STUDIES OF

PHYSICAL PROPERTIES OF CEMENTITIOUS MATERIALS IN RELATION TO HYDRATION PRODUCTS FORMED

THESIS SUBMITTED FOR THE AWARD OF THE
DEGREE OF DOCTOR OF PHILOSOPHY
IN CHEMISTRY

BY
S.K. CHOPRA, B.Sc. (Hons.), M.Sc

UNIVERSITY OF ROORKEE
ROORKEE

1964

C E R T I F I C A T E

Certified that the Thesis entitled " Studies of the Physical Properties of Cementitious Materials in relation to the Hydration Products formed " which is being submitted by Shree S.K. Chopra for the award of the Degree of Doctor of Philosophy in Chemistry of the University of Roorkee, is his own work carried out under my supervision and guidance. The matter embodied in this thesis has not been submitted for the award of any other Degree of any University.

This is to certify that he has worked on the above mentioned problem for a period equivalent to 24 months of full time research.

Waliullah Malik

(W.U. Malik)
Ph.D., D.Sc., F.R.I.C.(Lond.)
F.N.A.Sc.
Professor and Head of the
Chemistry Department,
University of Roorkee.

R O O R K E E)
)
)
D A T E 12.7.64)

ACKNOWLEDGEMENTS

The author gratefully thanks Prof. W.U. Malik, Head of the Chemistry Department, University of Roorkee for his able guidance and Dr. B.R. Aggarwal, Reader, Chemistry Department of the University of Roorkee for supervising the work in its early stages.

He is grateful to the Director of the Building Research Station, U.K., for providing the X-ray powder diffraction data of some of the samples, and the Director, National Physical Laboratory, India, for facilities of electron microscopic studies.

He is indebted to Prof. Dinesh Mohan, Director, Central Building Research Institute, Roorkee (India), for his encouragement by providing facilities to carry out this work and to management of the Iron & Steel Companies, the associated cement companies of India and the Clugston Foamed Slag Ltd. (U.K.) for supplying the samples.

C O N T E N T

Page No.

LIST OF TABLES

LIST OF FIGURES

Fig. No.

Fig. No.

GENERAL INTRODUCTION

Strength and dimensional stability are the two most important physical properties which a cementitious or binding material should possess for its successful application. Ordinary Portland cement, the well known cementing material, on hydration with water forms a 'cement gel' which fills spaces earlier occupied by water used in preparing a paste. A cement paste is normally constituted of residue of anhydrous cement, cement gel and the spaces. The latter are called capillaries or capillary cavities. According to Powers (1) the properties of cement gel and the degree to which the gel is "diluted" with capillary spaces, the effects of water in gel pores and capillaries are factors that determine important properties of cement pastes and products.

Ordinary Portland cement contains tricalcium silicate (C_3S*), β-dicalcium silicate (C_2S), tricalcium aluminate (C_3A) and a ferrite phase which until recently was regarded as C_4AF but which is now known to have a composition varying within the solid solution range C_6AF_2-C_6A_2F (2,3). The two silicates together constitute 70 - 85 per cent by weight of Portland cement. Steinour (4) reviewed the investigations on the hydration of C_3S and β-C_2S pastes in 1947. The main conclusions were that a very poorly

---

* $C = CaO$, $S = SiO_2$, $A = Al_2O_3$, $F = Fe_2O_3$, $H = H_2O$

This nomenclature is used interchangeably with ordinary chemical notations.

crystallized substance, generally described as a gel, was formed on the hydration of C_3S or β-C_2S and that a considerabl proportion of calcium hydroxide was formed in C_3S pastes but little or none in β-C_2S pastes. The hydrated calcium silicate was found to have a CaO/SiO_2 ratio of about 2. The gel formed on the hydration of a cement paste was believed to be no different (5).

Powers and Brownyard (6) studied the physical properties of hardened cement pastes and concluded that the hydration products of C_3A and C_4AF were colloidal and not microcrystalline. These authors gave the concept of gel-space ratio to explain the development of strength in cement pastes (7). The strength was considered proportional to the amount of cement gel formed in the space initially available to the gel; the latter being proportional to w_o i.e., the water content in the paste in the beginning. The empirical equation based on their data was

$$f_c = M \left[v_m/w_o - B \right] = M \left[K\,(w_n/w_o) - B \right]$$

where f_c is compressive strength, M, B and K are constants for a given cement; K being the ratio v_m/w_n. v_m is the weight of water required to cover the surface of a solid with one molecule thick layer and w_n is the non-evaporable water. The gel-space ratio is represented by the function v_m/w_o.

Powers (8) later modified the above function to

$$x = \frac{\text{gel volume}}{\text{gel volume + capillary space}}$$

where x is the gel-space ratio. The equation relating x with strength is

$$f_c = f_c^0 x^n$$

where f_c^0 and n are empirical constants. Since x is a fraction between 0 and 1, x^n operates as a reduction factor on f_c^0 which is considered to represent intrinsic strength.

One cc of Portland cement produces about 2.2 cc of cement gel (9). The cement gel is mostly colloidal in nature and has a specific surface of more than 2 million sq cm per g against about 2500 sq cm per g of the anhydrous cement. Thus the surface of cement increases about a thousand times in the course of hydration. The 'specific surface diameter' of the gel particle is about 120 A. The estimated figure for hydraulic radius is 7.0A and the corresponding average distance between solid surfaces in the gel being between 14 and 28A, 18A being a reasonable estimate (10). High strength of cement is thus considered by Powers and Czernin (11,12) primarily due to proximity of surfaces and Van der Waals forces. In fact this is an advanced and modern version of the old colloidal theory of Michaelis (13,14).

Powers (9,15) has built certain concepts of structure of cement gel and cement paste by which he has explained not only strength but several other important properties such as, stability and permeability etc. While his concept does not rule out the possibility of existence of many points of chemical bonding between gel particles, the latter's role in contributing towards strength and other properties was not brought out.

The other important theory of hardening of cement is based on the crystal structure of the hydrated phases formed. Though a beginning of this theory may be traced to the old crystal theory of Le Chatelier which explained cementing action on the basis of interlocking of crystals (13), the modern version of this theory has resulted mainly as a result of application of modern techniques for the identification of the hydrated phases.

The current approach started with the examination of set cement with differential thermal analysis by Kalousek, Davis and Schmertz (16), the synthesis of calcium silicate hydrates by Heller and Taylor (17), separation and identification of phases by X-ray technique by Nurse and Taylor (18) and Taylor (19), and new ideas of Bernal and Lea (20,13) in 1953 and 1956. Since then many important contributions have been made by Kalousek and his co-workers (21-24), Grudemo (25-27), Taylor and his co-workers (28-30), Sanders and Smothers (31), Midgley (32), Midgley and Rosaman (33),

Green (34) and Megaw and Kelsey (35).

Several new hydrates in the systems $CaO-SiO_2-H_2O$ and $CaO-Al_2O_3-H_2O$ have been reported (30,36). Determination of crystal structure of the important hydrates (30,35,37-39), morphological examination (25,40-46) and specific surface (1,6,47 and 48) of the pure hydrates and set cements have provided valuable evidence in support of the crystal theory.

It is now well established that the tobermorite-like hydrate in set cement is a very poorly crystallized variety of Taylor's calcium silicate hydrate (CSH II) showing no basal spacing but only one strong line at 3.05 - 3.07A and two weaker lines at 2.79 - 2.81A and 1.82 - 1.83A respectively. This phase is called as 'tobermorite gel' (49-51). A good deal of evidence from electron microscopy shows that tobermorite gel is present as fibres and the fibres are rolled up sheets (51).

According to Bernal, Jeffery and Taylor (52), the rapid growth of long fibres might well lead to production of interlocking crystals, similar in principle to those formed in gypsum plasters, but on a very much smaller scale. The interlocking of tobermorite fibres is considered to be the source of strength. According to Brunauer (50) the adhesion of tobermorite gel particles to each other and to other bodies is responsible for the engineering properties of strength and stability.

Grudemo (53) considers the evidence on the association of strength with any particular habit of crystal element in a paste structure rather inconclusive. Also, because of the great variability of microstructures, he considers the enormous specific surface of cement gel as the only important property in characterising cement pastes. These are very significant and important observations and show that the concept of cementing action based on the growth of interlocking crystals is not fully substantiated by experimental evidence.

Lea (54) has summarized the present state of knowledge as follows :

> "We can recognise that the conflict between crystal and colloid theories of set cement has been replaced by a more detailed description in which the large surface area underlying colloidal behaviour and crystal bond both play their parts".

Earlier estimates of the amount of $Ca(OH)_2$ formed from C_3S ranged from 0.6 to 1.4 moles per mole of C_3S (4). According to the latest estimate of Brunauer and Greenberg (51) the value is 1.5 moles. At complete hydration of C_3S, the stoichiometry of hydration of C_3S is represented by the equation

$$2Ca_3.SiO_5 + 6H_2O = Ca_3.Si_2O_7.3H_2O + 3Ca(OH)_2$$

The presence of calcium hydroxide in hydrated cement products is considered undesirable and even deterimental.

Slag and pozzolanic cements are actually mixtures of Portland cement with finely ground slag and pozzolana respectively. The main difference in their hydration from that of Portland cement is the reaction between liberated $Ca(OH)_2$ and constituents of slag and pozzolanas and consequently formation of cementing compounds which are known to have beneficial effects. This type of reaction also takes place on the hydration of cementitious materials such as mixes of lime with finely ground slag and pozzolana etc.

Studies of the activity of pozzolanas were critically reviewed by Lea (55) at the Stockholm International Symposium and more recently by Malquori (56) at the Fourth International Symposium on the Chemistry of Cement. Investigations on blastfurnace slag and slag cements were reviewed by Keil (57) and by Kramer (58) at the Third and the Fourth International Symposium.

No definite relationship has been found between the activity of a pozzolana and strength and other properties of the hardened pozzolanic cement mortar or concrete (56,87). In many instances the strengths of pozzolanic cements did not equal the strengths of that of the Portland cement even though the pozzolanic materials of high activity had been used. Similarly, some Portland blastfurnace cements have been found not to possess sulphate resistance greater than that of Portland cement (59-61). Williams and Chopra (62) found a great improvement in the properties of supersulphated

cement prepared from a low lime and high alumina slag by increasing the proportion of calcium sulphate. Examples of substantial improvements in the properties of cementitious materials by making small additions of chemicals are also available from the literature (63-65). However, many a times scientific explanations for a particular behaviour are lacking in the literature.

Investigations dealing directly with the theories of hardening of pastes of cementitious materials viz., slag and pozzolanic cements and mixtures of lime with slag or pozzolana are comparatively few (56,58). This appears to be primarily due to two reasons. Firstly, the chemistry of Portland cement itself is not very well understood. Secondly, the general belief has been that the hardening of clinker-based slag and pozzolanic cements would be no different from that of the Portland cement.

If the theories of hardening of Portland cement are assumed to be applicable to the hardening of cementitious materials, Lea's remarks about the conflict between the crystal and colloid theories will also hold equally well. In fact, there will be some additional questions.

According to Malquori (66) even if the end products of hardening in pozzolanic cements are qualitatively the same, there must be a considerable difference in the development of the process and in the final arrangement, because while the cementing compounds originate exclusively

from hydration of clinker constituents, with pozzolanic cements they originate partly from the reaction between lime from hydrolysis and the active constituents of the pozzolanic material. This statement holds equally good for the clinker-based slag cements.

Tobermorite gel having a CaO/SiO_2 ratio of 1.5 is considered to be the main cementing phase in hydrated Portland cement (51). The question is whether the slag and pozzolanic cements also produce tobermorite gel of this composition. The only answer available from the literature is that if the CaO content exceeds 0.020 mole per litre in solution, CSH-II (1.7 - 2.0 $CaO.SiO_2.aq.$) will form and at a lower concentration CSH-I (0.8 - 1.5 $CaO.SiO_2.aq.$) will be in the equilibrium (67,68). But, it is difficult to know the concentration of CaO in a hardened paste and further, experimental evidence regarding the presence or absence of $Ca(OH)_2$ in these hydrated cements itself is conflicting (69,70).

Tobermorite-like hydrates are identified by X-ray techniques and are characterized by their basal spacings (30). A review of the literature shows that so far it has not been possible to record the basal spacings in normally cured set cements (32,71).

Electron microscopy has also been employed in cement hydration studies (40-44, 72-75). Both the hydrated pastes of C_3S and β-C_2S as well as Portland cement pastes

have been examined. Buckle and Taylor (76) observed in C_3S pastes irregular masses possibly composed of small plates corresponding to very ill-crystallized tobermoritic material. Grudemo (43) found another phase present in almost equal amounts. It consisted of rather thick needles or rods, obviously composed of bundles of fibres or tubularly rolled sheets. The product was identified as fibrous tobermorite. Similar results were obtained for β-C_2S pastes. However, Funk (44) found β-C_2S pastes consisting almost entirely of fibrous C_2SH_2-type tobermorite.

Grudemo (25) has observed fibrous or bundled structures as well as amorphous masses in paste of ordinary Portland cement. Copeland and Schulz (45) have reported mostly clusters of acicular particles. The presence of laths and sheets, or flakes, in the more hydrated pastes has also been reported. The above description is for the C-S-H phase. Electron-microscopy studies on hardened cement pastes have also been reported by Iwai and Watanabe (40), Czernin (41),& Saji (75).

The crystal structure of tobermorite has been reported by Megaw and Kelsey (35) and Mamedov and Belov (37). The Megaw-Kelsey model is more widely accepted. Tobermorite has a layer type structure showing some analogies to the structure of clay minerals, especially to that of vermiculite (39). The structure contains discrete 3-metasilicate chains arranged in a structural unit consisting of two sheets of

parallel chains superimposed in such a way that free OH-OH edges of 7.3-A spacing are pointing outwards and are parallel to the plane of layer thus formed. Calcium ions are accomodated in internal positions in the planes of free OH-OH edges of 3.65A spacing, replacing all protons. This arrangement corresponds to a CaO/SiO_2 ratio of about 2/3. Though the positions of additional Ca and OH ions, and water molecules, were left undetermined, it is indicated that these groups can well be accomodated in lattice positions between the protruding OH-OH edges, which form a very open layer surface network of approximately hexagonal symmetry.

Taylor (77) has pointed out that tobermorite structure could 'go wrong' in many ways. According to Grudemo (78) the microstructural properties and particle habits of tobermorite phases can be influenced greatly by the nature of raw materials in synthesis mixtures and a number of other factors. Kalousek (22) had reported that some of Si^{4+} ions in tobermorite structure could be replaced by Al^{3+} ions and this influenced the morphology and also stabilized tobermorite phase. The tobermorite phase in hydrated slag and pozzolanic cements or mixes of lime and pozzolana thus could be significantly different from that of the hydrated Portland cement and so also its contribution towards strength development. The view expressed by some (79) that the final products of both cement hydration and pozzolanic reaction appear to be the same, therefore requires checking.

The important alumina bearing phases in set Portland cement are ettringite, C_4AH_{13}-$C_3A.CaSO_4.12H_2O$ solid solutions and hydrogarnet. While the contribution of tobermorite is probably more than the contribution of all the other hydrated phases put together, alumina bearing hydrated phases can influence the physical properties of hardened pastes differently depending on their composition, microstructure, crystal habit and relative amounts.

Alumina bearing hydrated phases may or may not be intimately mixed with silica bearing compounds. They may thus influence the intrinsic strengths of gels differently. Powers (80) found that Portland cement gels low in C_3A are stronger than those high in C_3A. In Portland cement alumina is present as C_3A. In other cementitious materials while the per cent alumina content may be higher, the actual C_3A content would be lower. The availability of alumina and its reactions to form hydrates will depend how alumina is present in the pozzolanas or slags. Al^{3+} ions can be present both in tetrahedral or octahedral coordination.

Attempts for the quantitative estimation of the hydrated phases formed on hydration of Portland cement have not proved fruitful so far (32,71) because the hydrated phases are generally present in poorly crystallized state. It is not surprising therefore that the relationship between strength and formation of a phase or phases are only of

general nature. This holds good also for the slag and pozzolanic cements and other cementitious materials (56,58, 64,65,81-88).

Presently it is not clear if the gel resulting from hydration of cement or from the reaction of calcium hydroxide with slag or pozzolana is a single phase or not. Also intrinsic strengths of gels formed on the hydration of different cementitious materials are not known and their comparisons with the intrinsic strength of gel produced on hydration of Portland cement are therefore not possible.

Reactions between added lime or that liberated from C_3S with alumina-silica bearing materials proceed slowly at ordinary temperatures but get very much accelerated under hydrothermal conditions and resulting in very high strengths of the mixes (30). Studies of such hydrothermal reactions have been made by Kalousek (89), Sanders and Smothers (31), Aitken and Taylor (90), Bessey (91), Taylor and Moorehead (92), Midgley and Chopra (93).

Most of the investigations show that high strengths are associated with the formation of tobermorite and low strengths are due to the formation of C_2S α-hydrate. However, it is not clear if the tobermorite gel or the crystalline variety result in comparatively higher strengths. Similarly, evidence on the association of crystal habit of tobermorite phase with strength is conflicting (30).

Kalousek (89) has reported that strength - unit weight of concretes prepared with cement or lime or a combination of the two with silica, pumice, shale and slag fines etc. showed nearly a straight-line relationship. Taylor and Moorehead (92) also found a correlation between tobermorite content and strength : weight ratio in light-weight lime-silica products. Midgley and Chopra (93) have also reported a relationship between strength and percentage of lime added for various periods of autoclaving of lime-slag mixes and formation of different cementitious phases. Bessey (94) has also reported similar relationships for sand-lime bricks. All these relationships are of general type and appear to be influenced by factors other than the phases formed as pointed out by some of the authors themselves.

Lea (54) concludes that we still are not clear about the relative importance of surface forces and chemical bonds; we cannot say that a large surface area is a necessary condition for hydraulic properties for this does not hold for the well crystallized product that act as the bond in cement cured in high pressure steam. A need for further work in this field is clearly indicated with a view to discerning the influences of the physico-chemical factors and understanding the mechanism of strength development.

A systematic and comprehensive investigation on the "Physical properties of cementitious materials in relation to hydration products" was therefore carried out. The cementitious materials studied were different types of slag cements, pozzolanic cements and a number of mixes of lime with siliceous fines. Though some of these are commonly termed as cements, others are not. But since all consisted of two or more than two constituents, the use of the wider term 'cementitious materials' was preferred. Similarly, the term hydration product has been used in a wider sense and implies the hardened paste (95).

The following aspects of the problem were chosen for investigations :

(1) the sedimentation characteristics and rheological properties of fresh pastes of cementitious materials as influenced by different physico-chemical factors,

(2) physical properties of hardened cementitious materials in relation to the structure of paste, nature of hydrated solid phases formed and 'intrinsic' strengths of the resulting gels, and

(3) hydrothermal reactions between lime and siliceous fines and the mechanism of strength development of the autoclaved compacts.

TABLE - 1

Designation, Description and Composition of the Cementitious Materials

S.No.	Designation	Description	Composition
1	PC	Ordinary Portland cement	*Portland cement clinker
2	PBF	Portland blastfurnace cement	*(65 parts of Portland cement clinker + 35 parts of granulated blast-furnace slag
3	BFP	Portland blastfurnace cement	*(35 parts of Portland cement clinker + 65 parts of granulated blast-furnace slag
4	PZC	Portland-pozzolana cement	*(75 parts of Portland cement clinker + 25 parts of fly ash**
5	SSC	Super-sulphated cement	(5 parts of Portland cement clinker + 25 parts of calcined gypsum + 70 parts of granulated blast-furnace slag
6	LS	Lime-slag	(15 parts of hydrated lime + 85 parts of granulated blast-furnace slag
7	LP	Lime-pozzolana	(30 parts of hydrated lime + 70 parts of calcined fly ash
8	E	Lime-ground sand	(30 parts of hydrated lime + 70 parts of ground quartz sand
9	F	Lime-fly ash	(30 parts of hydrated lime + 70 parts of fly ash

Table 1 (Cont'd.)

S.No.	Designation	Description	Composition
10	G	Lime-calcined fly ash	(30 parts of hydrated lime + (70 parts of calcined fly ash
11	H	Lime-granulated slag	(10 parts of hydrated lime + (90 parts of granulated (blastfurnace slag
12	I	Lime-foamed slag	(10 parts of hydrated lime + (90 parts of foamed slag

* 4 per cent gypsum was added for retarding setting times.

** Fly ash was used (a) in original state, (b) after calcination at 700°C so as to burn off unburnt carbon.

CEMENTITIOUS MATERIALS

The designation and composition of the twelve cementitious materials are reported in table 1. The compositions were selected on the basis of the earlier work (96-102).

The preparation of the cementitious materials involved two simple steps i.e., grinding of the oven dried constituents and their mixing. Each of the constituents of the cementitious materials was ground separately in a laboratory ball mill (0.5 cu.ft. capacity) to a fineness just short of the desired value. The ground constituents were then mixed in a vibratory ball mill for a short period of 15 to 30 minutes till the constituents got mixed homogeneously and the cementitious material possessed the specific surface (in sq cm per g) ultimately desired. The cementitious material thus prepared was sealed in an air-tight container.

A strict control was exercised on the quality of each of the constituent materials because a variability in quality can influence the results a good deal. Representative bulk samples were stored in sealed containers and standard methods of sampling were employed for drawing smaller lots. A brief description of the different materials together with their physico-chemical properties are reported below.

Ordinary Portland Cement

The ordinary Portland cement sample was prepared by grinding the clinker from the Bhupendra Cement Works Ltd., Surajpur (Punjab) with 4 per cent gypsum in a laboratory ball mill. A freshly ground batch of the Portland cement was prepared every time it was required for a programme of work.

The chemical analysis and the mineralogical constituents calculated from it by the Bogue formulae (103) are reported in table 2. The estimation of the mineralogical constituents of the clinker was also done by the microscopic examination (104) and employing the statistical method of point counting. The results are also reported in table 2. This clinker with normal C_3S (about 45 %) and β-C_2S (about 30 %) represents a typical Indian Portland cement clinker.

The physical properties of the cement (table 2) from the Surajpur clinker show that this cement passes the Indian Standard Specifications for the Ordinary Portland Cement (105).

Hydrated Lime

A high calcium limestone of purity not less than 98 per cent was burnt in a batch of 2 lb. in a laboratory furnace at 1000 $\pm$ 50°C for four hours. Lime thus produced

was cooled in a desiccator and afterwards hydrated with a quantity of water somewhat in excess of that required to convert CaO into $Ca(OH)_2$. The hydrated lime was dried in an oven avoiding carbonation and then stored in sealed containers. Since carbonation could not be avoided altogether, only samples with a hydrate content of at least 90 per cent were used.

Slags, Pozzolanas and other Siliceous Fines

The Indian slags are characterised by low lime and high alumina contents. A typical sample selected for the present investigation was the granulated slag from the Tata Iron & Steel Works (TISCO), Jamshedpur because most of the earlier work (96-100) on slag cements had been done with this sample. Also this slag is now being utilized commercially in producing a Portland blastfurnace cement.

A sample of the British foamed slag was obtained from Clugston Foamed Slag Ltd., Scunthorpe (LINCS), U.K. primarily for studies on hydrothermal reactions between lime and siliceous fines because some work on this type of slag had been reported earlier by Midgley and Chopra (93).

As a result of the evaluation of the Indian fly ashes (101), the sample from the West Bengal Government thermal power station at Durgapur was selected because of its low content of unburnt fuel (about 6 per cent). This fly ash was used either in its original state or after

TABLE - 2

Properties of Ordinary Portland Cement (Surajpur)

S.No.	Property/Test	Results		
1.	Chemical Composition	Constituents		Per cent
		SiO_2		21.90
		Al_2O_3		6.04
		Fe_2O_3		2.89
		CaO		63.73
		MgO		4.71
		Free Lime		0.42
2.	Mineralogical Composition	Compounds in per cent		
		Calculated		Microscopic Method
	C_3S	47		44
	β-C_2S	27		36
	C_3A	11	)	15
	Ferrite phase	9	)	
3.	Physical Characteristics			
	Specific gravity		3.13 g/cc	
	Fineness (Blain's)		3200 sq cm/g	
	Setting Times in minutes	Initial		Final
		110		280
	Soundness (Le Chatelier) expansion	1 mm		
	Compressive Strength, psi (1:3 Standard mortar cubes)	3 days		7 days
		2139		3994

TABLE - 3

Chemical Analysis of Siliceous Components of Cementitious Materials

Constituents	Slag granulated TISCO per cent	Slag foamed British per cent	Fly Ash 122C Durgapur per cent	Fly Ash 122C Calcined Durgapur per cent	Surkhi Roorkee percent	Ground Quartz (Ennore sand) per cent
Loss on ignition	- 2.28	- 1.16	5.53	1.81	0.33	- 0.25
Silica (total), SiO_2	33.61	31.40	51.65	53.61	72.21	97.92
Aluminium Oxide, Al_2O_3	21.85	20.94	18.80	20.02	14.63	2.08
Iron Oxide, Fe_2O_3	3.83	1.55	19.65	20.87	6.29	
Calcium Oxide, CaO	35.90	37.72	2.20	2.86	0.94	Nil
Magnesium Oxide, MgO	2.92	5.62	1.49	1.44	2.04	Nil
Available Alkalies, as Na_2O	-	-	0.70	0.73	2.53	Nil
Sulphur Trioxide, SO_3	1.94	2.77	trace	Nil	Nil	Nil

TABLE - 4

X-ray Powder Data of Representative Samples of Slags and Pozzolanas

Granulated Slag			Foamed Slag			Fly Ash 122C			Fly Ash 122C (Calcined)			Surkhi		
d (A)	I/I_o^*	Identification	d (A)	I/I_o^*	Identification	d (A)	I/I_o	Identification	d(A)	I/I_o	Identification	d (A)	I/I_o	Identification
1	2	3	4	5	6	7	8	9	10	11	12	13	14	15
						5.58	vvw	Mu						
			4.24	vvw	G	4.25	w	Q	4.30	vvw	Q	4.26	w	Q
			3.71	w	G				3.68	vvw	H			
			3.44	vvw	G	3.33	vvs	Q,Mu?	3.34	vvs	Q	3.34	vvs	Q
			3.07	w	G	2.93	vvw	M	2.94	vvw	M			
			2.86	vvs	G									
			2.74	vw	G	2.69	vvw	H	2.69	vvw	H			
			2.43	m	G	2.517	w	H,M	2.52	m	H,M	2.48	vw	A,H?
			2.29	vw	G	2.45	vvw	Q						
2.03	vvw	G?	2.03	m	G	2.275	vvw	Q	2.29	vvw	Q			
						2.209	vvw	H,Mu?	2.20	vvw	H			
						2.123	vvw	Q	2.12	vvw	Q			
			1.92	vvw	G	1.973	vvw	Q				2.00	vw	A
			1.83	ms	G	1.814	vw	Q	1.83	w	Q,H	1.82	w	Q,H
			1.75	s	G				1.685	w	H	1.67	w	H
			1.64	vvw	G	1.607	vvw	M,H	1.60	vw	H,M			
			1.52	vw	G	1.537	vvw	Q	1.54	vvw	Q	1.54	vw	Q
						1.522	vvw	H	1.51	w	H,M			
1.45	vvw	G?	1.43	vvw	G	1.472	vvw	Q,M	1.45	w	H,Q,M			

Table 4 (Cont'd.)

1	2	3	4	5	6	7	8	9	10	11	12	13	14	15
			1.37	w	G	1.37	vw	Q	1.37	w	Q	1.38	w	Q,A
			1.323	vvw	G				1.317	vvw	H			
			1.285	vvw	G				1.268	vvw	H			
1.17	vvw	?	1.247	vvw	G				1.193	vvw	H	1.185	vvw	Q
Gehlinite ? + Glass			Gehlinite (G) + Glass			∠-Quartz (Q) + Hematite (H) + Magnetite (M) + Mullite (Mu) ? + Glass			∠-Quartz + Hematite (increased) + Magnetite + Glass			∠-Quartz + Gamma alumina (A) + Hematite		

* The intensity scale used throughout the X-ray data is an arbitrary one :
vvs = very very strong, vs = very strong, s = strong,
ms = moderately strong, m = medium, w = weak
vw = very weak, vvw = very very weak

calcination at 700°C for burning off the unburnt fuel which can vitiate the results. Both the samples possessed the necessary pozzolanic activity as determined by the lime reactivity test (106) according to which a 1:2:9 mix of hydrated lime-pozzolana-sand on curing at 55 ± 2°C must have a minimum strength of 600 lb/in^2 or 40 kg/cm^2.

'Surkhi' is a well known pozzolana commonly used in India since long (107). Actually it is nothing but calcined clay. A sample of surkhi passing the Indian Standard Specifications (108) was used in the present investigation. The surkhi sample satisfied the requirement of the lime reactivity test mentioned above.

The quartz fines were prepared by grinding the Ennore sand which, like the Leighton Buzzard Sand of U.K., is the Indian Standard sand. It is a quartz sand with a total SiO_2 content of not less than 98 per cent.

The chemical and mineralogical constituents of slags, pozzolanas and other siliceous fines were determined by the standard chemical methods and X-ray powder analysis respectively. The latter was carried out on a Phillips X-ray unit (sealed) using a Debye-Scheerer camera of 114.6 mm diameter and molybdenum K alpha radiation. The results of the chemical and X-ray powder analyses are reported in tables 3 and 4 respectively.

The minerals identified in the different materials were as follows :

Material	Minerals Identified
Granulated Slag (TISCO)	None (only glass)
Foamed Slag (British)	Gehlinite and glass
Fly Ash 122 C (Durgapur)	Alpha quartz, hematite, magnetite, mullite?and glass
Fly Ash 122 C, calcined (Durgapur)	Alpha quartz, hematite, magnetite and glass
'Surkhi' (Roorkee)	Alpha quartz, gamma alumina and hematite

STUDIES ON THE FRESH CEMENTITIOUS PASTES

CHAPTER 1

SEDIMENTATION CHARACTERISTICS OF CEMENTITIOUS PASTES

Introduction

Grudemo (109) has described hardened cement paste as a complex and highly variable system of particles of a manifold of sizes, shapes and compositions, of water in different states of fixation, and of pores and voids, the sizes and distribution of which depend on how the particles of solid matter are aggregated and linked to each other. It is apparent that the initial chemical and mineralogical composition and the initial particle size distribution of cement; the water cement ratio; method of preparation of paste together with few other factors will govern the physical properties of a hardened paste. It is most likely therefore, that the early structure of paste may leave its imprint on the structures subsequently developing from it. Lea (110) had emphasized that the knowledge of early reactions of cement is not as much advanced as of those taking place at later ages.

Since the present investigation aims towards interpreting and correlating the physical properties of a variety of cementitious materials in relation to the hydration products formed, naturally in the first instance one would like to know how important are the differences in the structures of fresh pastes of slag and pozzolanic

cements and mixes of lime with slag or pozzolana from those of the Portland cement paste because improvements in the properties of the cementitious materials are possible only then. That such differences can be important is shown by the innumerable examples of additions being made in order to improve upon the early structure and properties of fresh cement pastes, mortars and concretes (63,111-113). Powers (114) has made a major contribution towards the understanding of the properties of fresh cement pastes and has applied the concepts of dispersion and flocculation in explaining these and the underlying phenonemon. The approach of the Russian scientists (115) who have also made several notable contributions in this field, is based on the colloid-chemical behaviour of the binding materials. The development of a self-stressed concrete by them (116,117) demonstrates how fruitful the understanding of the structure formation can be.

Many examples of improvements in the properties of existing cementitious materials or development of new binding materials from slag, pozzolanas etc. are also available in the literature (63-65). Changes in early structure are implied in many instances; but it appears those have not been studied. Further, it is difficult to deduce any information on the early structure of such pastes from the published work as both the materials and experimental conditions were highly variable. Moreover,

many a times no scientific explanations were given for a change in property or behaviour. In view of this, a study of the early structure of pastes of cementitious materials was considered important.

Pastes of cementitious materials are nothing but concentrated suspensions of powders in water. In the beginning particles are discrete. A study of the sedimentation characteristics will therefore provide information on the action of suspension medium on particles, interaction of particles amongst themselves and the physical state of the suspension.

Materials

The Surajpur Portland cement, two samples of pozzolanic cement and one sample of the Portland blastfurnace were used in this study. The pozzolanic cements were prepared by replacing 25 per cent of the Portland cement by fly ash (122C) and surkhi respectively. The fly ash sample was used in its original state. The Portland blastfurnace cement (65 clinker: 35 slag) was prepared from the TISCO slag, the glass content in the slag being at least 90 per cent. All these samples contained 4 per cent gypsum as a retarder of setting time.

The other materials studied were finely ground granulated slag, fly ash in its original state, surkhi and

ground quartz sand. The data on fineness as determined by the Blaine and Wagner methods (118,119) in table 5 show that the ground materials were of the same fineness as the Portland cement except the fly ash sample which was coarser. The results of the sedimentation analyses in table 6 show that the particle size distribution in ground samples of slag, surkhi and sand was more or less similar to that of the Portland cement; the fly ash sample being somewhat coarser. The values of the specific surfaces (S_1 and S_2 in table 5) of the ground materials were also determined from the particle size analyses and were found to agree well with those determined by the Blaine and Wagner methods (table 5).

Figs. 1 and 2 show the shape of coarse particles (-100+170 mesh B.S. sieve) of the ground materials and those of fly ash sample in their original states. The particles are mostly sub angular to angular. The quartz particles are sub angular to rounded. In fly ash samples sub-rounded particles were also seen sometimes. The presence of glass is also evident from the micrographs (Fig. 2).

The cementitious mixes used were one part of hydrated lime with two parts by weight of either ground slag and surkhi, and fly ash. A 1:3 mix of lime-fly ash was also included.

A. Granulated slag-showing subangular to angular grains (x 50)

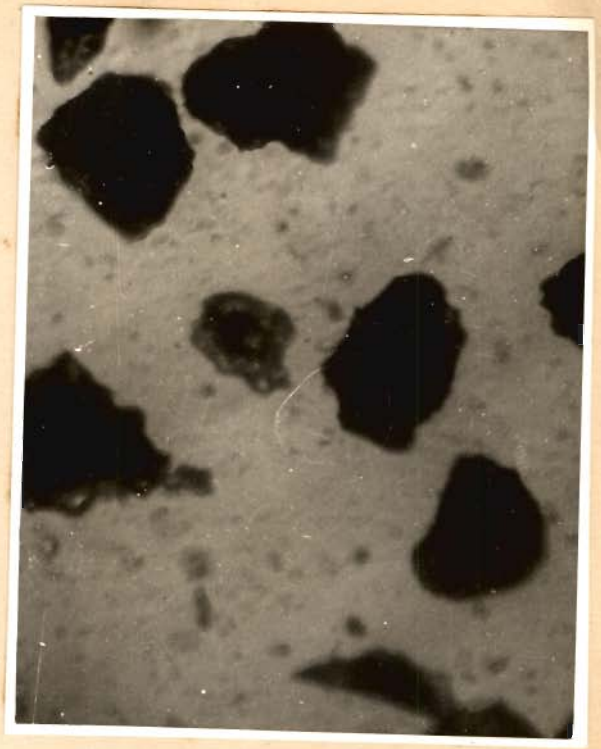

B. Foamed slag-showing angular grains (x 50)

C. Surkhi-showing subangular to angular grains (x 50)

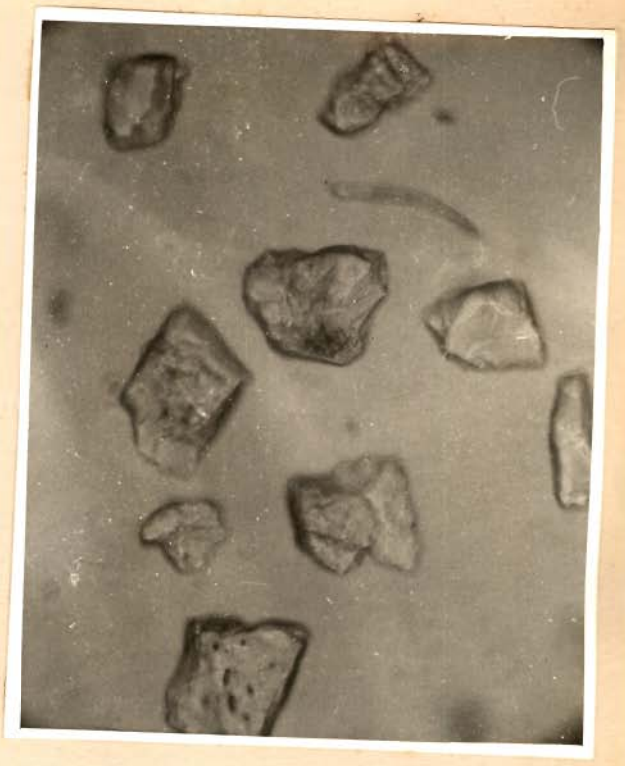

D. Quartz-showing subangular to rounded grains (x 50)

Fig. 1. Photomicrographs of different powders passing 100 mesh and retained on 170 mesh B.S. sieve

A. Original sample showing angular and rounded opaque grains and spheroids of glass (x 50)

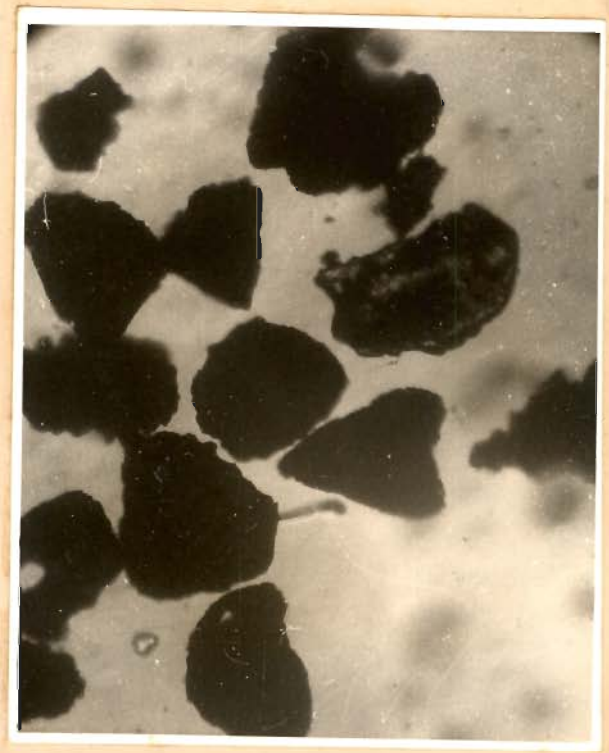

B. Fraction (-100+170 mesh B.S. sieve) showing subangular to angular grains, sometimes subrounded (x 50)

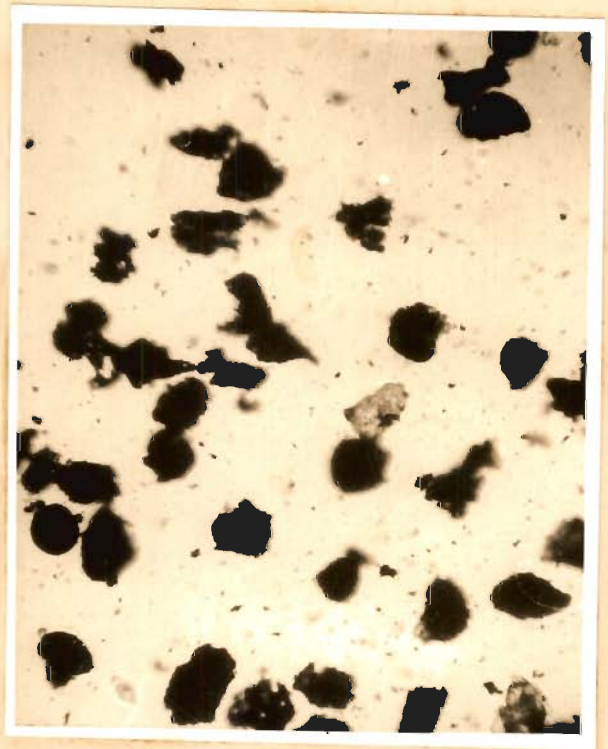

C. Fraction (-200+325 No. U.S. sieve)showing angular to rounded opaque grains (x 50)

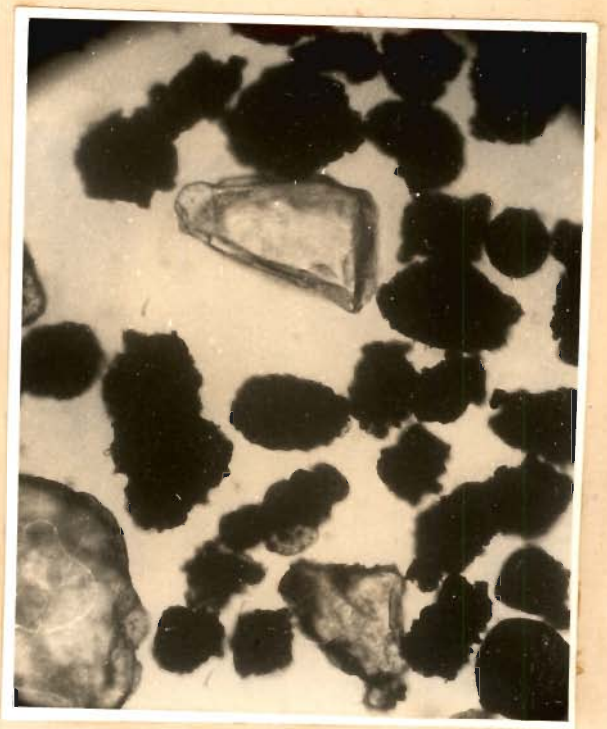

D. Calcined fraction (-100+170 mesh B.S. sieve) showing angular and rounded grains (x 50)

Fig. 2. Photomicrographs of the Durgapur fly ash (122C)

TABLE - 5

Fineness of Ground Materials by Different Methods

Sample	-325 U.S. Sieve per cent	Surface Area, sq cm/g		Surface Area, sq cm/g Sedimentation Analysis		Surface Area(S_1) sq cm/cc	Average Particle Diameter Microns	
		Blaine	Wagner	*S_1	*S_2			
Portland cement	81.94	3200	2144	3250	-	10080	5.9	
Slag	93.0	3209	1822	3486	1743	10179	5.8	
Surkhi	82.0	3200	1845	3316	1851	8622	6.9	
Sand (Quartz)	77.0	3227	2225	3130	1720	8138	7.3	
Fly Ash	55.8	2763	1450	2442	1520		10.2	**
Hydrated Lime	75.44	-	2261	7025	4060	15946	3.7	**

* S_1 and S_2 are surface areas calculated from sedimentation analysis assuming that (i) average diameter of all the particles below 2.5 microns is 1.25 microns and (ii) of all the particles below 7.5 microns is 3.75 microns.

** Average particle dia. is $\frac{6}{S_1}$ where S_1 is the surface area in sq.cm/cc

TABLE - 6

Particle Size Analysis of Ground Materials

Particle Size in Microns	Portland Cement	Slag	Surkhi	Ground Sand	Fly Ash (As received)	Hydrated Lime
	per cent	per cent	per cent	per cent	per cent	per cent
< 60	52.00	52.00	51.00	52.50	46.64	89.96
< 40	39.78	44.72	41.86	44.46	36.14	83.20
< 20	37.96	42.64	30.00	39.00	27.30	75.96
< 15	28.08	30.42	29.38	27.56	22.62	72.80
< 10	24.12	25.74	25.48	26.00	15.34	53.30
< 7.5	20.28	20.80	20.28	20.28	13.52	46.15
< 5.0	16.90	19.76	13.26	13.52	9.10	39.00
< 2.5	13.24	17.03	13.00	13.26	7.80	21.97
< 1.5	13.00	14.30	12.87	13.00	6.50	5.20

EXPERIMENTAL

Fineness by the Blaine Air Permeability Method

The Blaine air permeability apparatus (Fig. 3A) consists essentially of a means of drawing a definite quantity of air through a prepared bed of cement of definite porosity. The number and size of the pores in a bed of definite porosity is a function of the size of the particles and determines the rate of air flow through bed. While the detailed test procedure is described in the ASTM Book of Standards (118), the broad outline is given below.

The volume of the cement bed is determined by filling the permeability cell with mercury with and without the cement bed in place and noting the difference in weights. This divided by the density of mercury at the temperature of the test will give the desired volume.

The weight of cement to be taken for the test is given by the formula :

$$W = 3.15\ V(1 - e) \qquad \ldots \quad (1)$$

where W = weight of sample required in grams,

V = the bulk volume of the cement bed in cu.cm.

e = the required porosity of the bed of cement which is standardised as 0.500 ± 0.005.

The required weight of the standard cement (114 h) supplied by the United States National Bureau of Standards is placed

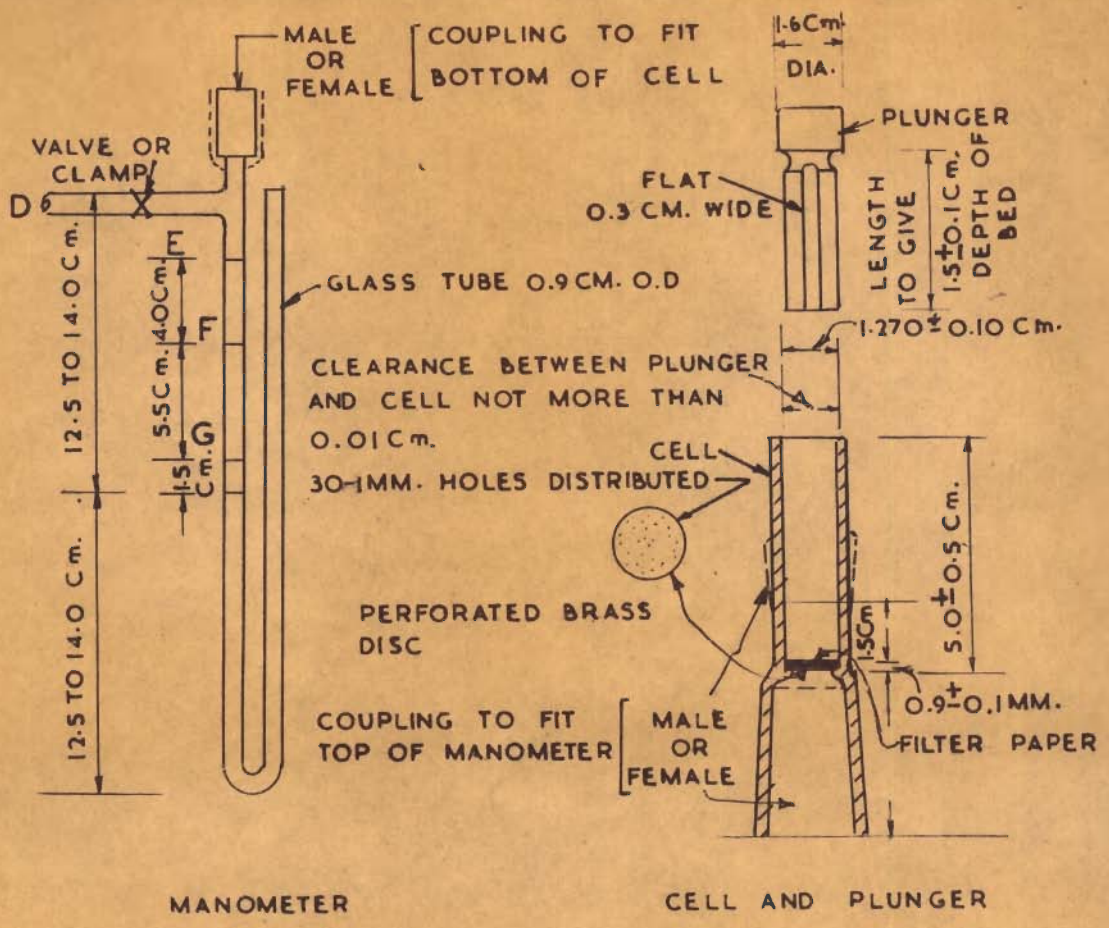

A. BLAINE MANOMETER (AFTER LEA)

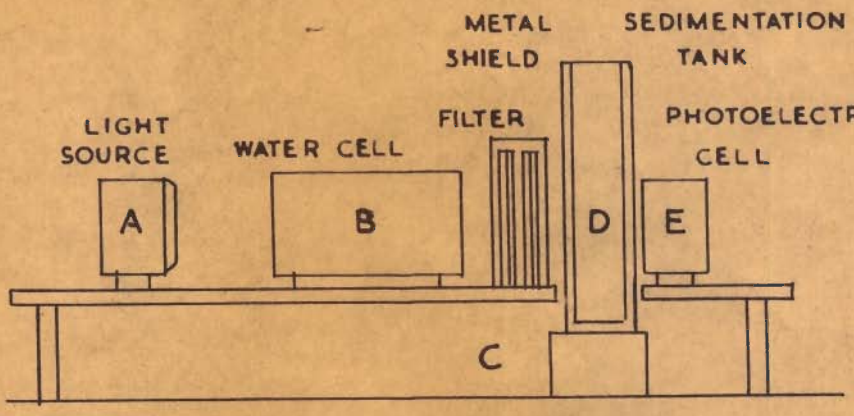

B. WAGNER TURBIDIMETER APPARATUS

FIG. 3. APPARATUS FOR DETERMINATION OF SPECIFIC SURFACE OF FINE POWDERS.

in the permeability cell and compacted to the standard volume with the half of the plunger (Fig. 3A). The air is evacuated through tube D until the liquid in the manometer reaches mark E. The valve or clamp is then closed and as the liquid in the manometer falls, it is timed between marks F and G. The mean of three tests is taken and the procedure is repeated with the cement whose specific surface (S) is to be determined.

$$S = \frac{S_s \rho_s (1 - e_s) \sqrt{\eta_s} \sqrt{e^3} \sqrt{T}}{\rho (1 - e) \sqrt{\eta} \sqrt{e_s^3} \sqrt{T_s}} \quad \ldots (2)$$

where S = the specific surface in sq cm per g of test sample

S_s = the specific surface of the standard cement sample used for calibration

T = time taken by manometer liquid in travelling from mark F to G with the test sample

T_s = the same as above for the standard cement sample

η = viscosity of air in poises when testing test sample

η_s = the same as above when calibrating the apparatus with the standard sample

e = porosity of test sample

e_s = porosity of calibration sample

ρ = specific gravity of test sample

ρ_s = specific gravity of calibration sample.

The terms $\sqrt{\eta}$ and $\sqrt{\eta_s}$ can be omitted from the above formula if the test sample is tested at a temperature within

$\pm$ 3°C of the temperature of testing the caliberation sample. If the test is employed for testing the fineness of cements only, the terms ρ and ρ_s may be omitted. If the porosity of the test sample is the same as that of the calibration sample then the terms containing e and e_s can be omitted from the above formula.

Fineness by Wagner Turbidimeter Method

In this method (119) parallel rays of light are passed through a suspension in kerosene of the cement or test sample, on to a photoelectric cell the resultant output of which is measured by a micro-ammeter. The reading is a measure of the turbidity of the suspension which in turn is generally held to be a measure of the surface area of the suspended matter.

Fig. 3B shows a schematic layout of the apparatus (120). The light source A, water cell B, shield and filter C and photoelectric cell E are all fixed to a moveable platform so that they can be raised or lowered together and a pointer is arranged to indicate the level of the light source below the liquid level in the sedimentation tank D. The latter is supported separately and independently. Observations are made at intervals according to the settling times for the different sized particles.

The settling time t is calculated for a range of particle diameters from the formula

$$t = \frac{1,837,000\ u}{(\rho_1 - \rho_2)} \times \frac{h}{d^2} \qquad \ldots \quad (3)$$

where t is time of settling,

u is viscosity of kerosene in poises,

ρ_1 and ρ_2 are the densities in g per cc of the solid particles and kerosene respectively,

h is depth of suspension to level of light in cm, and

d is diameter of particle in microns.

A burette is calibrated so that kerosene which it contains and which is allowed to run off passes the calibration points at these times, each point being marked with the particle diameter which it represents. The particle diameters taken are 60, 55, 50, 45, 40, 35, 30, 25, 20, 15, 10 and 7.5 microns. The kerosene to be used in the burette and the settling tank should be the same.

A suspension of the standard cement is made and the light intensity is adjusted up or down according to whether the specific surface so determined is too high or too low. The procedure is repeated until the correct value of specific surface is obtained within $\pm$ 15 sq cm per g. The micrometer reading is then taken with the light shining through the filter and a tank of similar dimensions to the sedimentation tank but filled with clear kerosene oil. This gives the reference value of microammeter reading for future adjustment of light intensity.

A suspension of the cement to be tested is made in a small quantity of kerosene to which a small amount of dispersing agent (oleic acid) has been added. This is transferred to the sedimentation tank and made up with clear kerosene to a total volume of 335 millilitres. This must be thoroughly agitated in a standard method.

The burette is filled above the zero mark and as soon as the kerosene in the burette reaches the zero mark the agitation of the sedimentation tank is stopped and the tank is placed in position and the light filter removed.

The microammeter is read as the kerosene in the burette passes the 60, 55, 50, 45, 40, 35 and 30 micron calibration marks. The moveable platform is then raised successively to the appropriate levels for the 25, 20, 15, 10 and 7.5 micron particles and the micrometer reading taken in each case as the kerosene passes the corresponding calibration point on the burette.

The filter is then replaced, the sedimentation tank is removed, and the lamp intensity is checked. Then

$$S = \frac{38\gamma(2 - \log I_{60})}{1.5+0.75 \log I_{7.5}+\log I_{10}+\log I_{15}+\log I_{20} \text{ ---} +\log I_{55}-11.5 \log I_{60}} \quad \ldots (4)$$

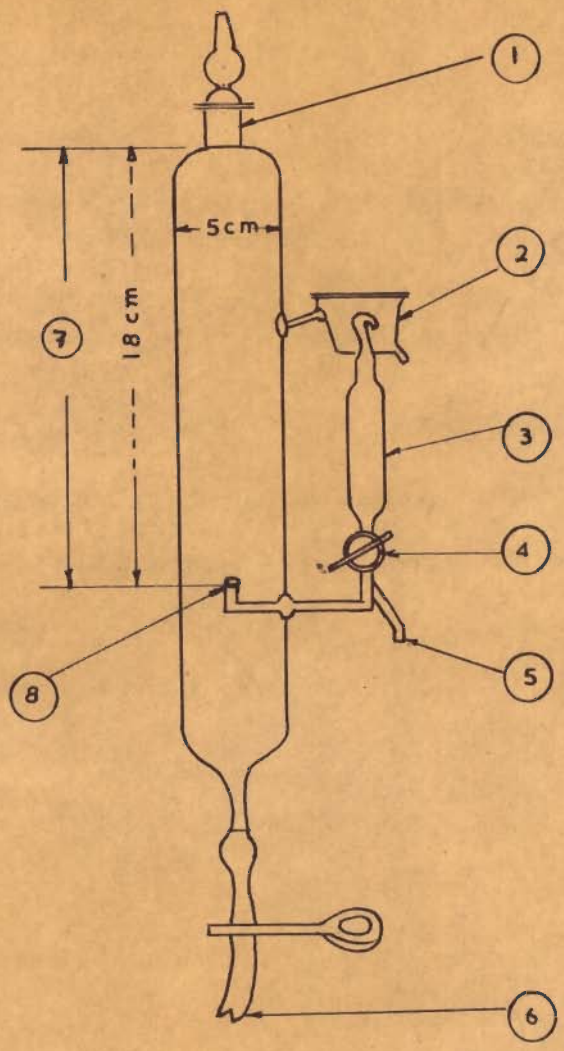

FIG. 4. THE SEDIMENTATION APPARATUS

1. GROUND JOINT.
2. OVERFLOW CONTAINER WITH DRAIN.
3. AUTOMATIC PIPETTE 10 CC. CAPACITY.
4. THREE-WAY STOPCOCK.
5. OUTLET DRAINING SAMPLES.
6. OUTLET FOR DRAINING.
7. EFFECTIVE SEDIMENTATION HEIGHT 18 Cm.
8. LEVEL AT WHICH SAMPLE IS DRAWN.

where S = specific surface of test sample in sq cm per g,

r = the corrected percentage of the sample of cement passing No. 325 U.S. sieve and

$I_{7.5}, I_{10}--I_{60}$ = the microammeter reading corresponding to 7.5, 10---60 micron calibration marks.

A correction factor is determined for the No.325 sieve by sieving a sample of standard cement. This correction factor is applied to the percentage of the sample of cement under test which passes the No. 325 sieve.

Particle Size Analysis

The particle size distribution was determined by the pipette method using the sedimentation apparatus shown in Fig. 4. This apparatus, originally designed by Carey and Stairmaid, was modified by Joglekar, Kumarswamy and Bhuchar (121).

5 grams of sample was dispersed in 455 ml of dispersion medium. 2 per cent sodium hexa metaphosphate solution was used for dispersing the samples of slag, fly ash, surkhi and ground sand etc. Aqueous dispersions were made for these samples but absolute alcohol was used for the samples of hydrated lime and Portland cement. Chemically pure anhydrous $CaCl_2$ (1 g/500 ml) was used as a dispersing agent for the Portland cement in alcohol. Further dispersion was obtained by blowing compressed air, freed from CO_2 and moisture, through the settling column

for about 5 minutes. The rest of the procedure of withdrawin portions of 10 ml of suspension at fixed time intervals, calculated for different particle sizes on the basis of the Stokes law, is the same as given in any standard book (122).

Fineness of Fly Ash by the Modified Method of Chopra and Narain

The determination of specific surface of fly ash by the air permeability method is known to give misleading information about its fineness (123). The specific surfaces of the Indian fly ash samples were determined both by the Blaine air permeability method (B) and the Wagner turbidimeter method (W). The ratio B/W which is known to be constant (1.8) for cements (124) was found to vary a great deal (3.18 to 5.66) for the fly ash samples. It was concluded that the specific surface of fly ash as determined by the current procedures (118,119) was in error.

Lea and Nurse (125) have listed the important factors which influence the results of specific surface measured by the air permeability method. Inhomogenity of the powder bed due to large particle-size ratios, presence of unburnt fuel and variations in porosity function were found to be the main sources of error in the measurement of the specific surface of the fly ash samples.

Chopra and Narain have modified the procedure of measuring the specific surface by the air permeability

method and the details are reported elsewhere (126). The main features of the method are the separation of fly ash into two fractions with the help of a No. 325 U.S. sieve and finding proportions of the two fractions quantitatively; firing the fine fraction (-325 U.S. sieve) at 700°C for removing unburnt carbon. The particle size analyses of the fired and unfired fractions of fly ash samples showed that the firing did not affect the particle size (table 7). The surface area of the fired fraction (-325 U.S. sieve) was determined by the Blaine method incorporating a modified porosity function. The surface area of the coarse fraction was determined by the sieve analysis. The true surface area was calculated by adding up the contribution of the coarse and fine fractions. The values for the different fly ash samples are reported in table 8. It may be noted that the ratio B/W is now constant and has the same value (about 1.8) as that of the Portland cement. The values for the fly ash sample No. 3 are for the Durgapur fly ash sample 122 C which was used in the present investigations.

Preparation of Paste

A paste is prepared by mixing dry cementitious material with water in a definite proportion. The preparation of a paste is an important step and the effects of different mixing schedules were studied earlier by Powers and Steinour (127,128). The mixing of a single batch of paste in the present study was done in a Waring Blender

T A B L E - 7

Particle Size Analysis of Unfired and Calcined Samples of Fly Ash (Fraction Passing 3 2 5 U.S. Sieve)

Particle size Microns	Per cent Cumulative					
	Sample No. 3		Sample No. 5		Sample No. 6	
	*A	*B	A	B	A	B
< 60.0	85.00	80.25	97.00	98.50	96.12	91.01
< 40.0	75.24	70.69	91.50	90.00	88.50	82.40
< 20.0	65.09	60.05	63.05	61.00	77.21	75.15
< 10.0	52.05	51.90	49.25	48.20	53.33	52.04
< 7.5	32.00	33.25	38.00	39.15	41.42	42.00
< 5.0	25.04	25.27	30.06	30.51	27.30	28.13
< 2.5	18.28	18.56	20.13	21.07	21.25	21.50
< 1.5	10.17	10.65	12.01	12.25	12.15	12.50
Surface Area Calculated from Sedimentation Data sq cm/g						
S_2 **	3055	2822	3588	3600	3890	3830
S_3 **	4365	4411	5155	5222	5358	5336
S_4 **	6055	6100	7300	7410	7530	7500

* A & B represent unfired and calcined samples of a particular fly ash.

** S_2, S_3 & S_4 are surface areas calculated by assuming (i) particles below 7.5 microns are assumed to be 3.75 microns in diameter, (ii) particles below 1.5 microns are assumed to be 1.5 microns in diameter, and (iii) particles below 1.5 microns are assumed to be 0.75 microns in diameter.

TABLE - 8

True Specific Surface of Fly Ash

Fly ash sample	Fraction passing 325 U.S. sieve		Surface area of calcined sample (-325 fraction) sq cm/g		Surface area of +325 fraction sq cm/g	True specific surface fly ash sq cm/g		Ratio B/W
	Content percent	Unburnt fuel percent	Blaine	Wagner		Blaine (B)	Wagner (W)	
No. 1	40.00	1.50	3273 (0.58)**	1824	100	1370	730	1.87
No. 2	48.6	2.50	4217 (0.58)	2499	300	2203	1215	1.81
No. 3* (Durgapur)	55.8	2.06	4700 (0.58)	2590	320	2763	1445	1.84
No. 4	77.5	5.35	5494 (0.58)	3024	310	4327	2343	1.84
No. 5	70.00	9.38	5560 (0.54)	3007	247	3966	2105	1.88
No. 6	60.00	4.89	6010 (0.53)	3456	300	3726	2073	1.80

* No. 3 sample is Durgapur fly ash 122 c used in the present investigations.

** Minimum porosity at which bed was made.

under vacuum so as to avoid the entrainment of air (129). The mixing schedule for the cement pastes was 1-3-2 minute cycle of mix-rest-mix as per the recommended practice (128). For the other cementitious pastes a 3-1-2 minute cycle of mix-rest-mix was adopted as the corresponding volume of solids to be mixed was greater than that of cement. The sequence in mixing was (i) adding the cement or solid to water with mild agitation; (ii) vigorous agitation for one or three minutes; (iii) rest for 3 (or one) minutes and finally (iv) vigorous agitation for two minutes. The mixing was done in a constant temperature laboratory ($27 \pm 2^{o}C$). The temperature of the paste after mixing was kept close to the laboratory temperature by using water whose temperature was so adjusted that the final temperature of the paste was close to $27 \pm 2^{o}C$. A single batch of paste was prepared from 450 - 600 g of solids with varying amounts of water.

Measurement of Bleeding of Paste

The accumulation of water on the surface of a settling fresh paste is known as "bleeding" which has been treated as a special case of sedimentation (127). The procedure followed in measuring bleeding was as recommended by Steinour (128). The paste was placed in a metallic cylindrical jar, about 4 in. diameter and 3 in. height. The height of the paste in the jar was measured with a guage of an accuracy of about 0.5 mm. Water was poured

from a small graduate down the side of the jar till it formed about 3 mm layer over the surface of the paste. A float was then placed on the surface of the paste without disturbing the paste. The main body of float was a bakelite disc 20 to 25 mm in diameter and about 2 mm thick. A fine wire 3 in. long was mounted vertically at the centre of the disc. After the float was seated in position, a low power microscope was focused on the tip of the float-stem and a reading was taken. The readings were taken at one or two minutes intervals during the period of constant bleeding rate and thereafter at an interval of five minutes. The readings were taken with an accuracy of 0.001 mm till the completion of bleeding.

Determination of Different Parameters in Bleeding (or Sedimentation) Studies

The equations (128) for bleeding rate and bleeding capacity respectively are :

$$Q = \frac{0.2g(d_c - d_f)}{\sigma_w^2 \eta} \quad \frac{(W - W_1)^3}{C} \qquad \ldots (5)$$

where

Q = the rate of bleeding, cm of subsidence per second

g = gravitational acceleration, cm/sec^2

d_c = density of cement, g/cc

d_f = density of water, g/cc

η = viscosity of the water, poises

σ_w = specific surface of cement sq cm/cc as determined by the Wagner turbidimeter

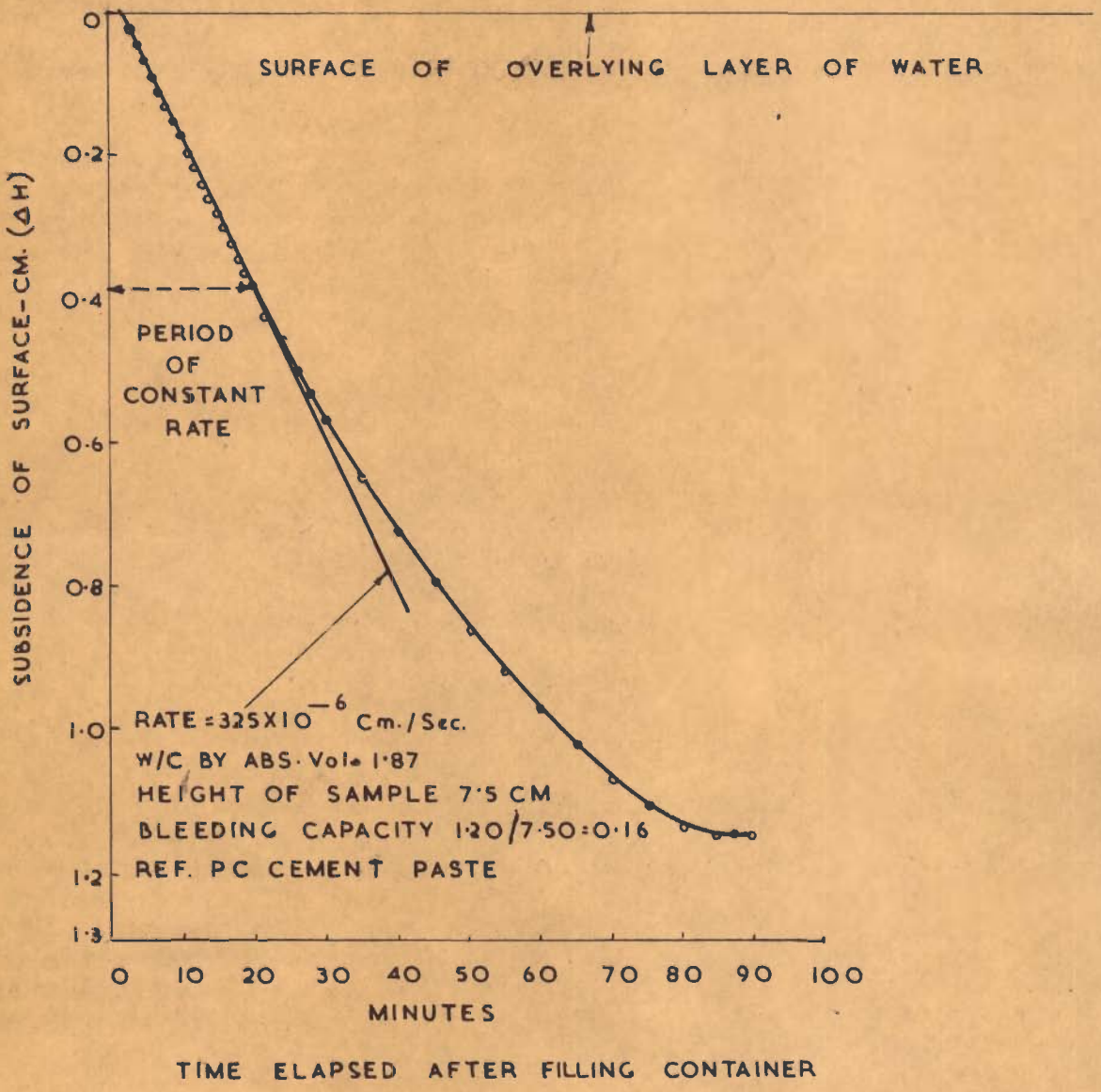

FIG. 5. TYPICAL BLEEDING CURVE (AFTER POWERS)

W = volume of water per unit volume of mix

C = volume of cement per unit volume of mix, $(C + W = 1)$

W_i = a constant for a given cement or solid at a given temperature, which, since it is subtracted from W, was assumed to represent a quantity of immobile water per unit volume of paste

and

$$\Delta H' = \frac{K^2 C \rho_C}{V} \left[(W/C) - (W/C)_m \right]^2 \quad \ldots (6)$$

where

$\Delta H'$ = bleeding capacity expressed as settlement per unit of original height

W = initial weight of water

C = weight of cement

ρ_C = density of cement

V = initial volume of paste

K and $(W/C)_m$ are experimental constants characteristics of a given cement and are dependent mostly on surface area of the cement. $(W/C)_m$ is defined as the water-cement ratio of a 'base' paste in which particles are so concentrated that bleeding cannot occur.

The equation (5) is only partly theoretical and embodies practical approximations. The equation (6) is an empirical equation.

The initial bleeding rate which is constant for about 10 to 20 minutes was determined from a plot of the change in height of paste versus time (Fig. 5). The slope of the straight portion of the curve gives the value of Q. The straight line was extended to the zero of the time

scale and the total settlement was figured from the zero position. The bleeding capacity ($\Delta H'$) was obtained by dividing this total settlement by the initial height of the paste.

For determining W_i of equation (5), values of $(QC)^{\frac{1}{3}}$ were plotted versus W. The plot is a straight line relationship and the line cuts the axis of W at W_i. The theoretical slope of the line is the cube root of $\frac{0.2g\ (d_c - d_f)}{\sigma_w^2\ \eta}$ and involves the determination of various physical quantities. The data lines were always drawn to the theoretical slope unless the experimental points showed discrepancies of significant magnitude.

Similarly, $\sqrt{\frac{\Delta H'}{C}}$ was plotted versus W/C (by volume). This is a straight line relationship. The point where the straight line cuts the W/C axis gives the value of $(W/C)_m$. The slope of the line gives the value of K in equation (6). The lines were always drawn for the best fit of the experimental points.

Steinour (128) had found the plots of $\sqrt{\Delta H'}$ versus water content (W) by absolute volume to be on a straight line. The straight line must pass through the point (1,1) since the bleeding capacity, $\Delta H'$ must equal 1 when W is equal to 1.

All the above relationships were determined experimentally for a variety of pastes and for this purpose at least three concentrations of solids in a paste were chosen to arrive at a particular relationship.

Sedimentation Volume and Porosity of Sediment

The bleeding capacity, $\Delta H'$ is the settlement per unit of original height of the paste. The final height of the paste is therefore $1-\Delta H'$. Knowing the internal diameter of the container, volume of the sediment can be calculated. When diameter is constant, the sedimentation volume can be expressed in terms of final height i.e., $1-\Delta H'$.

Knowing the volume of the sediment and volume of solids in settled paste, porosity can be calculated. The porosity has been expressed in terms of the final volume of the sediment (i.e., the settled paste).

"Pore" Sizes of Fresh Pastes and Width of 'Pores'

The mean size of pores in fresh paste can be estimated from hydraulic radius, that is, the quotient of water content and wetted surface area (130).

$$\text{Hydraulic radius} = \frac{\text{water-filled volume per unit volume of mix (W)}}{\text{water-covered surface per unit volume of mix (S)}} \quad \ldots(7)$$

If σ is the specific surface of solids in the mix in sq cm per unit of solid volume, then

$$S = C\,\sigma \qquad \ldots (8)$$

where C is the concentration of solids in unit volume of mix

$$\therefore \quad \text{Hydraulic radius (m)} = \frac{W}{C.\sigma} \qquad \ldots (9)$$

The average size of pore can be estimated from the hydraulic radius by assuming that the cross section of the pore resembles a rectangular slit. Powers and Brownyard (131) has shown that in a slit of width b, thickness h and length L, as h/b is made larger, hydraulic radius (m) approaches 1/2 b as limit. This means that the width of pores is at least twice and at most four times the hydraulic radius.

RESULTS

Bleeding (or Sedimentation) Characteristics of Pozzolanic and Slag Cements

Validity of the Equations

Pozzolanic and slag cements are prepared by replacing a part of ordinary Portland cement with a pozzolana or slag. Even when the latter possesses the same fineness as that of the cement it replaces, it is not possible to estimate the rate of bleeding of the former type of cements from the experimentally determined value of Q for the Portland cement paste. This is because the equation (5) is only partly theoretical and it is difficult to say how the introduction of pozzolana or slag will change the flocculent state. The bleeding characteristics

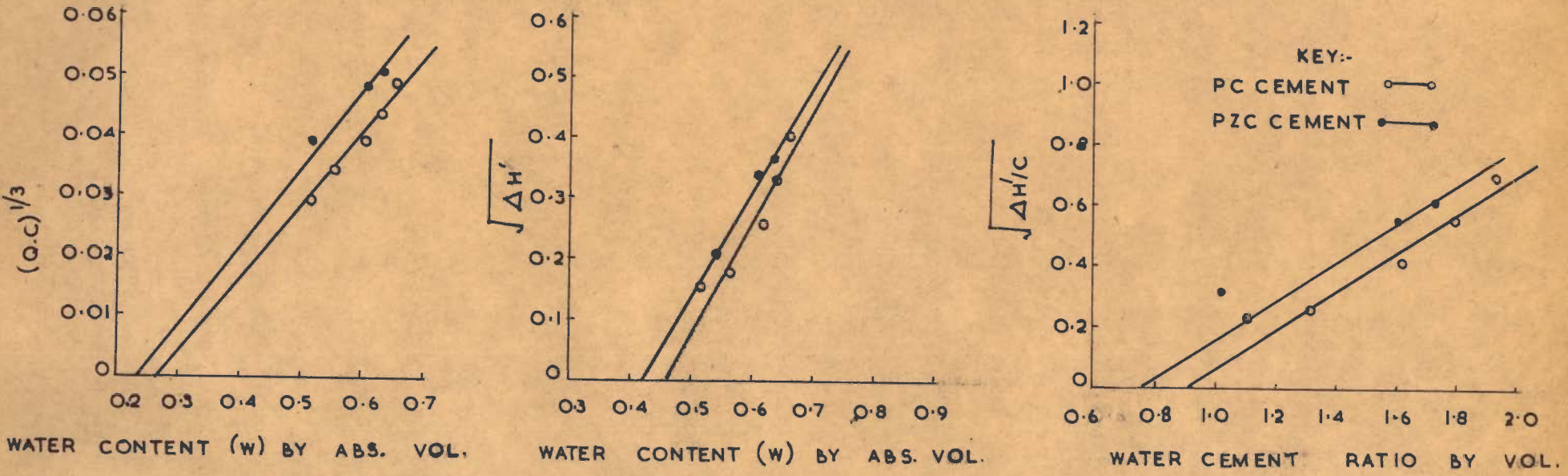

FIG. 6. TYPICAL RELATIONSHIPS FOR DIFFERENT CEMENTS.

were therefore determined experimentally.

Fig. 6 shows a typical plot of $(QC)^{\frac{1}{3}}$ versus W for a pozzolanic cement. Since the points lie on the straight line with a theoretical slope, it is inferred that equation (5) holds good. Even the empirical relationships between $\Delta H'$ versus W and $\sqrt{\frac{\Delta H'}{C}}$ versus (W/C) can be represented by a straight line (Fig. 6). The last mentioned relationship shows the validity of the equation (6). In short, the bleeding characteristics of the pozzolanic cements are not different from those of the Portland cement. This is also true of the Portland blast-furnace cement (table 9).

Comparison of Values of W_i and $(W/C)_m$

The values of W_i of pozzolanic cements differ significantly from those of the Portland cement while it is not so for the slag cement (table 9). To understand the effect of the presence of non-cementitious powders in a cement paste on the magnitude of W_i, the bleeding characteristics of ground slag, pozzolana etc. were also studied separately. For obvious reasons a saturated solution of calcium hydroxide was used for flocculating these concentrated suspensions of angular particle of powders having almost the same fineness (table 5 and 6). Differences in W_i appear to be mainly due to different states of flocculation (table 10).

TABLE - 9

Bleeding (or Sedimentation) Characteristics of Different Cement Pastes

Cement designation	Specific Surface (Wagner)		Density in kerosene	w/c Ratio of paste		Cement content of paste	Bleeding rate	Bleeding capacity	Porosity of sediment	Values of constants		
	sqcm/g	sqcm/cc	g/cc	wt.	vol.	Abs. vol.	$Q \times 10^6$	$\Delta H'$	% of settled volume	w_i	w	$(w/c)_m$
Portland cement	2144	6711	3.13	0.35	1.10	0.479	51.0	0.023	51.2			
				0.40	1.25	0.444	93.0	0.028	55.4			
				0.50	1.56	0.390	146.0	0.065	58.9	0.27	0.52	0.91
				0.55	1.72	0.367	221.0	0.109	59.8			
				0.60	1.87	0.347	325.0	0.160	59.4			
Pozzolanic cement (25 per cent cement replaced by flyash 122C)	1778	5736	2.96	0.35	1.10	0.479	122.0	0.047	49.9			
				0.50	1.56	0.390	277.7	0.116	56.2	0.23	0.44	0.76
				0.55	1.72	0.367	342.1	0.130	56.6			
Pozzolanic cement (25 per cent cement replaced by surkhi)	2091	6317	3.02	0.276	0.86	0.537	70.9	0.023	45.0			
				0.350	1.10	0.479	138.9	0.065	48.9	0.15	0.30	0.58
				0.45	1.41	0.414	330.0	0.176	49.6			
				0.50	1.56	0.390	855.0	0.250	47.5			
Portland blastfurnace cement (cement: slag 65:35)	2044	6390	3.09	0.40	1.25	0.444	63.5	0.020	54.2	0.26	0.52	-

TABLE - 10

Sedimentation (or Bleeding) Characteristics of Pastes of Different Powders
(Flocculating Agent - Saturated Lime Water)

Powder sample	Specific Surface Wagner sqcm/g	Specific Surface Sedimentation sqcm/g	Specific Surface Sedimentation sqcm/cc	Density in kerosene oil g/cc	w/c(vol.)	Solid content in Abs. vol.	Bleeding rate $Qx10^6$	Bleeding capacity $\Delta H'$	Porosity of sediment % of setteld vol	(w_1)	(w)	$(w/c)_m$
Slag	1822	1743	5320	2.92	1.17	0.461	172.0	0.035	52.2	0.18	0.44	0.70
					1.45	0.408	297.0	0.055	56.8			
					1.75	0.363	333.0	0.087	60.2			
					1.89	0.346	394.0	0.094	61.9			
Fly ash 122C	1450	1520	3648	2.40	1.73	0.366	477.0	0.073	60.5	0.24	0.50	0.56
					1.80	0.357	539.0	0.088	60.8			
					1.92	0.343	584.0	0.091	62.3			
					2.04	0.329	788.0	0.113	62.9			
					2.28	0.305	1285.0	0.127	65.1			
Surkhi	1845	1851	4869	2.61	1.17	0.461	229.1	0.051	51.5	0.12	0.35	0.53
					1.30	0.435	416.6	0.096	51.8			
					1.52	0.396	488.2	0.174	51.9			
					1.83	0.353	990.9	0.219	54.7			
					2.08	0.324	1666.0	0.224	58.2			
Quartz sand	2225	1720	4558	2.65	1.06	0.485	119.0	0.05	49.0	0.14	0.33	0.70
					1.32	0.431	261.0	0.13	50.3			
					1.59	0.386	515.0	0.21	51.5			
					1.86	0.350	783.0	0.31	50.0			

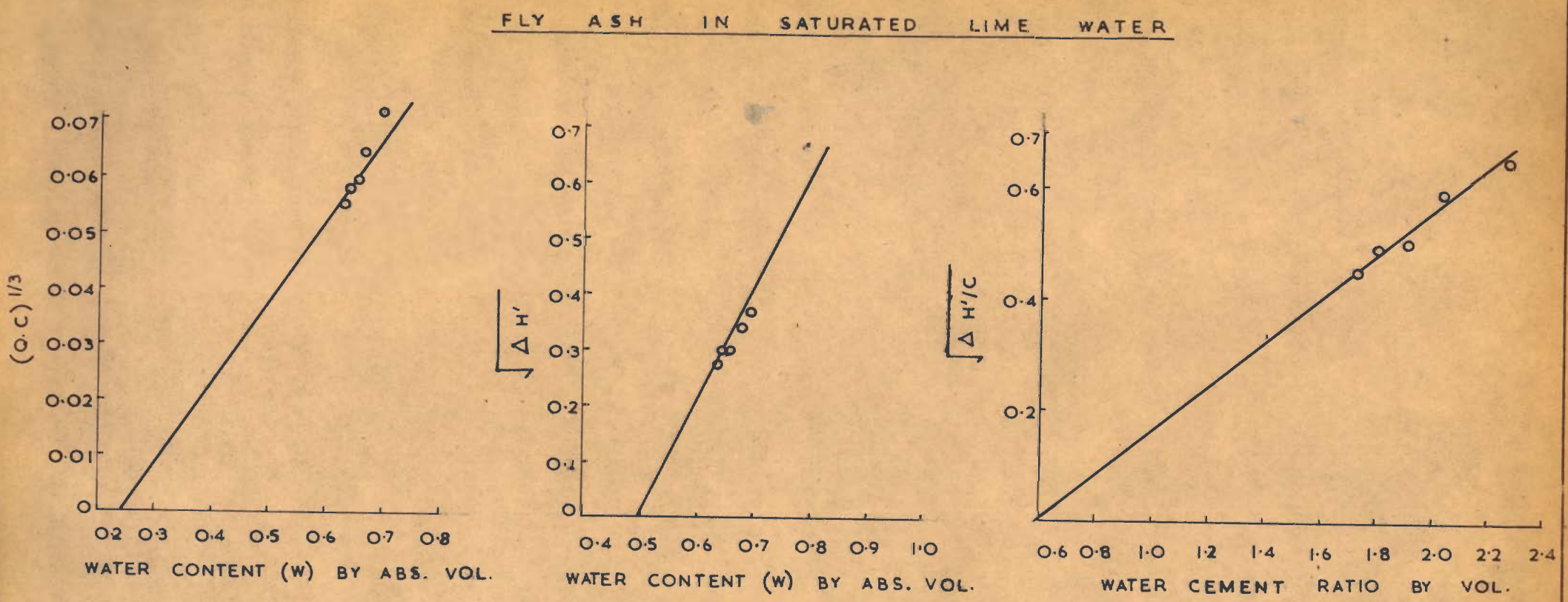

FIG. 7. TYPICAL RELATIONSHIPS FOR SUSPENSIONS OF POWDERS.

The suspension of surkhi is least flocculated because the bleeding rates are highest. The presence of alkalies (table 3) in this powder appears to be responsible for it. The value of W_i for the suspension of fly ash in saturated lime solution is based on experimental slope (Fig. 7) as the points did not fit the theoretical slope. The presence of carbon particles and the shape of particles of fly ash (Fig. 2) appear to be responsible for a higher value of W_i. W_i could not have been influenced by the particle size as the fly ash was somewhat coarser than the other non-cementitious powders. In short, W_i in the suspension of non-cementitious powders is influenced both by flocculating forces and particle shape. On the other hand, the magnitude of W_i in a Portland cement of paste is known to be more influenced by the chemical factors (132). A comparison of the values of W_i of the pozzolanic and slag cement pastes (table 9) with the value of ordinary Portland cement paste shows that the magnitude of W_i in the former pastes is a result of both the physical and chemical factors.

Steinour considers the differences in W_i in Portland cements of different compositions due to chemical reactions (128). According to him a significant amount of initial reaction takes place and reaction products form as coating on the cement particles, the latter increasing the immobile phase at the expense of mobile one (e.g., increasing W_i). Therefore, it follows a fine material which,

while replacing a part of the Portland cement does not change the pH of the solution as a result of its solubility or its reactivity, will not change W_i materially. Actually this was found to be so for cements in which replacement was done with slag. However, this does not appear to be so for the surkhi powder as it reduced W_i to almost half of its value. The 'surkhi' sample contains a good deal of alkalies which can reduce W_i by retarding the initial chemical reactions and also by reducing the degree of flocculation.

The degree of flocculation influences the bleeding capacity strongly. The data in table 9 show that the bleeding capacity of the pozzolanic cements was very much greater than that of the Portland cement; but the slag cement showed somewhat lower capacity. The values of $(W/C)_m$ were 0.58 and 0.76 for the two pozzolanic cements against the value of 0.91 for Portland cement showing thereby a lower strength of the floc structure of the pozzolanic cement pastes. Also in the latter cement the floc strengths fall off more rapidly as W/C ratio increases as the data on the porosity of the sediment (table 9) shows that the porosity of pozzolanic cements is lower than that of Portland cement and also a relatively smaller increase in porosity takes place on increasing W/C ratios. It may be concluded that the replacement of cement by pozzolanas may bring about a

sort of deflocculation of the Portland cement paste. A comparison of the values of bleeding capacity and of 'W' of the Portland blastfurnace cement (table 9) with those of the Portland cement do not show any significant differences and therefore it may be concluded that the degree of flocculation in the former paste is not any different.

Bleeding or Sedimentation Characteristics of Pastes of Cementitious Mixes

Powers (133) had given the equation

$$Q'' = \frac{C_t \quad (a + c)\,(d' - d_f)\left[W - P(W_i)_p\right]^3}{(C\,\sigma_c \;+\; a\;\sigma_a)^2} \qquad \ldots (10)$$

for calculating the bleeding rate of cement paste containing aggregate. Another relationship (133) given was

$$Q''/Q_p = p^2(a/c + 1)\;\frac{(d' - d_f)}{(d_c - d_f)}\;\frac{1}{(1+a/c\;\sigma_a/\sigma_c)^2} \qquad \ldots (11)$$

where Q'' = rate of bleeding of lime-surkhi mix

Q_p = rate of bleeding of a suspension of surkhi powder in saturated lime solution

a/c = ratio of added lime to the surkhi content

p^2 = $\dfrac{\text{the capillary area per unit volume of lime-surkhi paste}}{\text{capillary area per unit volume of surkhi paste}}$

σ_a/σ_c = $\dfrac{\text{Specific surface of lime-surkhi in sq cm per cc}}{\text{specific surface of surkhi in sq cm per cc}}$

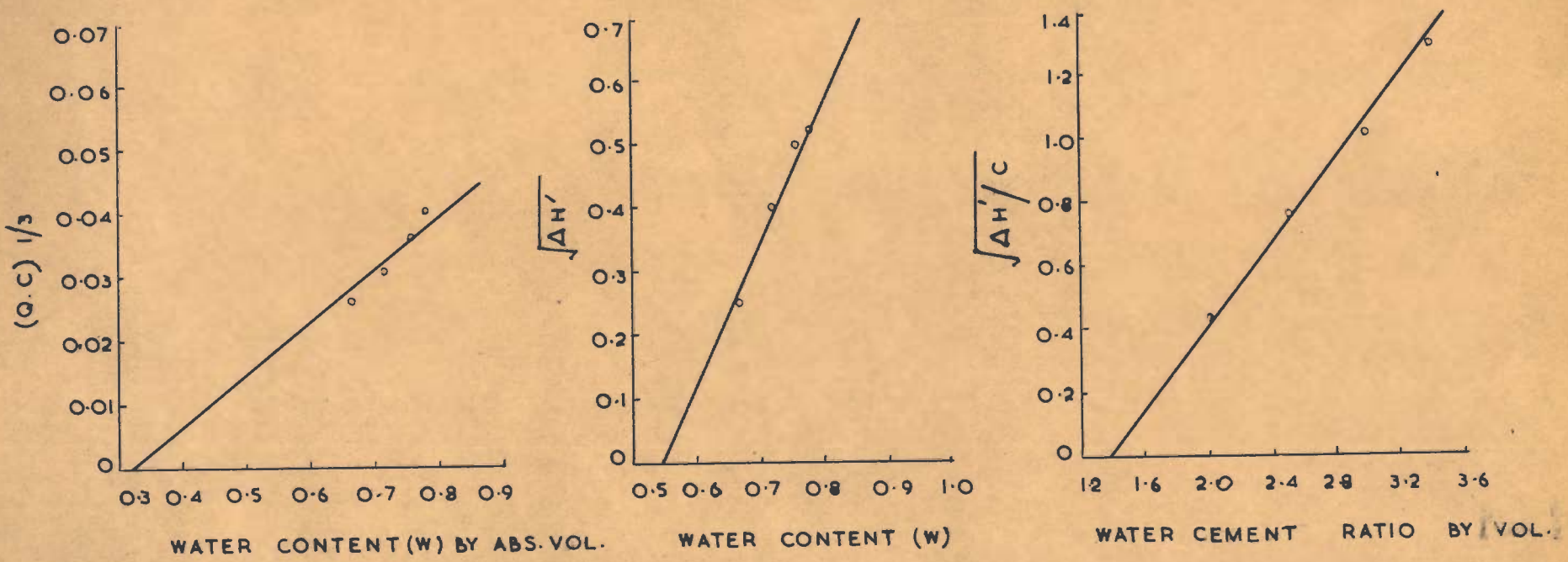

FIG. 8. RELATIONSHIPS FOR LIME PASTE

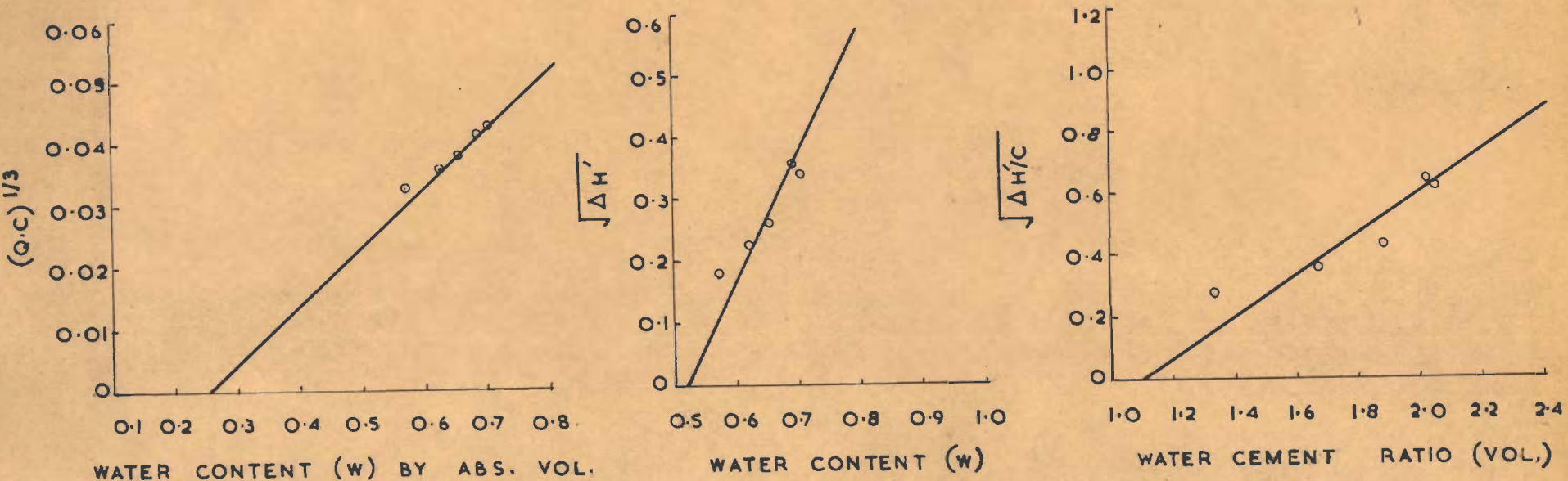

FIG. 9. TYPICAL RELATIONSHIPS FOR 1:2 LIME-SLAG PASTE

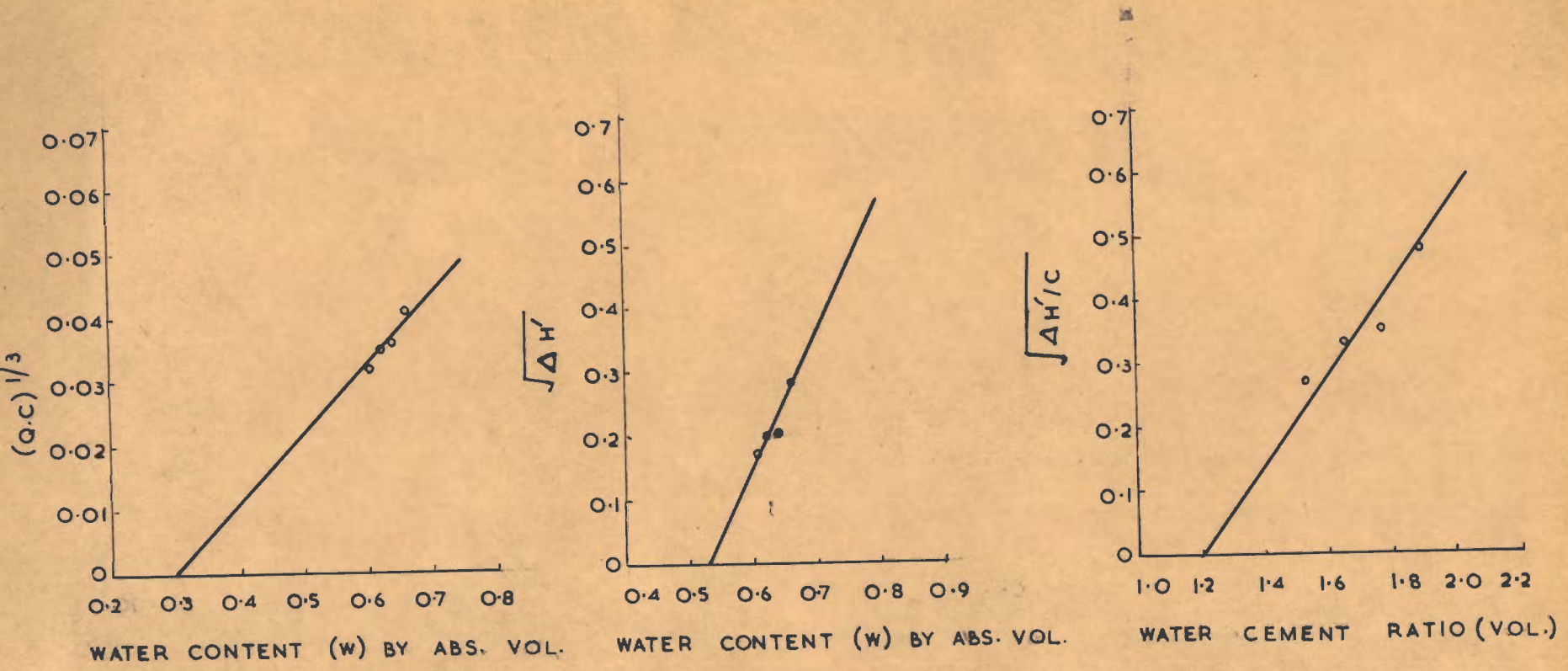

FIG. 10. TYPICAL RELATIONSHIPS FOR 1:2 LIME – FLY ASH PASTES

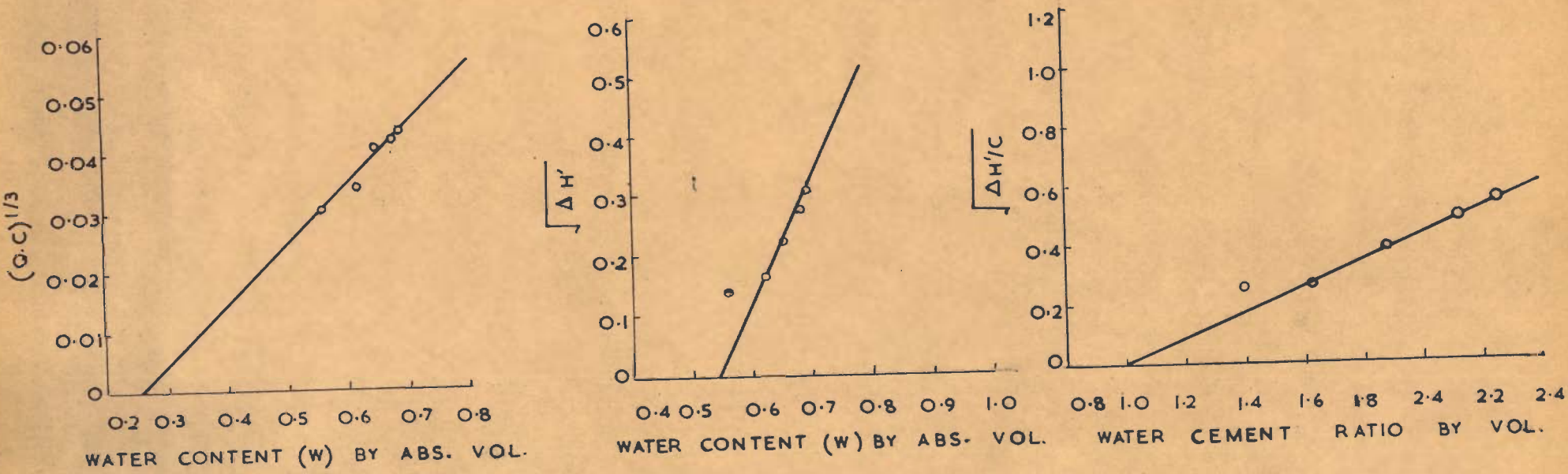

FIG. 11. TYPICAL RELATIONSHIPS FOR 1:2 LIME – SURKHI PASTE

Assuming that surkhi in 1:2 lime-surkhi was acting as an aggregate, estimate of Q'' were made from the bleeding of lime paste using the equation (10). The calculated values of Q'' were found to be far lower than the experimentally determined values showing that the assumption was not correct. An alternative assumption made was that lime is a fine powder added to a paste of surkhi in saturated lime water to reduce bleeding. By substituting the different values in equation (11)

$$Q'' = 0.243\ Q_p$$

$\because Q_p = 990.9 \times 10^{-6}$ cm/sec for a concentrated suspension of surkhi in saturated lime when W/C was 1.83 (by volume)

$$\therefore Q = 227.8 \times 10^{-6} \text{ cm/sec}$$

The actual value determined was 196×10^{-6} cm/sec. The agreement is satisfactory and supports the latter assumption.

The validity of the above assumption is also supported by the data which shows, that the values of W_i and $(W/C)_m$ for 1:2 lime-slag/fly ash/or surkhi mixes differ among themselves only slightly (table 11). The typical relationships are shown in Figs. 8 to 11. In all these mixes the particles of slag, fly ash or surkhi are always in contact with a saturated solution of lime and being coarser govern the packing arrangement. The particles of hydrated lime being finer get into the spaces between the bigger particles. The degree of flocculation of the various 1:2 mixes also could not be any different as conditions of lime saturation were always existing.

TABLE - 11

Bleeding (or Sedimentation) Characteristics of Lime-Slag/Pozzolana Pastes

Cementitious Mix	Specific Surface sq cm/cc	Density in kerosene g/cc	w/c ratio of paste vol.	Solid content of paste Abs.vol.	Bleeding rate $Q \times 10^6$	Bleeding capacity, ΔH	Porosity of sediment % of settled volume	Values of constants w_i	w	$(w/c)_m$
Hydrated Lime	9000	2.21	1.99	0.334	51.3	0.06	64.3			
			2.55	0.282	100.0	0.16	66.4	0.32	0.55	1.30
			3.12	0.242	194.4	0.20	67.7			
			3.41	0.227	277.7	0.27	68.5			
1:2 Lime-slag	6413*	2.68	1.33	0.426	78.8	0.032	55.6			
			1.67	0.374	116.6	0.048	60.7			
			1.88	0.347	158.3	0.066	62.8	0.26	0.52	1.14
			2.22	0.310	222.3	0.127	64.4			
			2.36	0.298	244.4	0.113	66.4			
1:2 Lime-fly ash	5312*	2.34	1.53	0.395	79.0	0.029	59.2			
			1.65	0.377	106.0	0.040	60.5	0.30	0.53	1.20
			1.77	0.361	117.0	0.042	62.2			
			1.89	0.346	196.0	0.077	62.4			
1:3 Lime-fly ash	4851*	2.35	1.53	0.395	116.0	0.048	58.4			
			1.65	0.377	153.0	0.067	59.4	0.28	0.49	0.88
			1.77	0.361	206.0	0.104	59.7			
			1.88	0.347	213.0	0.123	60.4			
1:2 Lime-Surkhi	6246*	2.48	1.25	0.440	62.5	0.020	53.3			
			1.62	0.380	105.5	0.026	60.8			
			1.87	0.348	196.0	0.051	63.2	0.26	0.55	1.00
			2.12	0.320	225.0	0.075	65.3			
			2.25	0.308	262.0	0.096	66.0			

* These values were computed from the specific surface of the individual constituents. The value for the hydrated lime was obtained from the sedimentation analysis as the Wagner's surface area value was low.

DISCUSSION

Bleeding (or Sedimentation) Characteristics of Portland Cement Paste

Cement is hydrophillic in nature and on coming in contact with water at ordinary temperature certain chemical reactions take place rapidly. But subsequently the paste of cement and water shows a low activity over a period of about an hour or two; the latter is termed as the 'dormant period' by Powers who found that the rate of bleeding of the paste (i.e., collection of water on the surface) or the rate of sedimentation of the solid particles during this period was constant (127). According to Powers the reaction products formed in this period do not effectively alter the surface centours of the particles or change the viscosity of the liquid and probably get accomodated in the loose layer of reaction product formed round the cement particles earlier (134).

Powers (127) likened the phenonmenon of bleeding of paste to the hydraulic flow of fluid through small capillaries and derived the equation (5) by the application of Poiseuille's law. This equation is a modification of the general equation

$$Q = \frac{0.2}{\sigma^2} \frac{g(d_c - d_f)}{\eta} \frac{W^3}{C} \qquad \ldots (10)$$

and was modified with a view to obtaining an agreement with the experimental data on cement pastes. σ in this

equation is the specific surface of solid sq cm per cc; the remaining notations are the same as in equation (5).

While the general equation assumes that all the water in the paste is taking part in the flow between the particles, some of the water, represented by W_i in Powers equation, is not taking part and is known as immobile water. Subsequently Steinour (135) carried out basic studies on the rate of sedimentation of non-flocculated suspensions of uniform spheres, suspensions of uniform-size angular particles and concentrated flocculated suspensions of powder. He found that the data of these studies supported the basic theory that led to general equation (10) with empirical proportionately constants introduced. Though Steinour too found it necessary to introduce the term W_i in the equation for a close agreement with the data, he showed that Power's concept of W_i was not wholly correct. Irrespective of different views on the causes of some of the water not taking part in flow, it is best to term it as 'immobile water'. Steinour (128) considered a properly prepared thick suspension of cement particles in water to be in a flocculent state. But he pointed out that the term flocculent state should not be construed to mean that the paste consists of a collection of more or less separate floccules. Instead, the whole body of paste constitutes a single floc, the floc structure being rather a uniform reticulum of cement particles. Nevertheless,

cement particles remain discrete during the dormant period and all sizes are forced to fall at the same rate under the pull of gravity and hence the bleeding of a paste.

In a non-flocculent state of particles, thick suspensions of emery were found by Steinour (135) to settle to the same final volume irrespective of the initial volume of suspension. This was not found true of the cement paste because of its flocculated state. The greatest possible amount of water that can be lost from a paste by bleeding under the force of gravity alone is known as bleeding capacity. The latter has been found to be a function of initial water content. The higher the initial water content, higher is the lowest possible water content of the completed sediment of the paste. Steinour (128) found that the bleeding capacity, $\Delta H'$ (expressed as settlement per unit of original height) bears an empirical relationship reported earlier in equation (6).

Differences in the Structure of Cements and other Pastes

The bleeding or sedimentation characteristics of different pastes are important because the properties of the hardened paste will be dependent on the structure of the sediment (i.e., fresh paste after bleeding). The study of the latter is difficult because experimentation in this state is rather limited.

While the total porosity of the sediment can be calculated easily, it is difficult to know the pore-size distribution. However, the mean size of pores can be estimated from hydraulic radius and is a useful guide for comparing the pore-size distribution. The hydraulic radius is a quotient of water content and wetted surface area. Estimated average width of pore reported in the last column of table 12 was calculated on the assumption that the section of a typical pore resembles a rectangular silt (131). The data for some typical pastes at the commonly employed W/C ratios shows that the mean pore size of pozzolanic cements is greater than that of Portland cement even when the total porosity after bleeding was lower.

The mean pore-size in pastes of lime and pozzolana/or slag was calculated from the equation (9) under three conditions i.e., (A) when 'W' is equal to the water content of paste before bleeding, (B) when 'W' is corrected by subtracting the immobile water (W_i), and (C) when water content of the paste is considered equal to water present in the paste after bleeding i.e., when volume of water corresponds to the porosity of the sediment of the paste. The data in table 12 show that under conditions (A) and (B) the mean pore-size of the pastes of lime and pozzolana/or slag are comparable to that of the Portland cement paste (W/C = 1.87), but under condition (C) i.e., when the bleeding is over the mean

TABLE - 12

"Pore" Sizes of Fresh Pastes of Cement and Cementitious Materials

S. No.	Paste Composition	w/c Ratios		Fineness of solids	*Water content (w)	Porosity of sediment	Hydraulic Radius**			Estimated Average width of pore***
		wt.	vol.	sq cm/cc	Absolute units	per cent	A	B	C	
							Microns			Microns
1	Portland cement(PC)	0.35	1.10	6860	0.521	51.2	1.586	0.764	1.558	Between 3 and 6
		0.40	1.25	6860	0.556	55.4	1.826	0.939	1.686	Between 3 and 6
		0.60	1.87	6860	0.653	59.4	2.740	1.610	1.807	Between 3½ and 7
2	PZC (75 PC: 25 F. Ash)	0.35	1.10	5736	0.521	49.9	1.897	1.059	1.816	Between 3½ and 7
3	PZC (75 PC: 25 Surkhi)	0.35	1.10	6317	0.521	48.9	1.721	1.226	1.616	Between 3 and 6½
4	PBF (65 PC: 35 Slag)	0.40	1.25	6860	0.556	54.2	1.959	1.067	1.910	Between 3½ and 7½
5	Hydrated lime	0.875	1.99	9000	0.666	64.3	2.220	1.152	2.138	Between 4 and 8½
6	1:2 lime-slag	0.60	1.67	6413	0.626	60.7	2.610	1.526	2.531	Between 5 and 10
7	1:2 lime-surkhi	0.65	1.62	6246	0.620	60.8	2.612	1.517	2.561	Between 5 and 10
8	1:2 lime-fly ash	0.70	1.65	5312	0.623	60.5	3.112	1.612	3.020	Between 6 and 12
9	1:3 lime-fly ash	0.70	1.65	4851	0.623	59.4	3.407	1.876	3.243	Between 6½ and 13

* $w = 1-c$ where c is cement or solid content per unit volume of the original paste.

** A is the hydraulic radius calculated from $w/c.\sigma$ considering 'w' equal to the water content of the paste before bleeding. B is the hydraulic radius calculated from the formula $w-w_i/c.\sigma$ where w_i is the immobile water. C is the hydraulic radius calculated from the formula $w/c.\sigma$ where w is the water present in the sediment after bleeding; the volume of water will correspond to the porosity in column 7

*** Values of hydraulic radius under column C were used for calculating average width of pores.

pore size is 1½ times of that of the Portland cement paste. It may also be inferred that comparisons of the mean pore size are realistic only under condition (C).

It would be desirable that the mean size of pores in the fresh pastes containing pozzolanas etc. after bleeding is very near or even smaller than that of Portland cement because pore size is probably more important than the total porosity. Since at a given water content pore size decreases if the specific surface area of the powder increases, grinding of pozzolanas to a slightly greater fineness suggests itself. But if, on the other hand, a pozzolana is ground very much finer than the Portland cement, the final porosity of the sediment may not be any different from that of the Portland cement paste because the magnitude of flocculation forces may change considerably and thus the advantage acruing from greater reduction in porosity of a pozzolanic cement paste may be lost. Broadly speaking, the fineness of the pozzolanic cement should be equal to that of the Portland cement in terms of sq cm per cc instead of sq cm per g because of widely differing densities of the two cements.

Flocculent State in Pastes

A paste is prepared by shaking cement with water in a mixer and as a result dispersion takes place. The term dispersion should not be taken to mean exactly

the same as in colloids, though some do believe in colloidization or self-induced dispersion of cement particles (115). According to Powers (114) a cement suspension is dispersed when the interparticle attraction is so weak that it has no appreciable effect on the behaviour and physical properties of a paste. Initially, during dispersion, the forces between cement particles and water are much greater than those between cement particles themselves and thus solution is favoured. But simultaneously gelatinous coatings are formed on cement particles and gradually the solution gets saturated with electrolytes. Consequently, after this initial period of few (2-5) minutes interparticle forces become greater and the suspension goes into a flocculent state.

Powers (130) considers the flocculent state to be explicable in terms of classical theory viz.,

> " the gel-coated grains carry a solvated layer and they have a positive zeta potential. The combined effect of solvated layer and electrostatic charge is such as to prevent actual contact between adjacent grains. But the grains are concentrated enough to experience interparticle attraction, at least over part of their boundaries. The effects of repulsion and attraction balance at a certain distance of separation where the potential energy of the particles is at a minimum. The cement grains tend to remain in 'potential troughs' which are so located as to require spaces between particles ".

From the foregoing discussion it can be inferred that the flocculent state of the Portland cement paste may change or get destroyed if part of the cement

particles in a paste are replaced by those of a pozzolana or slag. Strictly speaking, other things being equal, it will depend how such replacements affect the balance of attractive and repulsive forces.

Van der Waals forces will decrease when a reactive material like cement is replaced and the decrease will depend on the relative surface activity of the replacing particles. Amongst various powders tried only slag glass could be considered to have appreciable activity. In all other powders the decrease in attractive forces therefore would be considerable when part of Portland cement is replaced by such powders. When mixing with water is done in a mixer, the suspension will get dispersed to a greater degree because of reduced inter-particle attraction. This is an initial disadvantage to start with. No wonder workability of a cement paste is reduced many a times by replacing part of it with a pozzolana, particularly so when the water requirements increase.

The coulombic forces which depend on the net electric charge of the two particles may be attractive or repulsive. In Portland cement pastes only repulsive forces are operative due to the presence of counterions held close to each particle by electrostatic attraction. In pozzolanic and slag cement pastes the repulsive forces will still be present but if the charge on the replacing

powder is opposite, some attractive forces can also come into play and decrease the magnitude of repulsive forces. But in view of greater pore diameter in pozzolanic cement paste (table 12) and the fact that attractive forces decrease more rapidly with distance of separation, repulsive forces appear to have increased in magnitude appreciably particularly in pastes of pozzolanic cements.

The above discussion on the attractive and repulsive forces coming into play in pozzolanic and slag cement pastes shows that compared to Portland cement pastes the net interparticle attraction in the former type of pastes is likely to be weaker. In some cases net repulsive forces may be operative, i.e., conditions for flocculent state may be non-existent. This is evident from the bleeding characteristics of the mass concrete at a W/C ratio of 0.8 (table 13) reported by Mather (136) on replacing the Portland cement with a variety of replacement materials. His data clearly show that only the use of very fine replacement materials reduces the bleeding. Otherwise replacements increase the bleeding i.e., degree of flocculation is very much reduced. However, it may be pointed out that the presence of alkalies and salts etc. in the replacing materials may complicate the situation. This has been discussed in the next chapter.

T A B L E - 13

Bleeding Characteristics of the Mass Concrete Having Various Replacements of the Portland Cement (Type II)

w/c Ratio = 0.8
(After Mather)

Replacement material	Specific surface (Blaine) sq cm/g	Per cent of cement replaced	Bleeding of concrete per cent
None	3550	0	9.8
Slag I, RC-198	3605	30	15.7
Slag I, RC-198	3605	50	12.8
Slag I, RC-198	3605	70	17.7
Slag II, RC-216(B)	3695	50	13.3
Natural Cement I, RC-214	11260	20	5.3
Natural Cement I, RC-214	11260	35	2.3
Natural Cement II, RC-215	6420	35	11.2
Fly ash I, AD-3	3565	30	15.7
Fly ash I, AD-3	3565	45	9.9
Fly ash I, AD-3	3565	60	12.6
Fly ash II, AD-7	2940	45	15.2
Fly ash III, AD-8	2945	45	13.6
Fly ash IV, AD-9	4205	45	11.9
Pumicite I, AD-6	4410	25	6.9
Tuff, AD-II	10460	35	2.9
Obsidian, AD-12	3415	35	12.0
Calcined Shale I, AD-5	13685	20	5.8
Calcined Diatomite, AD-14	10450	30	5.3
Uncalcined Diatomite, AD-15	12125	8	6.0

CHAPTER 2

EFFECT OF ELECTROLYTES ON SEDIMENTATION (OR BLEEDING) CHARACTERISTICS OF PASTES

Introduction

Certain chemical additions are made to affect a variety of properties of cement paste and concrete; the more important ones being the bleeding, workability, setting times and rate of hardening etc. While the field of chemical additions and admixtures is very wide in scope (63), the present study is confined only to the effects of electrolytes which get introduced in the system because of the use of pozzolanic additions or replacements to cements. Sometimes electrolytes are added intentionally to enhance the grindability and activity of cementitious powders e.g., in the wet grinding of slags (97). A good deal has been published on the possible reactions which take place on the addition of calcium chloride, sodium carbonate, sodium sulphate and other inorganic salts. While the overall effects of such additions on the properties of cement pastes are well known (13,14,127,128) the mechanism of the action is not clearly understood. For example, the mode of action of gypsum which has been used as a retarder in cement since long is still not clearly understood (137). The main reason is that reactions of cement with water are already complex and introduction of chemical additions introduces further complications.

Earlier it was shown that the sedimentation rate and volume of a fresh paste, which in turn, affects the pore size distribution and porosity of the sediment, is also influenced by the surface forces and electrostatic charge on solid particles. In context of the present study of the properties of fresh paste and its structure, the effect of physical interaction of chemical additions was considered an aspect which has not been studied in the past to the extent as the resultant chemical reactions. The former is equally important. The present study was therefore confined to this aspect only.

The electrostatic charge on the particles of a sol depends to a great extent on electrolyte additions. Silica hydrosols are known to maintain their negative charge in fairly acidic, alkaline or neutral solutions. The pozzolanas are generally either siliceous or alumino-siliceous. Those used in this investigation i.e., ground quartz, surkhi and fly ash etc. belong to this category and carry a negative charge. Cement particles on the other hand, are known to be positively charged (138). But working with cement pastes is not likely to be fruitful as a good amount of gypsum is always present in the system and complicates the results. On this account, granulated slag which is also believed to carry a positive charge was selected for this study. The electrolytes used were saturated solutions of calcium hydroxide, calcium sulphate and a solution saturated with both of these;

sodium hydroxide and sodium sulphate; calcium chloride and aluminium chloride etc.

MATERIALS

The materials used were :

(i) granulated slag of specific surface of 3948 ± 50 sq cm per g (Blaine)

(ii) ground surkhi of specific surface of 3200 ± 50 sq cm per g (Blaine)

(iii) $CaCl_2.2H_2O$, $AlCl_3$, NaOH, Na_2SO_4, CaO and $CaSO_4.\frac{1}{2}H_2O$ of A.R. quality.

EXPERIMENTAL

The viscosity of the solution was determined by the Ostwald viscometer (139). The viscosity was measured at a temperature of 25 ± 2°C.

The experimental procedures for other determinations was the same as in the Chapter 1.

RESULTS

The data on bleeding rate, bleeding capacity ($\Delta H'$) and total bleeding time determined experimentally for pastes (i.e., concentrated suspension) of finely ground slag in different electrolytes are reported in table 14. A W/S ratio of 0.40 by weight or 1.26 by volume was selected because it is most commonly employed in the study of cement pastes. The sedimentation volume

T A B L E - 14

Effect of Additions of Electrolytes on Bleeding (or Sedimentation) Characteristics of Slag Pastes

(Slag of Fineness of about 4000 sqcm/g)

Concentration of solution	Solution content of paste Abs.Vol.	Bleeding rate $Q \times 10^6$	Bleeding capacity $\Delta H'$	Bleeding time Mts	Porosity of sediment per cent settled volume
1	2	3	4	5	6
		a. Paste made with distilled water			
Nil	0.539	148.0	0.030	38	52.4
		Pastes made with $AlCl_3$ solution			
0.0156 M	0.539	177.0	0.075	92	50.2
0.0315 M	0.539	190.0	0.0746	95	50.2
0.0625 M	0.539	161.0	0.044	50	51.4
0.125 M	0.539	54.0	0.021	70	52.9
		b. Pastes made with $CaCl_2$ solution			
0.0312 M	0.539	155.0	0.030	38	52.5
0.0625 M	0.539	180.0	0.043	50	51.9
0.1250 M	0.539	195.0	0.080	90	49.9
0.2500 M	0.539	192.0	0.068	78	50.5

Table 14 (Cont'd.)

1	2	3	4	5	6
	c. Pastes made with saturated calcium hydroxide and sulphate				
Sat. $Ca(OH)_2$	0.539	155.5	0.043	60	51.9
Sat. $CaSO_4$	0.539	148.1	0.033	40	52.3
Sat. $Ca(OH)_2$ and Sat. $CaSO_4$ solution	0.539	166.6	0.032	38	52.4
	d. Pastes made with Sodium Hydroxide				
0.0156 M	0.539	160.0	0.039	50	52.0
0.0312 M	0.539	127.2	0.034	52	52.3
0.0625 M	0.539	187.5	0.048	60	51.6
0.1250 M	0.539	133.3	0.038	47	52.1
	e. Pastes made with Sodium Sulphate				
0.0156 M	0.539	161.0	0.030	35	52.2
0.0312 M	0.539	154.0	0.032	40	52.4
0.0625 M	0.539	121.8	0.017	28	53.1
0.1250 M	0.539	127.0	0.026	40	52.7
0.2500 M	0.539	100.2	0.023	50	52.6
0.4000 M	0.539	105.0	0.028	45	52.6

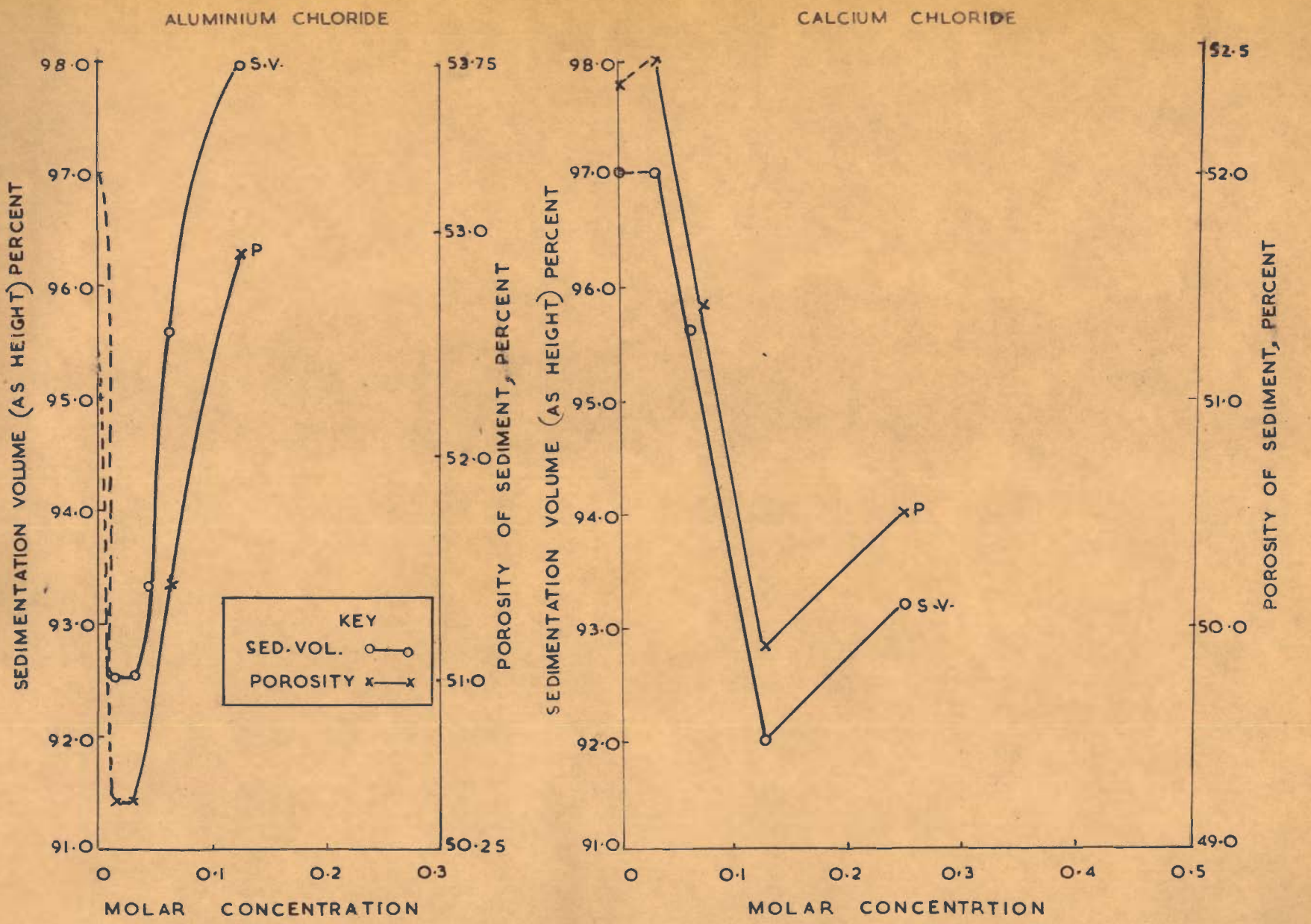

FIG.12. EFFECT OF CONCENTRATION OF ELECTROLYTES ON SEDIMENTATION VOLUME AND POROSITY OF SLAG PASTES.

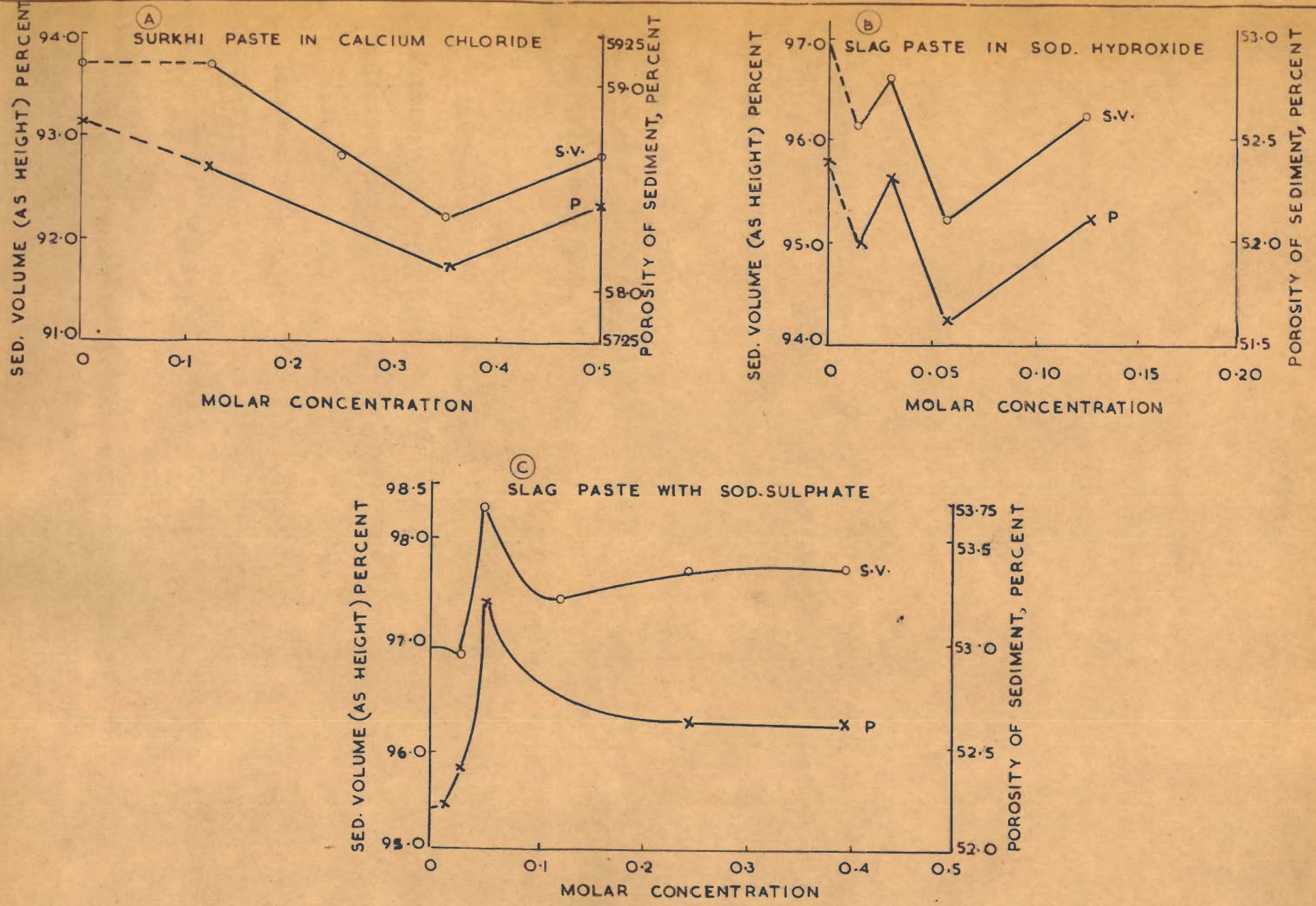

FIG.13. EFFECT OF CONCENTRATION OF ELECTROLYTES ON SEDIMENTATION VOLUME AND POROSITY OF SURKHI AND SLAG PASTES.

(in terms of sediment height) was computed from the values of bleeding capacity and Figs. 12 and 13 are plots of sedimentation volume and porosity versus the concentration of electrolytes. The sediment height would be $(1 - \Delta H') \times 100$ per cent.

The concentrated suspension of slag in water had a sedimentation volume of 97.0 and porosity 52.4 per cent respectively. This point has been plotted in Figs. 12 and 13 as the starting point but strictly speaking this is not correct because some ions do exist in the solution, and therefore this point is joined with the next point by a dotted line. The main idea of showing the dotted part of the curve is to show the degree of flocculation with different chemical additions in relation to when distilled water was used.

All the curves show sharp points corresponding to minimum and maximum sedimentation volumes. For calcium chloride and aluminium chloride solutions the sedimentation volume was minimum at concentrations of 125.0 millimoles and 15.62 millimoles per litre respectively. The maximum occured at a concentration of 31.25 millimoles per litre for calcium chloride and at 125 millimoles per litre for aluminium chloride solutions (Fig. 12). With sodium sulphate the sedimentation volume was highest; the minimum and maximum values of concentration were 31.25 millimoles and 62.5 millimoles per litre respectively. The second

minimum occurs at 125 millimoles and the sedimentation volume thereafter increases only slightly (Fig. 13C). With sodium hydroxide the first decrease occurs at 15.62 millimoles and for the second at 62.5 millimoles per litre. The sedimentation volume is lowest at the latter concentration. The maximum occurs at 31.25 millimoles per litre. Though the curve shows an increase after the second minimum at a concentration of 125 millimoles, the sedimentation volume was lower than the maximum value (Fig. 13B). The effect of addition of calcium chloride solutions on the sedimentation characteristics of the surkhi paste are shown in Fig. 13A; the data is reported in table 15.

The plots of total porosity of sediment versus concentration show a similar pattern i.e., when sedimentation volume is maximum the porosity is also maximum (Figs. 12 and 13). However, porosity was not sensitive to small changes in sedimentation volume. The curves of bleeding times against concentrations were not plotted but would be similar in nature.

Because of their low solubility, it was not possible to study the effects of calcium hydroxide and sulphate solutions on sedimentation volume in the manner described above. But since in pastes of cement or cementitious materials, their concentrations are mostly near saturation, the effects of saturated solution of either of the electrolytes or combination of the two was studied and the results are reported in table 14 and are self-

TABLE - 15

Effect of Addition of Calcium Chloride on Sedimentation Characteristics of 'Surkhi' Paste

Concentration of solution Molar	Volume of solution content of paste Abs.vol.	Bleeding rate $Q \times 10^{6}$	Bleeding capacity $\Delta H'$	Porosity of sediment % settled volume	Bleeding time Mts
		Pastes made with distilled water			
nil	0.539	83.0	0.063	58.8	166
		Pastes made with calcium chloride solution			
0.1250 M	0.539	83.0	0.063	58.8	162
0.250 M	0.539	69.0	0.072	58.4	185
0.350 M	0.539	82.0	0.078	58.1	200
0.500 M	0.539	74.0	0.072	58.4	168

explanatory.

Before discussing the results of sedimentation volume, two points deserve mention. These are the effects of viscosity of the solution and the chemical reactions possible as a result of action of solution on slag grains. Viscosity influences the sedimentation rate but when concentration of electrolyte is low, its influence will be negligible because the viscosity of the dilute solutions will not be different from that of water (table 16). Changes in sedimentation volume at higher concentrations however, could also result partly from the changes in viscosity of the suspension medium. Similarly, the effects of solution and precipitation reactions may begin to influence the sedimentation characteristics appreciably by formation of new reaction products only at higher concentrations. On this account only effects of very dilute solutions are considered important.

DISCUSSION

Electrostatic Charge, Flocculation and Sedimentation Volume

Starting with an apparently stable colloid and adding an increasing amount of a solution of an electrolyte, the limiting concentration at which the system becomes unstable and flocculates can be determined precisely under carefully controlled conditions. The limiting concentration is called the flocculation value.

T A B L E - 16

Viscosity of the Aqueous Solutions of Sodium Sulphate (at 25 ± 1°C)

Molar Concentration	Viscosity in Centipoises
0	0.8937
0.0156	0.894
0.0312	0.896
0.0625	0.897
0.125	0.911
0.250	0.961

The addition of electrolytes to fresh pastes i.e., concentrated suspensions of particles may also produce similar effects; but the determination of the so called 'flocculation value' cannot be precised for obvious reasons. However, the sedimentation volume itself can form a good basis to know if a system flocculates or deflocculates on addition of electrolyte because the particles in a deflocculated system settle down next to each other, each seeking the lowest possible point. The latter results in the formation of a compact layer at the bottom and the volume of the layer, known as sedimentation volume, will be less compared to when flocculation occurs during sedimentation.

The particles of a silica hydrosol and clay suspensions are negatively charged. While silica hydrosols always maintain their negative charge in acid as well as in neutral or alkaline solutions, reversal of charge for negatively charged silica particles, kaolin and serpentine etc. has been reported under certain pH conditions (140). Kandilarov's results of sedimentation rate and volume of polydisperse kaolin and quartz suspensions in solutions of sodium chloride and sulphate, calcium and aluminium chlorides are of particular interest because pozzolanas generally consist of either siliceous or alumino-siliceous powders. Since in the present study the pozzolanas (surkhi and fly ash) also belong to this category, the effect of addition of

electrolytes was not studied as the trends of results are not likely to be different from those reported by Kandilarov. This leaves the choice to the study of positively charged particles. The cement particles are positively charged, but the latter are difficult to study because of ensuing chemical reactions and large amount of heat evolved. Slag which is similar in nature, but possess a lower activity was therefore preferred. Also the latter is believed to carry a positive charge.

The granulated slag of specific surface of about 4,000 sq cm per g was used. Its extraction with distilled water showed that lime equivalent to 0.094 per cent was liberated immediately and that hardly any more lime was released on continued leaching with water due to the formations on the surfaces of the slag grains which stopped further action of water. However, when the slag grains were placed in continuous contact with water, the concentration of Ca ions first increased and then decreased. The decrease in concentration is due to the adsorption of calcium ions by the acid hydrate surfaces formed on account of dissolution effect. The solution contained mostly calcium, sulphate and hydroxyl ions (141). In this type of dynamic equilibrium, it is the concentration of the depositing species i.e., calcium ions that play an important role. Equilibrium involves both the concentration of calcium ions in the solution and in the surface and the potential.

Explanation of Effects of Electrolyte Additions

It is difficult to explain the curves in Figs. 12 and 13 on the basis of the chemical action of the electrolytes because the plots of sedimentation volume versus increasing concentration of an electrolyte do not follow a regular pattern. But the curves can be explained on the basis of differences in flocculation and structure of the double layer. However, it is pointed out that in these suspensions, unlike those of colloids, electrical effects are only of secondary importance; gravitational forces being primarily responsible for the phenomenon of sedimentation.

Effect of Aluminium and Calcium Chloride Solutions

Adsorption of trivalent aluminium ions should be greater than that of divalent calcium ions and the latter greater than monovalent sodium ions. At low concentrations when not many counter ions are present, repulsive forces will be stronger and particles will settle till their mutual repulsion stops further settling. The results show that for slag only 0.0156 M aluminium chloride was required for deflocculation (in relative terms) as against 0.125 M of calcium chloride. The reversal of phase seems to take place then and the particles now carry a negative charge. With an increase of concentration of aluminium chloride to 0.0625 M, flocculation seems to take place with a rise in the

concentration of counter ions i.e., aluminium ions now. However, it is not clear whether the reversal is due to the ions themselves or the products of hydration.

Surkhi particles are negatively charged and because of the presence of free alkalies in them (table 3) will fix sodium and potassium ions. The effect is not as specific in this case as in slag. On the addition of calcium chloride, calcium ions go on replacing the monovalent ions till the particle surface is fully covered. Effect of further additions of calcium chloride will be similar to that considered above (Fig. 13A). Deflocculation therefore ~~to~~ takes place at a higher concentration i.e., 0.35 M calcium chloride solution.

Effect of Calcium Hydroxide and Sulphate

In a paste of slag in water calcium ions are the stabilizing ions. Counter ions are important from the point of view of flocculation. The counter ions already present in water are sulphate and hydroxyl ions; sulphate were found to be predominant (141). Therefore with the addition of saturated solution of calcium hydroxide, the concentration of the depositing species i.e., Ca ions is important in this type of dynamic equilibrium. The latter involves both the concentration of calcium ions in solution and on the surface and the potential. The analysis showed that the concentration of calcium ions in solution had actually decreased showing

thereby that these ions had been adsorbed with a resultant increase in potential. Increasing this potential means increasing zeta potential of the particle. It may therefore be inferred that conditions for flocculation are not favoured. This is shown actually by a decrease in sedimentation volume on addition of calcium hydroxide (table 14). Addition of a saturated solution of calcium sulphate also results in more Ca ions being adsorbed but counter ions being divalent, steady state conditions are brought about quickly because of the greater shielding effect of the counter ions. Addtion of divalent counter ions therefore may increase the flocculation slightly as is evident from a slight increase in sedimentation volume (table 14).

Effect of Sodium Hydroxide Solution

The first decrease in sedimentation volume on the addition of a dilute solution of sodium hydroxide (Fig. 13B) may be explained on the basis that the calcium ions already present repel sodium ions and the shielding effect of counterions is not strong. However, with further additions double layer is built up because sufficient counterions are now present to flocculate it. This takes place at a concentration of 31.25 millimoles per litre. Subsequent deflocculation takes place in a manner explained earlier for Calcium hydroxide.

Effect of Sodium Sulphate Solution

The most important change takes place at a concentration of 62.5 mm per litre when sedimentation volume is greater than with any other electrolyte. (Fig. 13C). The explanation is that the divalent sulphate counterions are more tightly held and reduce attraction for the monovalent sodium ions effectively. The thickness of double layer is therefore decreased and zeta potential falls off more rapidly. These conditions lead to greater flocculation. Only further increase in concentration of sodium sulphate solution brings about a reversal in charge because potential determining ions (sodiums) do not have access across the double layer and the charge on sulphate ions is double that of sodium ions. But this effect is not much pronounced because sodium sulphate at higher concentrations does not dissociate much and remains as ionic pair.

The above discussion shows that the differences in sedimentation volume or porosity arise from differences in the degree of flocculation, the latter being explicable in terms of the Helmholtz double layer theory. In short, the effects of small additions of electrolytes on the properties of fresh pastes are due to their physical interaction, the electrostatic charge on the particles playing an important role.

Electrolyte or chemical additions are made to improve upon workability, accelerate or retard setting and enhance strengths. Recently Nagai (64) has reported success in accelerating development of strength of a high-slag-content lime cement by chemical additions. This is illustrated by some of his data in table 17. The improvement in strength with the addition of 2-3 per cent sodium sulphate is remarkable. Nagai has given no explanation but it is obvious that the changes in flow and setting times (table 17) could not have taken place without a change in the structure of fresh paste as brought out in the above discussion. And it follows that the changes in strengths must also be partly due to changes in the structure of fresh paste. How the additions affect the degree of flocculation and thereby flow properties is discussed in the next chapter.

TABLE - 17

Setting Time, Flow and Strengths of 1:2 Cement : Sand Plastic Mortar
(Composition of Cement - Slag : Fly ash : Lime as 60:30:10)
(After S. Nagai)

Salt	Mixing medium	Setting Time			Flow Test		Compressive Strength lb/in^2		
		Amount percent	Initial hr-min.	Final hr. min.	Amount percent	Flow percent	7 days in air	28 days in water	28 days in air
2% Na_2SiF_6	Fresh water	35.0	4-05	7-15	65	185	114	1053	1351
3% $Na_2O.3SiO_2$	Solution	39.5	2-13	6-10	65	154	967	1750	1337
2% Na_2SO_4	Fresh water	35.0	8-15	11-35	64	199	1607	2233	2275
2% $Na_2SO_4.10H_2O$	Fresh water	32.5	9-25	11-45	63	206	1067	2062	1792
3% Na_2SO_4	Solution	36.0	7-50	10-45	65	182	1351	2105	2645

CHAPTER 3

RHEOLOGY OF FRESH PASTES

Introduction

Earlier, the information on the early structure of cement and other pastes was obtained by studying their sedimentation characteristics. A study of the flow properties should, in fact, provide more direct information on the structure i.e., the initial framework resulting from the interaction of particles of different nature present in this thermodynamically unstable two phase system. An understanding of the effects of physico-chemical processes taking place in the paste on the flow properties may ultimately lead to improvement in the workability and placement of concrete. Such a study may also throw some light on the mechanism of setting, a phenomenon which puts an end to the flow properties of fresh pastes.

A study of rheological behaviour of cement pastes, however, presents difficulties as large particle sizes of cements do not permit the use of small clearances between the coaxial cylinders in rotational viscometers. Errors are introduced due to sedimentation at high water/cement ratios. Further, hydration of cement starts with the addition of water and the rheological behaviour of the resultant paste is thus time dependent. Nevertheless, the recent work of Dellyes (142), Papadakis (143),

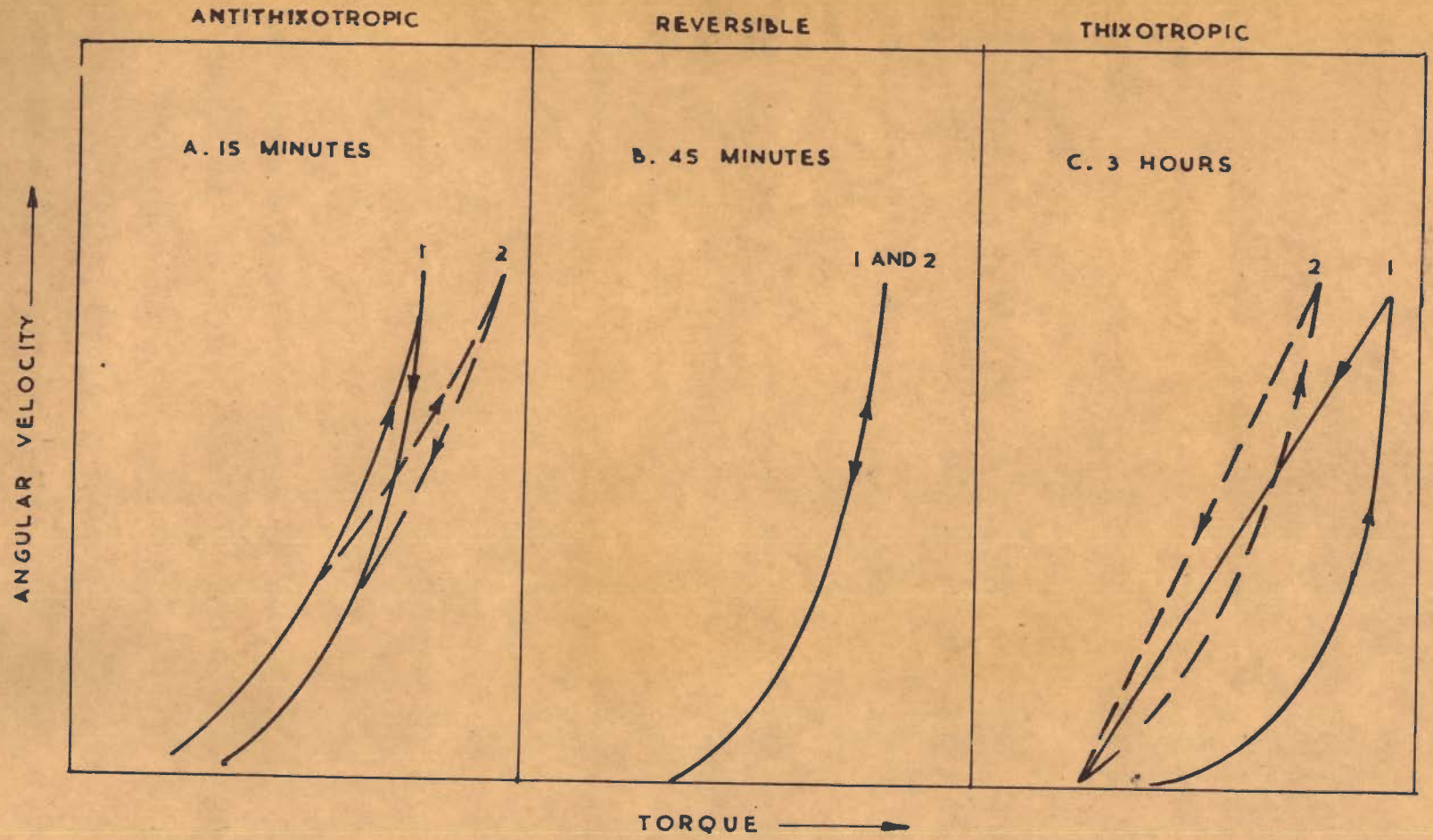

FIG.14. THREE TYPES OF FLOW BEHAVIOR FOR FRESH PORTLAND CEMENT PASTES.

(AFTER ISH — SHALOM AND GREENBERG)

NOTE :—

1. THE TIMES GIVEN ARE FOR THE PERIODS OF HYDRATION.
2. THE NUMBERS ON THE CURVES SHOW THE ORDER IN WHICH THE CURVES WERE MADE.

Tattersall (144,145) and Shalom and Greenberg (146) has contributed to the knowledge a good deal, particularly in quantitative terms and paved a way for a better understanding of this subject.

Shalom and Greenberg's work is latest and comprehensive. They have studied the effects of variables such as fineness, chemical and mineralogical composition of Portland cements, concentration, temperature of hydration and mixing conditions etc. on the flow properties of the pastes. Their pastes showed three types of rheological behaviour, i.e., (i) antithioxotropic, (ii) reversible and (iii) thixotropic (Fig. 14). Antithixotropic behaviour was characterized by a flow curve (rpm-torque) in which the descending portion (decreasing rpm) is to the right of the up-curve (increasing rpm) and was noticeable at 15 to 20 minutes after vigorous mixing. The reversible rpm-torque curves were obtained after 45 minutes of hydration. The predominant kind of flow was thixotropic and it was considered characteristic of the hydrogel formed by hydration of calcium silicates in cement.

Shalom and Greenberg believe the gels to be constructed of particles, which are plates or fibres, in contact only at certain points. This arrangement of flocculated particles leads to a loose three dimensional network of solids in a liquid medium. Thixotropy, an isothermal reversible sol-gel transformation, is attributed to the attracting and repelling forces between

particles. However, these authors point out that the application of the word thixotropic to cement paste is probably not entirely consistent with the definition because the transformation is not completely reversible. The irreversibility is probably due to chemical bonds or crystalline intergrowths of the various species which, when once broken, will not reform.

While it may be reasonable to assume that the rheology of the pastes wherein part of cement has been replaced by a pozzolana or slag will also be governed by the nature and amount of hydrogel formed on hydration, the present study is limited to seek information on two specific points arising from the work reported in chapters 1 and 2. Firstly, to know how the introduction of particles of different nature in the Portland cement paste will influence the intial framework resulting from their interaction and to what extent the latter influences flow properties. Secondly, since the additions of electrolytes had been found to change the degree of flocculation and structure of double layer in the slag paste with a variation in the concentration of the electrolyte, the effect of the latter on the flow properties requires to be known.

MATERIALS

The materials used in the present study were

(i) Portland cement (Surajpur) of fineness 3200 $\pm$ 50

(ii) two Portland blastfurnace cements e.g., PBF (65 clinker : 35 slag (g) and (35 clinker : 65 slag(g). The fineness was the same as above.

(iii) pozzolanic cement, PZC (75 clinker : 25 fly ash) having a fineness of 3194 sq cm per g (Blaine)

(iv) granulated slag (TISCO) of fineness of that of Portland cement i.e., 3200 ± 50 sq cm per g (Blaine)

(v) granulated slag (TISCO) of fineness 3948 ± 50 sq cm per g.

EXPERIMENTAL

Determination of Rheological Properties

The rotational viscometers of the type developed by Green (147) have been used for the determination of flow characteristics of cement pastes. The Mac Michael viscometer (148) was used in the present investigation. In this viscometer a spindle-plunger assembly is supported by a wire and dips into the sample which is contained in a rotable cup (Fig. 15). When the cup is rotated, the spindle-plunger assembly is subjected, through the sample, to rotational forces which are related to the viscous properties of the sample. The assembly continues to rotate until the torsional reaction of the wire suspension just balances the torque exerted by the cup through the sample. Thus a dynamic equilibrium results and the force is measured in empirical Mac Michael units which are based on the degree of rotation of the spindle. For obtaining the values in absolute units of viscosity, calibration was

Fig. 15. Showing Mac Michael rotational viscometer; the spindle-plunger assembly is suspended by a wire and dips into the rotatable cup.

done with a standard sample of mineral oil (Henry A. Gardner Laboratory, U.S.A.) having a viscosity of 8.5 poises at 25°C and using certified suspension wires. The measurements were carried out at a temperature of 25 ± 2°C.

The Mac Michael viscometer can be adapted to measure the viscous properties of materials over a wide range from water to heavy glues through suitable selection of suspension wires, cup speed, size of spindle, depth of sample and temperature etc. But on the whole, high shearing rates are not possible with this viscometer. The rheological measurements were obtained by the multiple point method. The speed of rotation of cup was varied from 5 to 40 revolutions per minute. The internal diameters of the rotational cup and the bob were 3.00 cm and 2.25 cm respectively. The bob was immersed to a depth of 4.5 cm in the sample under test and to reduce the end effects at the bottom of the bob, a recess was provided. The suspension wires used were mostly nos. 24 and 26; no. 30 was also used in a couple of measurements.

The Reiner and Riwlin equation (149) of plastic flow in a rotational viscometer is

$$\Omega = \mu \frac{T}{4\pi h}\left(\frac{1}{R_b^2} - \frac{1}{R_c^2}\right) - \mu_f \ln \frac{R_c}{R_b} \qquad \ldots (1)$$

where Ω is the angular velocity (ω) when torque (T) becomes sufficiently large so that all the material between the

walls of the cup and bob is in laminar flow. R_b and R_c are the radii of the bob and cup respectively, h the depth of immersion of the bob and f is the yield value. μ is mobility which is inverse of coefficient of viscosity (η).

The above equation is for the linear part of the curve only. However, when the curve is extrapolated to the torque axis, it cuts it at the point when angular velocity is zero and $T = T_2$. Then, according to Green (149)

$$\frac{T_2}{4\pi h}\left(\frac{1}{R_b^2} - \frac{1}{R_c^2}\right) = f \ln \frac{R_c}{R_b} \qquad \ldots (2)$$

Letting

$$\frac{\frac{1}{R_b^2} - \frac{1}{R_c^2}}{4\pi h} = S \qquad \ldots (3)$$

where S is the instrumental constant

and

$$\frac{S}{\ln R_c/R_b} = C \qquad \ldots (4)$$

where C is another instrumental constant,

the equation (2) therefore gives

$$f = CT_2 \qquad \ldots (5)$$

where f = yield value.

Substituting equations (3), (4) and (5) in equation (1) and writing U for $1/\mu$ gives

$$U = \frac{(T - T_2)S}{\Omega} \qquad \ldots (6)$$

where U = plastic viscosity

Now, $T = K\theta$ $\qquad \ldots (7)$

According to equation (7), the wire contant K when

multiplied by the number of degrees (Θ) through which the bob (and the wire) has been deflected gives the amount of torque (T). K is obtained by calibrating the wire with a Newtonian liquid of known viscosity. The equation for K is

$$K = \frac{\eta.\omega}{S} \qquad \ldots (8)$$

where η is viscosity of liquid,
Θ is the deflection,
S is a constant.

U and f now can be obtained from equations (6) and (7) respectively as $T = K\Theta$ and values of constants S and C can be obtained from the equations (3) and (4) respectively.

The method of making flow curve of a sample is well known and described in text books (150). The broad outline is to start at the lowest practical rpm of the cup and increasing rpm by the same number after a fixed time interval which should be as short as possible. The deflection (i.e., M) corresponding to each of the values of rpm is recorded. When a sufficient number of points have been taken to arrive at the desired top rpm, the down curve is commenced immediately. Descent on this curve is made by using the same intervals in rpm and in timing that were employed previously in ascending. This completes the cycle. Generally two cycles were performed.

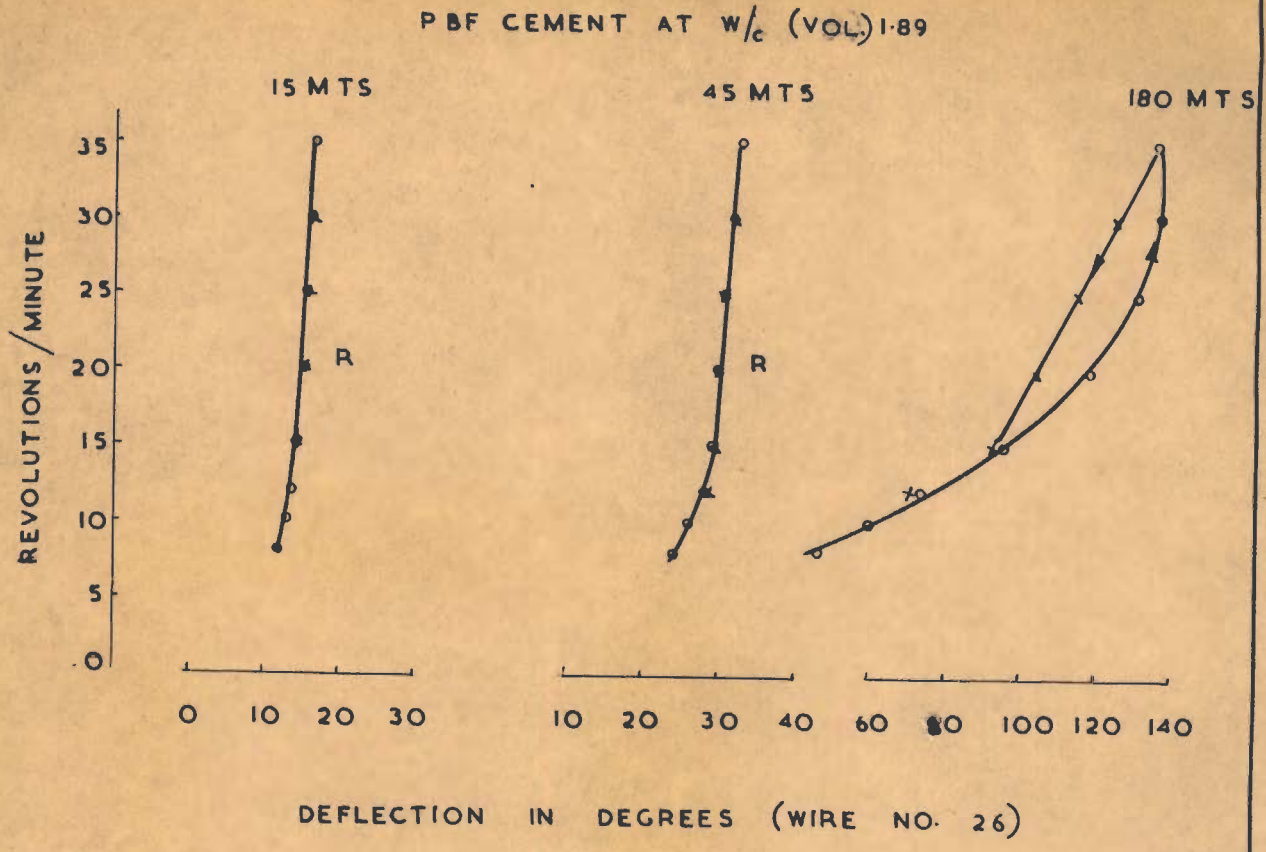

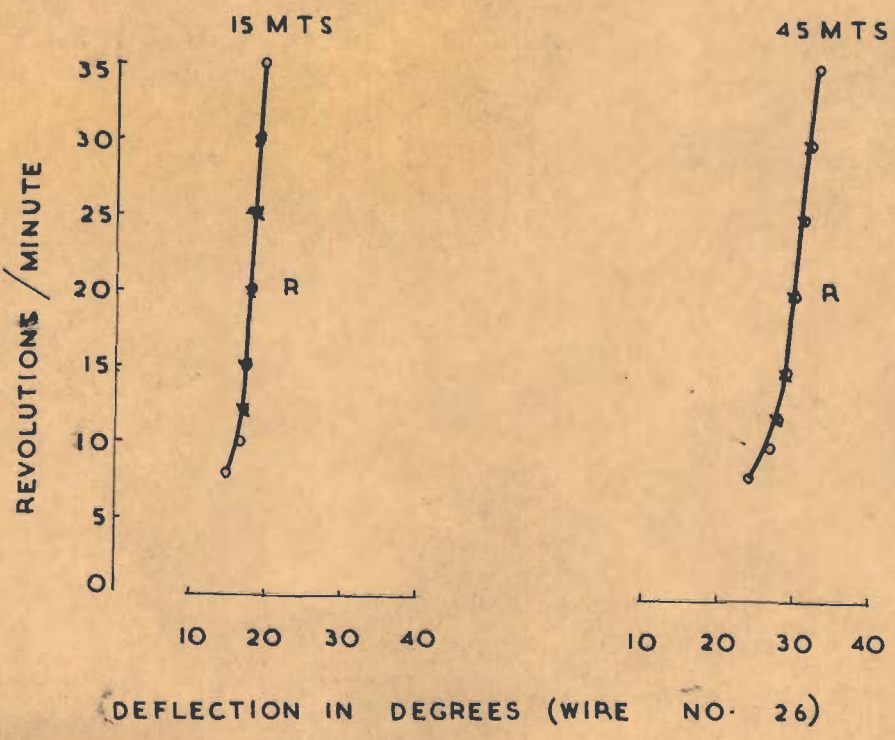

FIG. 17. FLOW CHARACTERISTICS OF CEMENT PASTES

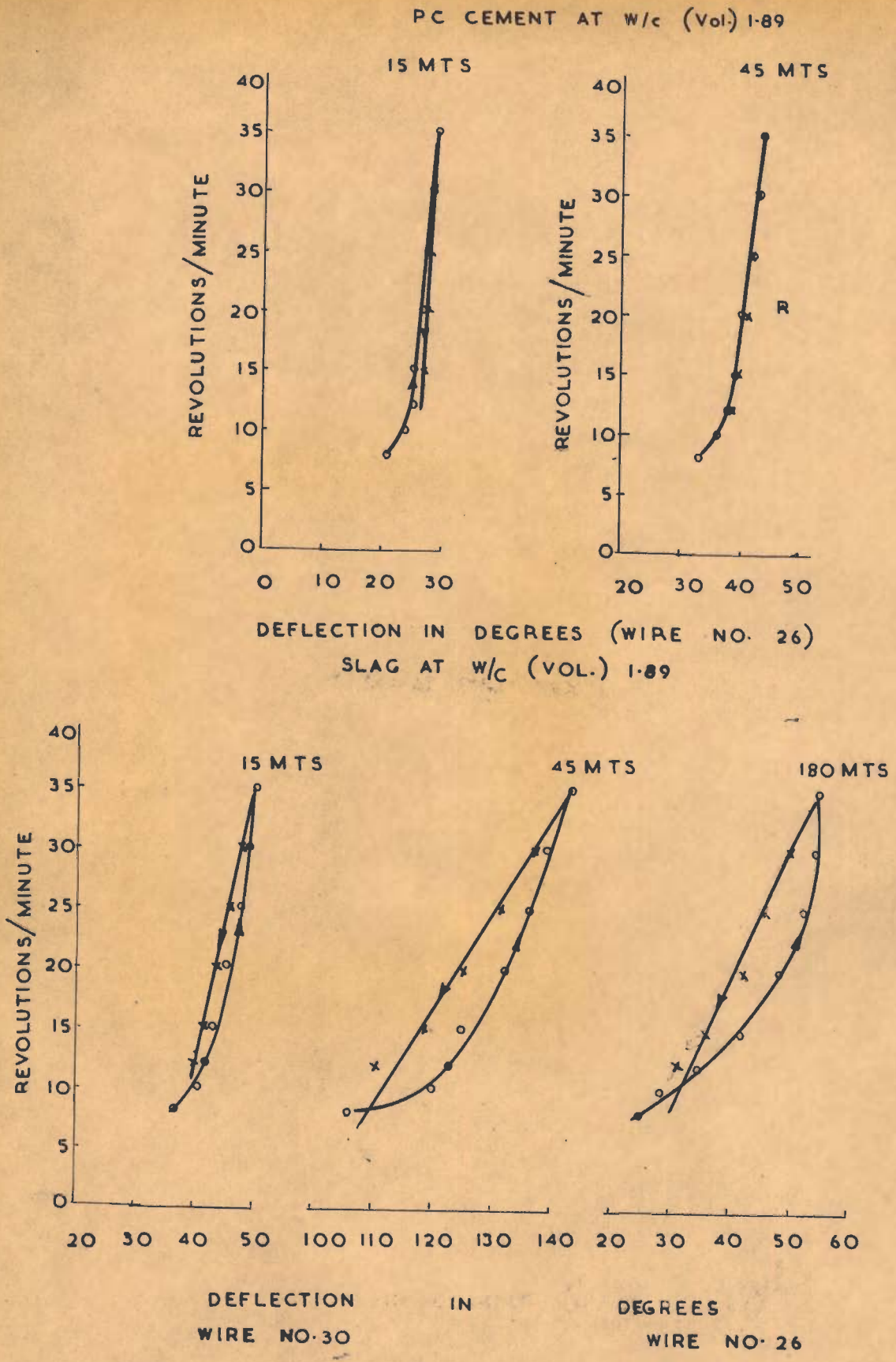

FIG. 16. FLOW CHARACTERISTICS OF PORTLAND CEMENT AND SLAG PASTES.

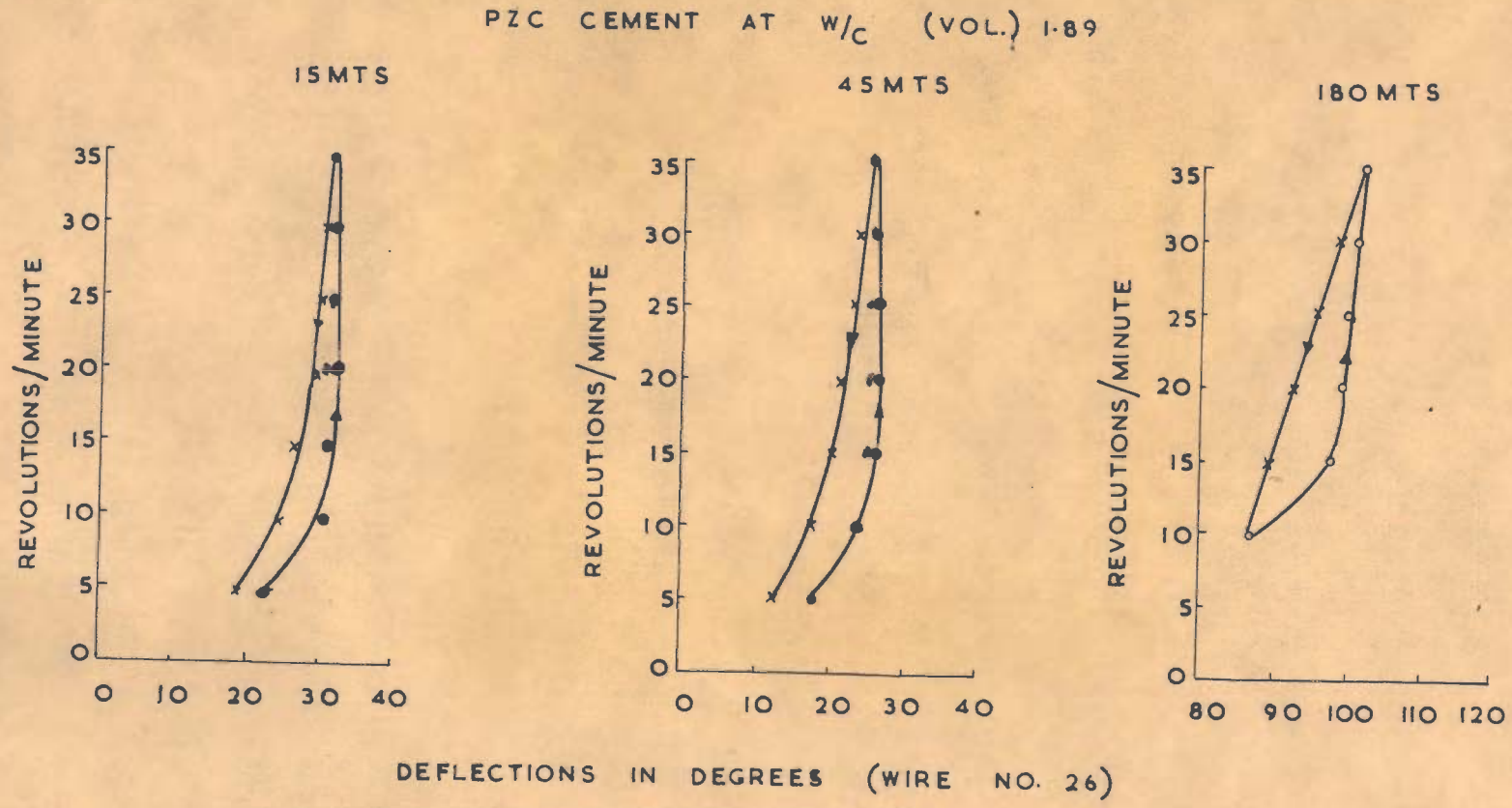

FIG. 18. FLOW CHARACTERISTICS OF CEMENT PASTES

RESULTS

Effect of Paste Composition

The curves of rpm versus torque for pastes of a Portland cement, two slag cements i.e., PBF (65 : 35) and BFP (35 : 65) and a pozzolanic cement (PZC 75 : 25) at a water cement ratio of 0.60 by weight are shown in Figs. 16 to 18. (Though two cycles were performed, only one has been shown. Except at three hours, the two cycles coincided at 15 and 45 minutes). The curves for Portland cement pastes (Fig. 16) are similar to those obtained by Shalom and Greenberg and, for the sake of simplicity, their terminology will be used herein to describe the rheological behaviour.

Only the Portland cement paste showed antithixotropy; some consider it dilatancy (151). However, the reversible behaviour was more commonly exhibited after 45 minutes of hydration by all the pastes excepting that of the pozzolanic cement (Fig. 18). Thixotropy was present in all pastes after longer hydration periods i.e., about 3 hours. Though the flow curve at 3 hours for the Portland cement paste is not shown in Fig. 16, it indicated thixotropy. The down curve for the pozzolanic cement pastes was always found to be on the left side of the ascending curve showing thixotropic behaviour at all periods. Similarly, a paste of granulated slag at an equivalent water solid ratio by volume also showed

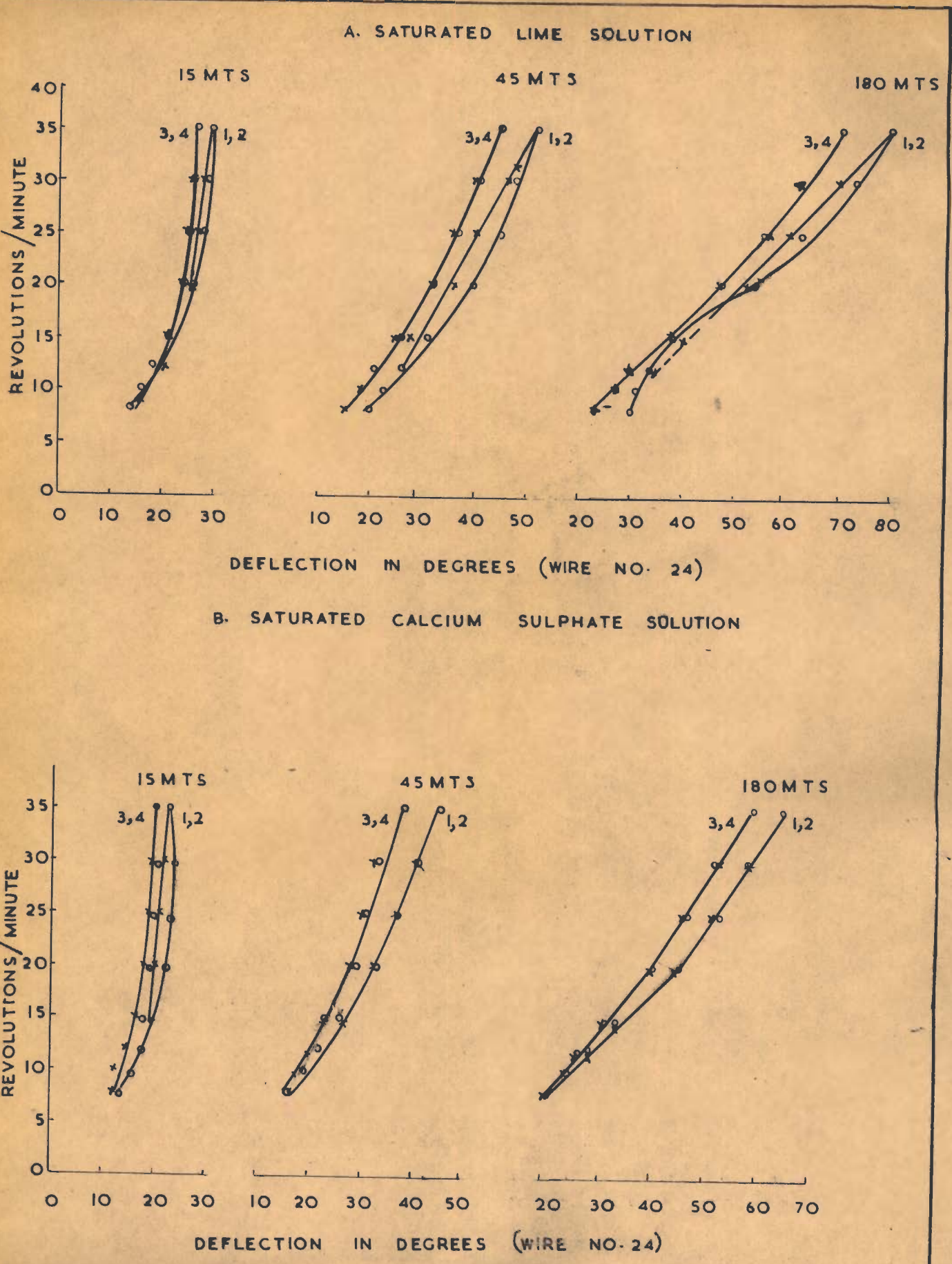

FIG.20. FLOW CHARACTERISTICS OF SLAG PASTES, W/S (Vol.) 1·26.

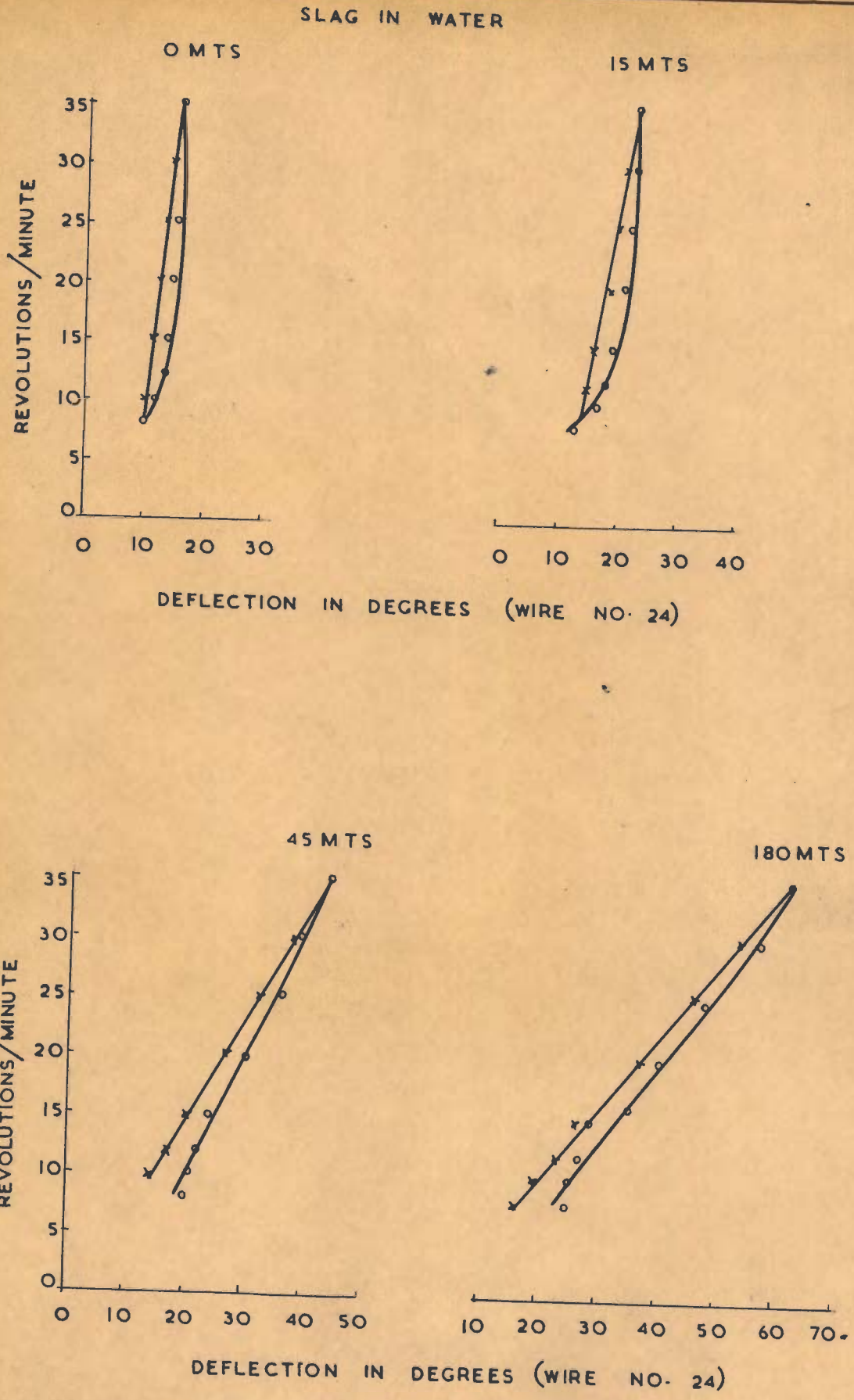

FIG.19. FLOW CHARACTERISTICS OF SLAG PASTES, W/S (VOL.) 1·26

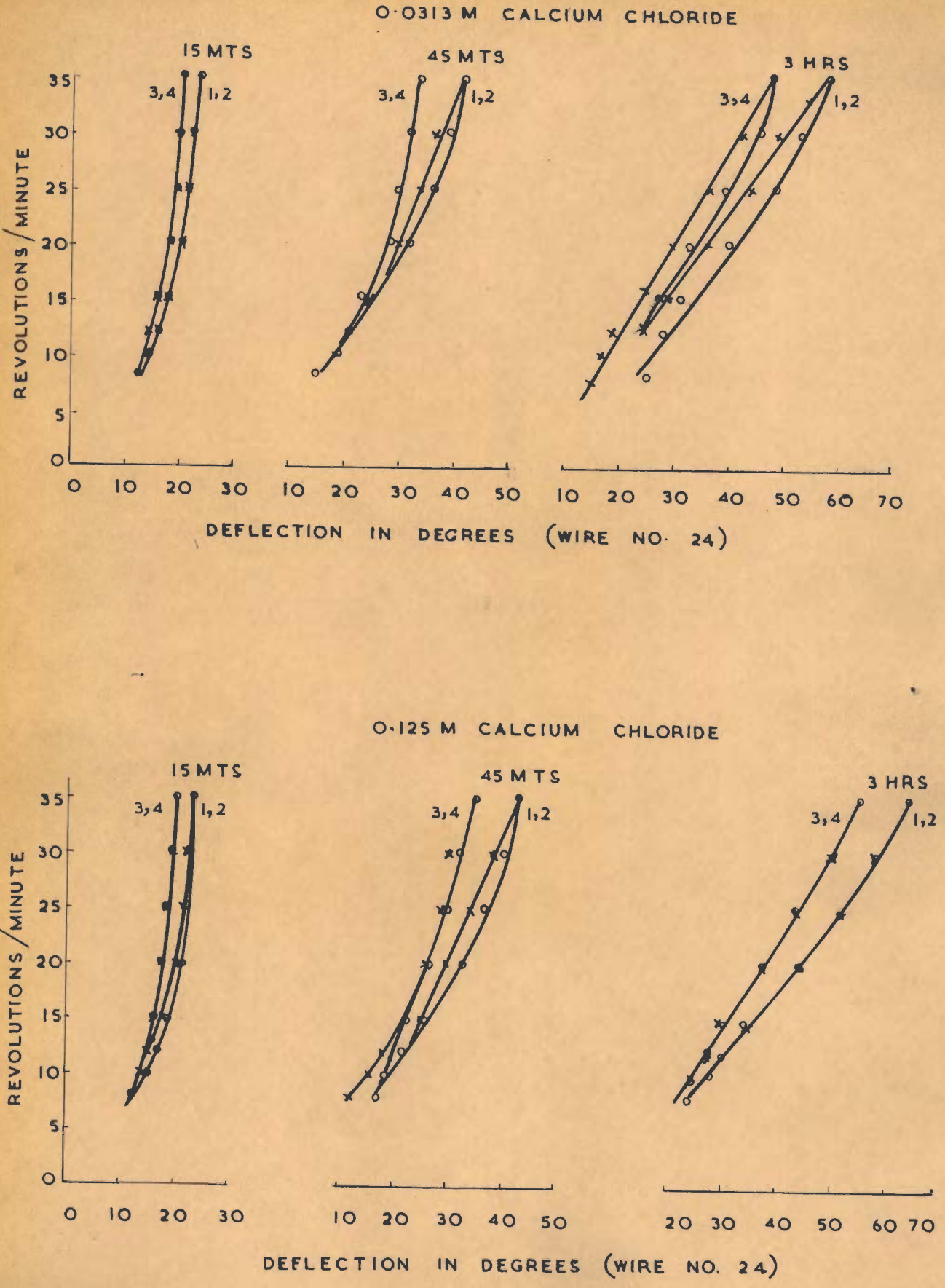

FIG. 21. FLOW CHARACTERISTICS OF SLAG PASTES W/S (Vol.) 1·26

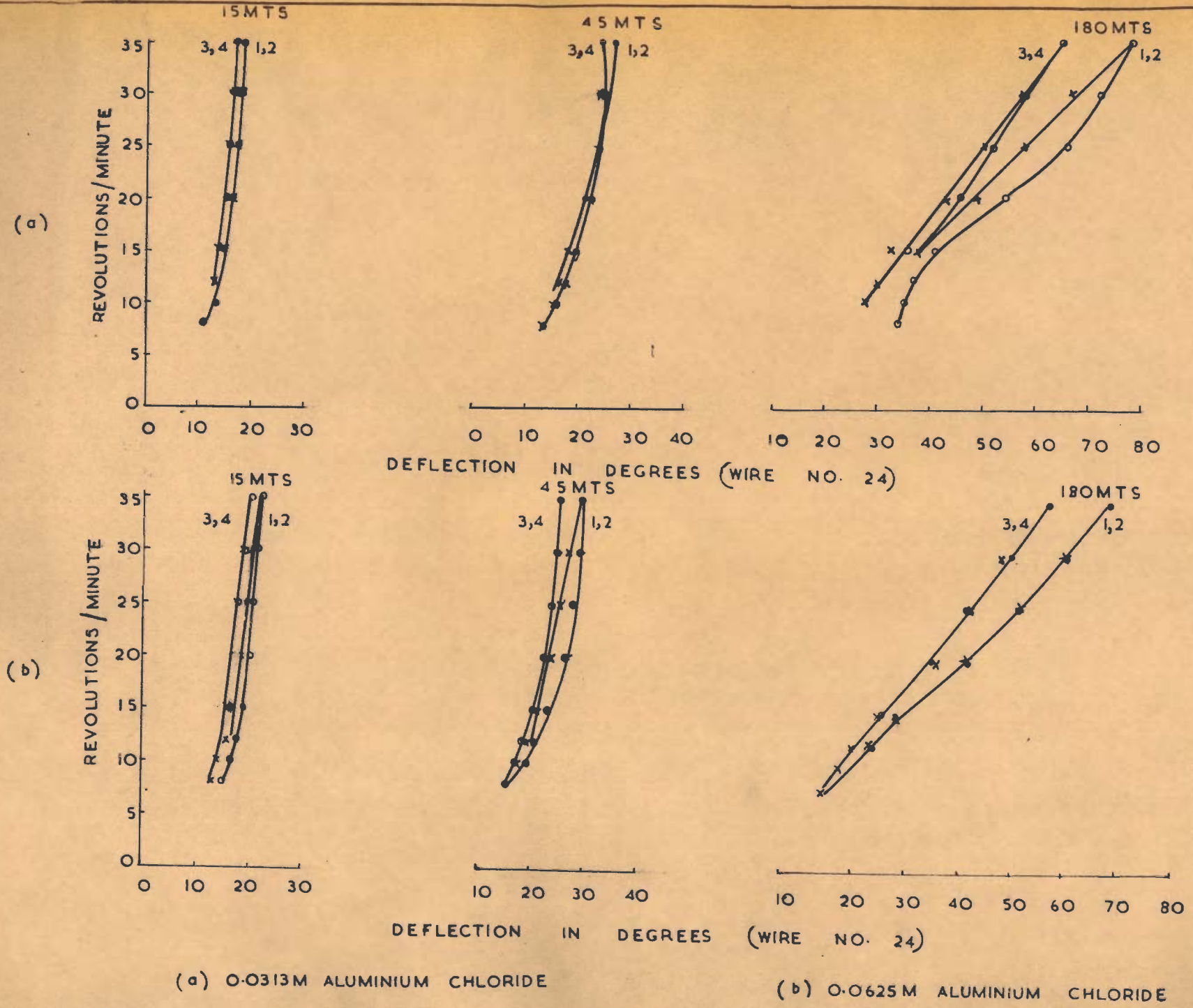

FIG.22. FLOW CHARACTERISTICS OF SLAG PASTES, W/S (Vol) 1·26

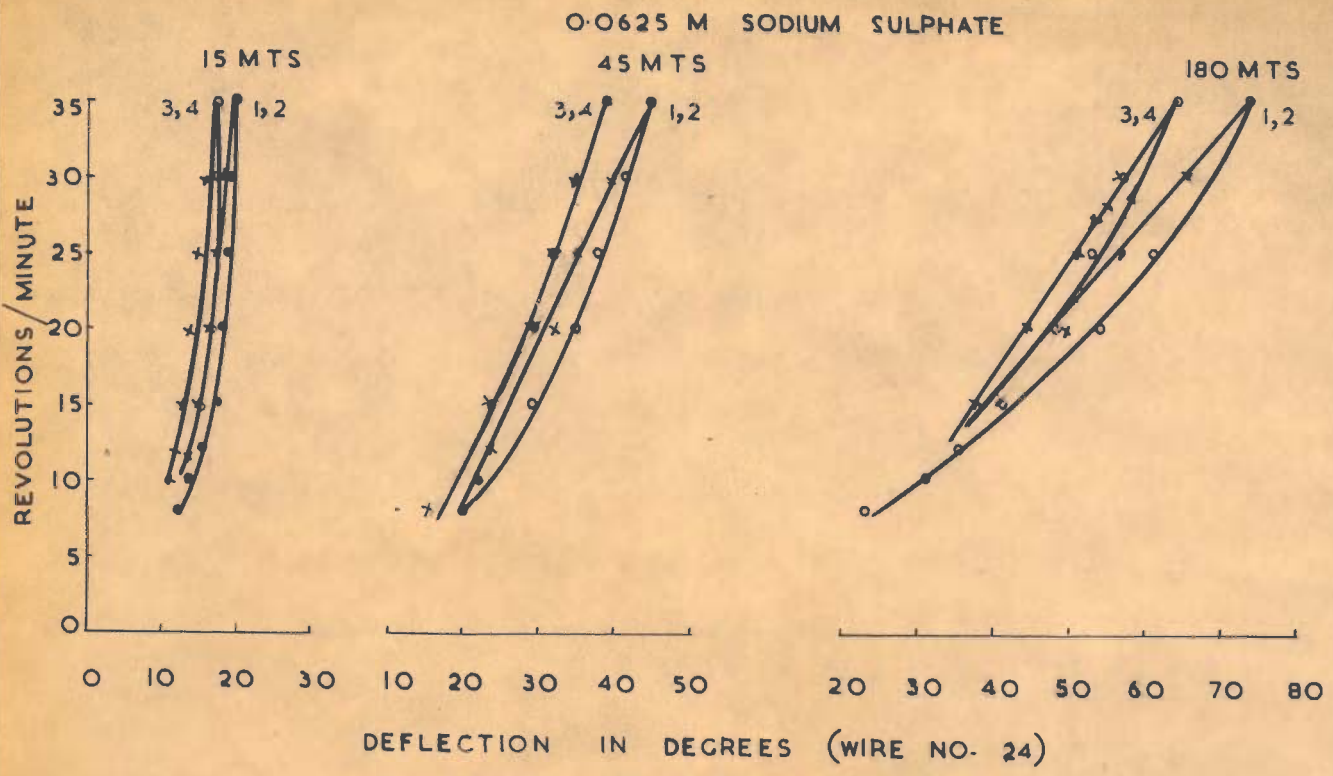

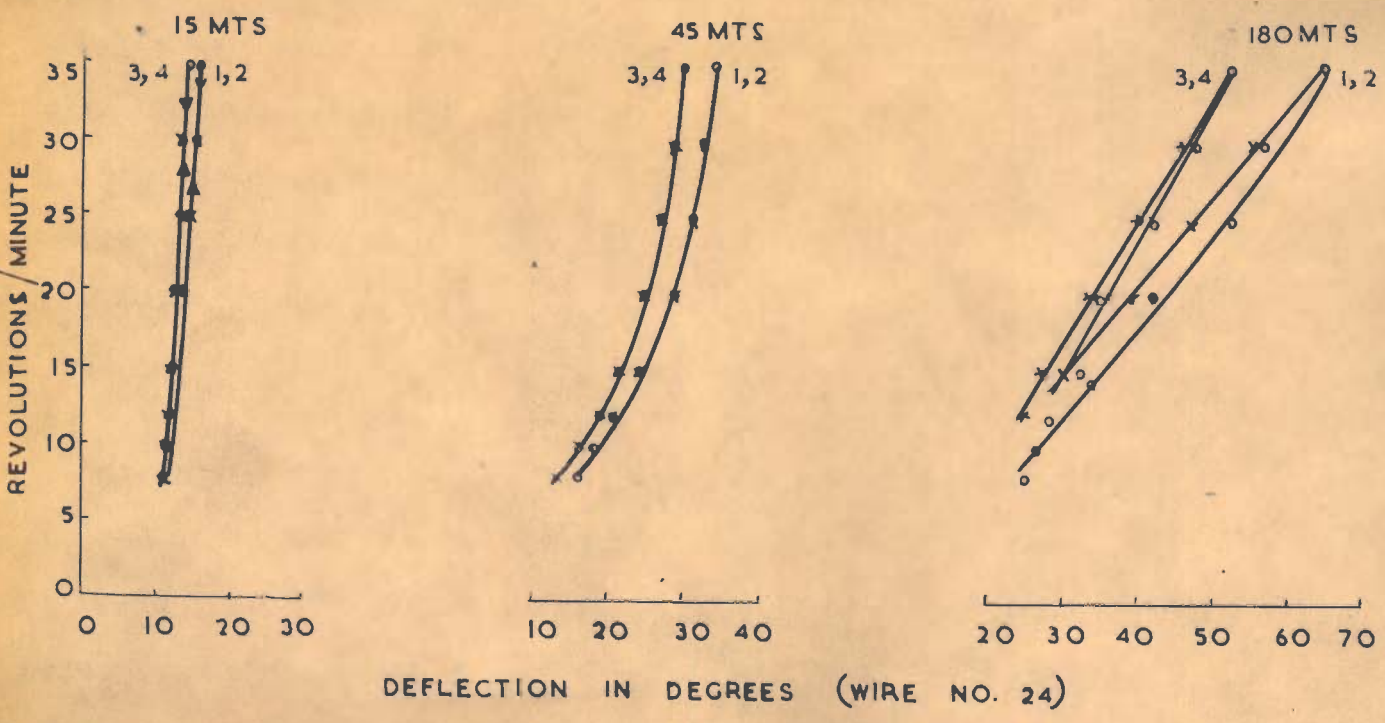

FIG.23. FLOW CHARACTERISTICS OF SLAG PASTE W/S (Vol.) 1·26

thixotropic behaviour from the very beginning (Fig. 16).

The plastic viscosity and yield values for the different pastes are reported in table 18. The plastic viscosity of Portland cement paste is highest while it is lowest for the pozzolanic cement, slag and slag cements having intermediate values. On the other hand, the yield value of the pozzolanic cement paste was found to be comparatively higher than that of slag cement pastes.

Effect of Addition of Electrolytes

Figs. 19 to 23 show flow curves for pastes of slag prepared with distilled water and electrolytes of different concentrations. The latter were selected on the basis of earlier results of sedimentation volume. It is interesting to note that though the water (or solution) to solids ratio in this series was lower (i.e., the ratio being 1.26 on volume basis against 1.87 in cements), antithixotropic or dilatant behaviour was absent. While reversible behaviour was observed in some of the pastes, thixotropic behaviour was more prominent.

Two cycles were performed in this series and the results showed thixotropy either did not exhibit itself or decreased a good deal after the first cycle. The data on plastic viscosity and yield value are reported in table 19. The nature and concentration of the electrolyte seems to influence the plastic viscosity to a far

TABLE - 18

Rheological Data on Pastes of Different Cements

Designation and composition of solids	w/s Ratio By vol.	Plastic*Viscosity(U_1), Cp			Yield Values(f_1), dynes/cm^2			Rheological Behaviour		
		15 Mts	45 Mts	180 Mts	15 Mts	45 Mts	180 Mts	15 Mts	45 Mts	180 Mts
Portland cement	1.89	76.0	85.5	1558.0	40.3	66.5	215.3	A	R	T
PBF 65:35	1.89	19.0	66.5	152.0	23.6	49.9	213.5	R	R	T
BFP 35:65	1.89	57.0	76.0	-	27.1	47.3	-	R	R	-
PZC 75:25	1.89	19.0	28.5	60.8	51.6	57.8	169.4	T	T	T
Granulated slag	1.89	33.6	54.4	123.5	10.9	35.2	80.5	T	T	T

* The plastic viscosity was calculated from the deflection values corresponding to 25 RPM on the upcurve.

TABLE - 19

Comparative Effect of Concentration of Electrolytes on the Rheological Behaviour of a Slag Paste

S.No.	Concentration of solution	*Plastic viscosity (U_1), Cp			Yield values (f_1) dynes/cm^2			Rheological behaviour, first cycle		
		15 Mts	45 Mts	180 Mts	15 Mts	45 Mts	180 Mts	15 Mts	45 Mts	180 Mts
1	Distilled water	365.6	1164.0	1649.0	35.4	8.9	7.0	T	T	T
2	0.0313 M Aluminium chloride	116.4	251.6	1973.7	49.6	63.7	24.8	R	R	T
3	0.0625 M Aluminium chloride	191.5	388.0	1707.2	49.6	53.1	60.1	T	T	R
4	0.0313 M Calcium chloride	232.2	793.4	1728.6	53.1	76.1	134.5	R	T	T
5	0.125 M Calcium chloride	212.9	890.1	1219.1	56.6	38.9	74.3	T	T	T
6	0.0625 M Sodium sulphate	232.5	890.1	1722.2	38.9	46.0	46.0	T	T	T
7	0.125 M Sodium sulphate	123.8	232.5	1769.5	38.2	86.7	15.9	R	R	T
8	Sat. $Ca(OH)_2$	270.9	1094.9	1044.0	67.3	44.3	56.6	T	T	T
9	Sat. $CaSO_4$	193.5	406.4	1335.2	17.5	58.4	65.7	T	R	R

* All values calculated from the down-curve of the first cycle if thixotropy (T) was present; otherwise from the upcurve of the first cycle, i.e., when the system was reversible (R)

greater extent than the yield values.

For each of the three electrolytes i.e., aluminium chloride, calcium chloride and sodium sulphate, two concentrations were selected i.e., the one giving a higher degree of flocculation compared to the other. The data (table 19) show that the plastic viscosities at 15 and 45 minutes were always higher for the concentration which produced the higher degree of flocculation. For example, the values were 191.5 and 116.4 centipoises for 0.0625 M and 0.0312 M aluminium chloride solutions respectively; the flocculation being higher at 0.0625 M. The differences in yield values are not significant. However, at 180 minutes the values of plastic viscosities were greater for concentrations which were expected to produce a lower degree of flocculation; but this change cannot be considered of any importance as the chemical reactions begin to show their effect at this stage.

DISCUSSION

Rheology of Fresh Portland Cement Paste

The constituents in Portland cement are di- and tricalcium silicates and tricalcium aluminate and a ferrite phase (2,3). The two silicates could be considered as hydrophillic gel-forming constituents. Without going into the mechanism of gel formation at this stage; it is sufficient to assume that it is built of individual

molecules held together, by relatively weak and non-directed forces because the gel has actually been found to be amorphous in nature. According to Forslind's theory the gelation mechanism is explained as a consequence of specific interaction of electronic structure of water molecule and arrangement of hydrophillic groups in the surface of the solid phase (152). The rheological behaviour is determined by the occurrance of lattice defects and dislocations in the stabilized liquid phase. The water in contact with silicate gel of large surface area in cement suspension or paste thus will possess a structure. Powers (153), Shalom and Greenberg (146) on the other hand, opine that it is the interaction of the solid particles which controls flow properties and water has no solidity. These workers contribute to the theories of Verwey and Overbeck and Kruyt. According to Powers (153) solvated surfaces and electrostatic charge, size, shape and concentration of particles and the viscosity of the fluid account for the rheological properties. Reiner (154) considers cement paste at W/C ratio of 0.4 and above as a first approximation to a Bingham body.

Thixotropy in Portland cement paste can be considered due to contacts between particles of calcium silicate hydrogel at certain points only. The hydrated particles of Portland cement carry a positive surface charge. The particles are probably in the form of plates,

fibres and needle-like crystals (146); the latter two are believed to be formed by rolling up of the plates. Shalom and Greenberg assumed these particles to be either fibres or plates and presented a model which is similar to that proposed by Van Olphen for the bentonite gels. Further, the forces between the hydrogel particles in paste are considered just strong enough to hold the system together requiring only small shearing stress to break the bonds or contacts and form a sol. The latter when allowed to stand for sufficiently long time again transforms slowly into gel. Though not above criticizm, this hypothesis appears to be reasonable in the light of the present state of knowledge and experimental evidence.

Rheology of Fresh Pastes of Slag and Pozzolanic Cements

Since the slag and pozzolanic cements are mixtures of Portland cement with slag or fly ash, their rheological behaviour will be dependent primarily on the relative amounts of each type of particles and their interactions. When Portland cement is present in a greater proportion, the resultant behaviour will be influenced more by it. But contribution of Portland cement may be proportionately greater even in mixes where it is not in excess because of its greater reactivity.

The different possible effects of the

Portland cement can be

(i) a change in the degree of flocculation,

(ii) a retardation of the gel formation,

(iii) an adverse effect on the formation of a continuous coherent framework of gel particles, and

(iv) a change in the nature of forces causing inter-linking between gel particles.

The rheological behaviour of the different cement pastes has been discussed in the light of the abovementioned effects.

Earlier it was concluded that the degree of flocculation in the PBF cement was only somewhat lower than that of the Portland cement whereas it was much lower in the paste of the pozzolanic cement (Chapter 1). This explains partly the lower values of plastic viscosity for the PBF and PZC cements (table 18); a greater reduction in the values of PZC cement being accounted by a greater reduction in the degree of flocculation in this paste compared to that of the PBF cement.

Both the conditions nos. (ii) and (iii) also will have an adverse effect because the degree of hydration in these cements at early ages is generally lower and consequently the quantity of calcium silicate hydrate, which in the intitial stages is formed primarily on the hydration of C_3S, will be lower. A continuous coherent framework is also less likely to result in the slag and pozzolanic cement pastes because of the presence of

less reactive particles of slag or fly ash. But the effects of this particular factor are of lesser importance and may influence the results only at very early ages.

C_3A content in slag and pozzolanic cements is lower, formation of needle-like crystals of ettringite which cause interlocking will therefore get reduced at early periods. The gels will be less rigid and yield values will be lower and the pastes may show enhanced thixotropy. Actually this is evident from the flow curves of the different cements (Figs. 16 to 18).

It is interesting to note that the plastic viscosity of BFP cement which contains 65 parts of slag is comparable to that of the Portland cement. This is understandable in the light of the values of the plastic viscosity of the granulated slag paste in water reported in table 18. The flow curves of a granulated slag (about 3200 sq cm per g) paste at a water-solid ratio of 1.87 showed thixotropic behaviour as early as 15 minutes (Fig. 16) as against a period of 3 hours for the Portland cement paste. Earlier, it was concluded in Chapter 2 that the slag particles carry a positive charge like Portland cement particles and that a paste of slag in water is in a flocculent state. The formation of colloidal hydrates is mostly favoured in the slag paste in water because of the absence of $CaSO_4$ and consequently that of the needle-like crystals of ettringite which provide cross linking. The flocculation in the slag glass paste will be thus less

oriented. The forces between gel particles in slag cement pastes, which show intermediate behaviour between a Portland cement and a slag paste, will therefore be comparatively weaker. This explains the lower plastic viscosities and yield values of these cements.

Though the plastic viscosity for the Portland cement paste at 3 hours is probably higher and yield value lower (table 18) than the real values because of the low rates of shear used (155), the flow curves of the different cement pastes showed thixotropy at 3 hours. It appears the number of junction points per unit volume was great enough in about three hours time to allow the formation of a more or less coherent structure and that after mechanical agitation, most of the junction points are restored at rest.

The yield values of the two slag cement pastes at 14 and 45 minutes are similar but lower than that of Portland cement. But the yield values of the pozzolanic cement are comparatively higher though, because of a lower degree of flocculation, lower yield values were expected. Since it is difficult to visualize that the energies of cohesion of gel particles will be widely different in the PZC paste, the size and shape of fly ash particles which are somewhat different (Fig. 2) appear to be partly responsible for this behaviour. It is quite likely that the particles of unburnt carbon and poorly crystallized oxides of silicon, aluminium and iron which

absorb moisture and swell like clays, are responsible for not only an increase in yield values but also for the thixotropic behaviour of the PZC paste from the very beginning (Fig. 18).

Effect of Electrolytes on the Rheology of Slag Pastes

The flow curves of the paste of slag (about 4000 sq cm per g) at a lower water-solid ratio (i.e., 1.26 by volume) are no different; again the thixotropy appearing from the very beginning (Fig. 19). Figs. 20 to 23 show the effect of electrolytes. The paste in saturated calcium hydroxide was found to be slightly less flocculated and hence shows lower viscosity values. But the rheological behaviour did not alter (Fig. 20A). An increase in the yield values (table 19) shows either an increase in number of junction points in the gel or an increase in the forces between gel particles. In fact, both of these are possible. As saturated calcium sulphate results in a slightly lower degree of flocculation the plastic viscosity decreases in the beginning but it would appear the formation of ettringite at later ages provides cross links in the hydrogel thus increasing the viscosity and yield values (Fig. 20B) and table 19. Since the chemical reaction may begin to show their influence after 45 minutes depending on the concentration of the electrolyte and even surpass the effects of physical interactions, greater importance is attached to behaviour at early periods.

Charge is known to increase the viscosity of a colloidal suspension. Dealing with rigid particles the effect may be taken due to an increase of the effective volume of the particle by its double layer (156). Earlier the differences in sedimentation volumes and bleeding times of pastes of granulated slag in different electrolytes were explained on the basis of electrostatic charge and the specific effects of electrolytes on flocculation. In short, the degree of flocculation was found to be governed by a balance existing at any stage between positive dispersing ions such as, aluminium, calcium and sodium and flocculating anions such as sulphate, chloride and hydroxyl etc.

The curves in Figs. 21 to 23 and data in table 19 clearly show that whenever electrolyte concentration brings about relatively a higher degree of flocculation, higher plastic viscosity results and thixotropic behaviour predominates. At concentration of 0.125 M calcium chloride, 0.0313 M aluminium chloride and 0.125 M of sodium sulphate, the flocculation was lower (Figs. 12 and 13) and so is the plastic viscosity at 15 minutes for the two concentrations of calcium and aluminium chlorides (Figs. 21 & 22) and sodium sulphate solutions (Fig. 23). Lower yield values were expected when degree of flocculation was lower. But it is not so (table 19). However, it may be observed under such conditions the curves show a reversible behaviour and a comparison of the values of the yield values calculated

the yield values calculated from these curves with those deduced from thixotropic curves, strictly speaking, is not rational. Comparison, under identical condition, say for example, for the two concentrations of calcium chloride at 45 minutes when both the curves show thixotropy is justifiable and the results clearly show that the yield value is lower when the degree of flocculation is lower in the paste.

CONCLUSIONS (Chapters 1 to 3)

The bleeding characteristics of the fresh pastes of the cementitious materials viz., pozzolanic and slag cements and mixes of lime with either slag or fly ash or surkhi or ground quartz sand etc., were found to be similar to those of the fresh Portland cement paste. The bleeding rate and the capacity of these pastes for the range of water content commonly employed in practice were found to conform respectively to the equations :

$$Q = 0.2 \; \frac{g(d_c - d_f)}{\sigma_w^2 \cdot \eta} \; \frac{(W - W_1)^3}{C}$$

and

$$\Delta H' = \frac{K^2 C \rho_c}{V} \left[(W/C) - (W/C)_m \right]^2$$

originally developed by Powers and Steinour for the fresh Portland cement paste.

The values of the immobile water per unit volume of the paste (W_1) of the pozzolanic and slag cements were found to be lower than that of the Portland cement; the differences being greater for the pozzolanic cements and only slight for the Portland blastfurnace cement. The differences were found to be due to the differences in degree of flocculation, the latter being influenced both by the physical and chemical factors; for example, the effect of size, shape and nature of fly ash particles or the presence of alkalies in the surkhi samples.

Corresponding differences in the values of bleeding capacity were also observed. The values of minimum water-cement ratio $(W/C)_m$ for the two pozzolanic cements were 0.58 and 0.76 against a value of 0.91 for the Portland cement showing thereby substantially lower strength of the'floc structure' of the pozzolanic cement pastes.

The pastes of one part of hydrated lime with two parts of either of the powders of slag, fly ash and surkhi did not show significant differences in the values of either W_i or $(W/C)_m$ showing thereby that the degree of flocculation and 'floc strength' did not vary in these pastes because the conditions of lime saturation were always maintained and the particles of slag, fly ash or surkhi etc. being coarser than lime, governed the packing arrangement. In other words as far as the structure of these pastes is concerned; the chemical nature of the powders does not appear to be important; only the physical characteristics of the fine powders are important.

The final porosity of the sediment of the fresh pastes of the pozzolanic cements was found to be considerably lower than that of the Portland cement paste; but the mean pore size was greater in the former paste. Similarly, though the porosities of the sediment of 1:2 and 1:3 lime-fines pastes were found to range from 59.4 to 60.8 per cent against 59.4 per cent of the

estimated average width of pore in the former paste was 1½ to 2 times of that in the cement paste. It is, therefore, concluded that the total value of porosity is not as important as what constitutes it i.e., how close are the particles to each other.

The net interparticle attraction in the slag and pozzolanic cement pastes was found to be comparatively weaker and that explains why replacements of the Portland cement with the pozzolanas having equal surface area (sq cm per g) in the present and earlier studies mostly increased the bleeding. Since at a given water content pore size decreases if the specific surface area of the powder increases, grinding of cement replacements to a slightly greater fineness suggests itself. The fineness should be equal to that of the Portland cement in terms of sq cm per cc and not sq cm per g because of the wide differences in the densities of the Portland cement and the replacing powders.

The sedimentation (or bleeding) rate and volume of a fresh paste, which in turn determine the porosity and 'mean' pore-size of the sediment, were found to be influenced greatly by the electrostatic charges on solid particles and the electrolytic additions such as solutions of aluminium and calcium chlorides, calcium hydroxide and sulphate, sodium hydroxide and sulphate etc.

The plots of both sedimentation volume and porosity of the slag pastes versus the increasing concentration (0.015 M to 0.50 M) of the different solutions showed well defined maxima and minima at certain concentrations. In view of this the changes in sedimentation volume could not be explained on the basis of the chemical action between slag particles and the different solutions. However, the former could be explained in terms of changes in the degree of flocculation which was found to be explicable in terms of the Helmholtz double layer theory. In short, the effects of small additions of electrolytes on the properties of fresh pastes are due to their physical interaction, the electrostatic charge on the particle, valence of the counterions and simillions playing an important role.

The important findings on the structure of fresh pastes obtained through the sedimentation studies were confirmed by the study of their rheological behaviour of the fresh pastes. Also the latter provided direct information on the initial framework resulting from the interaction of particles of different nature present in a paste. As against the Portland cement, the slag and pozzolanic cements did not show antithixotropy (or dilatancy). The reversible behaviour was more common after 45 minutes and thixotropy was observed after 3 hours of hydration.

The plastic viscosity of the Portland cement was highest while it was lowest for the pozzolanic cement, slag cements having intermediate values. The reason for lower plastic viscosity appears to be a lower degree of flocculation, retardation of gel formation, and the gel particles not forming a continuous coherent framework. Also the degree of flocculation in these pastes is lower and less oriented. The yield values were generally lower because of a lower degree of flocculation.

In view of the specific effects of electrolytes on flocculation, the degree of flocculation of slag pastes was found to be governed by a balance existing at any stage between the positive dispersing ions such as aluminium, calcium and sodium and flocculating anions of sulphate, chloride and hydroxyl etc. The rheological behaviour of these pastes at selected concentration of the electrolytes showed that relatively a higher degree of flocculation was accompanied by a higher plastic viscosity and the thixotropic behaviour was most predominant though at early periods of 15 and 45 minutes some pastes did show reversible behaviour. In short, small chemical additions were found to influence materially the structure of the fresh paste as was evident from the flow characteristics.

The data clearly demonstrated that even when the particle size distribution and specific surface (sq cm per g) of slags, pozzolanas and other fines were controlled,

differences in the structure of fresh paste of the cementitious materials existed in the form of differences in 'floc strength', porosity and 'mean' pore size. The latter eventually can affect the gel-space ratio differently and consequently the strength and other properties of the hardened paste.

STUDIES

ON THE HARDENED PASTES OF CEMENTITIOUS MATERIALS

CHAPTER 4

STRENGTH DEVELOPMENT AND THE FORMATION OF HYDRATED SOLID PHASES IN THE CEMENT PASTES

Introduction

A good deal of literature advocating the use of pozzolanic and slag cements and other cementitious materials has been published in India during the last decade or so. Hoon, Chopra and Vengupelarao (157) had studied the technology of artificial hydraulic limes. Hoon (158) investigated the activity of Talabira clay and other pozzolanas and properties of the pozzolanic cements prepared with different pozzolanas. Chopra and his co-workers (96 - 100) have reported on the hydraulicity of the Indian granulated slag and properties of the Portland blastfurnace cements and recommended the manufacture of the latter cement from the TISCO slag. Use of wet ground slag as a replacement of cement in concrete was also recommended by them (97). Puri and his co-workers (159) reported on the activity of calcined shale which was subsequently used as a pozzolana in mass concrete for the construction of the Bhakra Dam. Chatterjee and Lahiri (160) have also carried out investigation on the Indian slags and recommended their use. Chopra, Taneja, Rai and Kishan Lall (161) reviewed the work on this subject in 1958, high-lighted some of the important findings, made recommendations and indicated the scope of further research.

Subsequently Chopra and Kishan Lall (98) published their findings on the sulphate activation of the Indian slag and properties of the trial supersulphated cement prepared with it.

Investigations on Bokaro fly ash which was used subsequently as cement replacement (15 per cent) in the construction of the Rihand Dam were reported by Maheshwari, Aggarwal, Misra and Joshi (162). Rehsi and Garg (101) have evaluated the Indian fly ashes. Srinivasan (163) has studied the activity of calcined clays and recommended the use of active surkhi. Puri, Bawa and Srinivasan (164) have also reported on the strength and sulphate resistance of pozzolanic cement prepared with surkhi.

Most of the above publications report only on the suitability of the slags or pozzolanas and the results of the standard tests performed on the cements prepared with them. Very few (98,99,160,163) have attempted to compare the physical properties of the slag and pozzolanic cements with those being produced in other countries, and much less correlate the differences in properties of the slag and pozzolanic cements with the properties of the Indian slags or pozzolanas used in the preparation of the cements.

It is well known that the Portland blast-furnace cements develope strengths equal to those of the

ordinary Portland cement in about 28 days to 3 months depending on the type of Portland cement, nature of slag and its proportion and to a lesser extent on the procedure adopted for testing strengths (165).

As against Portland blastfurnace cement, the experimental evidence on equal strength development of pozzolanic cements is conflicting. While the differences in testing procedures may be partly responsible for it, some publications clearly bring out that the strength of concrete wherein cement is replaced by 20 to 30 parts of pozzolana of good activity does not equal the strength of concrete even in 90 days. For example, Mather (136) who used a single pozzolana in varying magnitude of replacements found only a few out of about 30 samples to give equal 90-days strengths. Fly ash concretes had strengths ranging from 3090 to 4940 psi as against 5470 psi of type II Portland cement at 90 days. Similarly, the data of Brink and Halstead (167) show that at a level of 20 per cent replacement none of the 34 fly ashes examined showed 90 days strengths equal to those of the Portland cement; only 14 fly ashes exceeded the strength of Portland cement at 365 days. Nurse (168) has also reported a similar findings.

No definite relationship has been found between strength of pozzolanic cement and the activity of pozzolana or its physico-chemical properties (167,101). One of the reasons is the variations in the properties of the

pozzolanas themselves. Vincent, Mateos and Davidson (169) have reported on the variation in pozzolanic behaviour of fly ashes. Their relationship between chemical composition (expressed in mole fractions on a triangular chart) and strength is a step forward, but appears to have a limited scope because fineness, which greatly influences activity, has not been taken into account. Moreover, the study was carried out only on lime-fly ash mixes.

In view of the above discussion, it may be concluded that there is need for a more basic approach to explain the development of strength in pozzolanic and slag cements and discern the influences of the resulting hydrated phases from those of the physical structure of the pastes or concretes. A study of the physical and strength properties of the cementitious materials in relation to the formation of hydrated phases was therefore carried out.

MATERIALS

The materials used were :

(1) PC cement

(2) PBF cement (65 clinker : 35 slag)

(3) BFP cement (35 clinker : 65 slag)

(4) PZC cement (75 clinker : 25 calcined fly ash)

(5) SSC cement (5 clinker : 25 calcined gypsum : 70 slag)

The samples nos. 1 to 4 contained 4 per cent gypsum as a

The cement nos. 1, 2, 3 and 5 were prepared in a manner described earlier under 'cementitious materials'. The fineness of the PC, PBF and BFP cements was 3200 ± 50 sq cm per g (Blaine) and 3918 sq cm per g for the SSC cement. The PZC cement was prepared from Durgapur fly ash calcined at 700 ± 10°C and Portland cement clinker. The fineness of the calcined fly ash was 3466 sq cm per g and that of the PZC cement prepared with it as 3161 sq cm per g (Blaine).

EXPERIMENTAL

Preparation of Paste

The pastes of cements were prepared in the manner described in Chapter 1.

Compressive Strengths of Hardened Pastes

The paste of a cementitious material was filled in a 2 in. cube mould immediately after the mixing was stopped. The filling was done in two layers and a light tamper was used for filling. Each layer was filled by giving it 25 tampings. The casting of specimens was done in a laboratory controlled at 50 ± 5 per cent of relative humidity at the standard temperature of 27 ± 2°C (105). The moulds were stored in a humidity of not less than 90 per cent for the first 15 hours. The specimens were then stripped and were placed under water at 27 ± 2°C for curing.

Fig. 24. Differential thermal analysis apparatus complete with a Leeds & Northrup programme controller.

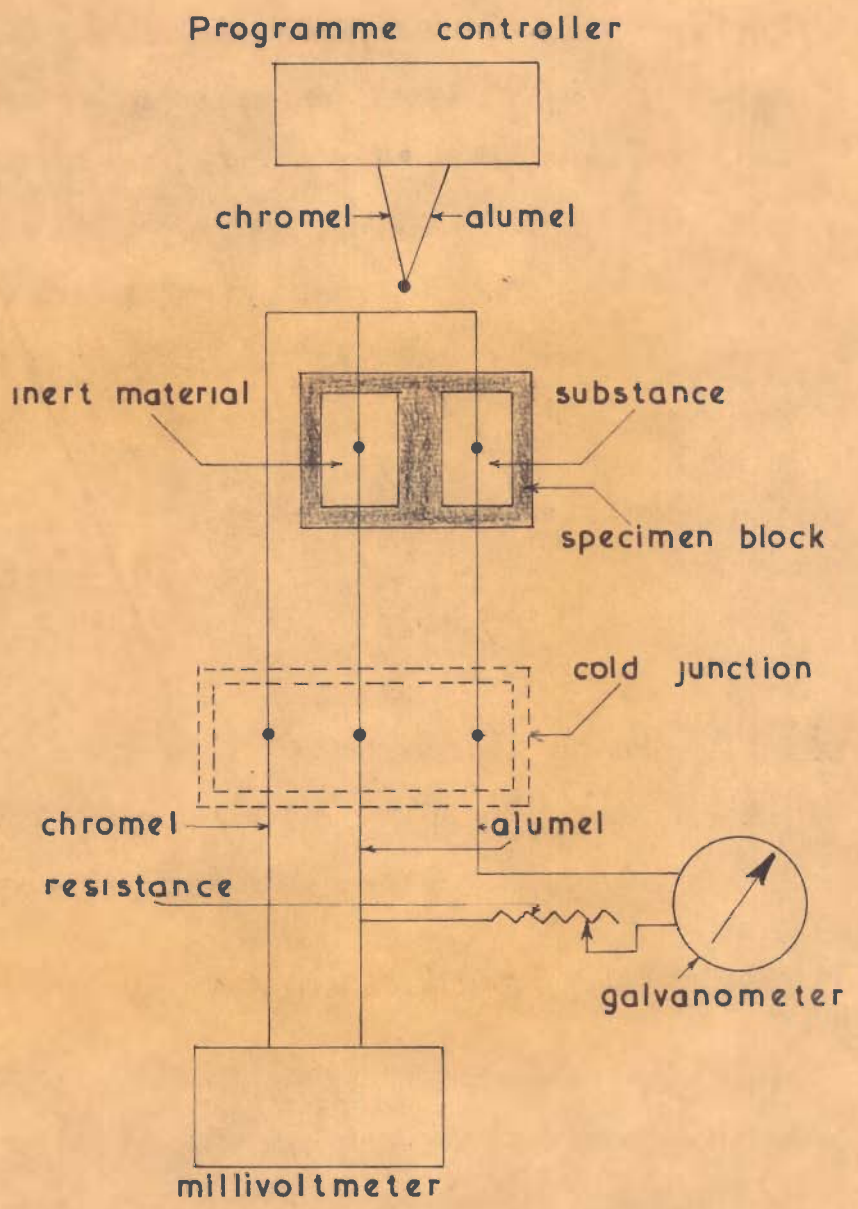

FIG.25. SCHEMATIC DIAGRAM OF D.T.A.

The compressive strenth of the hardened specimen was determined on a saturated surface-dry condition and at least four specimens were tested for each strength test. The average values have been reported. A variation of 10 per cent was allowed with the condition that at least three specimens must be left after rejection. Failing this, the test was repeated.

Preparation of Granular Samples

The material from the strength test was crushed further and passed quickey through sieves and a fraction between 30 and 80 U.S. sieve was separated out and stored in air-tight bottles. This granular sample was used for the determinations reported hereafter.

Differential Thermal Analysis

The experimental set up is shown in Fig. 24 and it consists of a furnace (upto 1000^{o}C), a refractory specimen holder, a pyrometer, a reflecting type galvanometer, resistances, thermocouples (chromel-alumel) and a Leeds and Northrupt Programme Controller. The schematic diagram is shown in Fig. 25. The heating rate of the furnace was controlled at 10 $\pm$ 1^{o}C per minute by the programme controller and a Dewars flask filled with powdered ice was used as a cold junction for the thermocouple.

Calcined aluminium oxide (γ-alumina) was used as an inert material and filled in one of the cavities of the specimen holder. The sample was filled in the other cavity. The atmosphere in the furnace during the experiment was 'air'. The analyses were carried out at the atmospheric pressure.

The galvanometer reading which measured the differential temperature was represented as ordinate and the temperature of the sample as recorded by pyrometer, as the abscissa in the thermograms. The curves were drawn showing the endothermal peaks downwards and the exothermal peak upwards with respect to the base line.

The granular sample prepared from the crushed material of a hardened paste was dried under vacuum of 1-2 mm of mercury for a few hours to remove free water. The sample was then ground to pass No. 100 U.S. sieve. The weight of sample used was 0.6 g.

X-ray Powder Analysis

The radiation used for X-ray powder analysis was Copper K alpha. A Guinier de Wolff focussing camera of a diameter of 114.6 mm was used for recording the powder diffraction pattern. This camera is fully focusing over the whole range.

The sample for X-ray analysis was dried under a vacuum of 1-2 mm of mercury for a few hours to remove

free water. The sample was then quickly ground very fine in an agate mortar and sealed in an airtight container till used.

RESULTS

Constitution and Hydraulicity of the Indian Slags

The Indian slags are characterised by comparatively a high alumina content resulting from the use of more aluminous iron ores and high ash metallurgical coke (170). On the other hand, lime content is pretty low (table 20A). According to the work of Osborne and his co-workers (171) the Indian slags are expected to fall generally in the phase assemblage C_2AS-C_2MS_2-CS-CAS_2. The mineralogy of the air cooled slag samples from the different iron and steel plants was studied by Chopra, Taneja and Mehrotra (172) with the help of microscopic and X-ray powder diffraction techniques. The mineralogical assemblages found are reported in table 21. Mellilite is the most predominant phase. The knowledge of phases, though not necessary, is considered desirable for a better understanding of the hydraulicity of a particular slag because the activity is known to differ with the nature of the slag glass (173,174).

Keil has discussed the various hydraulic indices employed for evaluating hydraulicity of slags

TABLE - 20(A)

Chemical Analysis of Air Cooled Blast Furnace Slags

S.No.	CONSTITUENTS	TISCO	DURGAPUR	BHILLAI	BHADRAVATI	ROURKELA
		per cent	per cent	per cent	per cent	per cent
1.	Silica (SiO_2)	31.68	33.12	39.07	42.16	29.96
2.	Aluminium Oxide (Al_2O_3)	24.49	24.27	18.76	21.28	26.25
3.	Iron Oxide (FeO)	0.73	1.02	-	-	0.70
4.	Manganous Oxide (MnO)	1.01	-	-	-	2.66
5.	Calcium Oxide (CaO)	37.97	33.20	37.36	30.41	33.04
6.	Magnesium Oxide (MgO)	3.52	6.79	4.54	6.32	6.41
7.	Sulphur (S)	0.84	0.71	0.74	0.61	0.72
8.	Acid Soluble Sulphate	tr	-	-	-	-

TABLE - 20(B)

Hydraulic Indices

	Formulae		TISCO	DURGAPUR	BHILLAI	BHADRAVATI	ROURKELA
F(I)	$\frac{CaO + MgO + 1/3\ Al_2O_3}{SiO_2 + 2/3\ Al_2O_3}$	≥ 1	1.03	0.97	0.93	0.78	1.02
F(II)	$\frac{CaO + MgO + Al_2O_3}{SiO_2}$	≥ 1	1.08	1.94	1.55	1.38	2.19
F(III)	$\frac{CaO+CaS+1/2\ MgO+Al_2O_3}{SiO_2 + MnO}$	≥ 1.5	1.98	1.85	1.50	1.31	1.94

TABLE - 21

Mineralogical Assemblages in Slags

S.No.	MINERALS		TISCO	DURGAPUR	BHILLAI	BHADRAVATI	ROURKELA
1.	C_2AS*	Melzilite	**OXC	OXC	OXC	OXC	OXC
2.	C_2MS_2		OXC	OXC	OXC	OXC	OXC
3.	CS	Wollastonite	OC	OC	OC	---	---
4.	C_2S	Calcium orthosilicate	---	---	---	---	---
5.	CAS_2	Anorthite	C	C	C	C	---
6.	MA	Spinel	---	---	---	OXC	OXC
7.	CMS_2	Diopside	---	OC	OC	---	---
8.	CaS	Calcium sulphide	OXC	OXC	OXC	OXC	OX
9.	MnS	Manganese sulphide	C	---	---	---	OC
10.	Fe_2O_3	Hematite	OC	OC	OC	OC	X
11.	FeS	Pyrrohotite	---	---	---	---	OC

*C stands for CaO
A " " Al_2O_3
S " " SiO_2
M " " MgO

**O observed optically
X determined by X-ray
C determined by calculation from chemical analysis.

and their limitations (57). It is quite apparent from the data in table 20B that, subject to the choice of an index, the same slag can be graded differently. The main difficulty, as in the past, is the placement of Al_2O_3 as an acid or base and in the evaluation of the Indian slag which has comparatively a high content of Al_2O_3, this makes all the difference to the values of indices. More recently luminescence under ultraviolet light has been recommended by Kramer (175) for evaluating the hydraulicity but Chopra and Taneja did not find this test reliable. (170). Welch (176) has also expressed a similar view.

Keil and Locher (174) have shown that the role of aluminium ions in glassy structure can be either as 'network former' or 'network modifier'. In the latter role aluminium ions act like calcium ions. Further, aluminium ions in the synthetic slag glasses containing 36 to 44 per cent CaO are considered to act partly like a base. Accordingly, this should be true of the Indian slag which contains low lime and high alumina and high strengths should be attainable with the Indian slag. But actually the strengths have not been found to be high (96,160). Chopra and Taneja (177) therefore studied the state of coordination of aluminium in synthetic $CaO-Al_2O_3-SiO_2$ glasses and have found that aluminium ions form part of the tetrahedra network and exist in fourfold coordination.

RANGES OF COMPRESSIVE STRENGTH

100—200 Kgs/Cm²

200—300 Kgs/Cm²

300—400 Kgs/Cm²

400—500 Kgs/Cm²

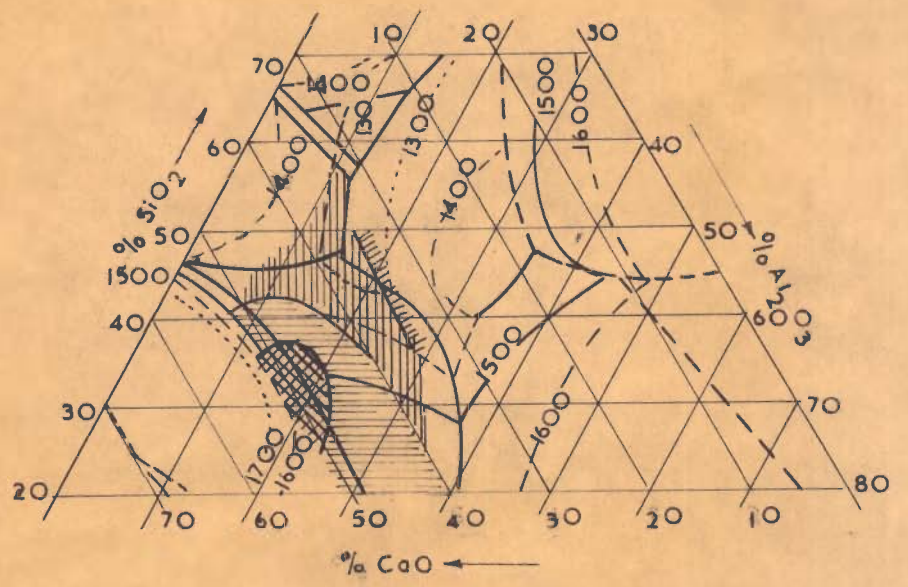

FIG.26. COMPRESSIVE STRENGTH VALUES, OBTAINED AFTER 28 DAYS, OF GLASSES OF THE $CaO - Al_2O_3 - SiO_2$ - MgO SYSTEM STIMULATED BY MEANS OF PORTLAND CEMENT CLINKER.

DATA REFERRING TO A 5 PERCENT MgO LEVEL
(ACCORDING TO KEIL & LOCHER, 1958.)

Activation of the Slag

Keil and Locher (174) have given diagrams (Fig. 26) showing ranges of optimum compressive strengths values of glasses under clinker activation in the field of a 5 per cent MgO content of the four-component system $CaO-MgO-Al_2O_3-SiO_2$. Similar diagrams for clinker and sulphate activation have been given by Tanaka, Sakai and Yanane (178). The compositions of the Indian slags are far removed from the optimum compositions e.g., 15.5 per cent Al_2O_3, 35 per cent SiO_2 and 51.5 per cent CaO for clinker activation and 18 - 20 per cent Al_2O_3, 50 per cent CaO and 30 - 32 per cent silica for sulphate activation. In fact, the compositions of Indian slags fall either very near the minimum ranges of compressive strengths or somewhat higher than those indicated in Fig. 26. But the work done by Chopra and Patwardhan (96) and Lahiri and Chatterjee (160) shows that actually the strengths are much better than predicted from their compositions. This could be due to the beneficial effects of minor constituents.

Pozzolanic Activity

According to Malquori (56) there are as yet no sufficiently reliable tests for predicting a prior how pozzolanic material mixed with hydrated lime or Portland cement in mortar or concrete will behave, either from the stand-point of mechanical-strength performance

or from that of reduction of free calcium hydroxide in the hardened binder. However, lime reactivity test and Fratini test (179) are considered to be most valuable. The lime reactivity of many Indian pozzolanic materials has been reported from time to time (101,158,159,162). The original and calcined fly ash sample (Durgapur) of this study passed the lime reactivity test (i.e., the value was more than 6000 p.s.i.). Fratini test also showed the samples to possess good pozzolanic activity.

Comparative Physical Properties of Cements

The important physical properties of the slag and pozzolanic cements and also that of supersulphated cement are summarized in tables 22 and 23. The main deductions from the published papers (96-101,157-163) and tables (22 and 23) are :

(1) the slag cements prepared from the low lime and high alumina slag develope strengths at a slower rate compared to those being produced elsewhere from slags of high calcium and low to medium alumina contents and consequently the former attains strengths equal to those of the ordinary Portland cement somewhat later i.e., at or after 3 months,

(2) for the same replacement, the reduction in strength of 1:6 concrete is not as much as in the standard 1:3 cement-sand mortar compacted on a standard vibrator (96). The differences arise probably from a higher initial volume of pores in mortar if the rate of formation of hydrated phases in mortar and concrete is assumed to be the same,

TABLE - 22

Physical Properties of Experimental Cements

Physical property	PBF Cement 65 clinker: 35 slag	PBF Cement 55 clinker: 45 slag	BFP Cement 35 clinker: 65 slag	PZC Cement 75 clinker: 25 F.as
1:3 Standard mortar strength per cent of control				
3 days	67.6	58.6	-	-
7 "	63.5	64.2	-	56.4
28 "	89.4	84.7	-	77.0
1:6 Concrete strength per cent of control				
28 days	83.3	72.8	72.3	-
3 months	91.9	82.7	76.7	-
6 months	99.4	88.0	-	-
Heat of hydration at 28 days in cals/g	55.3	39.1	-	-
Sulphate resistance compared to that of Portland cement	slightly greater	much greater	-	-

TABLE - 23

Comparison of the Physical Properties of the Trial Supersulphated Cement with Belgian and British Supersulphated Cements

S.No.	Property	Trial cement from Indian slag	Sealithor (Belgian)	Frodingham (British)
1.	Fineness			
	Specific surface (Blaine) cm^2/g	4,000	4,980	5,000
2.	Standard consistency			
	(Water required, per cent)	27.0	-	28.0
3.	Setting Time (minutes)			
	Initial	235	18 - 85	120 - 240
	Final	420	85 -205	180 - 360
4.	Soundness			
	Le Chatelier expansion, mm	0.0	0.5 -1.0	1.0
	Autoclave expansion, per cent	0.112	0.05	-
5.	Mortar compressive strength, kg/cm^2			
	1:3 cement-sand vibrated cubes			
	3 days	169	311	197
		(2403)*	(4423)	(2802)
	7 "	246	495	282
		(3498)	(7039)	(4010)
	28 "	449	671	493
		(6385)	(9572)	(7011)
	90 "	817	---	599
		(11618)		(8518)
	180 "	857	---	---
		(12201)		
6.	Concrete compressive strength, kg/cm^2			
	10 cm cubes, mix 1:6 by volume			
	w/c = 0.6	423 - 458	401	338
7.	Sulphate resistance	Resistant	Resistant	Resistant

*The values in Paranthesis give strengths in lb/in^2

(3) with an increase in the slag content, the decrease in strengths of the slag cements compared to that of Portland cement is comparatively lower. This may be due to a lower porosity of the sediment, differences in the nature of gels and hydrated phases produced on hydration, and the absence of $Ca(OH)_2$,

(4) the sulphate resistance of the Portland blast-furnace cements (table 22) is not as good as reported in the literature for similar type of cements (61). This may be due to higher content of alumina in the Indian slag and a slower rate of strength development

(5) though the supersulphated cement prepared from the Indian slag does not possess as high strengths as the Belgian cement 'Sealithor', it is comparable to the British supersulphated cement (table 23). The British cement is prepared from slag having comparatively a lower lime content (180),

(6) the trial supersulphated cement from the Indian slag, however, has shown excellent resistance to the effect of sulphate waters up to 4 years of storing (61),

(7) the strengths of Portland cement with fly ash replacement of 20 per cent do not equal those of the Portland cement even in six months (101), and

(8) the optimum temperature of calcination of clay for preparing surkhi should be chosen with the end use in view i.e., if strength is important, it should be 600 - 800°C and 1000°C if resistance to sulphate attack is important (163,164).

Hydrated Solid Phases Formed and Strength Development in the Hardened Pastes

Portland Cement Paste

The strengths of the pastes of the PC, PBF, BFP and PZC cements prepared at a W/C ratio of 0.40 and cured for different periods are given in table 24. The

TABLE - 24

Compressive Strengths of Different Cements at w/c Ratio of 0.40 (Curing in Water at 27 ± 2°C)

Designation of cement	Composition of cement	Strengths in Pounds Per Square Inch					
		24 hrs	36 hrs	3 days	7 days	28 days	90 days
PC	Ordinary Portland cement	1396	3071	3674	4637	7128	8040
PBF	65 PC: 35 SL(g)*	905	1985	2733	4368	6943	8288
BFP	35 PC: 65 SL(g)	400	1366	2019	3392	4625	6897
PZC	75 PC: 25 F(c)*	1177	1725	3084	3853	6418	9210
SSC	70 SL: 20 G: 5 PC*	-	-	3700	4920	5880	9978

* SL(g) stands for granulated slag, F(c) for fly ash calcined at 700°C and G stands for gypsum calcined at 750°C.

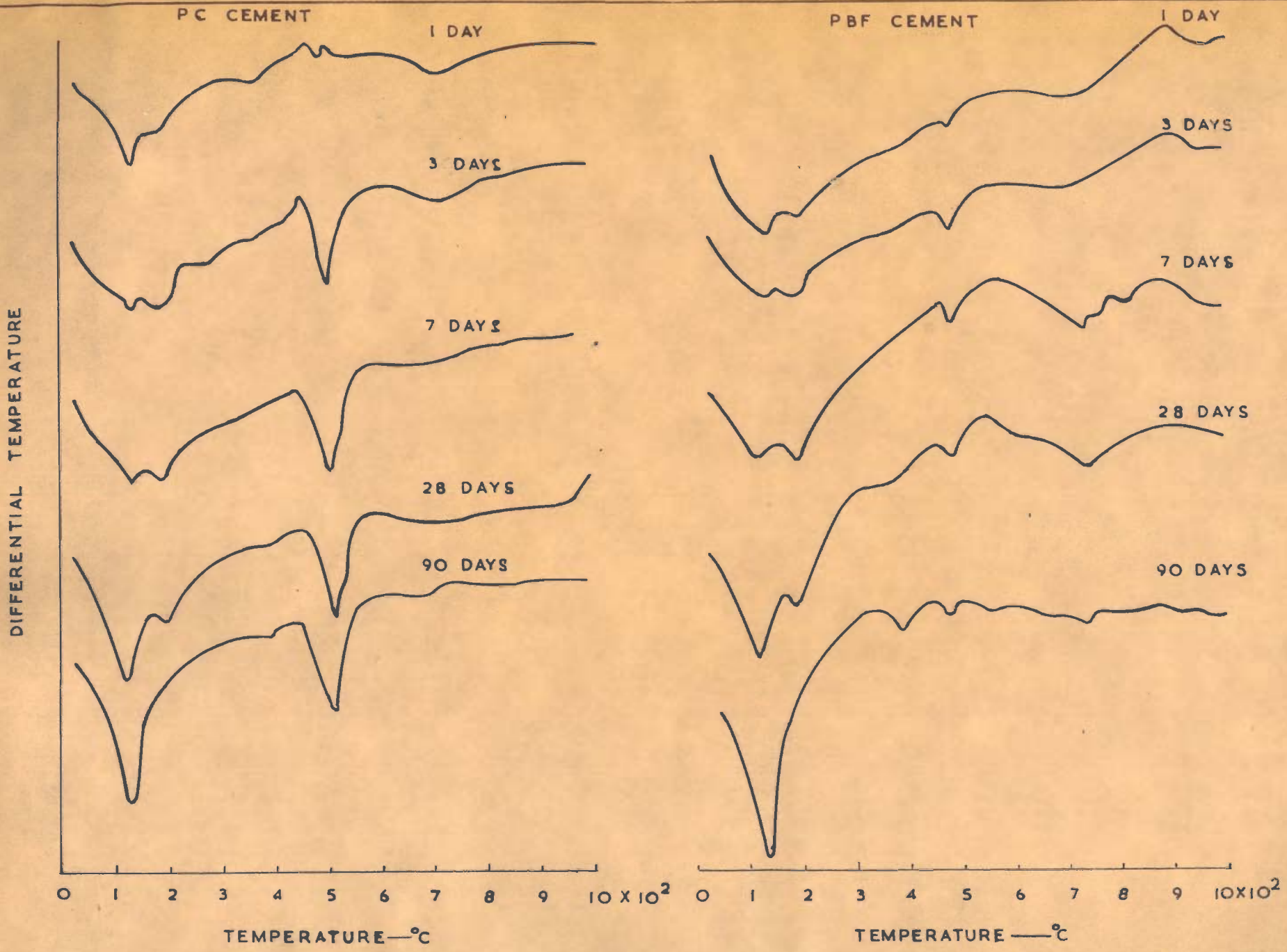

FIG. 27. DATA CURVES OF HYDRATED CEMENTS ($W/C = 0.40$)

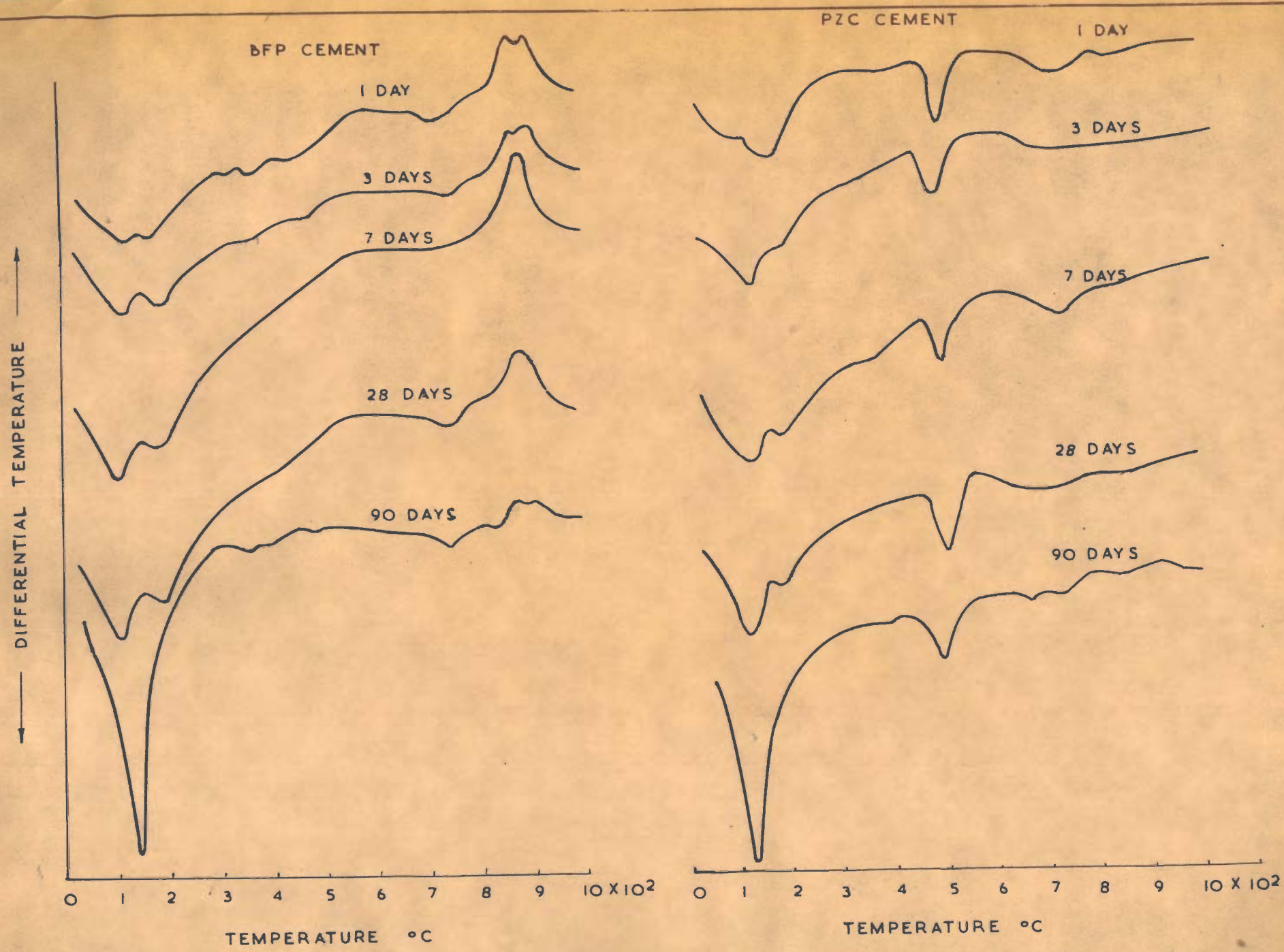

FIG.28. DTA CURVES OF HYDRATED CEMENTS ($W/C = 0.4$)

thermograms for each of the above four hydrated cements for ages of 1 to 90 days are shown in Figs. 27 and 28.

Ettringite, tetra and tri-calcium aluminate hydrate are formed in the Portland cement paste at one day as is evident from the endothermic peaks at 135°, 185° and 360°C respectively (Fig. 27). A small quantity of calcium hydroxide (495°C) and calcite (710°C) are also formed. The 3-days thermogram shows that tobermorite gel (Taylor's nomenclature for the tobermorite group is given at the end of this Chapter) is also formed since the first endothermic peak is no longer sharp. Also the quantity of C_3AH_6 has decreased and instead the quantity of $C_4A.aq.$ has increased as evident from the 185°C peak which is no longer shallow. This peak also may be due to monosulfoaluminate, formed probably by part transformation of ettringite. The quantity of calcium hydroxide has increased manifold. Because of the formation of tobermorite gel, gain in strength is more than 100 per cent.

At 7 days ~~there~~ no C_3AH_6 is present. There is a slight increase in the quantity of tobermorite gel and monosulfoaluminate. Correspondingly the strength gain from 3 to 7 days is not high. At 28 days the quantity of tobermorite gel has increased very much as evident from the extent of peak at about 130°C and as expected the strengths also rise by about 56 per cent.

The peak at 185°C is rounded now and a small inflection appears at 380°C, the latter is due to the formation of a hydrogarnet. From 28 days to 90 days the increase in strength is high and so is the increase in the quantity of tobermorite gel. A well defined peak at 380°C shows clearly the presence of hydrogarnet. The continuous slope from about 170° to about 360°C is probably due to dehydration of aluminate and related phases i.e., calcium aluminate hydrates (including $C_4A.aq.$), sulfoaluminate and carboaluminate. These phases appear to be present in amorphous state.

PBF Cement Paste

The thermograms of the PBF cement show similar patterns with few differences (Fig. 27). The peak development and therefore the formation of hydrated phases is no different from the PC cement. However, the quantity of calcium hydroxide is far less in the PBF cement paste. Also the presence of the hydrogarnet phase in greater quantities is evident from a shallow peak at 360°C and a sharp peak at 385°C in the 28 and 90 days thermograms respectively. It may be noted that the extent of tobermorite gel peak is nearly the same in the two cements i.e., PC and PBF at 28 days and so are the strengths. At 90 days though the strengths are equal, the first endothermic peak in the PBF cement occurs at somewhat higher temperature (142°C).

BFP Cement Paste

It may be concluded that $Ca(OH)_2$ is hardly present in any significant amount in the hydrated BFP cement (Fig. 28). This is expected as the clinker content is only 35 parts. The extent of endothermic peaks in 1 and 3 days thermograms together with exothermic peaks (850 - 900°C) due to crystallization of slag show a lower degree of hydration and therefore lower strengths (table 24). Calcium aluminate hydrate (C_3AH_6) formed at one day disappears in about 7 days time as is evident from the gradual disappearance of the endothermic peak at 355°C. It appears C_3AH_6 gradually changes into $C_4A.aq.$ or sulfoaluminate because of the growing endothermic peak at about 185°C. The curves show that the slope from 200 - 500°C due to oxidation is continuous and much more than in the PC and PBF cement.

It is surprising that the first endothermic peak in 90 days thermogram of this cement occurs at slightly higher temperature i.e., at 142°C and the extent of the peak is greater than even the Portland cement. It appears to be due either to the presence of tobermorite gel of different CaO/SiO_2 and SiO_2/H_2O ratios or the presence of ettringite in somewhat greater quantity in this paste or both. The amount of hydrogarnet present at 90 days is also greater as shown by

the shallow endothermic peak at 360°C. The strength gain from 28 to 90 days was also large. It is interesting to note that the exothermic peaks between 850 - 900°C characteristic of crystallization of slag diminish in extent with increasing period of hydration.

PZC Cement Paste

The thermograms for the PZC cement show the same pattern as PC and PBF cements (Fig. 28). Calcium hydroxide is present in amounts lower than that of PC cement showing that the hydration proceeds at a slower rate and strength development is also lower (table 24). Since the calcined fly ash contains SiO_2, Al_2O_3 and Fe_2O_3 oxides in a poorly crystallized state or with structural defects, lime released from C_3S combines immediately to form amorphous hydrated solids of mixed oxides of the type Kalousek, Davis and Schmertz had reported earlier (16). This is evident from the nature of endothermic peaks between 100° and 180°C in one-day thermogram. A small quantity of ettringite is also formed as in other cements. After 3 days' time the hydrated solids are better crystallized. The presence of tobermorite gel (127°C) and $C_4A.aq.$ or monosulfo-aluminate or monocarboaluminate (180°C) is also indicated. Their quantities increase from 3 to 7 days when a small quantity of hydrogarnet (390°C) is also formed.

The thermograms at 28 to 90 days are similar to those of the Portland cement but, as in the BFP cement, the extent of the endothermic peak at 132°C is greater than that of the Portland cement showing that either tobermorite gel with different H_2O/SiO_2 ratio is present or ettringite is present in greater quantity. It may be noted that strength gain from 28 to 90 days is comparatively greater in the BFP and PZC cements compared to those of the PC and PBF cements for the corresponding period. This is a significant observation and will be discussed later in greater details.

X-ray Powder Data of Hardened Pastes

Table 25 gives the X-ray powder data of the four hydrated cements i.e., PC, PBF, BFP and PZC after 90 days. Since these are clinker based cements, C_3S and C_2S were found in all the cement; ferrite phase only in PC and PZC cements. The X-ray data confirms that calcium hydroxide is present in decreasing order in PC, PZC, PBF and BFP cements. In the PBF cement it is present in a very small quantity.

Recently Midgley (32), and Copeland, Kantro and Verbeck (71) have discussed the different methods of examination of the set cement. The identification by the X-ray powder analysis (table 25) was done in the light of their findings and views.

T A B L E - 25

X-ray Powder Diffraction Data of Hydrated Cements

Hydrated PC Cement (Sample B)			Hydrated PBF Cement (Sample G)		
d (A)	I/I_o	Identification	d (A)	I/I_o	Identification
9.75	w	E*	9.00	vw	MS
9.00	w	E,MS	8.40	m/b	A
7.70	w/b	A,MC	7.60	m/b	A,MC
7.25	vw	F	4.90	s	CH
5.60	vw	E	3.90	vvw	A
5.10	vw	H	3.85	vw	C
4.89	vs	CH,E	3.79	vw	MC
4.65	vw	E	3.34	vw	H
4.40	vw	E,H	3.29	vw	H?
3.99	vvw	MS	3.24	vw	E?
3.86	w	C,E	3.11	m	CH
3.45	w	?	3.06	vw	T
3.33	vw	H	3.03	m	C,T,C_3S
3.10	ms	CH	2.88	ms	MS,MC,A
3.03	m/b	C,T,C_3S	2.79	ms/b	T,MS
2.97	vvw	?	2.75	m	C_3S,C_2S
2.875	m	MS,MC,A	2.725	w	C_3S,F
2.78	m/b	E,H,T,MS	2.63	s	CH
2.75	m	C_3S,C_2S	2.57	vw	E?
2.72	vw	C_3S,C_2S	2.48	vvw	C
2.68	vw	E,F	2.44	mw	CH
2.66	vw	E	2.41	vw	E?
2.625	vvs	CH	2.28	w	C
2.54	vw	MC,H	2.18	mw	C_3S
2.47	vvw	MS,A	2.16	vvw	A
2.44	w	CH	2.10	w	C
2.41	vw	E	2.05	vvw	MS,A
2.28	w	C	2.025	m/b	E?
2.20	vw	E	1.975	vw	MC
2.18	w	E,C_3S			
2.16	vw	Tc			
2.145	vvw	E,A			
2.10	vw	C			
2.045	w	MS,A			
2.025	w/b	E			
1.98	vw	MC			

* E= ettringite; T= tobermorite; MS= monosulfoaluminate; MC= monocarboaluminate; A= $C_4A.aq.$; H= hydrogarnet; CH= calciumhydroxide; C= calcite; C_3S= $3CaO.SiO_2$; C_2S= $2CaO.SiO_2$; F= ferrite phase; Q= quartz; M= melilite in unreacted slag.

Table 25 (Cont'd.)

Hydrated BFP Cement (Sample L)			Hydrated PZC Cement (Sample P)		
d (A)	I/I_o	Identification	d (A)	I/I_o	Identification
9.80	m	E	9.75	m	E*
8.95	vw	E,MS	8.25	vvw	A
8.25	vvw?	A	7.60	vw	A,MS
7.60	mw	A,MC	5.60	w	E
5.60	w	E	4.895	vs	CH
4.90	w	CH	4.69	vvw	E
4.69	vvw	E	4.25	m	Q
3.88	mw	E,A+?	3.875	w	E,A
3.35	s	H	3.69	vvw	?
3.11	vw	CH	3.59	vvw	E
3.07	vw	T	3.35	s	Q
3.04	m	C,C_3S	3.29	vvw	H?
2.88	s	MS,MC,A	3.11	m	CH
2.79	m	T,MS,C_3S	3.04	s	C,T,C_3S
2.75	m	C_2S	2.88	mw	MS,MC,A
2.72	vw	C_3S,C_2S	2.78	m	E,T,H,C_3S
2.67	vvw	E	2.75	mw	C_2S
2.63	m	CH	2.73	w	C_3S,C_2S
2.62	vw	?	2.69	mw	E,F
2.56	vw	E	2.63	vs	CH
2.49	w	C,E	2.61	vvw	E
2.44	w	CH	2.55	vw/b	E
2.41	vw	E	2.49	vvw	C,E
2.29	w	C	2.45	w	Q,CH
2.195	m	E	2.405	vvw	E
2.15	vvw	E,A	2.28	m	C,Q
2.125	vvw	E	2.205	w	E
2.10	vvw	C	2.19	vw	E,C_3S
2.09	vw	E?	2.12	w	E,Q
2.05	vw	MS,A	2.09	vw/b	E
2.025	s	E,M?	2.05	vw	MS,A
			2.025	w	E+?
			1.98	mw	MS

* E=ettringite; T= tobermorite; MS= monosulfoaluminate; MC= monocarboaluminate; A= $C_4A.aq.$; H= hydrogarnet; CH= calcium hydroxide; C= calcite; $C_3S = 3CaO.SiO_2$; $C_2S = 2CaO.SiO_2$; F= ferrite phase; Q= quartz; M= melilite in unreacted slag.

Table 25 (Cont'd.)

Hydrated SSC Cement (Sample T)		
d (A)	I/I_o	Identification
10.90	vvw	C_2AH_8?
9.80	vvs	E
8.90	w	E,MS
5.60	vs	E,C_2AH_8?
4.96	m	H
4.83	vw	E
4.69	vs	E
4.02	w	E
3.88	vs	E
3.68	w	M
3.60	mw	E
3.49	vs	E
3.47	w	M
3.34	s	H
3.27	vw	E
3.24	mw	E
3.03	mw	C,T,C_3S
3.01	w	?
2.85	ms	M,C_2AH_8
2.80	vw	
2.78	s	E,H
2.695	vvw	?
2.675	w	E
2.61	m	E
2.56	vs	E
2.525	vw	E
2.48	vw	C,E
2.465	vw	MS
2.45	vvw?	M
2.41	w/b	E?
2.34	vw	E+?
2.325	s	?
2.28	vw	C
2.225	w	H?
2.20	vs	E
2.18	mw	?
2.145	m	E,H?
2.12	vvw	E
2.08	mw	E+?
2.055	vw	MS
2.02	m/b	M
1.98	vw	MC

* E= ettringite; T= tobermorite; MS= monosulfoaluminate; MC= monocarboaluminate; A= $C_4A.aq.$; H= hydrogarnet; CH= calcium hydroxide; C= calcite; C_3S= $3CaO.SiO_2$; C_2S= $2CaO.SiO_2$; F= ferrite phase; Q= quartz; M= melilite in unreacted slag.

While discussing the calcium aluminate and calcium ferrite hydrates, Copeland, Kantro and Verbeck (71) mentioned a distinct group of lines appearing at 5.07, 4.40, 3.32, 2.26 and 2.01 and 1.72 A in all Portland cement pastes except type IV which is low in Al_2O_3 and in Fe_2O_3. After considering the various possible phases which could be present these authors have concluded that the lines are due to a ferrite-aluminate solid solution; the latter, i.e., the hydrogarnet, is believed to have a composition in the vicinity of $C_6AFS_2H_8$ (71).

It may be noted that the Portland cement paste shows lines at 5.1, 4.40, 3.33, 2.28, 2.05 A (table 25) and therefore the above hydrogarnet is present in it. But in the PBF, BFP and SSC cements the line at 3.33 A now occurs at 3.34 - 3.35 A and is much stronger in the BFP and PZC pastes; but there are no lines corresponding to 5.1 and 4.40 A. It is difficult to identify the hydrogarnet phase in the PBF, BFP and SSC cements but all the same its presence is evident from the X-ray data as well as the thermograms (Figs. 27 and 28).

Supersulphated Cement Paste

Chopra and Kishan Lall (98) have studied the sulphate activation of low lime and high alumina slag with a view to preparing supersulphated cement. The important findings are that for this type of slag, besides the activator calcined gypsum, the optimum

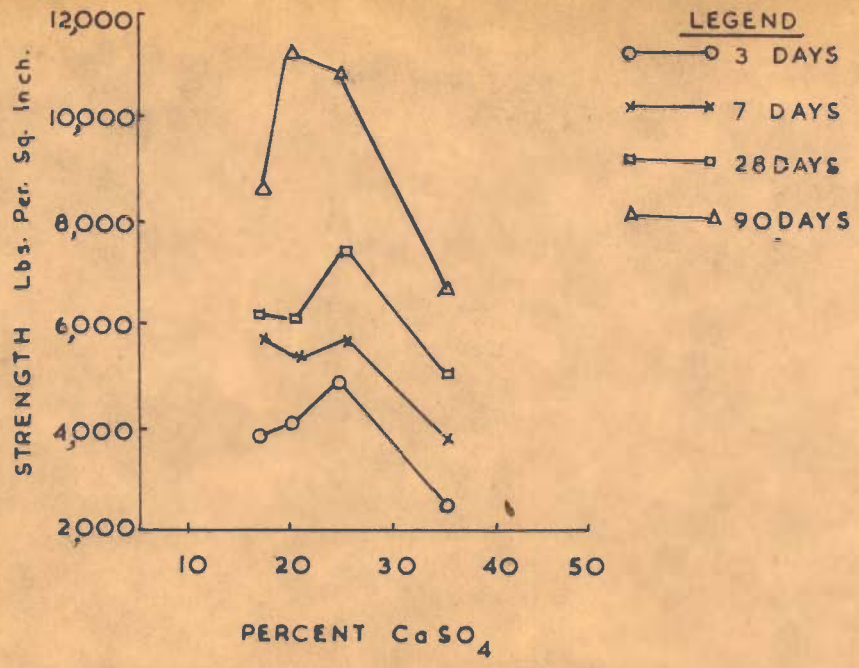

FIG.29A. EFFECT OF $CaSO_4$ ON STRENGTH

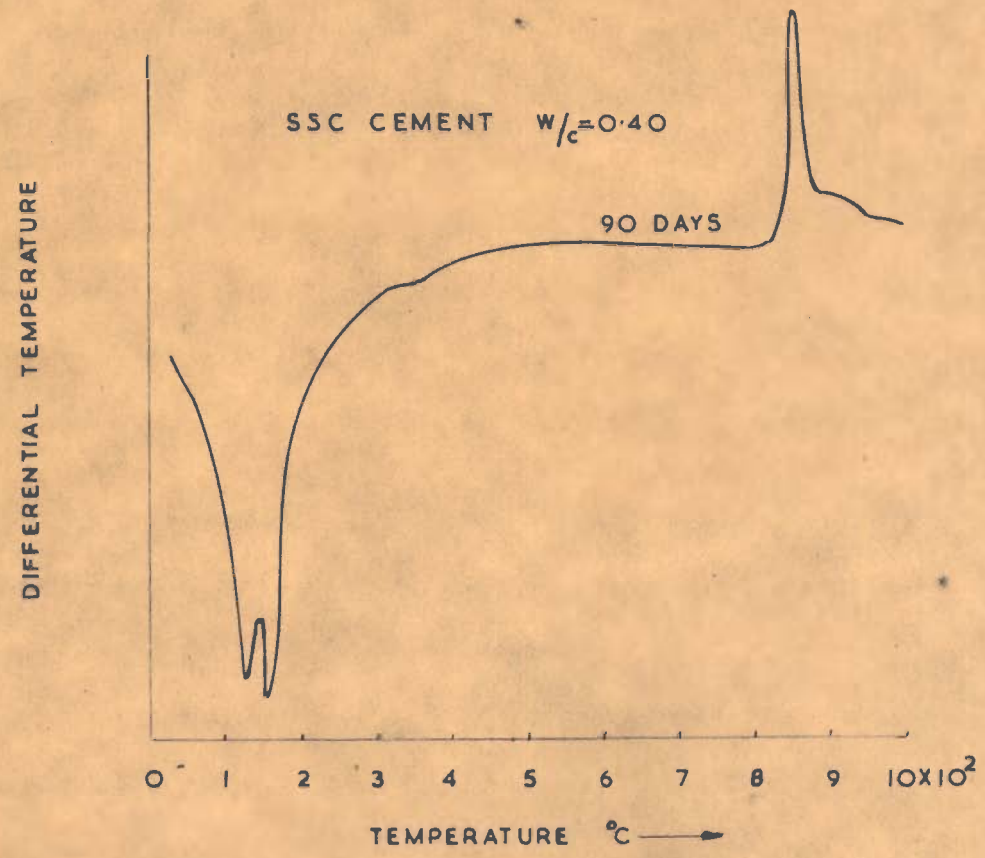

FIG.29B. D T A CURVE OF SUPER SULPHATED CEMENT

content of clinker is 5 per cent against 2 per cent recommended by Tanaka and Takemoto (181). The optimum temperature of calcination of gypsum was found to be 750°C.

The trial cements prepared by mixing slag, calcined gypsum and clinker in the proportions usually employed in the manufacture of supersulphated cement did not show good strength development. The determination of unreacted $CaSO_4$ in the set cement showed practically complete depletion of $CaSO_4$ in three days time. In view of these results and high alumina content (22.6 per cent) of the slag, the effect of increased amounts of $CaSO_4$ on the development of strengths was studied. The results in Fig. 29A show the optimum amount of $CaSO_4$ to be 25 per cent. The overall optimum composition of the SSC cement was thus 70/25/5 of slag/calcined-gypsum/clinker.

Chopra and Kishan Lall (98) had reported the differential thermal analysis of the supersulphated cements prepared from the Indian slag. The thermograms of the hydrated supersulphated cement of the above composition had shown the formation of the high sulphate form of sulfoaluminate (ettringite) at all ages as evident from the large endothermic peak at 150 - 175°C. The small inflection at 270°C in the 90 days curve was ascribed to the decomposition of the hydroxyl bound to Al in the ettringite. The extent of the endothermic

at about 160°C shows that the maximum quantity of ettringite had been formed at 28 days. The X-ray data (table 26) shows that the composition of the cementitious phase at 28 days was almost $3CaO.Al_2O_3.3CaSO_4.31H_2O$. At all other ages the ettringite phase seemed to have lower SO_3 and Al_2O_3 ratio. Since the longest spacing at these ages occurs at 9.71 A, the SO_3-Al_2O_3 ratio was more than 2.58 according to the findings of Midgley and Rosaman (33). The formation of a solid solution of $3CaO.Al_2O_3.3CaSO_4.aq.$ in $3CaO.Al_2O_3.3Ca(OH)_2$ aq. which has been reported by Nurse (180) as the cementing solids in set pastes of supersulphated cement prepared from the British slags of relatively low CaO/SiO_2 ratios, is quite likely. The lines at 5.02, 2.55 and 1.82 A in the 7 days old samples indicate the presence of di-calcium aluminate hydrate. The existence of Gehlinite hydrate was also indicated in one of the hydrated cements containing calcined gypsum in an amount lower than the optimum (98).

The supersulphated cement mix used in the present study was slag/calcined-gypsum/clinker as 70/25/5 and the 90 days thermograms (Fig. 29B) and X-ray data (table 25) are for the sample (i.e., T) prepared at a W/S ratio of 0.40. The thermogram shows the presence of calcium silicate hydrate, ettringite and a hydrogarnet corresponding to the endothermic peaks at 130°, 152° and 355°C respectively. The X-ray data shows additionally the presence of monosulfoaluminate (table 25).

T A B L E -26

X-ray Diffraction Data of the Trial Supersulphated Cement

Cement K 55 (25 per cent $CaSO_4$)							
3 days		7 days		28 days		90 days	
d(A)	I/I$_o$	d(A)	I/I$_o$	d(A)	I/I$_o$*	d(A)	I/I$_o$
9.71	vvs	9.71	vvs	9.82	vww	9.71	vvs
5.60	w	5.60	ms	5.68	vww	5.60	wm
4.69	vww	5.02	vw	4.67	vvw	4.69	vvw
3.88	vww	4.69	vw	3.91	vw	3.88	vww
3.49	w	3.88	wm	3.52	vw	3.49	vw
3.34	vw	3.49	w	2.79	vww	3.34	wm
3.02	vw	3.34	w	2.33	vvs	3.02	vw
2.55	vw	3.02	vww	2.20	vvw	2.55	vw
2.20	vw	2.86	vww	2.02	s	2.20	vvw
		2.55	vw			1.82	s
		2.28	vvw				
		2.20	vww				
		1.82	ms				

* Intensities in relation to the strongest line of Al at 2.23 A

DISCUSSION

Effect of Hydrated Phases on Hardening

A comparison of the thermograms (Figs. 27 and 28) and the different hydrated solids identified by the X-ray and D.T.A. techniques (table 27) showed only a general agreement between the results of the Portland cement and the three clinker-based cements. However, the following discussion will show the significance of differences as far as details are concerned.

Tobermorite gel is the main strength giving hydrate in the set Portland cement and it appears to be true of the PBF, BFP and PZC cements if the extent of the first endothermic peak is compared with the remaining peaks in each case. Tobermorite gel is believed to have a CaO/SiO_2 ratio not less than 1.5 (51). Compared to the thermograms of the hydrated pastes of PC, the PBF pastes show greater similarity than any other paste. Though the absence of the longest spacing (table 25) shows that the tobermorite phase is not well crystallized in the PBF cement and hence it could be designated as 'tobermorite gel', a higher peak temperature of the first endotherm suggests that the tobermorite phase is either having a different CaO/SiO_2 and H_2O/SiO_2 ratios or its microstructure is different.

The cements BFP and PZC, however, show differences in their first endothermic peak from the

TABLE - 27

Hydrated Solid Phases in Cements Cured for 90 Days

Designation of cement	Identification of Phases	
	DTA	X-ray Analysis
PC	End 130°C Tobermorite, Ettringite End 372°C Hydrogarnet End 510°C Calcium Hydroxide End 710°C Calcite	Tobermorite, Ettringite Monosulphoaluminate Monocarboaluminate Tetra calcium aluminate hydrate Hydrogarnet, calcium hydroxide calcite, C_3S, βC_2S, Ferrite
PBF	End 140°C Tobermorite, Ettringite? End 390°C Hydrogarnet End 482°C Calcium Hydroxide End 560°C (Small inflection) ? End 745°C Calcite	Tobermorite Monosulphoaluminate Monocarboaluminate Tetra calcium aluminate hydrate Hydrogarnet, calcium hydroxide calcite, C_3S, βC_2S
BFP	End 141°C Tobermorite, Ettringite End 375°C Hydrogarnet End 485°C Calcium Hydroxide End 745°C Calcite	Ettringite, Tobermorite Monosulphoaluminate Monocarboaluminate Hydrogarnet, calcium hydroxide calcite, C_3S, βC_2S
PZC	End 132°C Tobermorite, Ettringite End 385°C Hydrogarnet End 495°C Calcium Hydroxide End 660°C Quartz End 840°C Calcite	Ettringite, Tobermorite Monocarboaluminate Tetra calcium aluminate hydrate Hydrogarnet?, calcium hydroxide Calcite, C_3S, βC_2S, Ferrite, Quartz
SSC	End 130°C Tobermorite End 152°C Ettringite End 355°C Calcium Aluminate Hydrate (probably C_3AH_6)	Ettringite, Monosulphoaluminate Tobermorite Hydrogarnet Dicalcium aluminate hydrate ?

beginning. The shape of the endotherm and peak temperatures indicate that the composition of the tobermorite-like hydrates is probably different for these cements. In fact, formation of amorphous hydrated solids of mixed oxides of the type Kalousek had reported earlier (16), instead of tobermorite-like hydrates, is suggested in the PZC cement thermogram at one day. At 90 days the first endothermic peak in BFP cements occurs at slightly higher temperature than in the PC cement. This may be due to a greater quantity of tobermorite-like hydrates or due to the presence of a small quantity of ettringite as shown by X-ray data. The latter appears to be more true as the clinker content is low and so also the rate of hydration and hence formation of tobermorite in greater quantities is less likely. But differences in the microstructure of tobermorite can also account for the higher peak temperature.

Earlier it had been brought out that the requirement of SO_4 ions for the formation of ettringite was far greater when the slag is comparatively richer in alumina. The calcined fly ash used in the PZC also contained higher alumina (i.e., about 20 per cent compared to about 7 per cent in clinker). Consequently in the pastes of PBF, BFP and PZC cements, the sulphate ions from gypsum (retarder) first get chemisorbed on the surfaces of slag or pozzolana particles and form gelations coatings of sulfoaluminates probably with SO_3/Al_2O_3

ratios lower than 3 as is evident from a comparison of the shape and extent of endothermic peaks for ettringite (130°C) and monosulfoaluminate-monocarboaluminate and tetracalcium aluminate hydrate etc. (at about 180°C) in the 3 days thermograms of the above cements. These gelatinous coatings and those of calcium silicate hydrates formed on clinker hydration retard further action. This accounts for lower early strengths of the PBF, BFP and PZC cements. The strength development in these cements up to this stage appears to be entirely due to the hydrolysis of anhydrous constituents present in the clinker portion of these cements and obviously the strength is higher if the proportion of clinker is higher.

But when gelatinous coatings crystallize, reaction between lime and oxides, such as silica, alumina and iron oxide etc., takes place and give rise to the formation of hydrates of calcium silicate, aluminate and ferrite; and hydrogarnets etc., the gain in strengths is large. The gain in strengths at this stage will be mostly due to formation of additional quantities of calcium silicate hydrate phase (tobermorite gel) because $C_4A.aq.$, the most predominant aluminate phase may hardly contribute towards strength development. Since the thermograms show a rising slope in between 170° to about 360°C, the presence of one or more of the phases, such as aluminates, sulfoaluminate, gehlinite hydrate, hydrogarnet in poorly crystalline state which is indicated by the

X-ray data, is masked. But, it is quite likely that these phases are also contributing towards strength development.

According to Locher (69) three fields of high compressive strength exist. In the glasses containing large amount of silica and little alumina the hydraulic hardening is due to the formation of calcium silicate hydrate. In the field of alumina cement, hardening is due to formation of calcium aluminate hydrates poor in lime. In between these two areas of the 'silicatic' and the 'aluminatic' hardening lies the field of 'silico-aluminate' hardening which is responsible for the high strengths of glasses with medium contents of silica and alumina such as those present in slag. Formation of gehlinite hydrate is believed to be the cause of high strengths. This is silico-aluminic hardening of Locher. But it has also been reported that the gehlinite hydrate may react with calcium hydroxide to form a hydrogarnet (C_3ASH_4) and the transformation is accompanied by a decrease in strength. In short, the formation and stability of gehlinite hydrate is involved.

Gehlinite hydrate was not observed in any of the hydrated slag cements except one of the supersulphated cements (98). This is in conformity with the theory that it is not stable in presence of lime and accordingly its presence can be expected only in the SSC cement. Its presence in the PBF, BFP and PZC cements is also discounted because the strength gain from 28 to

90 days is higher in these cements compared to PC cement, showing that no transformation of gehlinite hydrate to hydrogarnet could have taken place. This is further supported by the observation that the composition of the hydrogarnet phase in the cements PC and PBF is not different (table 25). It may therefore be inferred that the high strength gain from 28 to 90 days is not due to silicoaluminic hardening. However, the alumina bearing hydrated phases such as aluminates and sulfoaluminates which are formed in greater quantities because of a high alumina content of the Indian slag may contribute towards strength development on account of Van der Waals forces, as these may be mostly present in poorly crystallized state.

Earlier it was concluded that ettringite is responsible for the early strengths of the SSC cement but secondary phases, such as calcium silicate hydrate and alumina gel contribute greatly towards the strengths at later ages. Since the hydrated SSC cement was found to possess high specific surface (table 35), it may be concluded that even in this cement wherein interacting surfaces are supposedly connected by strong chemical and mechanical bonds, the influence of enormous surfaces still plays a prominent role.

The above discussion shows that because of the variable degree of crystallinity of a hydrated phase;

deformed or restricted crystal structure of the others and colloidal nature of gel particles, the effect of the relative quantities of different hydrated phases in a paste is exceedingly difficult to estimate. It is not therefore possible at this stage to establish the relative influences of the physical and chemical bonds between surfaces on the strength of the cement. While such an estimation may be possible in the pastes of pure anhydrous compound, such an approach is not likely to lead to any tangible conclusion in a cement paste wherin the composition of the hydrated phases is hetrogeneous and complex.

APPENDIX

The tobermorite group. Tentative system of classification and nomenclature (after Taylor)

C/S ratio	Degree of crysallinity		
	High	Low	Very Low
	Complete X-ray powder pattern with hkl reflections	Poor X-ray powder pattern with (mainly) basal and hk or hk0 reflections	Very poor X-ray powder pattern consisting of one or more hk lines or bands. No basal reflections
Below 1.5 (near 0.83 when fully crystalline).	(14-A tobermorite [a]) (11.2-A tobermorite or tobermorite [b]) (9.35-A tobermorite or riversideite)	CSH(I) [d] ... Plombierite.[e]	
1.5 and over (probably 1.5-1.75 when fully crystalline).	("12.6-A tobermorite" [c]) ("10-A tobermorite" [c])	CSH(II) [f] .. CSH gel.[g]	

Notes and synonyms.

a Syn. plombierite

b Syn. $C_4S_5H_5$, well crytallized calcium silicate hydrate (I)

c The assumption that these species have C/S > 1.5 is purely tentative.

d Crumpled foils. CSH(I) is here short for "calcium silicate hydrate (I)" and does not imply CSH composition. Syn. CSH(B), 0.8-1.33 C/S hydrate etc.

e Gelatinous natural mineral of composition $C_{0.8}SH_2$

f Fibrous. CSH(II) is here short for "calcium silicate hydrate(I and does not imply CSH composition. Syn. C_2SH(II), C_2SH_2, 1.5-2.0 C/S hydrate etc.

g Short for "calcium silicate hydrate gel," the phase formed in C_3S pastes at room temperature; or any other similarly ill-crystallized material of similar composition. Syn. tobermorite (G), Hydrate (III) etc.

CHAPTER 5

PHYSICAL PROPERTIES AND THE MICROSTRUCTURE OF THE HARDENED CEMENT PASTES

Introduction

Powers (1,6) has made a comprehensive study of the physical properties of the hardened Portland cement paste. According to him the physical properties of a paste are not much influenced by differences in the chemical composition of the different Portland cements because any hydratedPortland cement is predominantly colloidal and this point of similarity outweighs the points of difference attributable to differences in chemistry. But this cannot be true of the slag and pozzolanic cements because the work reported in Chapters 1 to 4 has clearly shown that compared to the Portland cement the physico-chemical properties of formation of the slag and pozzolanic cement pastes and the development of hydrated solid phases are definitely different. The physical properties of the hardened pastes of slag and pozzolanic cements were therefore investigated. The important studies made were the fixation of water in different forms, capillary and gel porosity of the hardened pastes, specific surface and morphology of the hydrated phases, gel-space ratio versus strength and intrinsic strengths of'cement gels'etc.

MATERIALS

The samples of PC, PBF, BFP, PZC and SSC (table 1) were the same as those described in Chapter 4.

EXPERIMENTAL

Preparation of Paste

The pastes were prepared at W/C ratios of 0.40 - 0.60 in a Waring blendor as described in Chapter 1. The pastes at W/C ratio of 0.30 however, were prepared by hand mixing as these were too stiff for mixing in the blendor.

Compressive Strength of Hardened Paste

The compressive strengths were determined as per the method described in Chapter 4.

Preparation of Granular Samples

The granular samples were prepared according to the procedure outlined in Chapter 4.

Determinations on Granular Samples of Hardened Pastes

Determination of Non-evaporable Water (W_n/C)

Five to six grams of crushed material passing a no. 30 and retained on no. 80 U.S. sieve was spread in a weighing dish of about 5 cm diameter. The dishes were

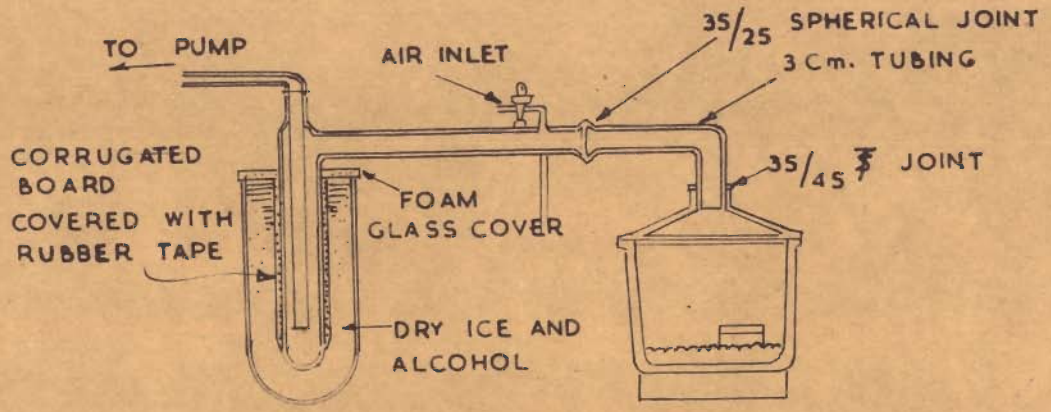

FIG.30. DIAGRAM OF APPARATUS

(AFTER COPELAND & HAYES)

transferred to a vacuum desiccator with concentrated sulphuric acid as desiccant. The desiccator was connected to a high vacuum pump which held the pressure in the system below 30 microns. The samples got dried in about 10 days' time as shown by constant weight. The dishes were then transferred quickly to a vacuum desiccator (Fig. 30)which contained no desiccant but was connected to a dry ice trap (-79 °C) which in turn was connected to a the high vacuum system mentioned above as per the method of Copeland and Hayes (182). The drying was continued until weighings on successive days indicated weight loss of about 1 mg of water per g of paste for one day of drying. The second drying was generally complete within 3 days.

After the drying was over the weighed sample was ignited at 1050°C in a platinum crucible for about 30 minutes, then weighed and replaced in a furnace for a second ignition period of 10 minutes and reweighed to check that there is no change in weight. The weight loss on ignition of the dried sample is due to the volatilization of non-evaporable water and volatile material present in the original cement. The loss on ignition of the original cement was determined separately. Then non-evaporable water was calculated from

$$W_n/C = \frac{W_1}{W_2}(1 - L) - 1 \qquad \ldots (1)$$

where W_n/C = non-evaporable water content, grams non-evaporable water per g of original cement,

W_1 = weight of granular sample before ignition, g,

W_2 = weight of granular sample after ignition, g,

L = ignition loss of original cement, grams per g of original cement.

Thermogravimetric Analysis

A Stanton thermobalance milligramme model HT-M was used for obtaining weight loss curves. The furnace is capable of heating the sample up to 1400°C. The heating rate was maintained at 6° per minute and the furnace temperature control was generally correct within ± 2°C. The thermocouple used was a platinum; 12 per cent rhodium/platinum couple with each wire of 0.5 mm. The chart speed was 6 inches per hour.

An alumina crucible (weighing about 14 g) for holding about 1 g of sample was used. The vacuum dried sample (containing only non-evaporable water) was ground to pass a no. 100 U.S. sieve. Sample weighing 1000 mg (accurate) was taken each time so that the weight loss could be read directly from the thermogram. The analysis was done at ordinary atmospheric pressure.

Determination of Total Water (W_t/C)

According to Powers method (183) about 5 g of the sample to be saturated was placed in a 50 ml Erlenmeyer flask fitted with a special stopper that

permits either the introduction of water from a burette or a stream of dried air free from CO_2. Water was slowly dropped on to the sample till the sample, upon being shaken, gathers into a lump and clings to the flask. Dry air is then passed over the sample for 2 minutes while it is being shaken. Drying by air is continued at intervals until the particles just fail to cling to each other and to the flask i.e., the particles are free flowing. The total water held by the sample in this condition corrected for the loss on ignition of the original cement is W_t.

Copeland (129) has determined W_t directly from the loss on ignition of the saturated paste at 1050°C by correcting for the ignition loss of the original cement. The results are expressed as total water per unit weight of cement, W_t/C. This method was employed throughout because the mixing of paste was done under vacuum thus eliminating air bubbles. Also it is simpler and quite accurate which is shown by the comparative values for the same samples by the two method.

Comparative Values of W_t/C for Hydrated Cement

Sample	Values of W_t/C	
	Powers Method	Copeland's Method
(1)	0.314	0.342
(2)	0.416	0.456
(3)	0.482	0.490
(4)	0.593	0.610
(5)	0.422	0.456
(6)	0.503	0.508

Determination of 'Apparent' Specific Volume of Total Water, V_t

The specific volume of the paste was determined (129) from the weighing of the samples of hardened pastes (2 in. cubes) in water and in saturated surface-dry condition in air. Since the pastes were mixed in vacuum, no air bubbles were present to vitiate the results. The apparent specific volume of total water, V_t, is simply the difference between the volume of a portion of the paste that contains 1 g of water and the original volume of cement in that. The latter is determined from the density of the cement itself.

Specific Volume of Granular Samples

Powers and Brownyard (184) had used both gaceous and liquid displacement fluids for determining the specific volume and found differences in results. The latter were explained on the basis of differences in size of molecule and differences in the interaction between solid and the fluid. Though the choice of displacement fluid is still controversial (185), Powers prefers helium for this purpose. Because of lack of facilities for determination of specific volume by helium displacement method, the choice in the present study fell on water because the size of molecules is in the same range as of various gases and much lower than that of organic liquids.

Specific Area of Hydrated Cements

The surface area was determined by exposing portions (about 5 g) of the previously dried (vacuum) granular samples of hardened pastes to atmospheres of different water vapour pressures. This was achieved by placing the samples over saturated solutions in evacuated desiccators until the weight of the exposed samples did not change more than 1 mg per g of dried sample per day (48) The equilibrium was considered to have been reached then. The desiccants used were $NaOH.H_2O$, $LiCl.H_2O$, $KC_2H_3O_2.1\frac{1}{2}H_2O$, sulphuric acid (55.01 per cent) and $K_2CO_3.2H_2O$ giving partial pressures (p/p_s) at 25 °C as 0.0703, 0.1105, 0.2245, 0.250 and 0.4276 respectively.

According to the BET Theory (186), the total amount of water vapour adsorbed at low partial pressures (up to about 0.40 p/p_s) is related to the amount of water vapour required to form a monomolecular layer on the solid by the equation

$$\frac{W}{V_m} = \frac{C\,(p/p_s)}{(1 - p/p_s)(1 - p/p_s + C\,p/p_s)} \quad \ldots (2)$$

where W = quantity of vapour adsorbed at any pressur p/p_s,

V_m = quantity of adsorbate required for a complete condensed layer on the solid, the layer being one molecule deep,

p = existing vapour pressure

p_s = pressure of saturated vapour

C = constant related to the heat of adsorption.

The BET equation (2) may be written in the form

$$\frac{1}{W}\left(\frac{X}{1-X}\right) = \frac{1}{V_m C} + \frac{C-1}{V_m C} X \qquad \ldots (3)$$

where $X = p/p_s$ and W = g of adsorbate per g of adsorbent. This is a straight line equation in which $\frac{(C-1)}{V_m C}$ is the slope and $\frac{1}{V_m C}$ is the intercept on Y-axis. By plotting the adsorption data in terms of $\frac{1}{W}\left(\frac{X}{1-X}\right)$ versus X, the values for C and V_m are obtained.

Since V_m is the amount of water vapour required to form one layer of molecules on the surface of the adsorbent, V_m is assumed to be proportional to the surface area, S. The equation relating these quantities is :

$$S = a_1 (V_m N/M) \qquad \ldots (4)$$

where S = surface area of adsorbent, sq cm per g,

a_1 = surface area covered by one molecule

N = 6.06×10^{23} = number of molecules in g - molecular weight,

M = Molecular weight of the adsorbate.

The latest value for a_1 is 11.4 A^2 per molecule (185). The above equation (4) therefore would be

$$S = (38 \times 10^6) V_m \text{ sq cm per g}$$

Thus surface area can be calculated if V_m is obtained by plotting the adsorption data as mentioned above.

Electron Microscopic Examination

It is necessary to break down hardened paste into a finely subdivided powder before the examination. The vacuum dried samples were lightly ground to a very fine powder avoiding contamination from extraneous matter. The fine powder was suspended in ethyl alcohol as per recommendations in the literature (25). Ethyl alcohol is said to give protection from CO_2 attack. The suspension was transferred to the support film on a 200 mesh grid and the specimens were examined in an electron microscope, RCA Emu - 2A Type, with 50 KV accelerating voltage. The order of the vacuum at the time of the microscopic examination was of the order of $5x10^{-5}$ mm of mercury. The magnification was x8800.

RESULTS

Hydration and Non-evaporable Water in Pastes

The data on non-evaporable water contents of saturated pastes prepared from five different cements at a water-cement ratio of 0.40 are reported in table 28. In the beginning all thewater in a paste is present in a free state i.e., the total water content of the paste should be equal to the mixing water. But since it was shown earlier that bleeding capacity of a paste is a variable factor, it is obvious that the total water content of the pastes to start with may be different

TABLE - 28

Effect of Curing Period on Progressive Fixation of Water and Reduction in Total Porosity of Hardened Pastes

Designation of cement	Period of curing hr/days	Water-cement ratio w_o/c	Non-evap. water w_n/c	Evap. water w_e/c	Total water w_t/c	Ratio w_n/w_t	Ratio w_n/w_o	Total porosity
1	2	3	4	5	6	7	8	9
PC	36 hrs	0.385	0.102	0.317	0.419	0.243	0.265	0.457
	3 days	0.368	0.107	0.291	0.398	0.269	0.291	0.403
	7 days	0.374	0.113	0.290	0.403	0.280	0.302	0.400
	28 days	0.376	0.156	0.258	0.414	0.376	0.415	0.355
	90 days	0.400	0.198	0.258	0.456	0.434	0.495	0.352
PBF	36 hrs	0.370	0.061	0.326	0.387	0.158	0.165	0.449
	3 days	0.355	0.097	0.288	0.385	0.252	0.273	0.397
	7 days	0.375	0.114	0.294	0.408	0.279	0.304	0.404
	28 days	0.363	0.159	0.238	0.397	0.400	0.438	0.340
	90 days	0.375	0.182	0.240	0.422	0.431	0.485	0.329

Table 28 (Cont'd.)

1	2	3	4	5	6	7	8	9
BPF	36 hrs	0.414	0.071	0.344	0.415	0.171	0.172	0.396
	3 days	0.407	0.074	0.374	0.448	0.167	0.183	0.503
	7 days	0.376	0.075	0.301	0.376	0.199	0.200	0.413
	28 days	0.379	0.118	0.276	0.394	0.290	0.311	0.380
	90 days	0.373	0.136	0.267	0.403	0.337	0.365	0.374
PZC	36 hrs	0.376	0.083	0.311	0.394	0.210	0.220	0.424
	3 days	0.374	0.091	0.308	0.399	0.228	0.242	0.423
	7 days	0.370	0.106	0.289	0.395	0.268	0.286	0.396
	28 days	0.365	0.153	0.245	0.398	0.384	0.419	0.336
	90 days	0.362	0.162	0.234	0.396	0.409	0.447	0.330
SSC	3 days	0.395	0.048	0.373	0.421	0.126	0.122	0.507
	7 days	0.379	0.071	0.310	0.380	0.169	0.187	0.423
	28 days	0.411	0.110	0.339	0.449	0.251	0.268	0.457
	90 days	0.398	0.152	0.298	0.450	0.337	0.382	0.404

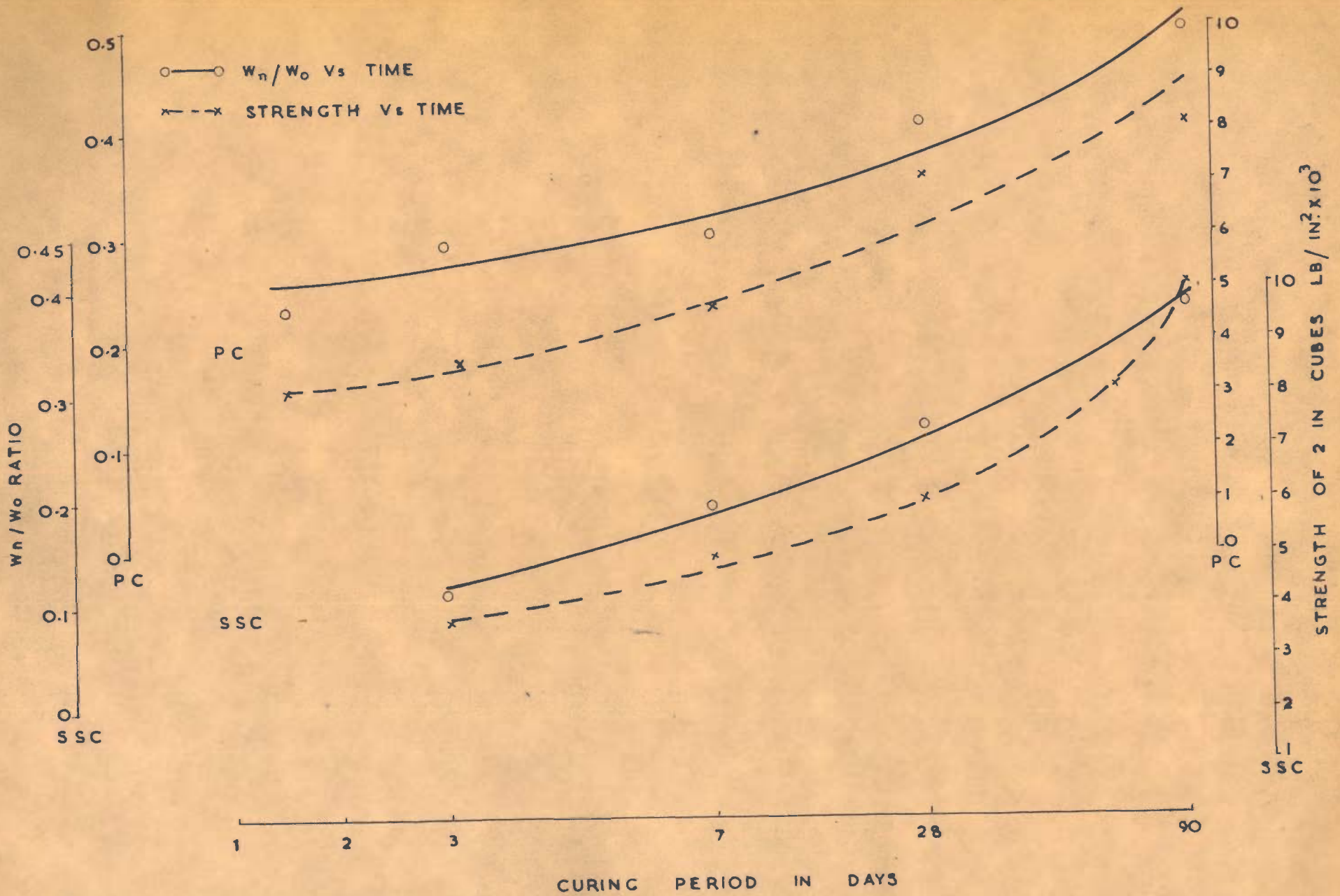

FIG. 31. PROGRESSIVE HYDRATION & STRENGTH DEVELOPMENT OF CEMENTS

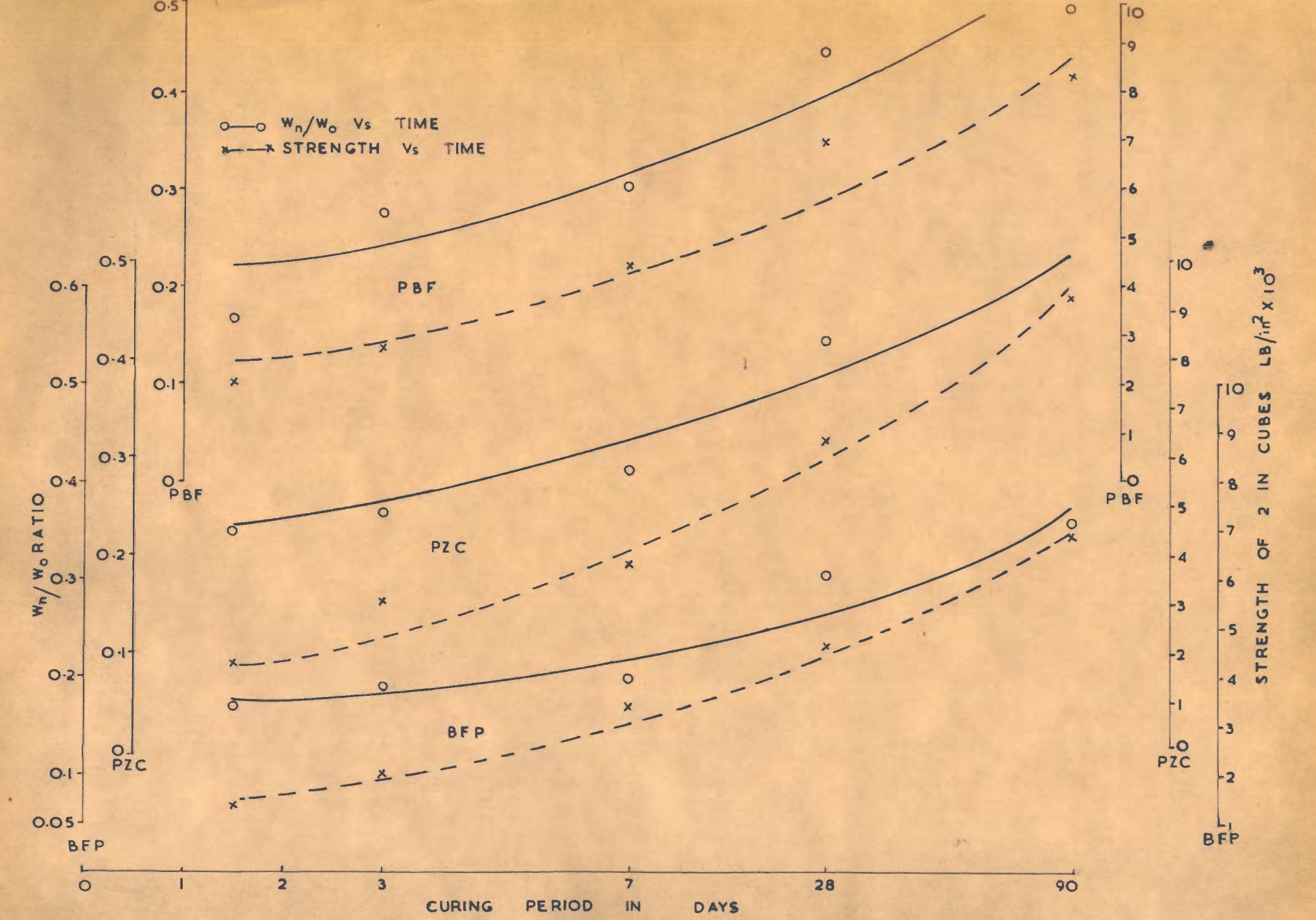

FIG. 32. PROGESSIVE HYDRATION AND STRENGTH DEVELOPMENT OF CEMENTS

even though the pastes might have been prepared at the same water-cement ratio under controlled conditions. In other words, while comparing the contents of non-evaporable water of different pastes, this factor should be taken into account.

As hydration progress, part of the total water present in a paste gets fixed up as water of hydration and a corresponding amount of water must enter the paste to maintain conditions of saturation. The data of total water content per g of anhydrous cement reported in tables 28 and 29 show that variations from specimen to specimen can be appreciable. Therefore, a comparison of the contents of non-evaporable water at different stages of hydration in a particular paste or at a particular stage of hydration in different pastes is strictly not correct. If, however, the non-evaporable water content is expressed as a fraction of the total water in a saturated paste, the comparisons would be more realistic. Such values of W_n/W_t are reported in the tables 28 and 29. Alternatively, the values of W_n/W_o i.e., the ratio of non-evaporable to total water present in the beginning can be compared (table 28 and 29).

Effect of Time on Hydration and Strengths of Different Cements

A plot of W_n/W_o versus time for the five cements are shown in Figs. 31 and 32 along with the curve

TABLE - 29

Effect of w/c Ratio on Fixation of Water and Total Porosity of Hardened Pastes at 90 days

Designation of cement	Water-cement ratio		Non-Evap. water	Evap. water	Total water	Ratio	Ratio	Total porosity
	w/c	w_o/c	w_n/c	w_e/c	w_t/c	w_n/w_t	w_n/w_o	
1	2	3	4	5	6	7	8	9
PC	0.300	0.276	0.147	0.167	0.314	0.468	0.532	0.243
	0.400	0.400	0.198	0.258	0.456	0.434	0.495	0.352
	0.500	0.460	0.199	0.311	0.510	0.390	0.433	0.414
	0.550	0.504	0.197	0.359	0.556	0.354	0.391	0.471
	0.600	0.557	0.210	0.400	0.610	0.344	0.376	0.516
PBF	0.300	0.313	0.162	0.147	0.309	0.524	0.517	0.213
	0.400	0.375	0.182	0.240	0.422	0.431	0.485	0.329
	0.500	0.467	0.204	0.312	0.516	0.395	0.428	0.411
	0.550	0.483	0.201	0.349	0.550	0.365	0.416	0.462
	0.600	0.492	0.185	0.368	0.553	0.334	0.376	0.483

TABLE - 28

Effect of Curing Period on Progressive Fixation of Water and Reduction in Total Porosity of Hardened Pastes

Designation of cement	Period of curing hr/days	Water-cement ratio w_o/c	Non-evap. water w_n/c	Evap. water w_e/c	Total water w_t/c	Ratio w_n/w_t	Ratio w_n/w_o	Total porosity
1	2	3	4	5	6	7	8	9
PC	36 hrs	0.385	0.102	0.317	0.419	0.243	0.265	0.457
	3 days	0.368	0.107	0.291	0.398	0.269	0.291	0.403
	7 days	0.374	0.113	0.290	0.403	0.280	0.302	0.400
	28 days	0.376	0.156	0.258	0.414	0.376	0.415	0.355
	90 days	0.400	0.198	0.258	0.456	0.434	0.495	0.352
PBF	36 hrs	0.370	0.061	0.326	0.387	0.158	0.165	0.449
	3 days	0.355	0.097	0.288	0.385	0.252	0.273	0.397
	7 days	0.375	0.114	0.294	0.408	0.279	0.304	0.404
	28 days	0.363	0.159	0.238	0.397	0.400	0.438	0.340
	90 days	0.375	0.182	0.240	0.422	0.431	0.485	0.329

Table 28 (Cont'd.)

1	2	3	4	5	6	7	8	9
BPF	36 hrs	0.414	0.071	0.344	0.415	0.171	0.172	0.396
	3 days	0.407	0.074	0.374	0.448	0.167	0.183	0.503
	7 days	0.376	0.075	0.301	0.376	0.199	0.200	0.413
	28 days	0.379	0.118	0.276	0.394	0.290	0.311	0.380
	90 days	0.373	0.136	0.267	0.403	0.337	0.365	0.374
PZC	36 hrs	0.376	0.083	0.311	0.394	0.210	0.220	0.424
	3 days	0.374	0.091	0.308	0.399	0.228	0.242	0.423
	7 days	0.370	0.106	0.289	0.395	0.268	0.286	0.396
	28 days	0.365	0.153	0.245	0.398	0.384	0.419	0.336
	90 days	0.362	0.162	0.234	0.396	0.409	0.447	0.330
SSC	3 days	0.395	0.048	0.373	0.421	0.126	0.122	0.507
	7 days	0.379	0.071	0.310	0.380	0.169	0.187	0.423
	28 days	0.411	0.110	0.339	0.449	0.251	0.268	0.457
	90 days	0.398	0.152	0.298	0.450	0.337	0.382	0.404

TABLE - 29

Effect of w/c Ratio on Fixation of Water and Total Porosity of Hardened Pastes at 90 days

Designation of cement	Water-cement ratio		Non-Evap. water	Evap. water	Total water	Ratio	Ratio	Total porosity
	w/c	w_o/c	w_n/c	w_e/c	w_t/c	w_n/w_t	w_n/w_o	
1	2	3	4	5	6	7	8	9
PC	0.300	0.276	0.147	0.167	0.314	0.468	0.532	0.243
	0.400	0.400	0.198	0.258	0.456	0.434	0.495	0.352
	0.500	0.460	0.199	0.311	0.510	0.390	0.433	0.414
	0.550	0.504	0.197	0.359	0.556	0.354	0.391	0.471
	0.600	0.557	0.210	0.400	0.610	0.344	0.376	0.516
PBF	0.300	0.313	0.162	0.147	0.309	0.524	0.517	0.213
	0.400	0.375	0.182	0.240	0.422	0.431	0.485	0.329
	0.500	0.467	0.204	0.312	0.516	0.395	0.428	0.411
	0.550	0.483	0.201	0.349	0.550	0.365	0.416	0.462
	0.600	0.492	0.185	0.368	0.553	0.334	0.376	0.483

TABLE - 31

Apparent Specific Volume of Total Water in Hardened Pastes and the Ratio w_n/w_t
(Pastes prepared at a w/c ratio of 0.4 and Cured for Different Periods)

Designation of cement	Age of Paste hr/days	Specific volume of cement v_c cc/g	Density of Paste Saturated g/cc	Specific volume of paste cc/g	Total Water wt/c	Apparent specific volume of total water v_t	Ratio w_n/w_t
1	2	3	4	5	6	7	8
PC	36 hrs	0.319	2.025	0.493	0.419	0.911	0.243
	3 days	0.319	2.035	0.491	0.398	0.925	0.269
	7 days	0.319	2.042	0.489	0.403	0.913	0.280
	28 days	0.319	2.045	0.488	0.414	0.898	0.376
	90 days	0.319	2.035	0.491	0.456	0.870	0.434
PBF	36 hrs	0.329	1.993	0.501	0.387	0.950	0.158
	3 days	0.329	2.003	0.499	0.385	0.942	0.252
	7 days	0.329	2.004	0.498	0.408	0.916	0.279
	28 days	0.329	2.030	0.492	0.397	0.903	0.400
	90 days	0.329	2.029	0.493	0.456	0.852	0.431

TABLE - 31

Apparent Specific Volume of Total Water in Hardened Pastes and the Ratio w_n/w_t
(Pastes prepared at a w/c ratio of 0.4 and Cured for Different Periods)

Designation of cement	Age of Paste hr/days	Specific volume of cement v_c cc/g	Density of Paste Saturated g/cc	Specific volume of paste cc/g	Total Water wt/c	Apparent specific volume of total water v_t	Ratio w_n/w_t
1	2	3	4	5	6	7	8
PC	36 hrs	0.319	2.025	0.493	0.419	0.911	0.243
	3 days	0.319	2.035	0.491	0.398	0.925	0.269
	7 days	0.319	2.042	0.489	0.403	0.913	0.280
	28 days	0.319	2.045	0.488	0.414	0.898	0.376
	90 days	0.319	2.035	0.491	0.456	0.870	0.434
PBF	36 hrs	0.329	1.993	0.501	0.387	0.950	0.158
	3 days	0.329	2.003	0.499	0.385	0.942	0.252
	7 days	0.329	2.004	0.498	0.408	0.916	0.279
	28 days	0.329	2.030	0.492	0.397	0.903	0.400
	90 days	0.329	2.029	0.493	0.456	0.852	0.431

Table 31 (Cont'd.)

1	2	3	4	5	6	7	8
BFP	36 hrs	0.335	1.896	0.527	0.415	0.989	0.171
	3 days	0.335	1.945	0.514	0.448	0.912	0.167
	7 days	0.335	1.961	0.510	0.376	0.974	0.199
	28 days	0.335	1.960	0.510	0.392	0.959	0.290
	90 days	0.335	1.989	0.520	0.403	0.918	0.337
PZC	36 hrs	0.341	1.954	0.512	0.394	0.956	0.210
	3 days	0.341	1.969	0.508	0.399	0.933	0.228
	7 days	0.341	1.970	0.507	0.395	0.937	0.268
	28 days	0.341	1.990	0.502	0.398	0.915	0.384
	90 days	0.341	1.996	0.500	0.396	0.908	0.409
SSC	3 days	0.336	1.941	0.515	0.381	0.983	0.126
	7 days	0.336	1.955	0.512	0.421	0.927	0.169
	28 days	0.336	1.950	0.511	0.449	0.907	0.251
	90 days	0.336	1.988	0.502	0.450	0.904	0.337

TABLE - 32

Apparent Specific Volume of Total Water in Hardened Pastes and the Ratio w_n/w_t
(Pastes Prepared at different w/c ratio but cured for 90 days)

Designation of cement	Water-cement ratio w_o/c	Sp.Vol. of cement v_c cc/g	Sp.Vol. of paste saturated cc/g	Total water w_t/c	Apparent Sp. Vol. of water v_t/	Ratio w_n/w_t
1	2	3	4	5	6	7
PC	0.276	0.319	0.452	0.314	0.875	0.468
	0.400	0.319	0.491	0.456	0.868	0.434
	0.460	0.319	0.516	0.510	0.892	0.390
	0.504	0.319	0.526	0.556	0.897	0.354
	0.557	0.319	0.541	0.610	0.904	0.344
PBF	0.313	0.329	0.460	0.309	0.884	0.524
	0.375	0.329	0.493	0.422	0.881	0.431
	0.467	0.329	0.520	0.516	0.869	0.395
	0.483	0.329	0.522	0.550	0.896	0.365
	0.492	0.329	0.525	0.553	0.880	0.334

Table 32 (Cont'd.)

1	2	3	4	5	6	7
BFP	0.289	0.335	0.473	0.312	0.917	0.371
	0.373	0.335	0.502	0.403	0.918	0.337
	0.478	0.335	0.535	0.505	0.931	0.311
	0.478	0.335	0.535	0.504	0.931	0.301
PZC	0.300	0.341	0.485	0.316	0.949	0.414
	0.362	0.341	0.500	0.396	0.912	0.409
	0.426	0.341	0.519	0.472	0.901	0.345
	0.444	0.341	0.524	0.490	0.905	0.324
SSC	0.310	0.336	0.480	0.339	0.904	0.413
	0.398	0.336	0.502	0.450	0.873	0.337
	0.472	0.336	0.526	0.509	0.897	0.257

TABLE - 34

Determination of Chemically Combined Water in Hardened Pastes by Thermogravimetric Analysis

Sample Particulars: Cement	w_o/c ratio	Loss in weight g/g of Dried Paste: Due to combined water 0-650°C	Due to $Ca(OH)_2$ 490-600°C	Due to carbonate 600-1000°C*	Total loss 0-1000°C	Water in cementitious hydrates, g/g (3) - (4)
1	2	3	4	5	6	7
PC	0.400	0.1780	0.0370	0.0195	0.1975	0.141
PBF	0.375	0.1560	0.0130	0.0050	0.1740	0.143
BFP	0.373	0.1090	0.0040	0.0070	0.1200	0.105
PZC	0.362	0.1410	0.0190	0.0210	0.1620	0.122
SSC	0.398	0.0900	0.0000	0.0020	0.0880	0.090
PC	0.557	0.1948	0.0330	0.0155	0.2103	0.161
PBF	0.492	0.1645	0.0135	0.0067	0.1847	0.151
PZC	0.444	0.1380	0.0170	0.0205	0.1585	0.121

* Loss from 600-1000°C may not be entirely due to calcium carbonate; some of it may be due to combined water. But the latter is neglected as it would be small.

Table 29 (Cont'd.)

1	2	3	4	5	6	7	8	9
BFP	0.300	0.289	0.116	0.196	0.312	0.371	0.401	0.313
	0.400	0.373	0.136	0.267	0.403	0.337	0.365	0.374
	0.500	0.478	0.157	0.398	0.505	0.311	0.328	0.524
	0.550	0.478	0.152	0.352	0.504	0.301	0.378	0.464
PZC	0.300	0.300	0.131	0.185	0.316	0.414	0.436	0.263
	0.400	0.362	0.162	0.234	0.396	0.409	0.447	0.330
	0.500	0.426	0.163	0.309	0.472	0.345	0.382	0.414
	0.550	0.444	0.159	0.331	0.490	0.324	0.358	0.440
SSC	0.300	0.310	0.140	0.199	0.339	0.413	0.451	0.282
	0.400	0.398	0.152	0.298	0.450	0.337	0.382	0.405
	0.500	0.472	0.131	0.378	0.509	0.257	0.277	0.500

for the development of strengths versus time of hydration. Though the curves show mainly the trends in progressive hydration and strength development, the differences in behaviour of the cements are clearly brought out. For example, all the clinker-based cements show at early ages lesser hydration and also a slower rate of strength development compared to that of the Portland cement.

Effect of W/C ratio on Hydration and Strengths

A comparison of the W/C ratios before and after bleeding (W_o/C) shows that the effects of bleeding on the hydration and strength development (tables 29 and 30) become increasingly important at higher water-cement ratios and these may be widely different in different types of cements (table 29). For example, the pastes of the BFP and PZC cements prepared at a W/C ratio of 0.55 finally had a W_o/C ratio of 0.478 and 0.444 respectively. Since W/C ratio influences strengths a great deal (table 30), these differences are important in any comparison of the strength properties of the different cements.

Apparent Specific Volume of Combined and Total Water in Hardened Paste

Though the non-evaporable water loses its identity in becoming an integeral part of the solid phase, Powers and Brownyard (187) considered the absolute volume of the hydrated solid phase as being equal to the original volume of the cement plus the volume of the non-evaporable

TABLE - 30

Compressive Strengths of Cements at Different w/c Ratios (After 90 days curing in water at 27 ± 2°C)

Designation of cement	Composition	Strengths in Pounds per Square Inch. Water to Cement Ratios				
		0.30	0.40	0.50	0.55	0.60
PC	Ordinary Portland cement	9691	8040	6944	4974	3320
PBF	65 PC: 35 SL(g)	11,181	8288	6944	6204	4378
BFP	35 PC: 65 SL(g)	9610	6897	6083	4116	-
PZC	75 PC: 25 F(c)	10,080	9210	5080	-	4906
SSC	70 S: 20G: 5PC	10,752	9978	7392	-	-

water and assigned a hypothetical specific volume to the non-evaporable water which, for obvious reasons, was found to be less than one. These workers also believed that the remaining water i.e., evaporable water could further be divided into gel water and capillary water on the basis of vapour pressure data. The gel water or the physically adsorbed part of the evaporable water was considered to possess specific volume less than 1.0. Thus the total water content of a saturated paste specimen was divided into (i) water with a specific volume less than 1.0, and (ii) free or evaporable water with a specific volume equal to 1.0. The apparent (or mean) specific volumes of total water in saturated pastes which were computed from the measured volumes of the saturated granular samples and the volumes and weights of the ingredients (assuming that the cement retained its original weight) were found by Powers and Brownyard to follow the relationship

$$V_t = 1 - 0.279\, W_n/W_t \qquad \ldots (5)$$

where V_t is apparent specific volume of total water, V_t was found to be a linear function of W_n/W_t and it was concluded that V_t in hardened paste containing no capillary space was 0.860. The mean specific volume of the gel water was estimated to be about 0.90 and that of capillary water as 1.0.

Copeland (129) also found that V_t was a linear

function of W_n/W_t but his best straight line did not pass through 1.0 when $W_n/W_t = 0$. He reported the mean specific volume of chemically free water in a saturated hardened Portland cement paste as 0.99, independent of the extent of hydration of the cement or the water-cement ratio of the paste. It was therefore concluded that there is no difference between the speicifc volume of gel water and capillary water in saturated pastes. The apparent specific volume of non-evaporable water, V_n, was found by extrapolation to be 0.74; the latter being lower than the value of Powers and Brownyard 0.82, which was calculated from helium displacement measurements. According to Copeland the use of the latter value appears to have led Powers and Brownyard to the conclusion that gel water was more dense than capillary water. This is supported by the thermodynamical treatment of the data by Copeland and his value of 0.398 for the specific volume of the hydration porducts which agrees very well with the 0.392 obtained by Powers and Brownyard using the water-displacement method.

Though there is no agreement between the views of different workers even upto-date (188) and there is a great scope of further research in this field which indeed is full of practical difficulties, the Copeland's approach was adopted in the present study because of its simplicity. Also the objective in the present study being limited to finding if the mean or

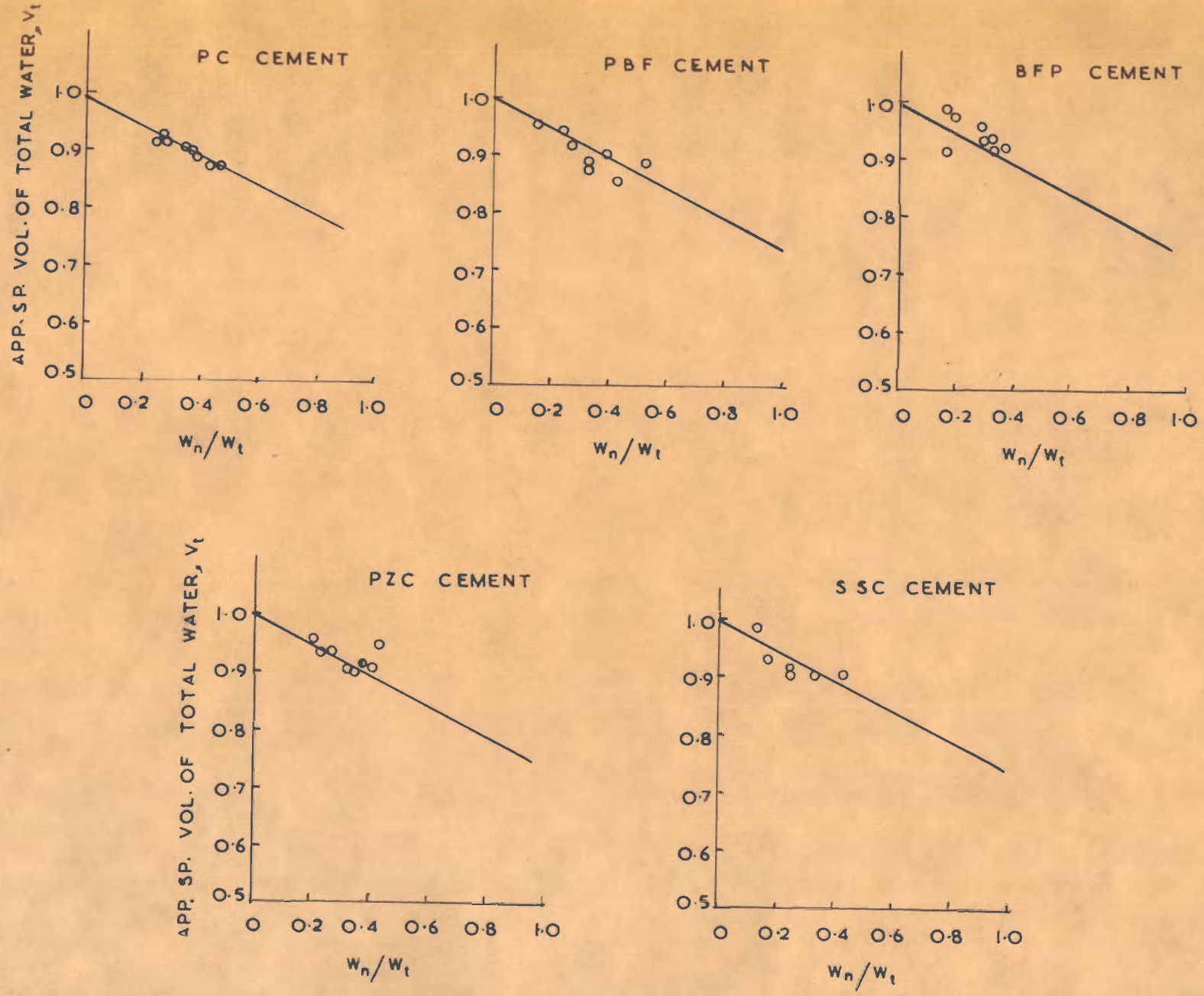

FIG. 33. RELATIONSHIP BETWEEN APP. SP. VOLUME OF TOTAL WATER (V_t) & W_n/W_t

apparent specific volume of the total water in a saturated hardened pastes of the cements such as PBF, BFP, PZC and SSC cements etc. is any different from that of the Portland cement and also if there are any differences in the apparent specific volumes of the evaporable and non-evaporable (or combined water).

W_n/W_t and density of a saturated paste were determined and V_t was calculated (tables 31 and 32). The plots of V_t versus W_n/W_t for saturated pastes of five different cements are shown in Fig. 33. The points represent different stages of hydration irrespective of the period of hydration or water-cement ratio of the paste. The relationship between V_t and W_n/W_t is a straight line relationship and for the Portland cement of this study the relationship (Fig. 33) is the same as reported earlier by Copeland i.e., $V_t = 0.99 - 0.25\ W_n/W_t$. According to it when $V_t = V_e = 0.99$ i.e., when all the water is present in free state i.e., the specific volume of evaporable water (V_e) is 0.99 And when $W_n/W_t = 1.0$, $V_t = V_n = 0.74$ i.e., the apparent specific volume of the non-evaporable water is 0.74.

The dispersion of points is such that no definite conclusions are possible but certain trends are obvious. For example, the mean specific volume of total water at a particular value of W_n/W_t is more or less the same in the PC, PBF and SSC cements but is slightly higher

TABLE - 31

Apparent Specific Volume of Total Water in Hardened Pastes and the Ratio w_n/w_t
(Pastes prepared at a w/c ratio of 0.4 and Cured for Different Periods)

Designation of cement	Age of Paste hr/days	Specific volume of cement v_c cc/g	Density of Paste Saturated g/cc	Specific volume of paste cc/g	Total Water wt/c	Apparent specific volume of total water v_t	Ratio w_n/w_t
1	2	3	4	5	6	7	8
PC	36 hrs	0.319	2.025	0.493	0.419	0.911	0.243
	3 days	0.319	2.035	0.491	0.398	0.925	0.269
	7 days	0.319	2.042	0.489	0.403	0.913	0.280
	28 days	0.319	2.045	0.488	0.414	0.898	0.376
	90 days	0.319	2.035	0.491	0.456	0.870	0.434
PBF	36 hrs	0.329	1.993	0.501	0.387	0.950	0.158
	3 days	0.329	2.003	0.499	0.385	0.942	0.252
	7 days	0.329	2.004	0.498	0.408	0.916	0.279
	28 days	0.329	2.030	0.492	0.397	0.903	0.400
	90 days	0.329	2.029	0.493	0.456	0.852	0.431

Table 31 (Cont'd.)

1	2	3	4	5	6	7	8
BFP	36 hrs	0.335	1.896	0.527	0.415	0.989	0.171
	3 days	0.335	1.945	0.514	0.448	0.912	0.167
	7 days	0.335	1.961	0.510	0.376	0.974	0.199
	28 days	0.335	1.960	0.510	0.392	0.959	0.290
	90 days	0.335	1.989	0.520	0.403	0.918	0.337
PZC	36 hrs	0.341	1.954	0.512	0.394	0.956	0.210
	3 days	0.341	1.969	0.508	0.399	0.933	0.228
	7 days	0.341	1.970	0.507	0.395	0.937	0.268
	28 days	0.341	1.990	0.502	0.398	0.915	0.384
	90 days	0.341	1.996	0.500	0.396	0.908	0.409
SSC	3 days	0.336	1.941	0.515	0.381	0.983	0.126
	7 days	0.336	1.955	0.512	0.421	0.927	0.169
	28 days	0.336	1.950	0.511	0.449	0.907	0.251
	90 days	0.336	1.988	0.502	0.450	0.904	0.337

TABLE - 32

Apparent Specific Volume of Total Water in Hardened Pastes and the Ratio w_n/w_t
(Pastes Prepared at different w/c ratio but cured for 90 days)

Designation of cement	Water-cement ratio w_o/c	Sp.Vol. of cement v_c cc/g	Sp.Vol. of paste saturated cc/g	Total water w_t/c	Apparent Sp. Vol. of water v_t/	Ratio w_n/w_t
1	2	3	4	5	6	7
PC	0.276	0.319	0.452	0.314	0.875	0.468
	0.400	0.319	0.491	0.456	0.868	0.434
	0.460	0.319	0.516	0.510	0.892	0.390
	0.504	0.319	0.526	0.556	0.897	0.354
	0.557	0.319	0.541	0.610	0.904	0.344
PBF	0.313	0.329	0.460	0.309	0.884	0.524
	0.375	0.329	0.493	0.422	0.881	0.431
	0.467	0.329	0.520	0.516	0.869	0.395
	0.483	0.329	0.522	0.550	0.896	0.365
	0.492	0.329	0.525	0.553	0.880	0.334

Table 32 (Cont'd.)

1	2	3	4	5	6	7
BFP	0.289	0.335	0.473	0.312	0.917	0.371
	0.373	0.335	0.502	0.403	0.918	0.337
	0.478	0.335	0.535	0.505	0.931	0.311
	0.478	0.335	0.535	0.504	0.931	0.301
PZC	0.300	0.341	0.485	0.316	0.949	0.414
	0.362	0.341	0.500	0.396	0.912	0.409
	0.426	0.341	0.519	0.472	0.901	0.345
	0.444	0.341	0.524	0.490	0.905	0.324
SSC	0.310	0.336	0.480	0.339	0.904	0.413
	0.398	0.336	0.502	0.450	0.873	0.337
	0.472	0.336	0.526	0.509	0.897	0.257

for the BFP and PZC cements.

V_n of the hydrated cement is a weighted average and depends upon the magnitude of the apparent specific volume of water of hydration in each of the individual hydrated phases and upon the weight fraction of each of the hydrated phases. In other words, composition of the cement may influence the value of V_n and this may be indicated by the position of the line. The plots of V_t versus W_n/W_t for the cements PBF, FBP, PZC and SSC also show a straight line relationship. The data indicate that V_n for the PBF and SSC cements is 0.74. On the other hand, Fig. 33 indicates that V_n for the BFP and PZC cements may be somewhat different than that of the Portland cement.

Porosity of the Hardened Paste

The pores in a paste are defined as spaces that can be occupied by water that is evaporable at a constant low external humidity at a given temperature. Pores are of two types, (i) gel pores - small pores between the gel particles, and (ii) capillary pores which are larger than gel pores and exist between aggregates of gel particles. Since both the capillary porosity and total porosity in a hardend paste have a profound influence on the physical properties, an accurate determination of porosity has been attempted by several workers; the work of Powers and Brownyard,

and of Copeland and Hayes and Powers being more important (6, 129).

Earlier it was shown that the partial specific volume of evaporable water in saturated Portland cement pastes was 0.99. The total pore volume of a saturated hardened paste would be the volume of the water present in the pores which can be estimated from the total water content and the partial specific volume of the water in a saturated paste. Similarly the gel pore volume can be estimated from the pastes which contain no capillary pores. The capillary pore volume is the difference between the total and gel pore volumes.

According to Copeland and Hayes (129), the total pore volume (p_t) and gel pore volume (p_g) are

$$p_t = 0.99 \ W_e = (W_t - W_n) \ 0.99 \qquad \ldots (6)$$

where 0.99 is partial specific volume of evaporable water i.e., W_e

$$p_g = 0.99 \times 2.38 \ V_m = 0.99 \times 2.38 \ k \ W_n = \ldots (7)$$

$$= 2.36 \ k \ W_n \qquad \ldots (7A)$$

where V_m is weight of water required to cover surface with ~~one~~ one molecule thick layer and
k is constant

amd $$p_c = p_t - p_g = 0.99 \left[W_t - (1 + 2.38 \ k) W_n \right] \ldots (8)$$

It may be noted from the above equations that pore volume is related to non-evaporable water and total water in a saturated hardened paste. Since porosity is the pore volume in unit volume of paste, it can be calculated from W_n/C and W_t/c by multiplying pore volume per

unit weight of cement by amount of cement in a unit volume of paste. The equations for total porosity (ϵ) and capillary porosity (ϵ_c) would be respectively

$$\epsilon = p_t/V_p = 0.99 \left[W_t/c - W_n/c\right] \frac{d_p}{1 + W_t/c} \quad \ldots (9)$$

$$\epsilon_c = p_c/V_p = 0.99 \left[W_t/6 - (1+2.38k)W_n/c\right] \frac{d_p}{1 + W_t/c} \quad \ldots (10)$$

where d_p is the density and V_p is the volume of paste. The values of the total porosity calculated as per equation (9) are reported in tables 28 and 29 respectively. The values of capillary porosity and gel porosity for 90 days cured pastes of different cements are areported in table 33.

Surface Areas of Hydrated Cements

The weight of water required to cover the surface of solid material with one molecule thick layer, V_m, is the most important quantity in the BET equation for determining the surface area. Recently Powers (185) has discussed the effects of various factors, including the proportionality between V_m and surface area, on the calculated surface areas of hydrated cement. While discussing as to how near one can get to the theoretical value of V_m, the practical difficulty of having a "bare" surface of hydrated cement has been mentioned by him. The other difficulty i.e., the calibration of V_m for a

T A B L E - 33

Porosities of 90 Days Cured Pastes of Different Cements

Designation of cement	w_o/c Ratio	Total porosity (1)	Capillary porosity (2)	Gel porosity (1) - (2)
PC	0.276	0.243	0.108	0.135
	0.400	0.352	0.166	0.182
	0.460	0.414	0.221	0.193
	0.504	0.471	0.266	0.205
	0.557	0.516	0.289	0.227
PBF	0.313	0.213*	0.063	0.150
	0.375	0.330	0.165	0.165
	0.467	0.411	0.261	0.150
	0.483	0.462	0.217	0.145
	0.492	0.483	0.294	0.189
BFP	0.289	0.313	0.175	0.138
	0.373	0.374	0.233	0.141
	0.478	0.524	0.284	0.240
	0.478	0.464	0.296	0.168
PZC	0.300	0.263*	0.158	0.105
	0.362	0.330	0.172	0.158
	0.426	0.414	0.250	0.164
	0.444	0.440	0.276	0.164

* Self desiccation might have taken place in these pastes because of low w_o/c.

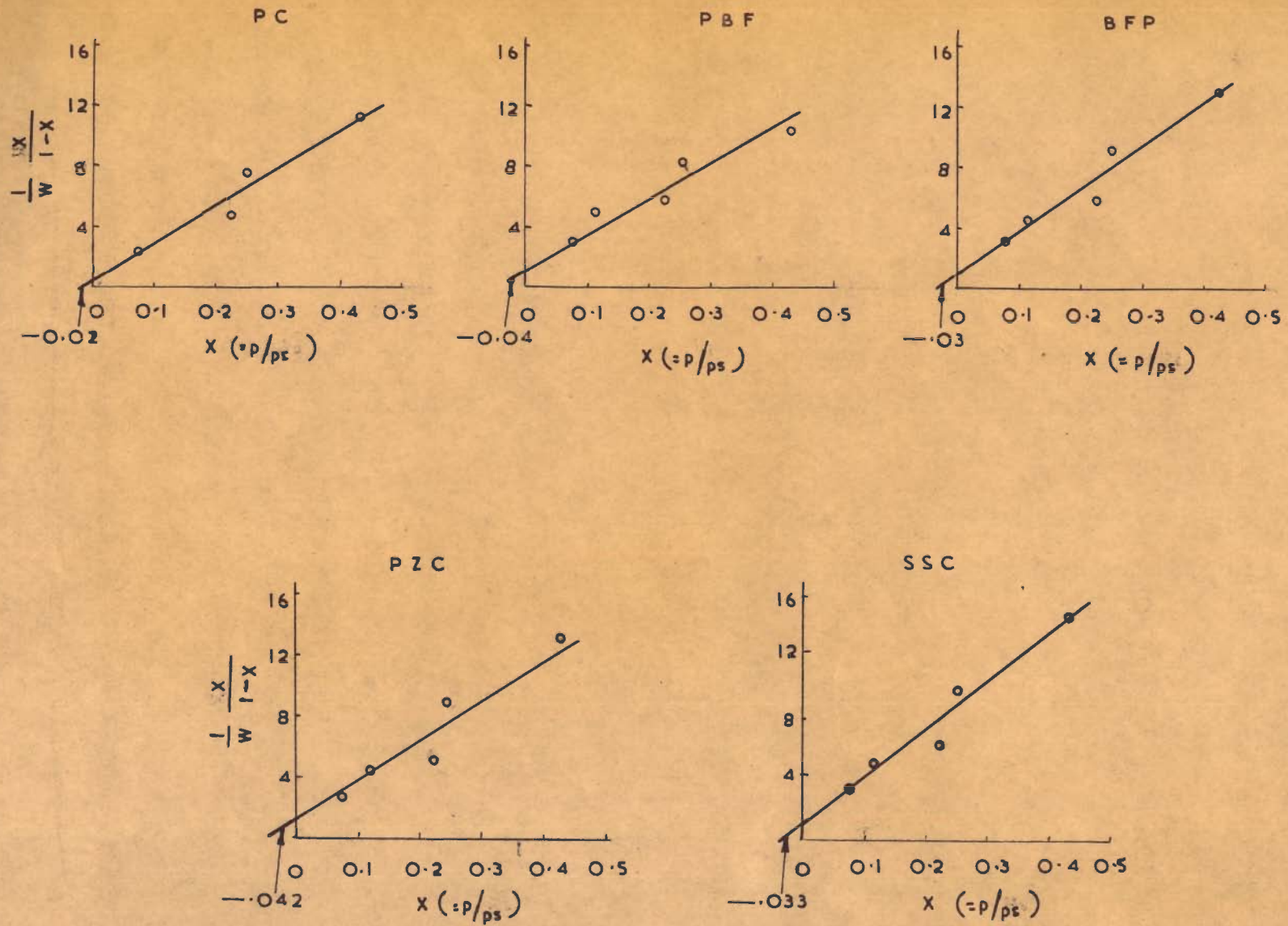

FIG. 34. TYPICAL PLOTS FOR EVALUATING C & V_m

FOR 90-DAYS HYDRATED CEMENT ($w/c = 0.40$)

given standard material and drying conditions seems to have been almost solved by determining surface areas of dried sample of a laboratory preparation of afwillite by nitrogen and water-vapour adsorption (189). Finally, Powers has concluded on the basis of various considerations and data that the surface areas determined by water vapour adsorption in the BET method are fairly accurate. Fig. 34 shows plots of $\frac{1}{W}\frac{X}{1-X}$ versus X for different hydrated cements from which values of c and V_m were obtained. The surface areas were calculated from the latter and are reported in table 35. The values of the Portland cement no. 15754 taken from Powers data show a good agreement with the Portland cement of this study (table 35).

Since the Portland cement is similar in composition to that of Powers cement, comparison of the PC cement with the other hydrated cements such as PBF, BFP, PZC and SSC becomes striking. The values of surface area per g of hydrated cement show that the cements can be arranged as PC, PBF, PZC, SSC and BFP in a decreasing order. Since the surface area of the SSC cement has not been reported so far, it is interesting to note that even supersulphated cement contains a good amount of either poorly crystallized sulfoaluminates or gels or may be both which contribute towards specific surface of this cement.

Relationship between V_m and W_n

The ratio V_m/W_n for Portland cement was found by Powers and Brownyard (190) to be independent of age or water cement ratio. The influence of various degrees of drying of test samples on the experimentally determined values of V_m and W_n was studied by Tomes, Hunt and Blaine (47). There is some uncertainty as to the relations between observed values of V_m and W_n and the theoretically correct values (185).

The V_m/W_n ratios for the PBF, BFP, PZC and SSC cements could be different from the value for the Portland cement as the ratio between colloidal to non-colloidal hydrated phases may be different. Earlier a mention was made of the differences in hydrated phases formed as a result of hydration of the above cements (table 27). The differential thermal analysis curves (Figs. 27 to 29) also show that the amounts of $Ca(OH)_2$ and carbonate are highly variable in the PBF, BFP, PZC and SSC cements. Since the latter hardly contribute towards V_m, the combined water in hydrates other than $Ca(OH)_2$ was determined by the thermogravimetric analysis (Fig. 35) and is reported in table 34. The ratios of V_m/W_n are reported in table 35. In view of the limited data, it is not possible to say anything about the constancy of the ratios. However, the data show that the cements BFP and SSC probably have values of V_m/W_n significantly different from those of the PC, PBF and PZC cements.

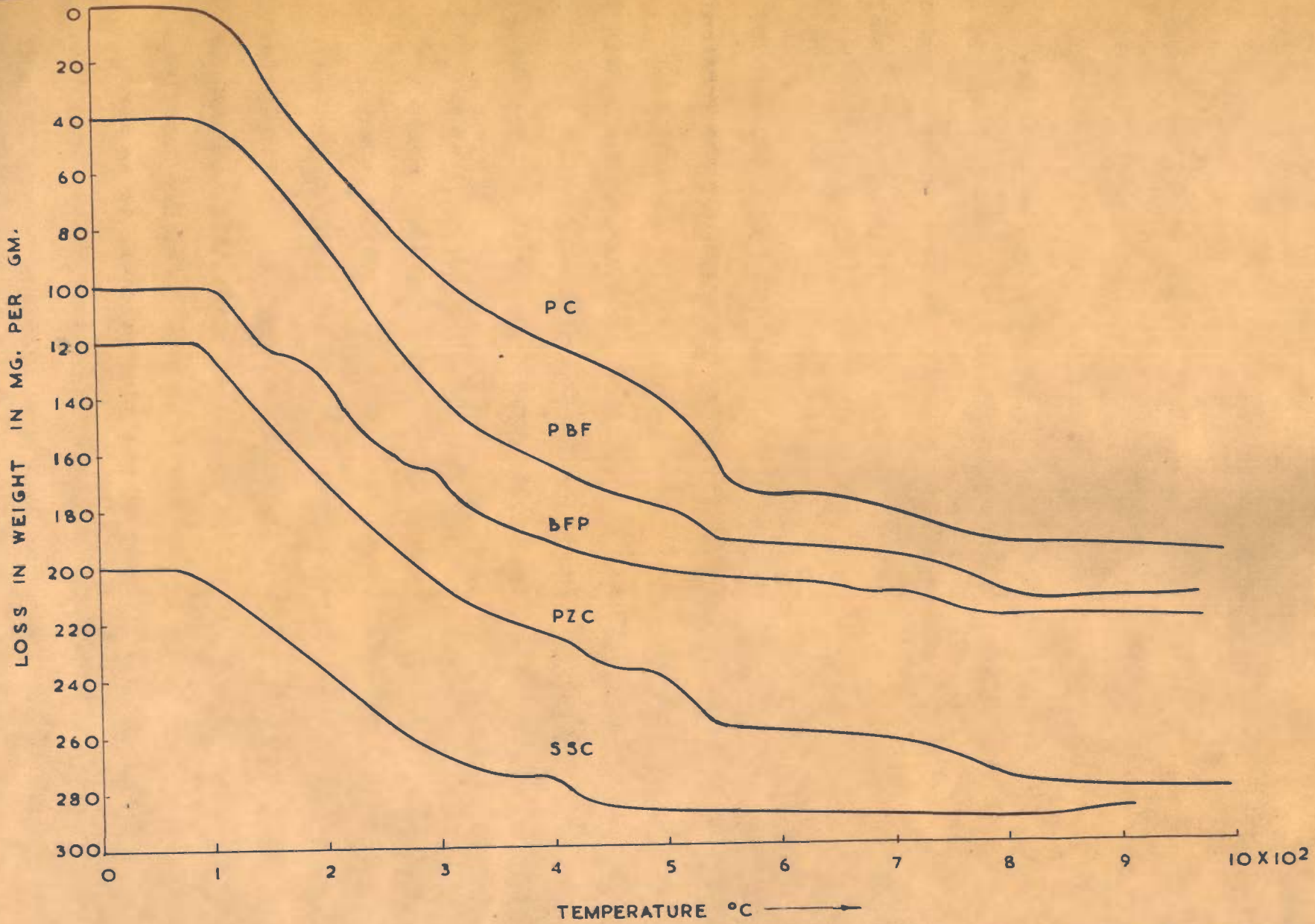

FIG.35. THERMOGRAVIMETRIC LOSS OF VACUUM DRIED HYDRATED CEMENTS

(W/C=0·4, AGE 90 DAYS)

NOTE:- THE CURVES HAVE BEEN SHIFTED FOR CLARITY

TABLE - 34

Determination of Chemically Combined Water in Hardened Pastes by Thermogravimetric Analysis

Sample Particulars: Cement	w_o/c ratio	Loss in weight g/g of Dried Paste: Due to combined water 0-650°C	Due to $Ca(OH)_2$ 490-600°C	Due to carbonate 600-1000°C*	Total loss 0-1000°C	Water in cementitious hydrates, g/g (3) - (4)
1	2	3	4	5	6	7
PC	0.400	0.1780	0.0370	0.0195	0.1975	0.141
PBF	0.375	0.1560	0.0130	0.0050	0.1740	0.143
BFP	0.373	0.1090	0.0040	0.0070	0.1200	0.105
PZC	0.362	0.1410	0.0190	0.0210	0.1620	0.122
SSC	0.398	0.0900	0.0000	0.0020	0.0880	0.090
PC	0.557	0.1948	0.0330	0.0155	0.2103	0.161
PBF	0.492	0.1645	0.0135	0.0067	0.1847	0.151
PZC	0.444	0.1380	0.0170	0.0205	0.1585	0.121

* Loss from 600-1000°C may not be entirely due to calcium carbonate; some of it may be due to combined water. But the latter is neglected as it would be small.

The most commonly observed particle habit of CSH-I or low lime-tobermorite is that of thin sheets or foils, estimated to be one or two molecular, units thick in extreme cases. The presence of small and comparatively flat platy particles, together with crinkly foils was also observed in another form of CSH-I. The CaO/SiO_2 ratio in the latter was about 1.1 and concentration of calcium hydroxide as 3.8 mM/litre (43). In the vicinity of lime saturation a finely fibrous or needle like growth is promoted. The solids have a ratio of CaO/SiO_2 ratio of 1.5 and higher&are known to occur mostly in fibrous form.

Fig. 36A shows a representative aggregate from a lightly ground set Portland cement paste (W/C = 0.40) at 90 days. A close examination of the edges reveals a fibrous structure. Some hexagonal plates probably belonging to the C-A-H compounds are also present. Such plates seem to be forming bridges between gel structures adhering to different parts of the plate surfaces.

The fibrous character of the tobermorite phase is very well illustrated by Fig. 36B which shows bundled fibres. The presence of bundled fibres in Type I (ASTM) cement paste has also been reported by Grudemo (43).

Little information is available in the literature on the electronographic study of the morphology of set pastes of slag and pozzolanic cements. Malquori, Sersale and Giordano-Orsini (191), however, have published electronmicrographs showing the morphological evolution

T A B L E - 35

Surface Areas of the Hydrated Cements and the Ratio v_m/w_n

Cement designation	w_o/c	v_m per g of dried paste	v_m per g of cement	Sp. surface of hydrated cement m^2/g	Ratio** v_m/w_n
PC	0.400	0.0412	0.0512	195	0.292
PBF	0.375	0.0399	0.0483	183	0.280
BFP	0.373	0.0341	0.0387	117	0.312
PZC	0.362	0.0372	0.0444	169	0.298
SSC	0.398	0.0306	0.0335	127	0.339
PBF	0.492	0.0437	0.0536	204	0.289
PZC	0.444	0.0363	0.0432	164	0.300
*PC 15754	-	-	-	219	0.311

* Powers data for the Portland cement 15754.

** The values of w_n employed are those reported under last column of Table 34.

Electron Microscopic Examination of Hydrated Pastes

Buckle and Taylor (76) found irregular masses, possibly composed of small plates, in hydrated C_3S pastes. The irregular masses were almost certainly identified as very ill-crystallized tobermoritic material. Grudemo (43) found the hydrated C_3S paste to be consisting of irregularly shaped agglomerates of small and thin particles, similar to those reported by Buckle and Taylor. But a second phase consisting of long and rather thick needles or rods, obviously composed of bundles of fibres or tubularly rolled sheets, was also found in an equal amount. Funk (44) found β-C_2S pastes consisting almost entirely of fibrous C_2SH_2 type tobermorite. Grudemo (43) found both distorted plates and coarsely fibrous or tubular particles in β-C_2S pastes.

Since ordinary Portland cement consists of 70 - 80 per cent of C_3S and β-C_2S, the predominant gel phase in the hydrated cement paste would correspond to that observed in C_3S and β-C_2S pastes. However, it is likely that the hydrated gel phase in the Portland cement is exceedingly ill-formed. The other phase in hydrated Portland cement paste would be relatively large-sized plates of calcium hydroxide and C-A-H crystals, the latter mostly appearing as hexagonal plates. However, these crystals together with those of the ettringite phase, in the form of needles or long rods, would be present in smaller amounts compared to the C-S-H phase.

A. Showing fibrous structure with some hexagonal plates of C-A-H (x 17600)

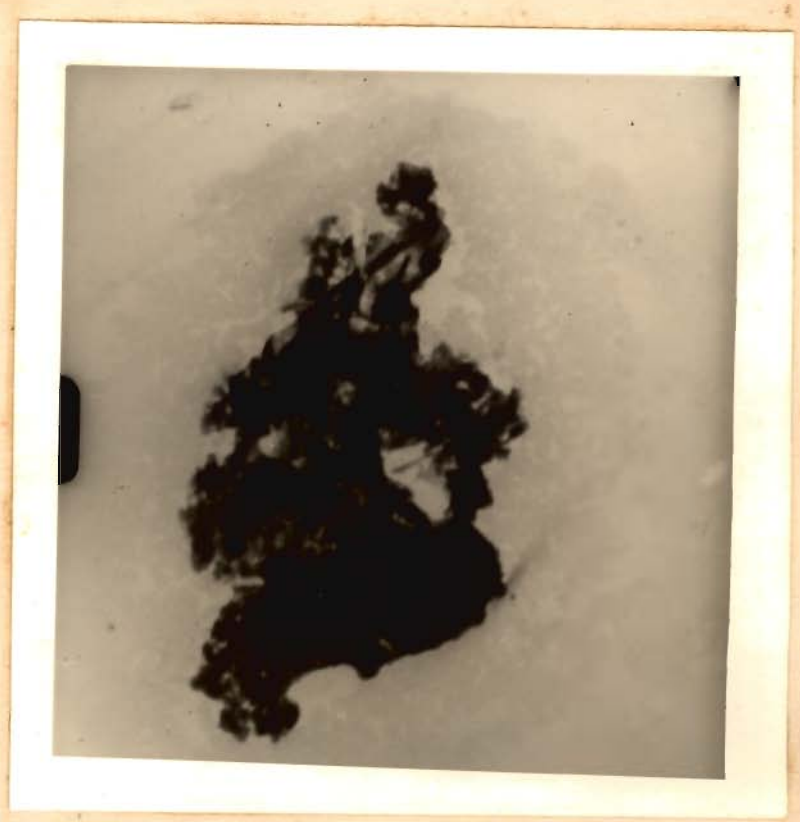

B. Showing bundled fibres (x 17600)

Fig. 36. Electron micrographs of representative aggregates from hydrated Portland cement (W/C = 0.40, age 90 days)

of hydration products of basic granulated slag in lime solution.

The electronmicrograph (Fig. 37A) of the aggregate of the set PBF cement (W/C = 0.40) at 90 days shows both fibrous and the platy structure. The plates belonging to the $CaO-Al_2O_3-H_2O$ phase are present to a greater extent than in the PC cement paste. This may be due to the higher alumina content of the slag. The fibrous structure is well illustrated in Fig. 37B. The fibres of the tobermorite phase in this paste are very much finer and shorter in length compared to the PC cement paste. At places the fibres are so fine that the material appears to be amorphous in nature.

The platy and fibrous structures were also observed in the set pastes of the BFP (W/C = 0.40) at 90 days. As against the PC and PBF pastes, some of the aggregates in Fig. 38A show sharp edges and bear resemblence to the original slag grains (Fig. 1). The presence of hydrated phases on unreacted slag grains is indicated. A few lath-like crystals, probably belonging to the ettringite phase, can be seen projecting from the main aggregate bridging between the aggregates. The tobermorite phase in the BFP paste consists of fine and short fibres (Fig. 38B). But presence of this phase in the form of flakes is also indicated in the electronmicrograph (Fig. 38B).

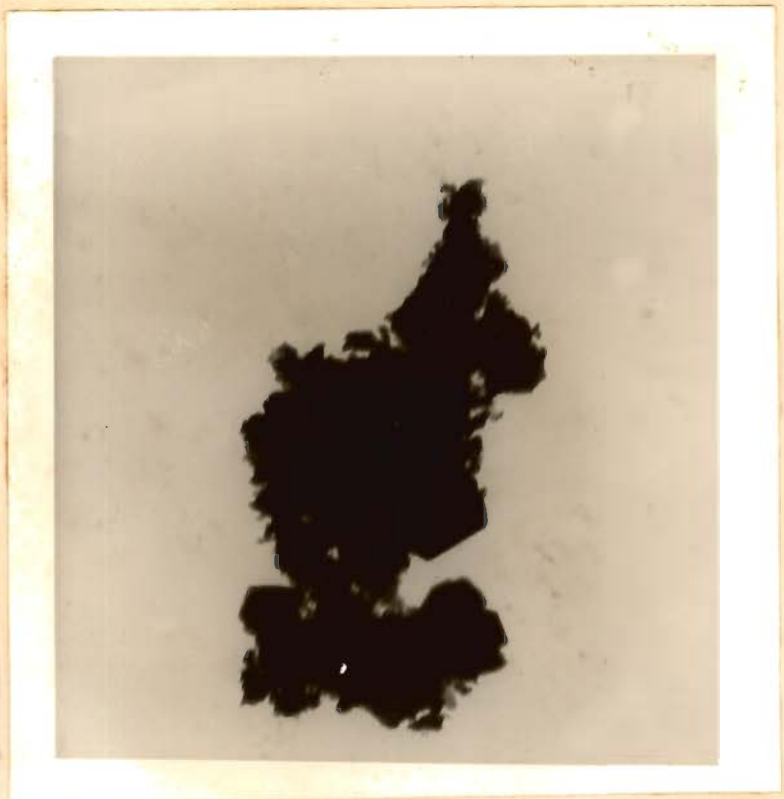

A. Showing fibrous structure and hexagonal plates (greater numbers) of C-A-H (x 17600)

B. Showing very fine and short fibres.

Fig. 37. Electron micrograph of representative aggregates from hydrated Portland blastfurnace cement(65C:35BL) (W/C = 0.40, age 90 days)

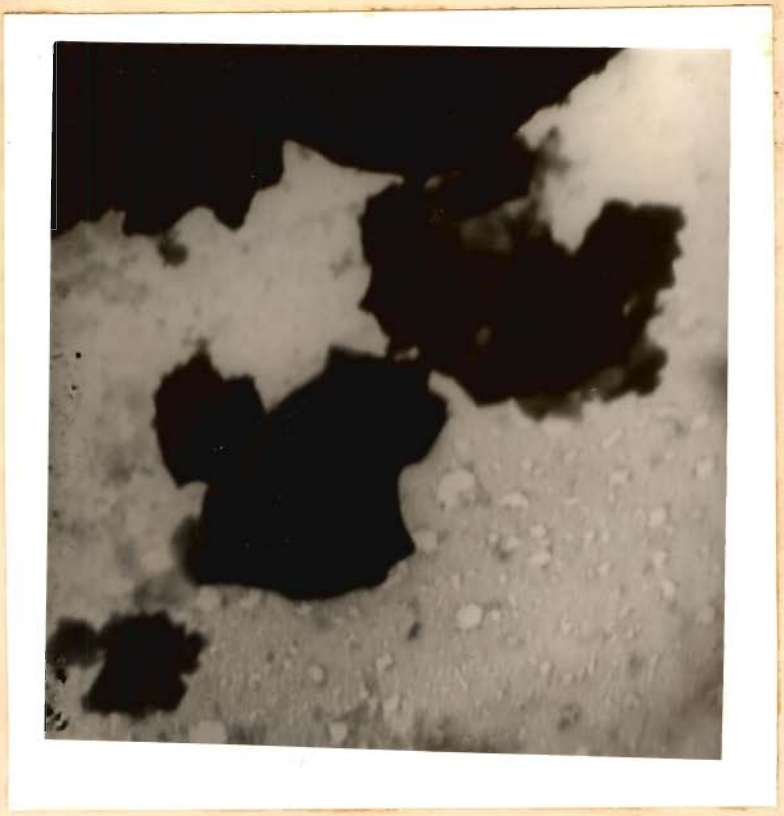

A. Showing both fibrous and platy structure (x 17600)

B. Showing fine and short fibres and some flakes (x 17600)

Fig. 38. Electron micrographs of representative aggregates of hydrated BFP cement (35C:65SL) (W/C = 0.40, age 90 days)

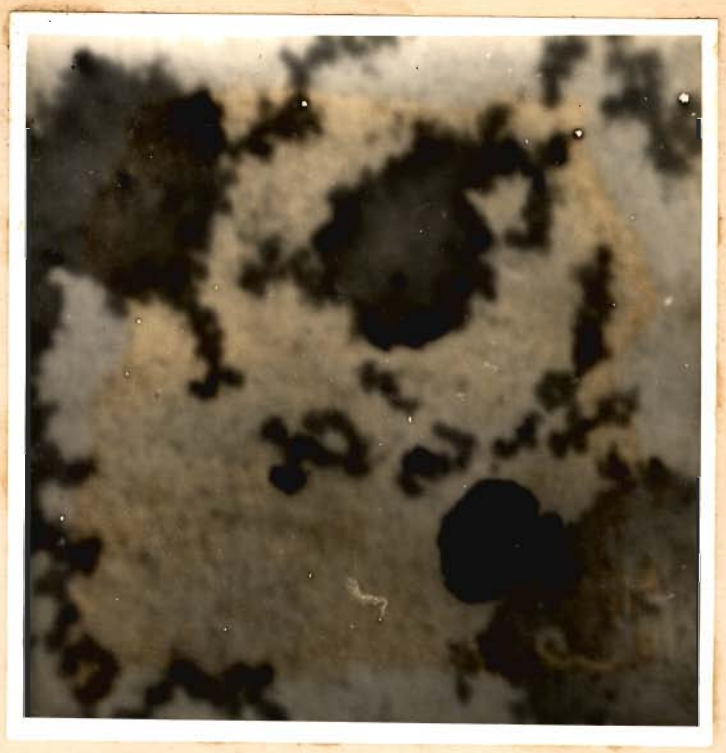

A. Showing fibrous (top left) and platy structure (x 17600)

B. Showing platy and lath-like crystals, and some foils belonging to C-S-H phase

Fig. 39. Electron micrographs of representative aggregates of hydrated pozzolanic cement (75C:25 fly ash) W/C = 0.40, age 90 days)

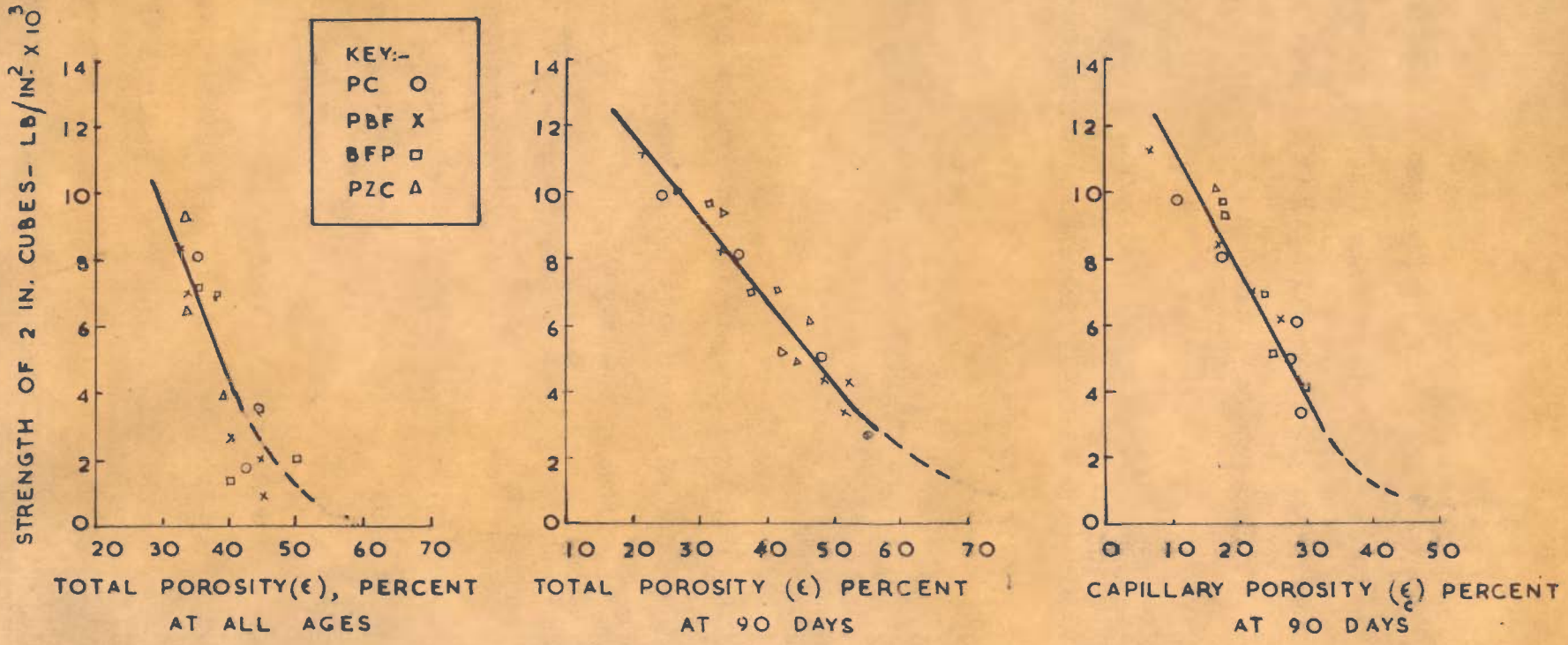

FIG.40. RELATIONSHIP BETWEEN STRENGTH & POROSITY OF CEMENT PASTES

The representative aggregates of the set PZC cement (W/C = 0.40) at 90 days show fibrous structure (Fig. 39A) and platy structure (Fig. 39B). The presence of several lath-like crystals of the ettringite phase is indicated in both the micrographs. Evidence of rolling of sheets or foils belonging to the C-S-H phase is also available in the electronmicrographs. Unreacted fly ash particles in form of chains are also visible.

DISCUSSION

Porosity and Strength

Some physical properties of cement paste depend upon total porosity while others, for example, compressive strengths and resistance to freezing are better related to capillary porosity (129). Fig. 40 shows the plots of the total porosity versus strength for the hardened pastes of each of the four cements PC, PBF, BFP and PZC at ages varying from 36 hours to 90 days. The scatter of the points is too much for drawing a definite relationship between total porosity and strength. But when total or capillary porosity values were plotted against strengths at 90 days, better relationships were obtained (Fig. 40). At 90 days when hydration reactions are in advanced stages the differences in the porosity values are very much narrowed down (particular for those cements which are clinker-based) because the hydrated phases tend to be

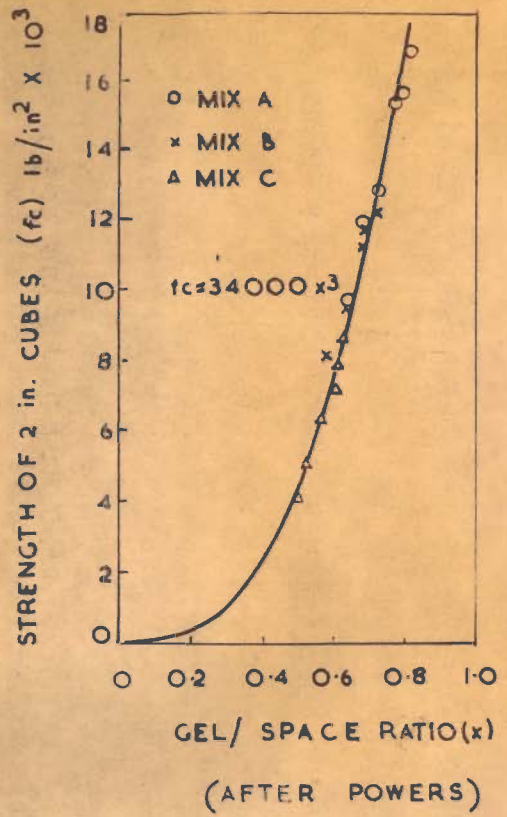

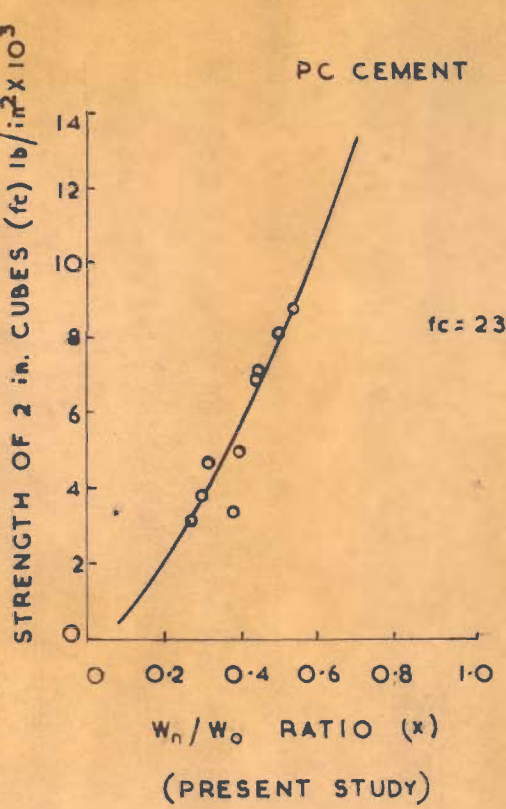

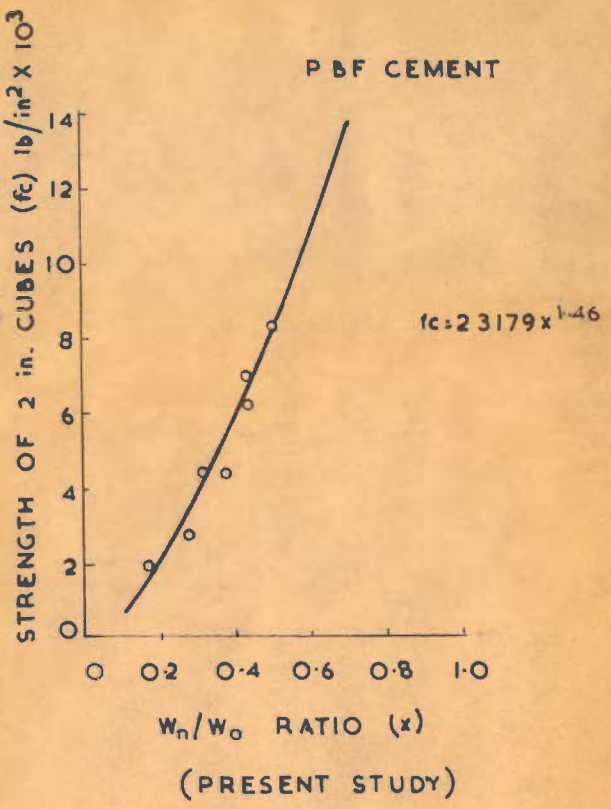

FIG.41. RELATIONSHIPS BETWEEN STRENGTHS & W_n/W_o RATIOS FOR DIFFERENT CEMENTS

more homogeneous as evident from the low temperature endotherms (Figs. 27 and 28). But it is obvious no precise relationship is possible if data for all ages and all cements is plotted together.

Gel-space Theory and Strength

According to Powers a given cement gel should have a characteristic strength, but the strength of the structure built of it that is, the paste as a whole, should depend upon the amount of gel in the space available to it (8).

Fig. 41 represents Powers relationship between compressive strength and gel-space ratio. The gel-space ratio, x, is evaluated from the equation

$$\frac{2.06\ C\ V_c \alpha}{C\ V_c \alpha + W_o} \qquad \ldots (11)$$

where 2.06 cm^3 is the volume of gel plus the non-gel constituents produced on the hydration of 1 cc of Portland cement and α is the coefficient of hydration i.e., the fraction of cement that has become hydrated, 2.06 C $V_c \alpha$ is the amount of gel produced, C is the weight of cement, V_c is the specific volume of cement and W_o is the volume of water-filled space originally present.

α is known only for a couple of Portland cements (1,8,129). Because it involves the determination of non-evaporable water for conditions of ultimate hydration

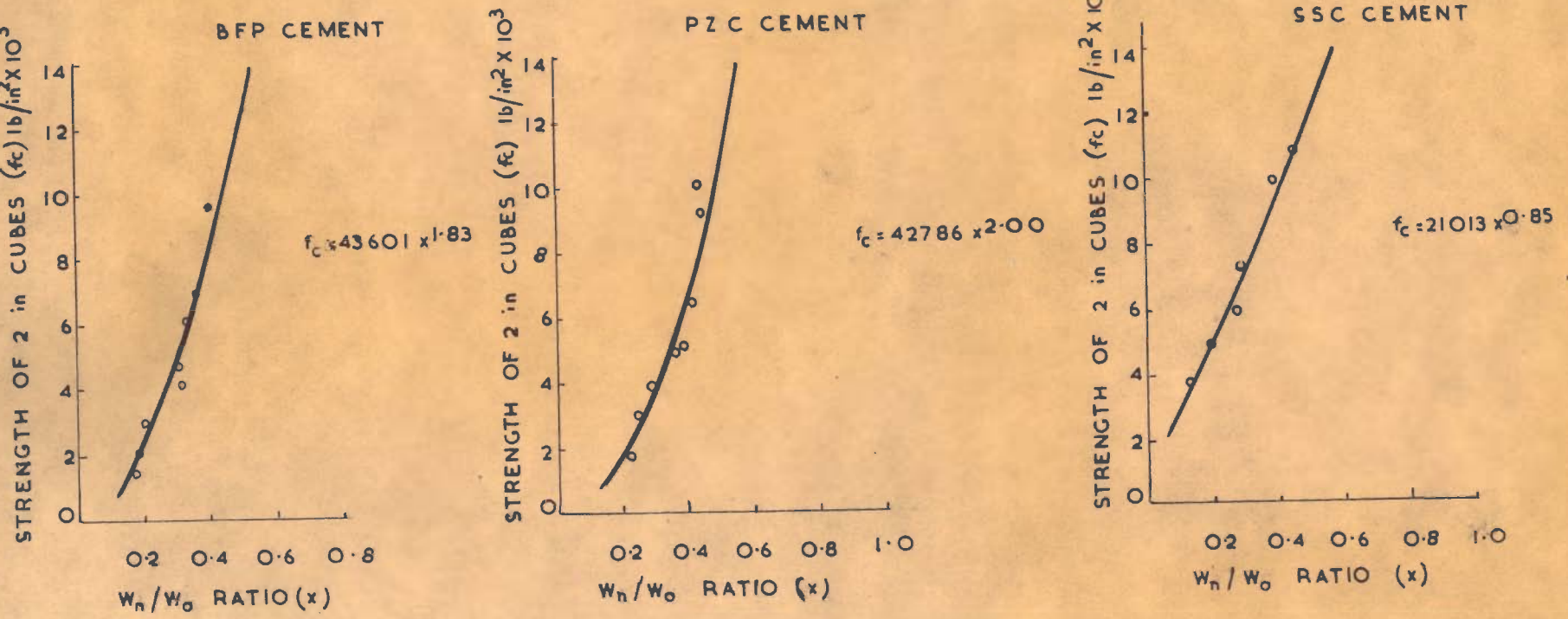

FIG.42. RELATIONSHIPS BETWEEN STRENGTHS & W_n/W_o RATIOS FOR DIFFERENT CEMENTS

its determination for PBF, BFP and PZC cements is rather difficult.

An estimate of α is also not possible. In view of this the ratio of W_n/W_o was taken up for plotting against strength instead of x. Though, W_n/W_o does not strictly represent the gel-space ratio, it is a good substitute as is evident from the relationships (compare in Figs. 41 and 42). Since the primary object was to find if relationships for the slag and pozzolanic cements are similar to those of the Portland cement, and if so, what are those; the plots of strength versus W_n/W_o should serve this purpose. By doing so, at the most, it may not be possible to compare numerical constants of this study with those reported by Powers (8) but the latter himself has pointed out that these are empirical relations and do not amount to a law of strength.

Powers (8) experimental data conformed closely to an equation

$$f_c = f_c^o x^n \qquad \ldots (12)$$

where f_c = compressive strength and f_c^o and n are empirical constants. Since x is a fraction between 0 and 1, x^n operates as a reduction factor on f_c^o. The intrinsic strength is represented by f_c^o.

Figs. 41 and 42 show the relationships between compressive strengths and values of W_n/W_o for the PC, PBF,

BFP, PZC and SSC cements which are similar to those reported by Powers. The equations representing relationships are given below. The relationships were obtained by the least square method. These are :

(i) $f_c = 23169\ x^{1.52}$ for the Portland cement

(ii) $f_c = 23179\ x^{1.46}$ for the PBF cement

(iii) $f_c = 43601\ x^{1.83}$ for the BFP cement

(iv) $f_c = 42786\ x^{2.00}$ for the PZC cement, and

(v) $f_c = 21013\ x^{0.85}$ for the SSC cement

Intrinsic Strength of Cement Gel

The above equations show that the intrinsic strength of the 'cement gel' in the pastes of the two slag and one pozzolanic cements (i.e., PBF, BFP and PZC) are not lower than the strength of the Portland cement gel. In fact, the intrinsic strengths of the two cements BFP and PZC are higher. The presence of comparatively a lower amount of calcium hydroxide or its absence, differences in the microstructure of the tobermorite phase and presence of ettringite (table 25) may be responsible for the higher intrinsic strengths of the two cements.

The SSC cement forms on hydration ettringite, monosulfoaluminate and secondary phases of calcium silicate hydrate and alumina gel. Since the secondary phases are not present in quantities greater than that of sulfoaluminates (Fig. 29B) and the intrinsic strength of the SSC cement is almost equal to that of the PC cement, it may be

concluded that the chemical species like ettringite etc. could have contributed more towards strength of the pastes of BFP and PZC cements.

While discussing the intrinsic strength of the Portland cement, Powers had indicated that there could be many points of chemical bonding between the particles but he was not clear whether or not all chemical species contribute to the intrinsic strength. But the discussion in the above para shows that higher intrinsic strengths of the BFP and PZC could be due to the presence of relatively a greater amount of ettringite in these two cements. The differences in the microstructure of the tobermorite phase in the BFP and PZC cements may also be responsible for higher intrinsic strengths of the cement gel in these cements as shown little later.

Comparison of Particle and Pore Size of Cement Gel

The particle size and pore size in the different hydrated cements were calculated and are reported in table 36. The results are self explanatory. The 'specific surface diameter', which is equal to 6/sp. surface (specific surface in m^2/cc), for the Portland cement is 124A against the reported value of 118A (1). The 'specific surface diameter' for the other cements is greater; being highest for the BFP cement. The value for the PZC cement, which together with BFP cement has shown higher intrinsic strength, is also greater than that of the Portland cement.

T A B L E - 36

Estimated Particle and Pore Size of Gel in Hydrated Cements

(90-Days Cured)

Designation of cement	w_o/c ratio	Sp. Vol. cc/g	Surface Area m^2/g	Surface Area m^2/cc	Sp. Sur Dia. A units	Non-Eva. water W_n	v_m/w_n = k	Pore* size in A units
PC	0.400	0.412	195	473	124	0.165	0.292	5.8
PBF	0.375	0.404	183	453	132	0.154	0.285	5.7
BFP	0.373	0.389	117	300	200	0.120	0.312	7.6
PZC	0.362	0.397	169	425	140	0.139	0.299	5.8
SSC	0.398	0.371	127	342	175	0.082	0.339	5.7

* Pore size calculated from hydraulic radius.

Estimation of pore-size is probably more important. This is calculated from the hydraulic radius,m

where $m = \frac{\text{volume of pores per g hydrated cement}}{\text{surface of walls per g of hydrated cement}}$

The volume of gel pores according to Copeland is given by 2.36 k W_n (129) and values in last column of table 36 were calculated from this formula. The data shows that the hydraulic radius for all the cements except BFP is 6A. The average pore width is thus between 12A to 24A against the reported value of 14A to 28A; the latter having been calculated by Powers and Brownyard on the assumption that the specific volume of gel water is 0.9 (6). The agreement is good. It is interesting to note that the average width of pores in the hydrated supersulphated cement is not different which implies that the colloidal portion of the hydrated phase is probably no different from that of the Portland cement. However, this is only an observation. But the BFP cement has a higher pore size width (ranging between 16A to 32A) in conformity with its higher 'specific surface diameter'.

The data discussed above is good only for the sake of making comparisons because it is now known from the studies of the morphology of the hydrated cement that gel particles are not spherical. A realistic estimate of particle dimensions and its influence on strengths are given below.

Differences in Microstructure and Effects on Intrinsic Strengths

The differences in the microstructure of the pastes can be summarized as follows :

(i) both fibrous and platy structures were present in all the pastes but the fibrous structure was more predominant in the paste of the Portland cement than in any other paste,

(ii) the fibrous phase of tobermorite-like hydrates in the slag and pozzolanic cements consists of very fine and short fibers as against the bundled fibres in the Portland cement paste. The DTA curves (Figs. 27 and 28) had also indicated differences in C-S-H phase in the slag cement pastes as evident from the peak temperature of the low temperature endotherm. For example, the peak temperature was 142°C for the two slag cements against 135°C for the PC cement,

(iii) the electronmicrographs showed a definite evidence of the existence of the flakes or sheets in the BFP and PZC pastes; but their presence in the PBF cement paste is not certain. This phase probably shows the presence of calcium silicate hydrates with a low CaO/SiO_2 ratios,

(iv) the hexagonal plates belonging to C-A-H phase were present in the PBF cement to a greater extent than either of the PC, BFP and PZC cement pastes. This is also evident from the X-ray powder data (t.25) which shows the presence of $C_4A.aq.$ in the PBF cement in an amount greater than any other cement paste, and

(v) the presence of lath-like crystals of the ettringite phase is indicated in the BFP and PZC pastes. The presence of ettringite in these pastes in amounts greater than that of the PC paste is also supported by the X-ray data (table 25). Neither X-ray nor electron micrographs showed the presence of ettringite in the PBF paste. Its presence in PC was indicated only by X-ray data.

While it is difficult to say how the above mentioned differences influence the strength characteristics of the different hardened pastes, certain deductions are possible from the published data (40-44,72-75). For example, the presence of hexagonal plates of C-A-H phase (i.e. $C_4A.aq.$) in the PBF to a greater extent are probably responsible for a comparative lower intrinsic strength of the cement gel. On the other hand, the presence of lath-like crystals of ettringite phase in the pastes of BFP and PZC cements probably is responsible for comparatively higher intrinsic strength of cement gel as these crystals provide cross links in the network formed by the calcium silicate hydrate phase. The 'self-stressing cement' of Mikhailov provides an analogy of the role of ettringite in forming a framework leading to very high strengths (116,117).

It appears from the results that the presence of slag or pozzolana modifies the crystal habit of the tobermorite phase resulting from the hydrolysis of clinker constituents in the PBF, BFP and PZC cements because, if it were not so, bundled fibres should have also been formed in the set pastes of the slag and pozzolanic cements as in the set Portland cement paste, the W/C ratio and period of hydration being the same. But very fine and short fibres were found to be present in the pastes of the slag and pozzolanic cements. The additional presence of flakes or rolled foils etc.

indicates that probably these phases were formed in the beginning and changed subsequently into fine fibres. Malquori and his co-workers have also reported a similar evolution of hydration products of slag in contact with lime solution (191).

Evidence on the influence of the crystal habit of the C-S-H phase on the mechanical strength is confusing and also there is lack of fundamental theories on the influence of the shape and size of gel particle elements on hardening (25). It is difficult to say which of the two morphological characters i.e., the bundled fibres or the very fine fibres, is likely to give higher strengths. But since the intrinsic strengths of the cement gel in the BFP and PZC cements were found to higher and that of PBF cement equal to that of the PC cement (P 184), it appears the tobermorite phase in the form of very fine fibres or flakes or foils results in higher strengths. This is supported by the observation that the $(SH)_3$ chains are longer and more isolated from each other in fibrous particles, shorter and more aggregated in coherent sheets in layer-like particles (25).

The ratios of V_m/W_n for the set BFP, PZC, PC, and PBF cements pastes (W/C = 0.40) were found to be 0.312, 0.298, 0.292 and 0.280 (table 35). It is obvious that the cements can be arranged as BFP, PZC, PC and PBF respectively according to a decreasing value of the specific

surface per unit non-evaporable water. It may be seen that the cements can be arranged more or less in the same order on the basis of decreasing intrinsic strengths. This indicates that higher intrinsic strengths probably result from the greater surface area and probably greater surface forces in hydrated cements wherein tobermorite is not present as bundled fibres as the latter tend to reduce surface area of the tobermorite phase.

CHAPTER 6

HYDRATION AND HARDENING OF LIME-SLAG AND LIME-POZZOLANA MIXES

Introduction

Investigations on reactions between lime and pozzolanas (including slags) with a view to understanding the mechanism of strength development are much older than those of the hydration and hardening of cement. In 1956 Lea had examined the two main theories, i.e., base exchange and direct combination, aiming towards explaining the mechanism of the lime-pozzolana reactions and had concluded that the base exchange theory was not tenable (192). Though many have believed in the explanation based on the chemical combination of lime with the constituents of a pozzolana or slag for sometime past, difficulties such as estimation of free lime, identification and estimation of hydrated phases, differences in the nature of materials and experimental variables have stood in the way of direct testing of this hypothesis.

However, recently many advances have been made in this field. Improved techniques have resulted not only in estimating free lime accurately (81, 179) but also in identification and possibly qualitative estimation of the main cementititous phases i.e., calcium silicate and aluminate hydrates (81-86), though as pointed out by Lea the role of iron oxide and alkalies in pozzolanas is still not clear (54). Notable contributions have been made by the

Russian scientists in explaining pozzolanic reactions (193). Malquori (56) has provided excellant information on the prehistory and constitution of pozzolanas leading to differences in activity. Ludwig and Schwiete (87) have reported the hydrates as $Ca(OH)_2$, $3CaO.2SiO_2.aq$, $4CaO.Al_2O_3.13H_2O$, $3CaO.Al_2O_3.3CaSO_4.32H_2O$, $3CaO.Al_2O_3.CaSO_4.12H_2O$. The presence of carboaluminates and hydrogarnets has also been reported (84). But unless the CaO/SiO_2 ratio in the calcium silicate hydrate or tobermorite phase is known and so also the relative amount of the latter amongst the different hydrated phases in the hardened paste, correlations between combined lime or the nature of hydrated phases will continue to be general in nature.

The effect of increased fineness of the pozzolana on strengths is well known but Alexander (193A) has shown that siliceous materials which are not normally pozzolanic become highly reactive when ground to ultrafine powders. This is an important observation and shows that how great the influence of a single physical property can be. On the other hand, in his recent review Malquori (56) has cited many examples emphasizing the effects of chemical and mineralogical composition of pozzolanas (including slags on their activity. It may therefore be concluded that there is a need for a balanced appraisal of the relative influences of the physical and chemical factos on the strength and other properties of cementitious materials and that the situation is not any different from that discussed

earlier in respect of cements.

MATERIALS

The cementitious materials used were LS and LP (table 1). Their compositions were 15 parts of hydrated lime with 85 parts of granulated slag and 30 parts of hydrated lime with 70 parts of calcined fly ash respectively.

The granulated slag and calcined fly ash had a fineness of 3200 ± 50 sq cm per g and 3466 sq cm per g respectively. The specific surface of the hydrated lime was 6329 sq cm per g.

The preparation of the cementitious materials was done in a manner described earlier.

EXPERIMENTAL

Preparation of Pastes

The method of preparation of paste at different W/C ratios was the same as described in Chapter 1

Determinations

The experimental procedures for the differential thermal, thermogravimetric and X-ray powder analyses and for determinations such as compressive strength, non-evaporable water, apparent specific volume of total water

etc. were the same as those described in Chapters 4 and 5. The samples for the differential thermal and X-ray powder analyses were dried for few hours under 1-2 mm of vacuum to remove free water. For all other determinations, granular sample (-30 + 80 U.S. sieve) dried under vacuum in a manner described in Chapter 4 were used.

Choice of Mixes and Experimental Conditions

The choice of mixes and experimental conditions in reactions of lime with ground slag and pozzolanas are more important than in the study of cement reactions because the reactions proceed slowly at room temperature and equilibrium is reached after long times. Since the quantity of the hydrated phases formed at early ages is small in relation to the quantity of unreacted lime, the errors in estimation of non-evaporable or combined water in the hydrated phases could be serious. Also the contribution of the cementitious phases towards strength development cannot be evaluated satisfactorily as unreacted lime, which is known to have adverse effects on strength, is a highly variable quantity. Attempt in the present study was therefore to select mixes and time of processing so that practically the entire quantity of lime enters into combination and the errors in making determinations are thus minimized.

The two mixes selected were (i) 15 lime : 85 slag (granulated), and (ii) 30 lime : 70 fly ash (calcined).

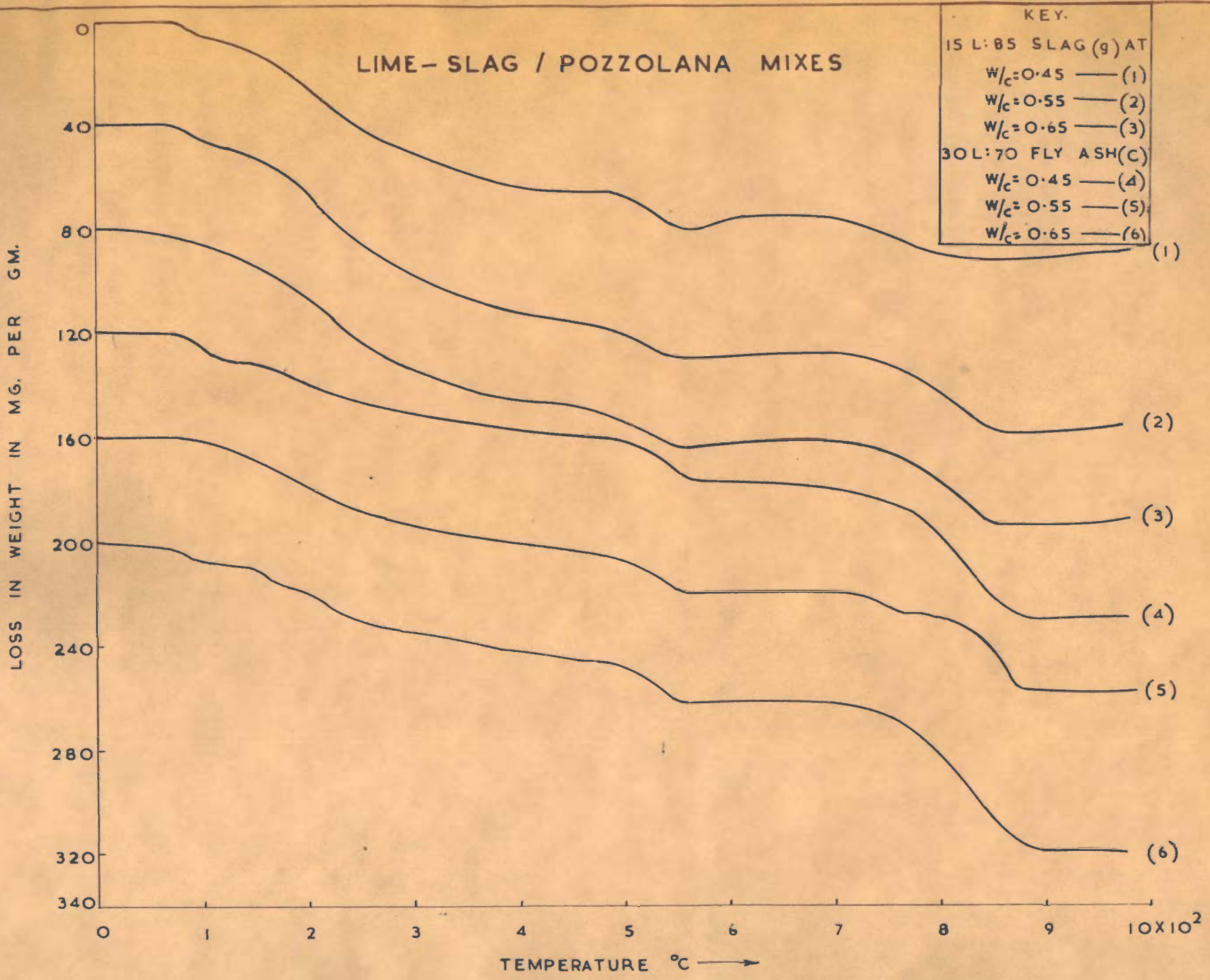

FIG. 43. THERMOGRAVIMETRIC LOSS IN VACUUM DRIED SAMPLES

The former was selected on the basis of an earlier study of activation of slag with lime (100). In view of the deleterious effect of unburnt carbon in fly ash on strength, calcined fly ash was used in the lime-pozzolana mix. The mix proportion employed was 30 lime : 70 fly ash by weight in the light of earlier work on lime-pozzolana mortars (102) and hydrothermal reactions (93). The period of curing was 3 months since chemical combination between lime and constituents of slag or pozzolana was expected to complete by that time and also transient phases formed at early periods were expected to enter stable arrangements.

RESULTS

Non-evaporable Water and Apparent Specific Volume of Total Water

The values of W_n/S (for W_n/C) (table 37) were calculatd in a manner similar to that used for the hydrated cement except that in place of loss on ignition of anhydrous cement, the value of the ignition loss of slag or pozzolana was used because most of the lime present in the original mix had been consumed as shown by weight loss curves in Fig. 43. The values of W_n/S for the three lime-slag mixes ranged between 0.094 to 0.113 and between 0.085 to 0.107 for the three lime-fly ash mixes. But on the other hand, the strengths of the lime-slag mixes are about 100 per cent more (table 37). This shows that the values of W_n/S were

TABLE - 37

Physical Properties of Hardened Cementitious Pastes

Mix Composition	Water-solids ratio* w/s	w_o/s	Non-Evap. water w_n/c Ignition method	Non-Evap. water w_n/c Thermogravimetric method	Evap.** water w_e/c	Total** water w_t/c	Ratio** w_n/w_t	Ratio** w_n/w_o	Total porosity ϵ	90-Days strength p.s.i.
15 Hyd. Lime	0.45	0.428	0.094	0.087	0.375	0.462	0.188	0.203	0.472	3024
+ 85 SL(g)	0.55	0.503	0.113	0.102	0.437	0.539	0.189	0.198	0.502	2139
	0.65	0.509	0.106	0.094	0.418	0.512	0.184	0.184	0.476	2027
30 Hyd. Lime	0.45	0.477	0.085	0.065	0.447	0.512	0.136	0.136	0.492	1321
+ 70 F(C)	0.55	0.531	0.107	0.066	0.524	0.590	0.124	0.124	0.546	1008
	0.65	0.519	0.101	0.070	0.520	0.590	0.134	0.135	0.548	1030

* w/s and w_o/s correspond to w/c and w_o/c in cements.

** Values of w_n determined by thermogravimetric method were used in calculating the ratios and also w_e/c and w_t/c.

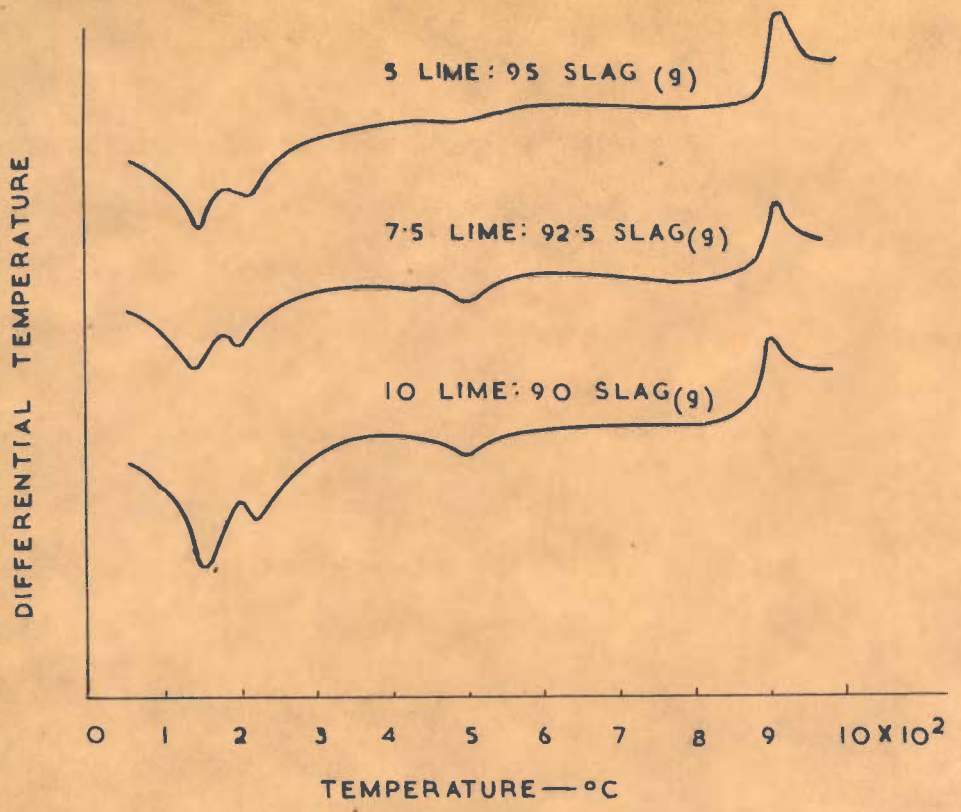

FIG.44A.D T A CURVES OF LIME-SLAG MIXES (AGE 7 DAYS)

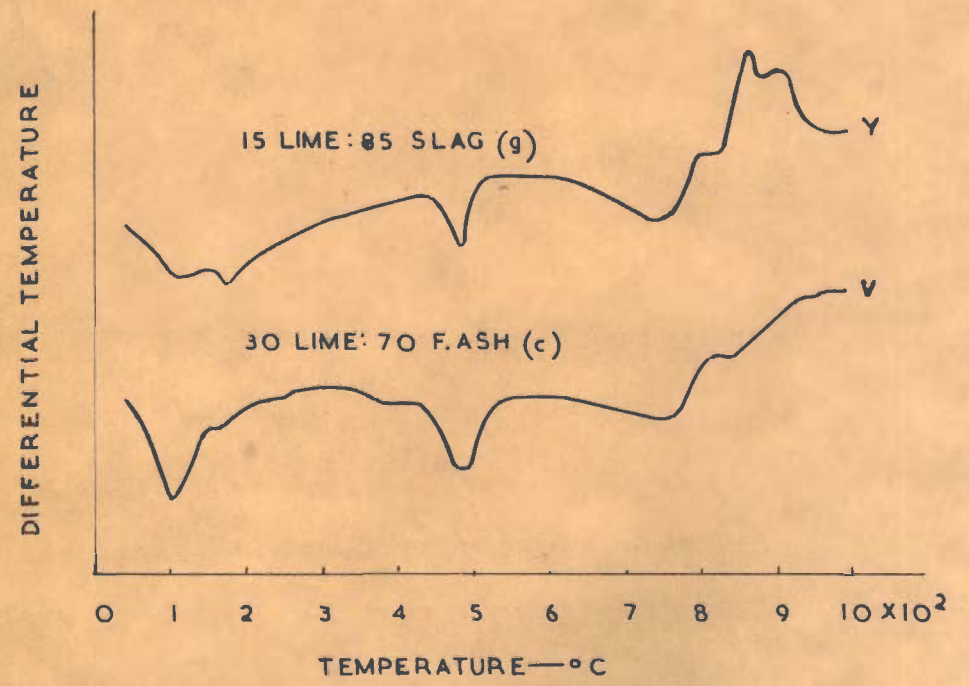

FIG·44B.D T A CURVES OF 90 DAYS CURED LIME SLAG / POZZOLANA MIXES.

not altogether satisfactory. This is also apparent from the values of W_n/S calculated from the thermogravimetric loss of the dried samples from 0 to 650°C and reported in table 37. The latter were reliable as shown below.

The data on loss in weight of the dried pastes (table 38) clearly shows that the loss due to the presence of carbonate is a highly variable factor. The weight loss from 0 to 650°C was therefore taken equal to the combined water and this data reported in table 37 show that actually the values of W_n/S for all lime-fly ash mixes are considerably lower than the corresponding values for lime-slag mixes and so are the strengths.

The values of the apparent specific volume of total water in the hardened mixes are reported in table 39 but the data was inadequate to derive any relationship between V_t and W_n/W_t.

Hydrated Phases in the Lime-Slag and Lime-Pozzolana Mixes

Chopra and Kishan Lall (100) had studied the activation of slag with small quantities of clinker and lime. Fig. 44A shows differential thermal analysis curves of the hydrated lime-slag mixes after 7 days of curing of 2 in. cube specimens. The first curve shows that in a mix of 5 : 95 lime-slag, all the lime had been consumed within 7 days. The first small inflection at about 120°is due to combined water and indicates the presence of tobermorite-

TABLE - 38

Non-Evaporable Water in Hardened Cementitious Pastes By Thermogravimetric Analysis

Mix Designation	Water-solids ratio (wt.) w/s	w_o/s	Loss in weight g/g of dried paste 0-650°C	490-600°C	650-1000°C	0-1000°C	Carbonate (Loss 650-1000°C) per cent	w_n/s*	w_n/w_o**
15 Hyd. Lime + 85 SL(g)	0.45	0.428	0.080	0.012	0.008	0.088	1.82	0.087	0.203
	0.55	0.503	0.090	0.008	0.028	0.118	6.36	0.102	0.198
	0.65	0.509	0.084	0.010	0.036	0.121	8.17	0.094	0.184
30 Hyd. Lime + 70 F(C)	0.45	0.477	0.058	0.018	0.052	0.110	11.89	0.065	0.136
	0.55	0.531	0.060	0.013	0.038	0.098	8.62	0.066	0.124
	0.65	0.519	0.062	0.014	0.058	0.120	13.16	0.070	0.135

* w_n/s is the loss in weight from 0-650°C for 1g of ignited paste and corresponds to w_n/c

** w_n/w_o is obtained by dividing w_n/s by w_o/s

T A B L E - 39

Apparent Specific Volume of Total Water in Hardened Cementitious Pastes

Mix Designation	Specific volume of dry mix v_c cc/g	Density of paste saturated g/cc	Specific volume of paste cc/g	Total water wt/c	Average specific volume of water v_t	Ratio w_n/w_t
15 Hyd. Lime + 85 SL(g)	0.361	1.858	0.538	0.462	0.924	0.188
	0.361	1.791	0.556	0.539	0.925	0.189
	0.361	1.743	0.573	0.512	0.975	0.184
30 Hyd. Lime + 70 F(C)	0.425	1.683	0.594	0.512	0.925	0.136
	0.425	1.672	0.598	0.590	0.891	0.124
	0.425	1.693	0.591	0.590	0.872	0.134

like hydrate. The endothermic peak at 215°C is due to the presence of C_4A aq. or a small quantity of monosulfoaluminate because of the presence of a small quantity of sulphate in the slag. With an increase in the proportion of lime in the mix, the magnitudes of the above mentioned peaks were found to increase and so also the peak temperature from 120 to 140°C, an additional endothermic peak appeared at 500 ± 5°C showing the presence of unreacted lime (Fig. 44A). The X-ray data also indicated the presence of C_4A aq., calcium hydroxide, calcite and tobermorite-like hydrate, probably of 14A tobermorite (100).

The mixes Y and V consisting of 15 parts of lime with 85 of slag and 30 parts of lime with 70 parts of fly ash respectively were prepared in the present study at a W/S ratio of 0.45 and cured for 90 days. The D.T.A. curves and X-ray data for the hydrated mixes are given in Fig. 44B and table 40 respectively. The mixes prepared at higher W/S ratios were not examined because the results are not expected to be any different as evident from the similarity between the weight loss curves at higher W/S ratios and that at 0.45 W/S ratio (Fig. 43).

The dta curve of the mix Y (Fig. 44B) shows the presence of tobermorite-like hydrate (118°C), C_4A. aq. and carboaluminate (188°C), unreacted lime (480°C) and carbonate (740°C). Because of the absence of ettringite peak (130 to 140°C), it is inferred that the peak at 182°C

T A B L E - 40

X-ray Powder Diffraction Data for Hydrated Lime-Slag/Pozzolana Mixes

Sample Y (Hydrated Lime-Slag)			Sample V (Hydrated Lime-Fly Ash)		
d (A)	I/I_o	Identification	d (A)	I/I_o	Identification
14.5	vw	T ?	9.8	w	T or $C_3F.3CaSO_4.aq.$
8.2	vw	A	7.95	vvw	?
7.9	mw	?	7.6	w	A
7.6	vw	MC, A, H	5.4	mw	Mu
5.3	vgw	H	4.9	m	CH
4.9	s	CH	4.28	s	Q
4.19	vw	Gh	3.86	mw	C
4.05	vvw	H	3.79	vvw	?
3.96	vvw	A	3.69	mw	He
3.87	vw	C	3.44	mw	Mu
3.83	vw	?	3.39	mw	Mu
3.11	m	CH	3.35	vvs	Q
3.07	vvw	T	3.11	w	CH
3.04	ms	C	3.07	ww	T
2.88	m	Gh, A	3.04	vs	C
2.73	vvw	H	2.96	vw	T
2.63	vs	CH	2.89	vw	Mu
2.53	vvw/b	H	2.70	s	He, Mu
2.49	vvw/b	Gh	2.63	s	CH
2.44	vvw/b	Gh	2.54	mw	Mu
2.36	vw	Gh	2.515	ms/b	He
2.33	vvw	?	2.50	w	C
2.29	vw	C	2.46	m	Mu
2.12	ww	Gh	2.28	s	Mu
2.09	vw	Gh	2.23	m	Q
2.03	ms/b	Gh, H	2.20	ms	Mu
1.93	s	CH, C	2.125	ms	Mu
			2.10	m	Mu
			1.98	m	Q

Tobermorite (T*)
+
Gehlinite hydrate (Gh)
+
Hydrogarnet (H)
+
Tetra calcium aluminate hydrate (A)
+
Monocarboaluminate (MC)
+
Calcium hydroxide (CH)
+
Calcite (C)

Tobermorite
+
Tetra calcium aluminate hydrate
+
Calcium hydroxide
+
Quartz (Q)) Unreacted
Mulite (Mu)) fly
Hematite (He)) ash
+
Calcite (C)

may also be due to monosulfoaluminate formed on account of the presence of a small quantity of sulphate in the slag. Also it may be noted that the extent of endothermic peak at 182°C is now greater than that of the peak at about 120°C (compare in Fig. 44A & B). It is clear that with an increase in lime content and period of curing C_4A aq. - carboaluminate are formed in greater amounts. This can affect the strength development adversely.

The X-ray data (table 40) also shows the presence of all the above mentioned hydrated phases and further indicate that the tobermorite phase is probably 14A tobermorite. The X-ray data, however, showed additionally the presence of gehlinite hydrate. It is quite likely that the upward slope from 200 to 380°C in the thermogram of Y mix (Fig. 44B) may be due to gehlinite hydrate present in poorly crystallized state.

The mix V shows the presence of free water (100°C), $C_4A.aq.$ - carboaluminate hydrate (178°C), hydrogarnet (400°C), calcium hydroxide (490°C) and calcite (750°C) respectively. The small inflection at 255°C is considered by Benton (84) to be due to C_2ASH_8. The small exothermic peaks at 310°C is due to some oxidation reactions, probably of α-Fe_2O_3 whose presence is indicated by the X-ray data (table 40). α-Fe_2O_3 together with quartz are constituents of the unreacted fly ash.

The X-ray data (table 40) confirms the presence of $C_4A.aq.$, carboaluminate, calcium hydroxide, calcite, quartz and α-Fe_2O_3 from fly ash. Since no sulphates were present either in lime or fly ash the line at 9.8A together with other lines at 5.40, 3.07, 2.96 and 2.28A shows the presence of 10A-tobermorite.

DISCUSSION

Effect of Total Porosity on Strength

Since one of the objects was to find how the early structure of the paste of cementitious materials influences the strengths of the hardened paste, attention is drawn to the values of water/solids ratio after bleeding (i.e., W_o/S) in table 37. A comparison of these values with those used for preparing the pastes (table 37) shows that the bleeding influences the final W/S ratio a great deal. While comparing strengths of cementitious materials, many earlier workers do not seem to have taken into account the differences in strengths which can arise from differences in bleeding characteristics.

Schiller (194) had found that the strength is related to the porosity. The data on porosity in table 37 show that in a particular set when porosity is higher, the strength is lower, otherwise, if the data is considered collectively irrespective of the mix composition, no relationship between strength and porosity is possible.

Hydrated Phases and the Strength Development

Malquori (56) has summarized the findings of several workers on the formation of hydrated phases in lime-pozzolana mixes as follows :

(a) the presence of calcium silicate hydrate of the tobermorite type has been ascertained as an apparently amorphous groundmass, in the form of a gel and in any case having a low degree of crystallization. Since the tobermorite highest in lime is stable in a calcium hydroxide solution having a near saturation titre, while the lower-lime forms are stable in weaker solutions (0.28 g per litre of CaO), the composition of the calcium silicate hydrate, although remaining within the tobermorite range, must vary,

(b) the presence of calcium aluminate hydrate, probably C_4A,H_{13} was ascertained, and

(c) the presence of C_2ASH_n was not sufficiently established.

The hydrated phases identified by the dta and X-ray powder analysis of the hardened pastes of lime-slag and lime-pozzolana of the present study are tobermorite-like hydrate, $C_4A.aq.$, carboaluminate and sulfoaluminate hydrates. The presence of a hydrogarnet and Stratlings compound (C_2ASH_8) is also indicated by the dta curves. However, a comparison of the dta curves (Fig.44) with those of the slag and pozzolanic cement (Figs. 27 and 28) shows that in lime-slag/or pozzolana mixes, the relative amounts of $C_4A.aq.$ - carboaluminate-sulfoaluminate hydrates (end. peak at 180°C) to that of tobermorite-like hydrates (end. peak at 120°C) are much greater. In other words, the quantities of the tobermorite hydrates are not

as high in lime-slag/pozzolana mixes as in the hydrated slag and pozzolanic cements at the corresponding age i.e., 90 days. This may explain the development of comparatively lower strengths in lime-slag/or pozzolana mixes.

The data of the present study indicates the presence of 14A-tobermorite hydrate and 10A-tobermorite hydrate in the slag and pozzolana mixes respectively. But in view of the conflicting evidence on the effect of microstructure of tobermorite-like hydrates on strength (46), it is difficult to say if the higher strength of the slag mixes is due to the presence of 14A-tobermorite hydrate. But the formation of gehlinite hydrate in lime-slag mix appears to be partly responsible for higher strengths of the lime-slag mixes.

The work on lime-slag/or pozzolana mixes was not carried out as extensively as planned originally because of the publication of results of a detailed study on several lime-pozzolana mixes by Jambor (88) and a similarity between his approach and that of the present investigation.

As far as the effect of the hydrated phases is concerned, it may be noted that Jambor's findings show two important differences from the results of the present study. Firstly, $C_4A.aq.$ whose presence is now well established (56) was not found by him even though the lime content in his mixes was quite high and the alumina

content of many of the pozzolanas was also high. Secondly, the tobermorite-like hydrate in his pastes was characterized by the longest spacing at 11.3 - 11.7A and consisted chiefly of irregular film-like formations or foils which is characteristic of CSH I. In this phase CaO/SiO_2 ratio is lower than in the 10A tobermorite (30) which was found to be present in the lime-pozzolana mixes of the present study.

Jambor's results also differ from those of Ludwig and Schwiete (87) who had studied reactions of lime with trass. Since it is believed that the ratio of CaO/SiO_2 in calcium silicate hydrate or tobermorite is 1.5 or more under conditions of lime saturation, Jambor's results would thus appear contrary to expectations because substantial quantities of unreacted lime were present in all his hardened pastes. It may therefore be inferred that unreacted lime in 400 days old pastes is probably heavily covered with gelatious coatings and thus is rendered inactive. Under these circumstances high lime tobermorites may ultimately change into low-lime tobermorites. Finally, it may be concluded from the above discussion that the theories which relate the absolute value of strength to the development of tobermorite phase are not fully substantiated as believed by Jambor, and there is scope for further work.

Gel-Space Theory and Instrinsic Strength

Jambor has shown that the compressive strengths

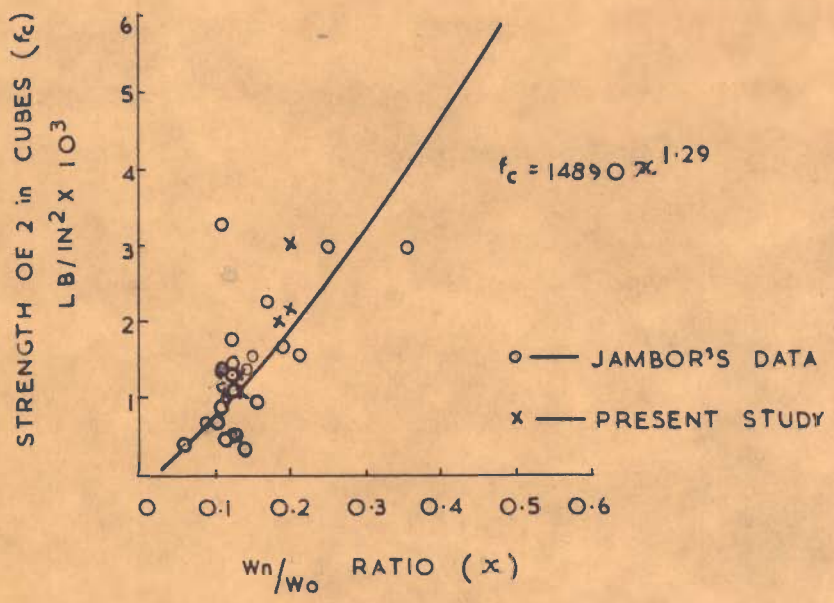

FIG. 45. RELATIONSHIP BETWEEN STRENGTH AND W_n/W_o RATIO FOR LIME-SLAG/POZZOLANA MIXES

of hardened lime-pozzolana pastes is a power function of the volume of the hydrated phases formed. This is in agreement with the gel-space theory of Powers (8). Earlier, the relationship $f_c = f_c^0 x^n$ was worked out for different hydrated cements and values of intrinsic strengths were reported in Chapter 5. Such a relationship was also attempted for lime-slag/or pozzolana pastes. For this purpose the values of W_n/W_m (corresponding to W_n/W_o) were calculated from the Jambor's data of the loss on ignition at 1000°C and 600°C respectively and the amount of unreacted lime (table 41) in a large number of pastes. The plot of strengths versus W_n/W_m values (Fig. 45) gives the relationship $f_c = 14890\ x^{1.29}$. It may be noted that the values of strengths and W_n/W_o of the lime-slag/or pozzolana pastes of the present study also satisfy the above relationship (Fig. 45).

The value of the intrinsic strength is 14890 p.s.i. which is much lower than that of the Portland cement i.e., 23169 p.s.i. Assuming that the tobermorite related phases are mainly responsible for strength as in cements, the factors which can lower the intrinsic strength of hardened lime-slag/pozzolana mixes are mostly calcium aluminate hydrates, unreacted lime, carbonate and unreacted residue of slag or pozzolana etc. As far as the results of this study are concerned, the presence of calcium aluminate hydrate ($C_4A.aq.$) in hardened lime-slag/or pozzolana pastes is mainly responsible for lowering the

TABLE - 41

Strengths of Lime-Pozzolana Pastes Versus W_n/W_m Calculated from Jambor's Data

1	2	3	4	5	6	7	8	9	10
No.	Paste	Mix proportions by weight	Mixing water, w_m per cent of wt. of mix	Strength of paste at 400 days p.s.i.	Hydrated Paste: Loss up to 1000°C (per cent by weight)	Hydrated Paste: Loss up to 600°C (per cent by weight)	Hydrated Paste: Amount of $Ca(OH)_2$ (per cent by weight)	*Non-Evap. water (w_n) g/g	** W_n/W_m
1	Dacite tuff	2:1	60.5	2258	14.5	9.1	1.5	0.102	0.169
2	+	1:1	55.0	1605	18.0	9.8	5.6	0.103	0.187
3	$Ca(OH)_2$	1:2	73.5	1065	23.6	10.8	15.2	0.093	0.126
4	Basalt tuff + $Ca(OH)_2$	1:1	47.0	1534	18.5	9.4	9.3	0.100	0.212
5	Diatomite I	2:1	99.2	1335	15.4	10.4	1.9	0.117	0.118
6	+	1:1	87.0	1051	18.7	10.6	5.6	0.114	0.130
7	$Ca(OH)_2$	1:2	86.7	653	21.6	11.3	18.3	0.088	0.101 ..
8	Diatomite II	2:1	72.0	3294	12.9	7.4	2.2	0.079	0.109
9	+	1:1	67.0	2982	15.9	9.3	6.2	0.170	0.253
10	$Ca(OH)_2$	1:2	80.6	1392	21.9	11.9	19.0	0.094	0.117 ..
11	Activated kaolin + $Ca(OH)_2$	1:1	69.0	2940	24.8	19.4	3.4	0.247	0.358
12	Fly Ash I	2:1	49.7	1718	12.7	7.0	7.2	0.060	0.121
13	+	1:1	55.0	1334	17.9	8.4	10.0	0.073	0.133
14	$Ca(OH)_2$	1:2	67.4	823	22.4	11.3	23.6	0.072	0.107
15	Fly Ash II + $Ca(OH)_2$	1:1	67.0	1363	19.0	9.4	9.0	0.089	0.133

Table 41 (Cont'd.)

1	2	3	4	5	6	7	8	9	10
16	Silica Gel	2:1	108.0	667	11.5	9.6	0.9	0.106	0.099
17	+	1:1	100.0	483	16.7	11.0	1.9	0.125	0.125
18	$Ca(OH)_2$	1:2	86.5	326	22.2	12.3	12.4	0.119	0.137
19	B Quartz + $Ca(OH)_2$	1:1	51.0	340	18.3	7.0	18.7	0.031	0.061
20	Sial	2:1	44.0	1406	11.3	6.3	7.5	0.051	0.116
	+	1:1	56.0	909	18.3	8.8	14.6	0.086	0.153
	$Ca(OH)_2$	1:2	76.0	497	23.1	11.1	23.6	0.07	0.116

* W_n = $\frac{\text{Loss in wt. at } 600^\circ C - \text{water in } Ca(OH)_2 \text{ unreacted}}{100 - \text{Loss in wt. at } 1000^\circ C}$

** Since W_o is not known, the ratio W_n/W_m was calculated instead of W_n/W_o; W_m is the mixing water.

intrinsic strengths because the quantities of unreacted $Ca(OH)_2$ were indeed small and carbonate was also not present in any unduly large quantity (table 38).

CONCLUSIONS (Chapters 4 to 6)

The effects of the period of curing and W/C ratio on the degree of hydation and strengths showed that all the clinker-based cements hydrated and developed strengths at a slower rate than that of the Portland cement.

The strength data of the PC, PBF, BFP, PZC and SSC cements hydrated at a W/C ratio of 0.4 showed that the strengths of the PBF cement equalled after 28 days; the gain in strength for the BFP and PZC cements from 28 to 90 days was higher than any other cement, and that at 90 days all cements, excepting the BFP, showed strengths equal or higher than those of the Portland cement.

The phases identified in the Portland cement paste were tobermorite-like hydrate (gel), ettringite, monosulfoaluminate, tetracalcium aluminate hydrate, a hydrogarnet and calcium hydroxide. Small quantities of calcite and monocarboaluminate were also present.

Most of the above hydrated phases were also found to be present in the pastes of the other clinker-based cements but with some differences. For example, at 90 days when the strengths were mostly equal to those of the Portland cement paste, the differences observed were

(a) the tobermorite phase appeared to be different in nature; either in having different CaO/SiO_2 and H_2O/SiO_2 ratios, or in microstructure,

(b) ettringite was not present in PBF cement but in the BFP and PZC cements it was present in quantities greater than that in the PC cement,

(c) the hydrogarnet phase in the PC cement could be identified as $C_6AFS_2H_8$ by the appearance of lines at 5.1, 4.40, 3.33, 2.28 and 2.05A. In the PBF, BFP and PZC cements there were no lines corresponding to 5.1A and 4.40A and also the line at 3.33A occurred at 3.34-3.35A in these cements. Moreover, the intensity of the line in the BFP cement was much stronger. Differences in the hydrogarnet phase in the PBF, BFP and PZC cements are indicated. The thermograms show that its quantity in the PBF cement is greater than in any other cement paste, and

(d) calcium hydroxide was present in a decreasing order in the PZC, PBF and BFP cements.

The hydrated silica and alumina bearing phases appeared to mix intimately only after 28 days of paste hydration. There were indistinguishable in the thermograms of 90 days old pastes.

There was no evidence of silico-aluminic hardening in the PBF and BFP cements. However, the presence of gehlinite hydrated showed evidence of this type of hardening in SSC cement.

The main hydrated phase in the SSC cement was ($3CaO.Al_2O_3.3CaSO_4.31H_2O$) ettringite. The sulphate activation of the low lime and high alumina slag had shown that the strengths were highest when ettringite with SO_3/Al_2O_3 ratio of 3 was formed and it was possible only when calcined gypsum was used in a quantity (20-25%) greater than that recommended (10-15%) in the literature. The other phases present were tobermorite-like hydrate,

gehlinite hydrate and a small quantity of monosulfoaluminate. Tobermorite-like hydrate was present in substantial quantities at 90 days as evident from the differential thermal analysis and specific surface measurement.

The hydrated solid phases in the hardened pastes of lime-slag and lime-fly ash were tobermorite-like hydrates, tetracalcium aluminate hydrate, carboaluminate & monosulfo-aluminate hydrates and a hydrogarnet.

The X-ray data indicated the presence of 14A-tobermorite hydrate in the lime-slag mix and 10A-tobermorite in the lime-fly ash mix. The formation of gehlinite hydrate in the lime-slag mix indicates the possibility of the silico-aluminic hardening.

The relationship between the apparent specific volume of total water (V_t) and the ratio of non-evaporable water to the total water (W_n/W_t) for the hydrated PC, PBF and SSC cements was found to be a straight line relationship and satisfied the Copeland's equation i.e.,

$$V_t = 0.99 - 0.25\, W_n/W_t$$

The apparent specific volume of the non-evaporable water thus appears to be 0.74. However, no conclusion could be drawn in respect of the BFP and PZC cements because of the dispersion of the experimental points.

The specific surface of the cement pastes (W/C = 0.40) hydrated for 90 days were found to be 195,

183, 117, 169 and 127 sq m per g for the PC, PBF, BFP, PZC and SSC cements respectively.

The values of the specific surface diameter and average pore width of the hydrated phases in the different cement pastes were estimated but these were found to be of limited use in revealing differences in the microstructure of the hydrated pastes.

Electronmicrographs, on the other hand, showed important differences in the hydrated cement pastes of 90 days age. For example, the micrograph of the hydrated PC cement showed entirely fibrous structure characteristic of the tobermorite phase. The bundled fibres were clearly visible. Some plates, probably of hexagonal symmetry and belonging to the calcium-aluminate hydrate phase, were also seen. The PBF cement also showed fibrous structure but the fibres were much finer and shorter in length. Sometimes the fibres were so fine that the material appeared to be amorphous in nature. The platy crystals, hexagonal and probably belonging to C-A-H phase, were present in a greater quantity in this cement.

In the BFP cement the tobermorite phase consisted of fine fibres and thin sheets. The hydrated PZC cement showed fibrous structure as well as foils, the latter being characteristic of the low-lime-tobermorite phase. Lath-like crystals of ettringite were also present in significant amount in the pastes of both the BFP and

PZC cements. No such structures were seen in the electron-micrographs of the PC and PBF cements.

The capillary or total porosity of the hardened pastes did not show a precise relationship with the strength. But the strengths of all the cements, including that of supersulphated cement, could be explained on the basis of the gel-space theory. The equations correspond to that of Powers viz., $f_c = f_c^o x^n$ where f_c is the absolute strength, f_c^o is the intrinsic strength and x is the gel-space ratio (W_n/W_o in the present study) and n is a reduction factor.

The relationships for the hardened pastes of the different cements were as follows :

(i) $f_c = 23169\ x^{1.52}$ for the Portland cement

(ii) $f_c = 23179\ x^{1.46}$ for the PBF cement

(iii) $f_c = 43601\ x^{1.83}$ for the BFP cement

(iv) $f_c = 42786\ x^{2.00}$ for the PZC cement, and

(v) $f_c = 21013\ x^{0.85}$ for the SSC cement , and

(vi) $f_c = 14890\ x^{1.29}$ for lime-pozzolana/slag

It was concluded from the above relationships that the intrinsic strength of the cement gel in each of the cements PBF, BFP and PZC is not lower than that of the PC cement. On the other hand, the intrinsic strengths of the BFP and PZC cements are higher. The presence of tobermorite phase in the form of very fine and short fibres and also as flakes or foils (characteristics of calcium silicate hydrate with low CaO/SiO_2 ratio) and

that of ettringite in greater quantities appeared to be responsible for higher intrinsic strengths of the BFP and PZC cements. The presence of hexagonal plates of C-A-H phase ($C_4A.aq.$) in the PBF cement in a greater quantity than in any other cement appears to affect the strength of this cement adversely.

The relationship $f_c = 21013\ x^{0.85}$ and the specific surface of 127 sq m per g of the hydrated cement show that even the secondary phases of tobermorite-like hydrate, gehlinite hydrate and probably alumina gel contribute a good deal towards the strength development of the supersulphated cement.

The reason for the lower intrinsic strength of the hydrated lime-pozzolana/slag pastes were found to be due to the presence of comparatively a greater proportion of the hydrated alumina bearing phases in comparison to that of the tobermorite-like hydrates.

STUDIES ON THE AUTOCLAVED CEMENTITIOUS PRODUCTS

CHAPTER 7

HYDROTHERMAL REACTIONS AND PROPERTIES OF AUTOCLAVED CEMENTITIOUS MATERIALS

Introduction

Both equilibrium and non-equilibrium studies of the hydrothermal reactions in the system $CaO-SiO_2-H_2O$ have been made with a view to understanding the processes of hydration of cement and cement-silica products at elevated temperatures. In his excellent review of the advances made during the last ten years or so in this field as well as the study of hydrothermal reactions in lime-silica (or siliceous) mixes, Taylor (30) has brought out that equilibrium studies, though important and valuable, provide little direct information on the reactions likely to occur and hence are of limited application in the technology of steam pressure curing of cement products or in the manufacture of sand-lime bricks, lightweight heat-insulating materials and other similar products. On the other hand, non-equilibrium studies provide information for direct technical application. But strictly speaking the information gathered from one particular non-equilibrium study may not hold true for another one because at the commonly employed temperatures (below 220 ^{o}C) the approach to equilibrium is slow and small variations in experimental conditions may influence the sequence of reactions. At this stage

it would be appropriate to emphasize the effect of the starting materials on the sequence of reactions and the formation of intermediate and final phases. For example, Midgley and Chopra (195) who had studied hydrothermal reactions in the lime-rich part of the system $CaO-SiO_2-H_2O$ found that the form of the starting material had a considerable influence on the nature of metastable phases produced.

Inspite of the above mentioned difficulties, the hydrothermal reactions which take place on the hydration of C_3S, β-C_2S and cement pastes are now well established. The different phases detected by various workers are listed by Taylor (30) and the phase assemblages which develop at successively higher temperatures for all $CaO:SiO_2$ ratios in the system $CaO-SiO_2-H_2O$ are now available from the excellent representations of the reactions in a series of triangular diagrams constructed by Roy and Harker (196).

Hydrothermal Reactions in Wet Mixes of Cement-Silica or Siliceous Fines

Briefly speaking, the successive formation of a modified form of CSH gel and of C_2S β-hydrate, together with $Ca(OH)_2$ result from the hydrothermal reactions of β-C_2S and C_3S in ordinary cement. Effect of addition of silica or quartz in cement pastes has been studied by Thorvaldson and Skelton (197), Kalousek

and Adams (198), Sanders and Smothers (31) and Neese, Spangenberg and Weiskirchner (199). All these investigators show that high strengths in autoclaved cement-silica products are associated with the formation of tobermorite which can be present in gelatinous as well as crystalline forms. On the other hand, the formation of crystalline C_2S α-hydrate is associated with low mechanical strengths.

Similarly, hydrothermal reaction in lime-silica pastes studied by Bessey (91), Kalousek (89), Aitken and Taylor (90) and Assarson (200) have shown the hydration phases to be poorly or well crystallized tobermorite, CSH gel, zonotlite, CSH(I), C_2S α-hydrate, gyrolite, hillebrandite and 'Phase F'. Again the development of strength was related with the formation of the different phases in a general way and conclusions were no different from those stated in the foregoing para.

Hydrothermal Reactions between Lime and Siliceous Fines

In view of the rapid technological advancements and application in the field of precast autoclaved building units, prepared from mixes of lime with ground quartz-sand, fly ash, calcined shales, slags etc. (201), it has become increasingly important to understand better the factors which govern the strength and other properties. The investigation reported in this Chapter has been carried out with this object in view.

Studies on hydrothermal reactions between lime and alumina-silica bearing materials are comparatively few. Kalousek had reported on the cementitious phases of autoclaved concrete products in 1954 (89). Ordinary Portland cement or lime or a combination of the two with silica, pumice, shale and slag fines etc. were used as cementitious fines for producing concrete. Kalousek found, in general, that strength-unit weight of concretes showed nearly a straight line relationship. The examination of the autoclaved lime-cement-silica (or pumice, slag etc.) product was done mostly by the chemical method and differential thermal analysis. The cementitious phases formed in the autoclave as a result of hydrothermal reactions were characterized as hydrates of 0.9 - 1.3 CaO/SiO_2 series and a poorly crystallized form of alpha-type dicalcium silicate hydrate. No attempt was however, made to correlate the formation of cementitious phases with the strength of concrete blocks.

Subsequently Midgley and Chopra (93) studied hydrothermal reactions between lime and fines such as fly ash, expanded colliery shale, ground quartz, granulated and foamed blastfurnace slags. Moist mixes of lime and fines in different proportions (maximum lime being 40 parts by weight) were moulded into cylinders at a pressure of 2 tons per sq in. and autoclaved at 160 lb per sq in. for 2, 6, 16 and 48 hours. The cementitious phases formed on autoclaving were examined

with the help of differential thermal analysis, X-ray powder diffraction photographs and chemical methods. An attempt to correlate strengths of compacted cylinders with the cementitious phases was made. Their main findings were :

(i) in all the mixes the development of strength was associated with the reaction of lime with silica to form tobermorite, the degree of crystallinity increasing with lime/silica ratio and processing time,

(ii) when the fines also contained alumina, a hydrogarnet was formed. The most probable composition of the hydrogarnets was $3CaO.Al_2O_3.SiO_2.4H_2O$ when fly ash or shale was reacting with lime and $3CaO.Al_2O_3.2SiO_2.2H_2O$ when slag glass was reacting,

(iii) Zonotlite and tobermorite were formed in lime-quartz mixes. At high CaO contents and long processing times, Flints CSH(A) was also formed,

(iv) the strength data indicated that the strengths were maximum in the 30 : 70 (lime : fines) mix processed for 16 hours except for slags. The CaO/SiO_2 ratio in these mixes was about 1.0, and

(v) mixes of lime and slag in proportions of 5 : 95 and processed for about 6 hours gave the maximum strengths. With an increase of either the proportion of lime or processing time greater quantities of C_2S α-hydrate were formed and there was a fall in strengths.

Though Midgley and Chopra were able to identify the different calcium silicate hydrates and hydrogarnet phases formed as a result of hydrothermal reactions and also relate the strengths, in general, with the nature and quantity of the strength giving calcium silicate hydrate phases, their experiments and results emphasized the need for further work. In a way

the present work could be taken as a continuation of the earlier work of Midgley and Chopra.

MATERIALS

Five mixes of lime and fines viz., E, F, G, H and I (table 1) were used in the present study. The sample of hydrated lime was the same as used in earlier studies (Chapter 6). The fines of each of the materials viz., quartz sand, granulated slag (TISCO) and foamed slag (British) had a specific surface of about 3200 $\pm$ 50 sq cm per g. The samples of fly ash (unfired) and calcined fly ash had a fineness of 2763 and 3466 sq cm per g respectively.

The composition of the five mixes E, F, G, H and I is given in table 1. In the mixes of E, F and G the ratio of hydrated lime to each of the ground quartz and fly ashes were 30 : 70. In the other two mixes e.g., H and I the ratio of lime to slag fines was 10 : 90. These mixes had been selected in the light of the earlier work of Midgley and Chopra (93) who had found a ratio of 30 lime : 70 fines to result in highest strengths. However, for lime-slag fines a ratio of 10 : 90 was selected,(instead of 5 : 95) as the Indian granulated slag has a CaO/SiO_2 ratio lower than that of the British granulated slag.

EXPERIMENTAL

Moulding of Compacts

Moulding of cylindrical compacts from moist mixes of lime and aggregate fines is an important step. Midgley and Chopra had moulded their specimens at a uniform pressure of 2 tons per sq in. The amount of water used was arrived at by trial and error and was 12 per cent for all the mixes except those prepared with quartz fines. Since this process does not ensure a uniform degree of compaction of solids which in turn may influence the strengths of the autoclaved specimens, it was considered important to control this unknown factor. For this purpose the influence of moulding pressure on deformation (i.e., degree of compaction), density and porosity of cylinders prepared from different solids at varying water/solids ratios was studied. The optimum moulding pressure for each of the cementitious mix at water/solid ratio of 0.12 was then chosen. Cylindrical compacts (3 in. ht. x 2 in. dia) were thus prepared under controlled conditions.

Autoclaving of Compacts

The cylindrical specimens were autoclaved at a steam pressure of 160 p.s.i. in a laboratory autoclave (Cenco) fixed with a pressure stat. In the light of previous experience of Midgley and Chopra only one

processing time of 16 hours was employed. At the conclusion of autoclaving period, the specimens were removed, placed in a desiccator to cool and were stored in dry CO_2 - free conditions till required for various physical determinations.

Water Absorption of Compacts and W_t

For Water absorption weighed specimens were immersed in water till the weight change was negligible. Generally this period was never more than 48 hours. Weight of saturated surface-dry specimens was taken accurately. The specimens were then crushed and a representative granular sample passing No. 30 and retained on No. 80 U.S. sieve was prepared for determining loss on ignition immediately. W_t was calculated from it as described earlier in Chapter 5.

Compressive Strength of Compacts

The procedure was the same as described in Chapter 4.

Preparation of Granular Sample

Crushed material from the autoclaved compacts was ground further and quartered. A representative sample of granular sample was prepared by passing it through U.S. sieve Nos. 30 and 80. The fraction (-30+80) was collected and stored for different determinations.

Differential Thermal X-ray Powder Analysis

The procedure for the differential thermal analysis of the granular sample was the same as reported in Chapter 4.

The X-ray powder analysis of the granular samples was done by the procedure described on page 24.4.

Non-Evaporable Water

The granular samples were dried under vacuum and non-evaporable water was determined in a manner similar to that described in Chapter 5.

The non-evaporable water content of the granular samples was also estimated from the thermo-gravimetric loss of vacuum dried granular samples.

RESULTS

Effect of Moulding Pressure on Deformation and Porosity of Green Compacts

Recently Lecnazar (202) studied the effect of moulding pressure on the properties of pastes, mortars and concretes prepared from a prematurely hydrated cement. As is well known the density of a compacted mass of granular solids depends to a great extent on the internal friction arising from the relative motion of the grains. When moulding pressure is applied continuously, the mass offers resistance and a characteristic deformation curve

is obtained. The data on the deformation of moist mixes of lime-siliceous fines can be interpreted as a relationship between moulding pressure and density of the compacts. Since the density of the aggregate and so also the internal friction are variable in the mixes of lime and fines, it was considered desirable to study the relationship between moulding pressure and porosity coefficient (m), the latter being the ratio of volume of pores (n) and volume of solids (V_c) in a unit volume.

Before the addition of water to a mix of lime and aggregate fines

$$V_c + n = 1 \qquad \ldots (1)$$

$$\text{and} \quad n/V_c = m \qquad \ldots (2)$$

By combining (1) and (2), volume of solids can be expressed as

$$V_c = 1/1 + m \qquad \ldots (3)$$

Similarly,

$$n = m/1 + m \qquad \ldots (4)$$

On the addition of water the system consists of three phases i.e., solid, water and air. If a unit volume of paste is denoted by V_z

$$V_c + V_w + n = V_z = 1 \qquad \ldots (5)$$

where V_w is volume of added water.

If z represents a unit weight of paste and C, W, p_a are the respective weights of components i.e., solid, water and air,

$$C + W + p_a = z \qquad \ldots (6)$$

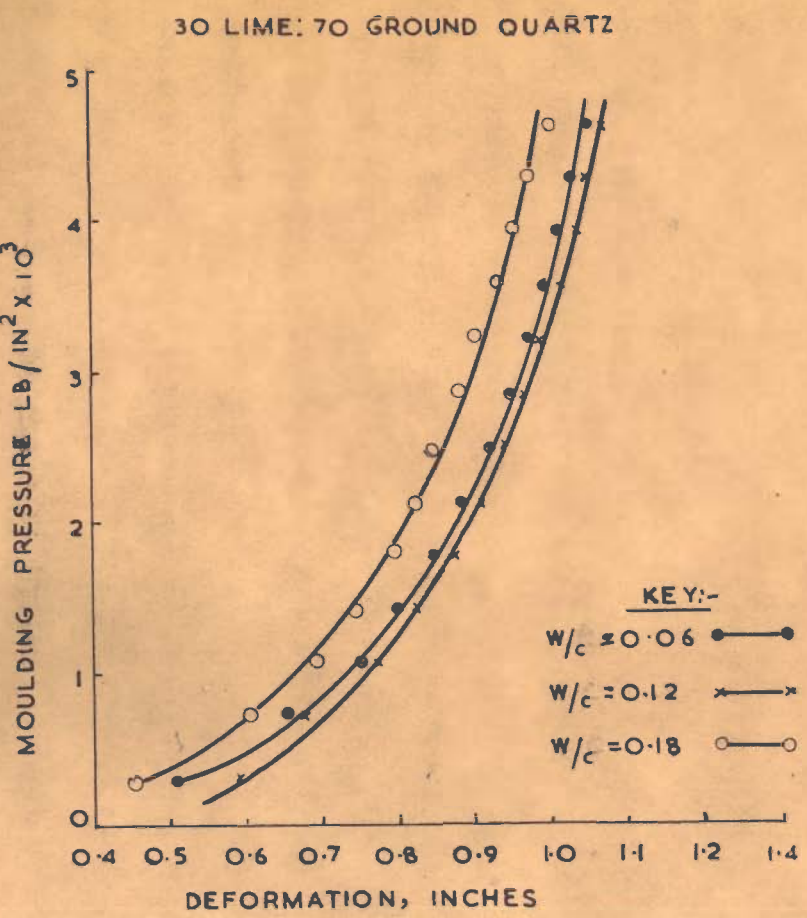

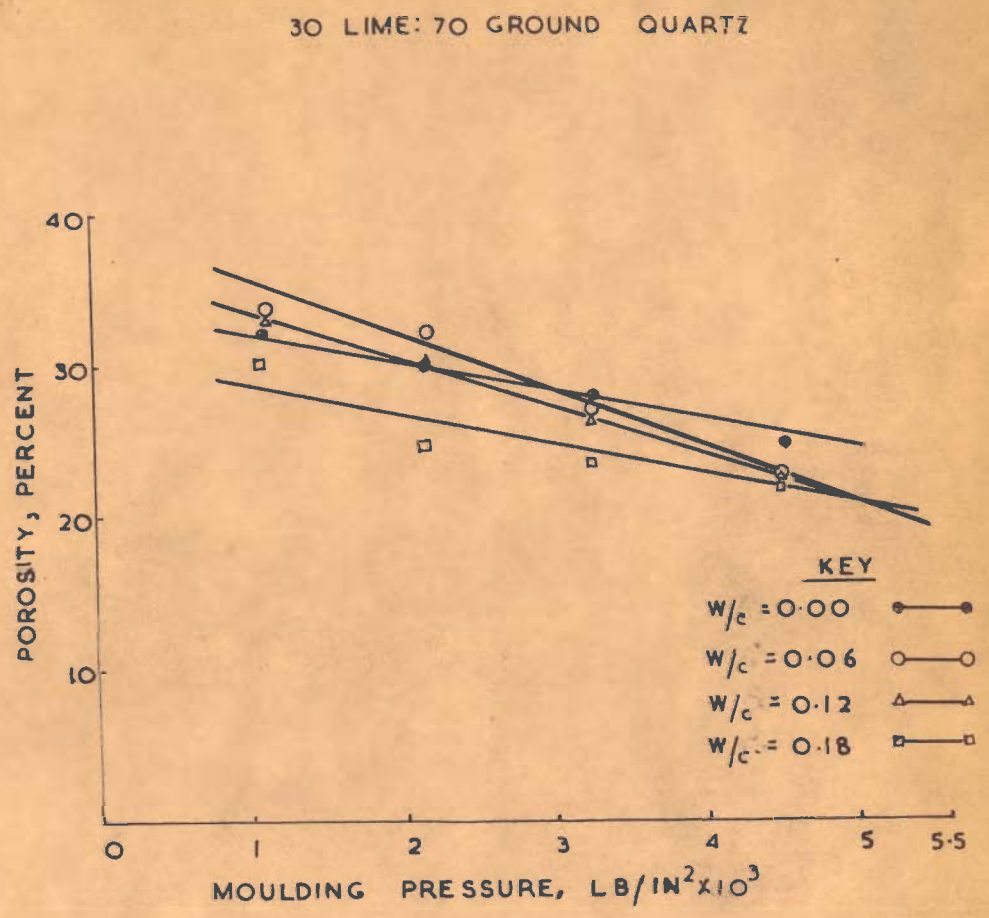

FIG. 46. TYPICAL RELATIONSHIPS FOR MOIST MIXES OF LIME - FINES

Equation (6A) can also be expressed as

$$V_z \cdot q_z = V_c \cdot q_c \cdot (1 + W/C) + p_a \cdot q_a \qquad \ldots (7)$$

where q_z, q_c and q_a are specific densities of paste, solids and air respectively. Since the specific density of air is very small compared to that of paste, the term $p_a \cdot q_a$ can be neglected. Substituting the value of V_c from equation (3) and if V_z is considered equal to a unit volume,

$$q_z = \frac{q_c}{1 + m} \cdot (1 + W/C) \qquad \ldots (8)$$

and porosity coefficient

$$m = \frac{q_c}{q_z} \cdot (1 + W/C) - 1 \qquad \ldots (9)$$

Fig. 46 shows a typical curve of deformation of a lime:fine mix as a function of moulding pressure. Water/solid ratio was varied in steps from 0 to 0.24. The results showed that deformatio-n increased with moulding pressure up to W/S = 0.12 for 30 lime : 70 ground quartz or slag and up to W/S = 0.18 for 30 lime : 70 fly ash (unfired) and then decreased for higher W/S ratios. The increase in deformation appears to result from the lubrication effect of water and reduction in internal friction. When quantity of water is more than necessary for lubrication, probably it exists as hydrospheres around lime particles and is shed at high moulding pressures. The porosity was found to decrease with increasing moulding pressure. This is shown in

Fig. 46 which is for a 30 lime : 70 quartz fines mix.

Midgley and Chopra had moulded cylindrical compacts at a pressure of 2 tons per sq in. and W/S ratio was 0.12 except for quartz fines. Values of porosity coefficient (m) and volume of pores (n) for four different lime-fines mixes and for two W/S ratios i.e., 0.06 and 0.12 were determined in the present study and are given in table 42. The data show that while the selections of W/S ratios based on trial and errors by Midgley and Chopra were very near the maximum deformations and hence maximum densities of each of the moist mixes, the values of porosity (n) were perhaps considerably different in their mixes. The present data indicate that for a moulding pressure of 2 tons per sq in. and W/S ratio of 0.12, the porosity could vary within wide limits (0.193 to 0.315 in the series under consideration). The 28 days compressive strengths of compacts cured under normal conditions together with other relevant data are reported in table 43.

From the above it may be concluded that for analysing the respective effects of porosity, nature and quantity of cementitious phases formed in hydrothermal reactions, on the strength of compacts it is important to prepare cylindrical compacts at the same porosity. But in practice moulding of cylindrical compacts absolutely at the same porosity was found very difficult because of

TABLE - 42

Porosity Coefficients of Compacts Moulded from Different Mixes

Specimen Designation	Mix Composition (By weight	Ratio water/solid (By weight)	Weight of specimen g	q_c g/cc	q_z g/cc	Porosity coefficient (average) m	Volume of pores (average) n
A_1	30L : 70F*	0.06	160.0	2.34	1.69	0.47	.319
A_2	30L : 70F	0.12	167.0	2.34	1.89	0.46	.315
B_1	30L : 70S	0.06	206.0	2.52	2.04	0.30	.231
B_2	30L : 70S	0.12	216.0	2.52	2.15	0.30	.231
C_1	30L : 70SL(f)	0.06	216.0	2.69	2.15	0.32	.242
C_2	30L : 70SL(f)	0.12	231.0	2.69	2.33	0.24	.193
D_1	10L : 90SL(g)	0.06	232.0	2.83	2.21	0.35	.259
D_2	10L : 90SL(g)	0.12	246.0	2.83	2.38	0.30	.231

L = Hydrated lime; F = fly ash; F(c) = calcined fly ash;
S = ground quartz sand; SL(g) = granulated slag; SL(f) = foamed slag.

TABLE - 43

Compressive Strength of Compacts Cured Under Normal Conditions for 28 Days

Specimen Designation	Weight of solid g	Volume of solid cc	Water absorbed after curing g	Water used in moulding g	Total water g	Porosity coefficient (average) m	Volume of pores (average) n	28 Days crushing strength (average) lb/in^2
A_1	151.0	64.0	35.96	9.00	44.96	0.70	0.412	293
A_2	149.1	63.7	27.20	17.90	45.10	0.70	0.412	378
B_1	194.5	77.2	22.72	11.50	34.20	0.44	0.305	357
B_2	192.9	76.1	10.30	23.10	34.40	0.45	0.310	378
C_1	203.8	75.7	16.60	12.20	28.80	0.38	0.275	799
C_2	206.3	76.9	7.67	24.70	32.37	0.41	0.284	792
D_1	219.0	77.3	27.80	13.00	40.80	0.52	0.342	742
D_2	219.7	77.3	6.70	26.30	33.00	0.42	0.295	956

variables. Nevertheless, the data in table 44 show that the value of 'n' for the four mixes varied from 0.31 to 0.33 and it was 0.35 for the mix of lime : fly ash (unprocessed) (in the latter mix presence of unburnt fuel was an additional variable). The average porosity of the four former mixes could be taken as 0.32 $\pm$ 0.01 before the processing in an autoclave.

Uncombined Lime in the Autoclaved Compacts

The processing time of 16 hours was decided on the basis of earlier results of Midgley and Chopra. The amount of unreacted calcium hydroxide was determined by the Franke method (table 45). The values may be slightly higher because of the slight decomposition of calcium silicate hydrates. But the results show that in all the mixes $Ca(OH)_2$ had been consumed almost completely. This is in accordance with the earlier results of Midgley and Chopra (93).

Non-Evaporable Water in the Autoclaved Mixes

The determination of non-evaporable water in the autoclaved mixes by the usual method of finding loss on ignition of the vacuum dried granular sample is rather difficult because while it is possible to account for the loss on ignition of the unhydrated cement in cement pastes, this is a variable quantity in the autoclaved mixes under discussion. But, since calcium hydroxide

TABLE - 44

Values of 'm' and 'n' of Cylindrical Compacts Moulded at w/c = 0.12

Specimen Designation	Mix composition	Average weight of specimen g	Average height of specimen in.	Specific density of mix (q_c) g/cc	Specific density of paste (q_z) g/cc	Porosity coefficient m	Volume of pores n
E	30L : 70S	276.0	2.71	2.52	1.94	0.46	0.32
F	30L : 70F	252.0	2.85	2.34	1.67	0.56	0.35
G	30L : 70F(c)	265.0	2.77	2.42	1.85	0.46	0.32
H	10L : 90SL(g)	306.6	2.84	2.79	2.08	0.50	0.33
I	10L : 90SL(f)	311.0	2.71	2.87	2.23	0.43	0.31

TABLE - 45

Amount of Unreacted $Ca(OH)_2$ after Hydrothermal Reactions

Specimen designation	Mix composition	$Ca(OH)_2$ before reaction per cent	Free $Ca(OH)_2$ after reaction per cent	Combined $Ca(OH)_2$ per cent
E	30L : 70S	28.75	1.06	27.69
F	30L : 70F	28.80	0.95	27.85
G	30L : 70F(c)	27.98	1.64	26.34
H	10L : 90SL(g)	9.62	1.76	7.86
I	10L : 90SL(f)	9.48	0.76	8.72

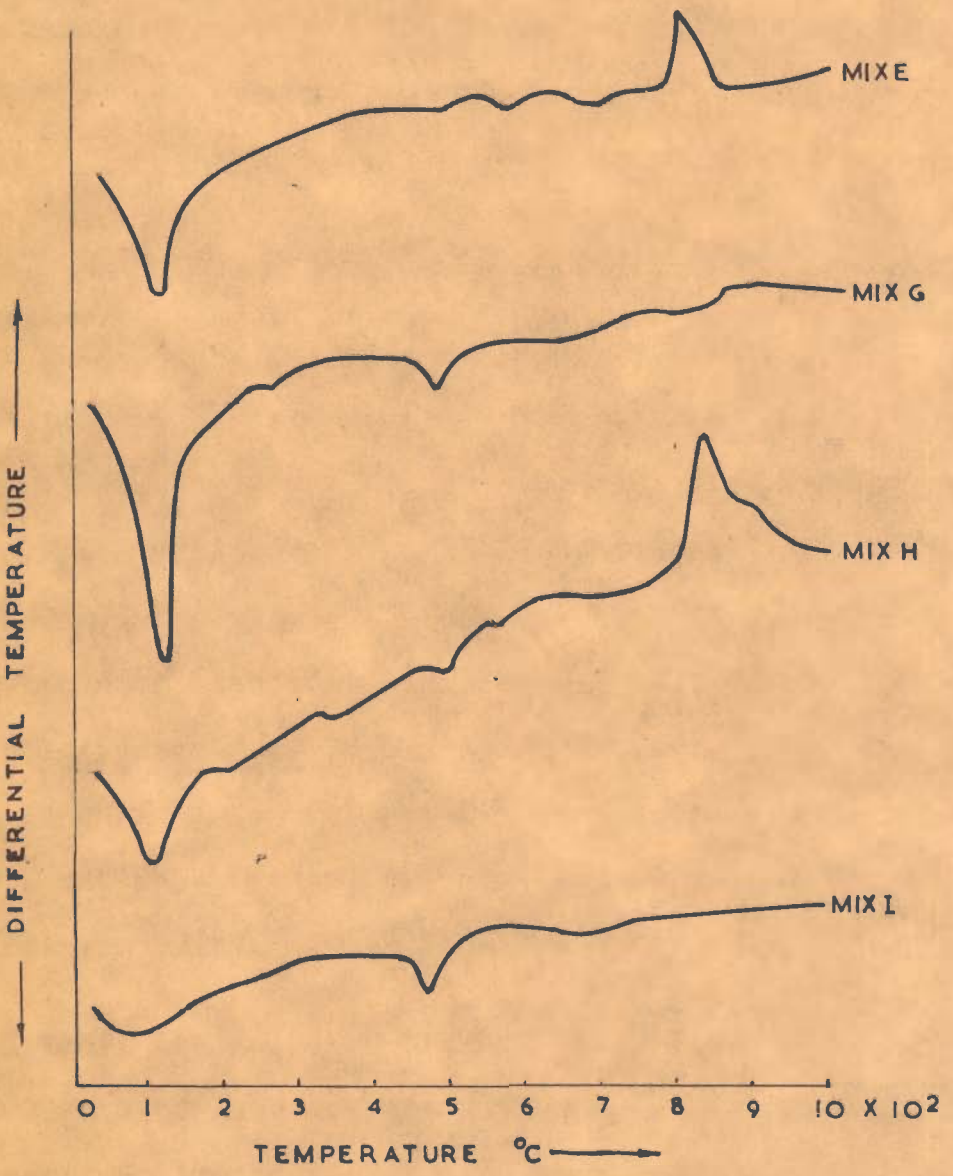

FIG. 47 D T A CURVES OF AUTOCLAVED LIME - FINES MIXES

was found to be present in the mixes in very small quantities (table 45), the determination of total loss on ignition, when corrected for the loss on ignition of the aggregate fines, gave fairly accurate values of the non-evaporable water (table 46).

Mineralogy of the Autoclaved Products

The mineralogical examination of the Mix E carried out with the help of X-ray powder diffraction analysis (table 47) showed the presence of poorly crystallized tobermorite and zonotlite in a smaller quantity. The large endothermic peak above 100°C is due to tobermorite gel and the exothermic peak at 805°C is due to the heat of formation of wollastonite (Fig.47). The poorly crystallized tobermorite gel is Taylors CSH(I). The inflections at 575° and 690°C are due to the conversion of quartz and decomposition of calcite respectively.

The longest spacing at 11.44 and other lines show the presence of a well crystallized tobermorite in lime-fly ash mixes F and G. A line of medium intensity at 2.76A together with some other weaker lines suggests the presence of a cubic phase of the hydrogarnet series, unit cell a_o = 12.37A which suggests an approximate composition of $3CaO.Al_2O_3.SiO_2.4H_2O$. The strong endothermic peak at 125°C (Fig. 47) is due to the presence of poorly crystallized tobermorite gel. The

TABLE - 46

Comparison of Non-Evaporable Water with Chemically Combined Water

Autoclaved Mix Designation	Non-Evaporable Water		Chemically Combined Water (Calculated)
	Thermogravimetric loss upto 650°C mg/g	Method of loss on ignition at 1000°C mg/g	mg/g
Mix E			
30 Lime:70 Quartz	0.059	0.064	0.064
Mix F			
30 Lime:70 F.Ash(u)**	0.122	0.016*	0.075
Mix G			
30 Lime:70 F.Ash(c)	0.089	0.084	0.075
Mix H			
10 Lime:90 Slag(g)	0.062	0.096	0.105
Mix I			
10 Lime:90 Slag(f)	0.025	0.039	0.066

* Not reliable as presence of unburnt fuel vitiated the results.

** u = unfired sample.

T A B L E - 47

X-Ray Powder Analysis of Autoclaved Lime-Fines Mixes

Mix E 30 Lime : 70 S			Mix F 30 Lime : 70 F		
d (A)	I/I_o	Identification	d (A)	I/I_o	Identification
11.40(b)	vw	T	11.44	s	T
4.72	vvw		7.22	vw	?
4.23	vw	Q	6.38	w	H
3.64	vw	Z	5.47	vvw	T
3.33	vvs	Q	5.04	vvw	H
3.05	vw	T,Z	4.30	vw	F
2.73	vvw	Z	3.73	vw	F
2.46	vvw	Q	3.36	vs	F+H
2.367	vvw		3.08	vvs	T
2.28	vvw?	Q	2.98	w	F+T
2.23	vvw?	Q	2.76	m	H
2.128	vvw?	Q	2.53	vvw	F+H
2.016	vvw	T	2.258	vw	H
1.976	vvw	Q	2.217	vw	F+T
1.824	vw	Q+T	2.14	vw	F+H
1.708	vvw	Z	2.094	vvw	T
1.672	vvw	Q+T	1.994	vw	T+H
1.546	vw	T+	1.824	w	T+H+F
1.523	vvw	T+Z	1.708	vw	H+F
			1.645	vw	H
			1.575	vvw	F
			1.517	vvw	T
Tobermorite (T) + Zonotlite (Z) + Quartz (Q)			Tobermorite + Hydrogarnet (H) ($3CaO.Al_2O_3.SiO_2.4H_2O$) + Unreacted fly ash (F)		

Table 47 (Cont'd.)

Mix H 10 Lime : 90 S(g)			Mix I 10 Lime : 90 S(f)		
d (A)	I/I_o	Identification	d (A)	I/I_o	Identification
11.35	w	T	11.00(b)	w	T
7.56	vw	H	6.92	w	H
6.93	vvw	H	4.98	vvw	CH
4.98	w	H+CH	4.21	vvw	S+$\mathcal{L}$
4.32	vvw	H	3.87	vvw	$\mathcal{L}$
3.84	vvw	$\mathcal{L}$	3.70	vvw	S+$\mathcal{L}$
3.42	w	H	3.41	vvw	S+H
3.26	vvw	$\mathcal{L}$	3.27	w	$\mathcal{L}$
3.06	vs	T	3.07	vw	S+T
2.74	vs	H	2.85	vs	S
2.63	vw	CH	2.74	w	S
2.49	w	H	2.627	vw	CH
2.398	vw	$\mathcal{L}$	2.44	vvw	S
2.24	m	H	2.397	vw	$\mathcal{L}$
2.033	ms	$\mathcal{L}$+S+H	2.292	vvw	S+H
1.982	ms	H	2.24	vvw	H
1.926	vw	H	2.038	vw	S+H+$\mathcal{L}$
1.878	vw	H	1.99	vvw	H
1.81	vw	T	1.822	vvw	S+T
1.76	vvw	H	1.768	m	S+H+$\mathcal{L}$
1.69	m	H+T	1.640	vw	S+$\mathcal{L}$
1.63	m	H	1.538	vw	S+$\mathcal{L}$
			1.435	vvw	S+$\mathcal{L}$
			1.388	vw	S+$\mathcal{L}$

Tobermorite (T)
+
Hydrogarnet (H)
($3CaO.Al_2O_3.2SiO_2.2H_2O$)
+
C_2S $\mathcal{L}$-hydrate
a small quantity
+
$Ca(OH)_2$ (CH)
trace

Unreacted slag (S)
+
C_2S $\mathcal{L}$-hydrate ($\mathcal{L}$)
+
Tobermorite
+
Hydrogarnet
($3CaO.Al_2O_3.2SiO_2.2H_2O$)
+
Calcium hydroxide
trace

small inflection at 270°C is probably due to the hydrogarnet and the small peak at 490°C is due to calcium hydroxide.

Both tobermorite and C_2S α-hydrate were found in mixes of lime and slag i.e., H and I. With granulated slag C_2S α-hydrate was formed in very small quantity but with foamed slag it was formed in a greater quantity. This is evident from the thermograms (Fig. 47). A hydrogarnet phase with a unit cell a_o = 12.13A and an approximate composition $3CaO.Al_2O_3.2SiO_2.2H_2O$ i.e., plazolite, was formed in the two lime-slag mixes. An endothermic inflection at 335°C may be due to the presence of the hydrogarnet. The presence of the large endothermic peak above 100°C shows the presence of tobermorite gel when granulated slag is used. This peak is absent in the thermogram for the lime-foamed slag mix. The endothermic peak at 468°C in the latter thermogram is characteristic of C_2S α-hydrate. A summary of the hydrated phases identified by X-ray powder technique in the autoclaved mixes are reported in table 46.

DISCUSSION

Nature of Hydrothermal Reactions

Formation of cementitious phases as a result of hydrothermal reactions in the mixes of lime and fines

compacted at W/S ratio of 0.12 is not likely to take place through solution and precipitation reactions as the solubilities of lime and silica etc. at the higher temperature (180°C) are very low. The likelihood of solid state reactions is far greater. The participation of a small quantity of water probably is responsible for rapid reaction between solids. Since a certain portion of the solid particles may not be in contact with another solid reactant, such reactions cannot be considered to have reached thermodynamic stability. But in the hydrothermal reactions under discussion since one of the reactant, $Ca(OH)_2$, got almost consumed (table 45), the reactions therefore may be deemed to have been completed in the limited sense.

The above reactions could be assumed to be of simple additive type i.e., mixed oxide from its component oxides. For example, reaction of lime, silica (from quartz) and water (oxide of hydrogen) to form calcium silicate hydrates. Lime attacks the mineral surface and the latter gets covered with a cryptocrystalline layer. According to Assarson (203) the reaction layers are of two types, forming monocalcium or dicalcium silicate hydrate as first crystallizing product and the thickness of the reaction layers at the boundary for a lime-quartz reaction (200 mg CaO per sq meter of mineral surface) are given as 2.1×10^4 and 1.2×10^4 microns. Though the solubility of lime at the reaction temperatures is

probably lower than that of (SiO_4) ions, the diffusion of the former through the reaction layers will be comparatively easier. Lime combines with silicate ions at the interface of the reaction layer and the solid (e.g., quartz). True growth of the reaction layer will therefore take place on the quartz crystal side, where reaction occurs; the apparent reaction on the other side is really a process of dissolution by which lime enters the reaction product layer. The growth of the reaction product layer then occurs by consumption of both adjacent reactant masses. The different stages of a typical solid state reaction are given by Garner (204) but the formation of aggregates of imperfectly crystallized product into coherent crystallites, which may still be more or less defective in structure, seems to be the end point in the reactions under consideration. This should be accompanied by an increase in density.

The above is also true of reactions of lime with other fines. The slag fines already contain some calcium ions. According to Assarson (203) when silicate lattice initially contains Ca ions, a portion of ions are already occupied to some degree, a certain part of the formation energy is consumed and the conditions of formation of hydration products are limited. When the surplus of formation energy between the stable and unstable compounds in question is insignificant, the phases formed on hydration behave as metastable compounds, and the

real equilibrium is not reached. This appears to be true as the non-evaporable water in the slag mix 'I' was indeed small (table 46).

The foregoing discussion shows how important is the nature of fines in such hydrothermal reactions. Some of the other important factors are chemical and mineralogical composition of the fines, lattice defects, impurities etc. Thorvaldson (205) had observed highest strengths only with the aggregates composed of free silicon dioxide in its various forms; the other minerals containing combined silica gave about 50 per cent of the strength obtained with quartz. This shows the effects of chemical nature of aggregates on strength. The effects of lattice defects and impurities etc. in solid state reactions are well known.

Though intermediate phases might have been formed in the hydrothermal reactions under discussion, the consumption of the added lime in all the mixes could be taken as a sign of completion of the reactions in the 'limited sense' as pointed out earlier. In the light of the information on the final hydrated phases formed and discussed earlier, the different hydrothermal reactions can now be written in the form of chemical reactions. (But this should not be taken to mean that reactant molecules are available to one

another for reaction in fluid media and kinetic effects are predominant).

The equations (1 - 4) are for a few general type of reactions; the equations (5 - 8) given below are for reactions presumed to take place in lime-fines mixes.

General Reactions

$$5Ca(OH)_2 + 6SiO_2 \text{ (quartz)} = 5CaO.6SiO_2.5H_2O \text{ (tobermorite)} \quad ...(1)$$

Weights	370	+	360	=	730
Volumes	165.9	+	135.9	→	304.2
Void space	(301.8)	-	(304.2)	=	- 2.4

$$2Ca(OH)_2 + SiO_2 \text{ (quartz)} = 2CaO.SiO_2.H_2O + H_2O\uparrow \text{ } (C_2S\ \alpha\text{-hydrate}) \quad ...(2)$$

Weights	148	+	60	=	190
Volumes	66.4	+	22.6	→	68
Void space	(89.0)	-	(68.0)	=	21

$$2CaO.Al_2O_3.SiO_2 \text{ (gehlinite) glassy} + Ca(OH)_2 + 3H_2O = 3CaO.Al_2O_3.SiO_2.4H_2O \text{ (hydrogarnet)} \quad ...(3)$$

Weights	274	+	74		+ 54	
				=	402	
Volumes	91	+	33.2		+ 54	
				→	143.6	
Void space	(178.2)	-	(143.6)	=	34.6	

$$2CaO.Al_2O_3.SiO_2 \text{ (gehlinite)} + CaO.SiO_2 \text{ (wollastonite)} + 2H_2O = 3CaO.Al_2O_3.2SiO_2.2H_2O \text{ (hydrogarnet)} \quad ...(4)$$

Weights	274	+	116	+	36	=	+426
Volumes	91	+	40	+	36	→	136
Void space	(167)	-	(136)			=	31

Reactions in the Lime-Fines Mixes

Mix E (30 lime : 70 quartz sand)

$$5Ca(OH)_2 + 6SiO_2 = 5CaO.6SiO_2.5H_2O \quad \text{(tobermorite)} \quad ...(5^*)$$

* The reaction (5) would be the same as in equation (1) when the formation of zonotlite in the lime and quartz reaction is neglected.

Mixes F and G (30 lime : 70 fly ash)

$$8Ca(OH)_2 + 7SiO_2 + Al_2O_3 + H_2O = 5CaO.6SiO_2.5H_2O + 3CaO.Al_2O_3.SiO_2.4H_2O \quad ...(6)$$

(reactive part of fly ash)* (tobermorite)

Weights	592	+ 420	+ 102	+ 18	= 730	+ 402	
Volumes	265.5	+ 158.5	+ 29.1	+ 18	→ 304.2	+ 143.6	
Void space	(498.3)		- (447.8)		= 50.5		

* Density of fly ash is 2.43 g per cc.

Mix H (10 lime : 90 granulated slag)

$$0.12CaO + 2CaO.Al_2O_3.SiO_2 + 2(CaO.SiO_2) + 3H_2O =$$

(slag constituents)

$$1.12CaO.SiO_2H_2O + 3CaO.Al_2O_3.2SiO_2.2H_2O \quad ...(7)$$

(tobermorite) (hydrogarnet)

Weights	6.72	+ 274	+ 232	+ 54	= 140.7	+ 426	
Volumes	2	+ 91	+ 80	+ 54	→ 58.6	+ 136	
Void space		(227.0)	- (194.6)		= 33.4		

Mix I (10 lime : 90 foamed slag)

$$Ca(OH)_2 + 2CaO.Al_2O_3.SiO_2. + 2(CaO.SiO_2) + 2H_2O =$$

(slag constituents)

$$2CaO.SiO_2.H_2O + 3CaO.Al_2O_3.2SiO_2.2H_2O \quad ...(8)$$

(C_2S α-hydrate) (hydrogarnet)

Weights	74	+ 274	+ 232	+ 36	= 190	+ 426	
Volumes	33.2	+ 91	+ 80	+ 36	→ 68	+ 136	
Void space		(240.2)	- (204.0)		= 36.2		

Chemically Combined Water

The chemically combined water was calculated on the basis of the equations (5 - 8) for the reactions described above and are reported under the last column (table 46). Considering the different assumptions made, the values agree reasonably well with the determined values. Also, the non-evaporable water is an arbitrary quantity dependent on the drying conditions and does not necessarily represent the chemically combined water and hence the slight differences in the two values are admissible.

Density of the Autoclaved Mixes

Earlier it was stated that the last stage in the hydrothermal reactions would be the formation of aggregates of imperfectly crystallized products into coherent crystallites; This may be accompanied by an increase in density. The density of the granular samples prepared from the dried crushed material from different compacts is reported in table 48. The density in some cases is higher than that of the original mix from which the compacts had been made (table 44). It may be noted that the density of the autoclaved productlis little higher than the true density (2.90) of the aggregate, i.e., ground foamed slag. This is an important observation showing that aggregation has taken place and possibly

TABLE - 48

Values of 'm' and 'n' of Autoclaved Cylindrical Compacts

Specimen designation	Dry weight of solids g	Moulding water g	Absorbed water g	Total water g	Density of autoclaved of solids g/cc	Volume of solids cc	Porosity coefficient m	Volume of pores n
E	246.4	29.6	19.3	48.9	2.49	98.9	0.49	0.329
F	225.0	27.0	25.2	52.2	2.51	89.6	0.58	0.366
G	235.8	29.2	24.4	53.6	2.64	89.3	0.60	0.370
H	273.7	32.9	15.3	48.2	2.73	100.2	0.48	0.324
I	276.8	34.2	25.9	60.1	2.93	94.4	0.63	0.389

this may be accompanied by an increase in porosity of the autoclaved product.

Porosity of the Autoclaved Mixes

Since physical properties of the autoclaved compacts may depend a good deal on their porosity, it was desirable to know how the hydrothermal reactions influence the porosity. While discussing the reactions, the weights and volumes of the reactant and the reaction products were given under each equation (The values of densities used are given in table 49A). In all reaction equations except (1) the volume of reactants is more than that of the reaction products and the difference between the two gives the void space created as a result of the reaction. The porosity values in respect of the different reaction equations were calculated and are reported in table 49B. The calculations show that formation of C_2S α-hydrate from lime and quartz fines would be accompanied by a greater increase in porosity compared to if tobermorite is formed. Similarly, the increase in porosity is more when hydrogarnet $C_3AS_2H_2$ is formed from gehlinite as against C_3ASH_4.

The calculation of total porosity (ϵ) in Chapter 5 was made from $\epsilon = \cdot 99 \left[(W_{t/c} - W_{n/c})\right] d_p/1 + W_{t/C}$. It is difficult for the autoclaved mixes because the determined values of $W_{t/c}$ and d_p for the granular crushed material were not found to be reliable. The porosity

TABLE - 49 A

Values of Density for Reactants and Reaction Products

S.No.	Reactant or Reaction product	Density g/cc	Reference
1.	Calcium hydroxide	2.23	F.M. Lea (206)
2.	Silica	2.65	determined
3.	Gehlinite	2.90	Taken equal to the density of slag
4.	Wollastonite	2.90	
5.	Tobermorite	2.44	W.C. Hansen (207)
6.	C_2S α-hydrate	2.80	L. Heller & H.F.W. Taylor (208)
7.	Hydrogarnet $3CaO.Al_2O_3.SiO_2.4H_2O$	3.00	Calculated
8.	Hydrogarnet $3CaO.Al_2O_3.2SiO_2.2H_2O$	3.13	C.O. Smith (209)

T A B L E - 49B

Effects of Hydrothermal Reactions on the Porosity Change of Autoclaved Compacts

Equation No.	Reaction	Weight of solids g	Volume of solids cc	Volume of mixing water cc	Volume of combined water cc	Void space created cc	Volume of free water cc	Volume of total pores cc	Vol. of total pores / Vol. of solids m	Porosity $(\frac{m}{1+m})$ n
1,5	$Ca(OH)_2$ with Quartz i.e., Mix E	730.0	301.8	87.60	90.0**	+ 2.4	-	- 2.4	- 0.008	- 0.007*
2	$Ca(OH)_2$ with Quartz	208.0	89.0	24.96	18.0	21.0	6.96	27.96	0.314	0.238
3	$Ca(OH)_2$ with Gehlinite	378.0	178.2	41.76	72.0	34.6	-	34.6	0.194	0.162
4	Formation of $3CaO.Al_2O_3.2SiO_2.2H_2O$	390.0	167.0	46.80	36.0	31.0	10.80	41.8	0.250	0.200
6	$Ca(OH)_2$ with fly ash (Mix F & G)	1114.0	498.3	133.7	162.0	50.5	-	50.5	0.101	0.092
7	$Ca(OH)_2$ with Granulated slag (Mix H)	512.7	227.0	61.5	54.0	33.4	7.5	40.9	0.180	0.153
8	$Ca(OH)_2$ with Foamed slag (Mix I)	580.0	240.2	69.6	54.0	36.2	15.6	51.8	0.216	0.177

* Minus sign means a reduction in porosity.

** Specific volume of combined water is assumed to be no different from that of evaporable water.

of the autoclaved mixes was therefore calculated in a manner similar to that used for calculating the porosity of the green compacts. The results are reported in the last column of table 48. The data bear out mostly what is postulated by the reactions in table 49B. For example, in lime-quartz mix porosity does not decrease at all. The porosity increase in the lime-fly ash compacts is comparatively greater because of the formation of the tobermorite and the hydrogarnet C_3ASH_4. (The difference in the values of the two lime-fly ash mixes is due to the presence of unburnt fuel in the mix F). The formation of both C_2S α-hydrate and the hydrogarnet $C_3AS_2H_2$ in lime-slag mixes should result in higher porosities; but if tobermorite is also formed, the ultimate value of porosity would be lower. This is shown by the data for the two slag mixes H and I. Since tobermorite is in greater quantity in the mix H than in I, consequently the porosity of the former mix is also lower (table 48).

Surface Areas and Strengths of the Autoclaved Products

The values of surface areas of the autoclaved products of hydrothermal reactions between lime and fines are reported in table 50. The surface areas of products of lime with either ground quartz or fly ash are nearly the same i.e., about 70 sq m per g. The value is lowest for the lime-foamed slag mix i.e., about 20 sq m per g

TABLE - 50

Surface Areas of Autoclaved Lime - Fines Mixes
(16 hours at 160 lb/sq.in. pressure)

Sample designation	p/ps (= x)	w g/g of dry autoclaved product (granular sample)	$\frac{x}{1-x}$	$\frac{1}{w}\frac{x}{1-x}$	C	v_m g/g of adsorbent	Surface area of solids sq m/g
Mix E	0.0703	0.0191	0.076	3.97			
	0.1105	0.0205	0.124	6.04			
30 Lime: 70 Quartz	0.2245	0.0225	0.189	8.40	101	0.0205	78
	0.2500	0.0224	0.333	14.86			
	0.4276	0.0324	0.747	23.06			
Mix F	0.0703	0.0178	0.076	4.27			
	0.1105	0.0191	0.124	6.48			
30 Lime: 70 F. Ash	0.2245	0.0217	0.189	8.71	101	0.0188	71
	0.2500	0.0222	0.333	15.00			
	0.4276	0.0304	0.747	24.55			
Mix G	0.0703	0.0160	0.076	4.74			
	0.1105	0.0204	0.124	6.07			
30 Lime: 70 F. Ash(c)	0.2245	0.0213	0.189	8.87	101	0.0179	68
	0.2500	0.0191	0.333	17.41			
	0.4276	0.0305	0.747	24.49			
Mix H	0.0703	0.0093	0.076	8.17			
	0.1105	0.0117	0.124	10.59			
10 Lime: 90 Slag(g)	0.2245	0.0112	0.189	16.86	101	0.0100	38
	0.2500	0.0121	0.333	27.48			
	0.4276	0.0141	0.747	52.96			
Mix I	0.0703	0.0032	0.076	23.75			
	0.1105	0.0043	0.124	28.91			
10 Lime: 90 Slag(f)	0.2245	0.0051	0.189	37.41	101	0.005	18
	0.2500	0.0065	0.333	51.16			
	0.4276	0.0075	0.747	99.77			

and intermediate for the lime-granulated slag i.e., about 40 sq m per g.

The compressive strengths for the autoclaved mixes are reported in table 51. The mixes of 30 lime : 70 quartz sand and 10 lime : 90 slag (granulated) show the highest strengths (about 10,000 p.s.i.) and the mix 10 lime : 90 slag (foamed) the lowest strength (about 2,500 p.s.i.). The two mixes of 30 lime : 70 fly ash possess intermediate strengths i.e., about 4,300 p.s.i. The magnitude of strengths in all the mixes is what Midgley and Chopra had reported earlier on the basis of limited tests. The only difference being that the mix of 10 parts of lime and 90 parts of granulated slag in the present series has shown higher strengths i.e., 9,203 p.s.i. as against 4,639 for the corresponding mix. However, it may be noted that highest strength obtaible by Midgley and Chopra in lime-granulated slag mixes was 8,589 p.s.i. and the mix composition was 5 lime : 95 slag. The explanation for the need of using a higher lime content in the present series for equivalent strengths is comparatively a lower CaO/SiO_2 ratio in the Indian granulated slag.

Strength and the Current Theories of Hardening

Theories of hardening of cement are generally

T A B L E - 51

Water Absorption and Strength of Cylindrical Specimens (Autoclaved for 16 Hours at a Pressure of 160 psi)

Specimen designation 1		Water absorption after 48 hours per cent 2	Density of saturated specimens g/cc 3	Crushing strength lb/in^2 4	Splitting strength lb/in^2 5	Ratio 4/5 6
E	(i)	7.67	2.08	11,614	907	
	(ii)	7.71	2.04	12,445	901	
	(iii)	7.39	2.04	10,666	770	
	Av.	7.59	2.05	11,542	859	13.4
F	(i)	12.52	1.90	3,899	416	
	(ii)	12.06	1.93	4,413	398	
	Av.	12.54	1.92	4,156	407	10.2
G	(i)	7.59	1.99	4,743	630	
	(ii)	8.47	2.00	4,566	703	
	(iii)	10.37	1.99	4,636	771	
	Av.	8.81	2.00	4,648	701	6.6
H	(i)	5.18	2.25	8,418	980	
	(ii)	6.53	2.24	10,486	861	
	(iii)	4.91	2.25	8,704	1141	
	Av.	5.54	2.25	9,203	994	9.2
I	(i)	10.54	2.28	2,780	230	
	(ii)	6.44	2.23	2,568	211	
	(iii)	-	-	-	288	
	Av.	8.49	2.26	2,674	223	12.0

extended to explain the development of strength in autoclaved products. But now there is sufficient experimental evidence to show that gel-space theory does not hold good (48). The correlation of strength with the formation of either some definite hydrated solid phase or phases or microstructure, though more widely accepted, is also not firmly established as pointed out by Lea (54). Czerin's (12) explanation that powerful surface forces arising from large surface areas of hydrated phases are responsible for strength development also does not hold as autoclaved products possess low values of specific surface.

The data on strengths, non-evaporable water contents, surface areas, porosities etc. are summarized in table 52 and show that explanation of strength development in terms of specific surfaces or gel-space theory is not tenable. It is interesting to note that while the strengths of the autoclaved lime and fines mixes are as high or even higher than those reported for the cement pastes of Ludwig and Pence (table 53), the values of the non-evaporable water contents of the former are much lower. The values of the specific surface of the lime-fines mixes are on the whole comparable with the values for the cement pastes.

The three mixes E, F and G have near about the same specific surface but when compared amongst themselves do not show any relationship with strengths which vary between 4,000 to 11,500 p.s.i. Similarly,

T A B L E - 52

Summary of Data on Autoclaved Compacts

Specimen designation	Non-Evap. water w_n mg/g	Surface area of solids sq m/g	Porosity of autoclaved compact n	Compressive strength of compact p.s.i.
Mix E	0.059	78	0.329	11,542
Mix F	0.122*	71	0.366	4,156
Mix G	0.089	68	0.370	4,648
Mix H	0.062	38	0.324	9,203
Mix I	0.025	18	0.389	2,674

* The value is high because of the presence of unburnt fuel in the unreacted fly ash.

TABLE - 53

Properties of Portland Cement Pastes Cured at Elevated Temperatures and Pressures After Ludwig & Pence (48)

Cement	Autoclaving Temp.	Autoclaving Time in days	Non-Evap. water w_n mg/g cement	Surface area of solids sq. m/g	Compressive strengths lb/in^2
A at w/c = 0.46	80	7	0.142	103.4	3825
	150	7	0.162	122.6	6141
	200	7	0.152	74.7	5086
	260	7	0.139	30.3	1281
	320	7	0.139	9.4	1331
B at w/c = 0.40	80	7	0.113	83.9	5458
	150	7	0.135	129.9	8100
	200	7	0.138	114.9	9478
	260	7	0.132	62.8	6623
	320	7	0.123	13.6	2618

though the mixes E and H show similar strengths, their values of specific surface differ by about 100 per cent. In short, strength cannot be related to the volume of hydrated phases formed in the compacts.

Though the data in table 52 indicate in a general way that strengths are low when total porosity is high, the explanation of strengths development in terms of porosity values also suffers from limitations. For example, the increase in porosities of the compacts of the mixes on autoclaving is of the same order but the difference in the ultimate strengths are far greater. This indicates that the absolute value of strength also depends on the nature of the hydrated phase.

Though the present data supports the earlier finding of Midgley and Chopra (93) that high strengths are associated with the formation of tobermorite phase and poor strengths with the formation of C_2S α-hydrate, there are some unanswered questions. Firstly, the contribution of hydrogarnet phase towards strength development is not clear except that it may increase the porosity and thus lower the strengths. But in the mix H of 10 parts lime with 90 parts slag, it does not seem to have any adverse effects on strength development because the mix of 30 parts of lime and 70 parts of quartz sand has near about the same strength and porosity but no hydrogarnet. Secondly, it may be deduced from the X-ray

data and surface area values that the tobermorite phase in the mix 10 lime : 90 slag is better crystallized than in the 30 lime : 70 ground quartz mix. The degree of hydration in the former mix is also lower but surprisingly the two mixes show the same magnitude of strengths. It may be inferred that differences in the morphology of the tobermorite phase and other factors such as the cohesive and adhesive properties of the hydrated phases may also play a part.

Compressive Strength as Influenced by Adhesion

The above discussion shows that as far as compressive strengths are concerned, some other factors are also coming into play. The principal stress which in the case of unconfined compression is the compressive strength is known to increase rapidly with an increase in cohesion and also with an increase in the friction angle. Gorden and Gillespie have concluded (210) that cohesion is also a function of the surface area and surface texture of the aggregate and believe that the total bond strength (adhesion) between aggregate particles and paste controls the cohesive value and as the quality of paste increases, failure in bond controls of the strength of concrete. The latter appears to be an important observation as will be clear from the following discussion.

Mixes of lime and fines could be likened to

those of cement and fine aggregate. The surface areas of the fines in the present study were the same, while small differences in surface texture are probably there. The observation that little water is squeezed out from mixes at some water/solid ratio above 0.12 and under high moulding pressures shows that most of the water is held tightly by lime (having internal surface as well) and its contribution towards promoting deformation and thereby adhesion is a variable factor. Since the compacts for compressive strength test were prepared at a W/S ratio of 0.12 and different loads were applied for achieving the same value of porosity, and adhesion between particles is improved by application of pressure, differences in degree of adhesion could have arisen at the stage of moulding the compacts themselves.

The green strength of the compacts (table 43) arises probably from primary bonds resulting from bridging between particles in contact and also van der Waals forces. As a result of hydrothermal reactions the strengths of compacts increase manifold. For example, the compressive strength of the compact H (10 lime : 90 slag) was about 956 p.s.i. after curing in 99 per cent relative humidity for 28 days and 9,203 p.s.i. after steam curing at 160 lbs per sq in. for 16 hours, the increase being ten times. Similarly, Midgley and Chopra had found the strengths of compacts containing 95 - 100 parts of slag fines with 5 to 0 parts of lime ranging between 8,589 to 3,780 p.s.i.

Surely, presence of this small quantity of lime will not result in the formation of hydration products in any substantial quantity. The increase in strength is primarily due to the strengthening of the primary bonds resulting from bridging between particles in contact, where surfaces are under pressure or deforemed and will hydrate or react more readily than other surfaces. Solid state reactions are postulated for the formation of bridges and also the formation of Bernals' welds by intergrowth of the lattices of crystals in contact due to some re-arrangement of the lattice as postulated by Lea (54) in explaining bond of cement to aggregate. The adhesional strength of the interparticulate bridges, number and strength of welds seem to be important factors in governing the strength and other properties of the compacts. Though difficult to assess, some information on this was obtained by subjecting the cylindrical compacts to direct tensile stresses by performing the splitting test (211). The results are reported in table 51 together with the ratios of compressive to splitting strengths under column 6 . The ratios in mixes, F, G and H are different from those of E and I.

A lower ratio (table 51) indicates comparatively a lower adhesion of particles of cementitious phase to each other but a better adhesion to other particles in the system (excluding those of calcium hydroxide). The former is mainly dependent on the

crystal structure and size of the cementitious phase and the latter on the shape and size of particles, their mutual orientation, chemical and mineralogical composition, lattice defects and impurities etc. Because in the present study the fineness of reactants, W/S ratio and porosity etc. of the compacts were the same, the major factors responsible for differences in adhesional strengths would be the chemical and mineralogical compotion, lattice defects and impurities in the constituents of fines which in turn influence the nature of hydrothermal reactions. It is not surprising to find better adhesional strengths of reactive solids i.e., two samples of fly ash and a granulated slag against ground quartz and foamed slag. The reason of the relative inactivity of the latter is due to its higher lime content as discussed earlier.

Mechanism of Strength Development

Application of pressure improves the adhesion between particles by formation of primary interparticulate bridges. Strengthening of the latter and formation of Bernals' welds through solid state reactions form an initial framework within few hours of autoclaving. Further increase in strength can take place by a further conversion of the reactants into reaction products of high specific surface i.e., by increasing the cohesion. Alternatively, the strengths can be increased by

increasing the number and strengths of welds i.e., working through adhesion. Both the approaches can lead to high strengths by a judicious choice of materials and methods. However, the practical limitation in either case is the aggregation which beyond a certain degree will reduce strengths through an increase in porosity.

CONCLUSIONS (Chapter 7)

The deformation characteristics of the moist mixes of hydrated lime with fines (viz., ground quartz sand, fly ash, granulated and foamed slag) were found to be governed by the water-solid ratio and the moulding pressure. The green compacts from the different lime fines mixes should therefore be moulded at the same value of porosity rather than under the same moulding pressure.

The hydrated solid phases formed were poorly crystallized tobermorite and xonollite in lime-ground quartz mix, 11A-tobermorite and hydrogarnet of composition C_3ASH_4 in lime-fly ash mixes, and poorly crystallized tobermorite, C_2S α-hydrate and hydrogarnet of composition $C_3AS_2H_2$ in lime-slag mixes.

The hydrothermal reactions between lime and fines were found to be almost complete in 16 hours time at 160 lbs per sq in. as evident from the very small quantities of the unreacted lime.

The reactions have been shown to take place in the solid state and are considered to be of simple additive type i.e., mixed oxides from the component oxides. However, it was found possible to describe the hydrothermal reactions in the form of chemical equations and estimate the chemically combined water and the changes

in porosities of the compacts on autoclaving. The latter were found to agree well with the experimentally determined values of non-evaporable water and porosity changes respectively.

The values of surface areas of the autoclaved products were found to be about 70 sq m. per g for the hydrated lime-quartz or fly ash mixes, about 40 sq m. per g for the lime-granulated slag mix and about 20 sq m. per g for the lime foamed slag mix.

The mixes of lime ground quartz and lime-granulated slag showed the highest strengths (10,000 p.s.i.) and the mix of lime-foamed slag the lowest strength about (2,500 p.s.i.). The two mixes of lime fly ash possessed intermediate strengths i.e., about 4,300 p.s.i.

The strengths could not be explained on the basis of gel-space ratio. The relationship between strength and nature of hydrated phase or total porosity of the autoclaved compacts were also not found satisfactory as these were only of general nature.

The two most important findings were that the ratio of the compressive and adhessive (or splitting) strength was not the same for the compacts prepared from different mixes, and that, in some instances, the density of the autoclaved product was greater than even the

density of the fines used in that particular mix. The explanation appears to be the adhesional strength of interparticulate bridges and formation of the Bernals' welds. The mechanism of strength development is visualized as follows :

> " Application of pressure improves the adhesion between particles by formation of primary interparticulate bridges. Strengthening of the latter and formation of Bernals' welds through solid state reactions form an initial framework within few hours of autoclaving. Further increase in strength can take place by a further conversion of the reactants into reaction products of high specific surface i.e., by increasing the cohesion. Alternatively, the strengths can be increased by increasing the number and strengths of welds i.e., working through adhesion. Both the approaches can lead to high strengths by a judicious choice of materials and methods. However, the practical limitation in either case is the aggregation which beyond a certain degree will reduce strengths through an increase in porosity ".

RÉSUMÉ

RÉSUMÉ

The chemistry of the hardening of the cementitious materials, like slag and pozzolanic cements and mixes of lime with slag or pozzolana etc., is not well understood. Controversy exists regarding the points of similarity and dissimilarity between the hardening process of these materials and that of the Portland cement, although many believe that the end products of hardening are qualitatively the same. Malquori (56), however, points out that there should exist a considerable difference in the development of the process and in the final arrangement because while the cementing compounds originate in Portland cement exclusively from hydration of clinker constituents, with pozzolanic cements they originate partly from the reaction between lime from hydrolysis and the active constituents of the pozzolanic materials. This is also true of the clinker-based slag cements.

According to Grudemo (25) the initial chemical and mineralogical composition, initial particle-size distribution of cement, the water-cement ratio, method of preparation of paste together with few other factors determine the physical properties of a hardened Portland cement paste. In the cementitious pastes hydraulicity of slag and activity of pozzolana are the additional important factors which will govern the physical properties.

From the investigations of the above authors and so also from the published work of others, many new points arise which either need a more elaborate treatment or a modification of the existing view point on the hardening of the cementitious materials. Firstly, is the problem of the maintenance of the separate identity of the hydrated calcium silicate phase (developed either from the hydrolysis of clinker or pozzolanic reaction) which needs a closer study. Secondly, there is the problem of the nature of the hydrated phases vis-a-vis the physical properties of the hardened cementitious materials that has to be more carefully examined. A systematic investigation, incorporating these and other aspects, was, therefore, thought worth undertaking and forms the main theme of the experimental work described in this thesis.

Structure of Fresh Pastes

It is most likely that the early structure of paste may leave its imprint on the structure subsequently developed from it. The possible influences of the initial framework established within the first few hours of the preparation of a paste on the subsequent hardened paste were, therefore, studied in terms of the sedimentation characteristics and the rheological properties of fresh pastes.

The sedimentation or bleeding characteristics of fresh pastes of the cementitious materials were found to be similar to those of the fresh Portland cement. The bleeding rate and capacity of the former pastes for the range of water content commonly employed in practice were found to conform to the equations :

$$Q = \frac{0.2\, g(d_c - d_f)}{\sigma_w^2 \cdot \eta} \quad \frac{(W - W_i)^3}{C}$$

and $\Delta H' = \frac{K^2 c \ell}{v}\left[(W/C) - (W/C)_m\right]^2$

originally developed by Powers and Steinour for the fresh Portland cement paste.

The values of the 'immobile' water per unit volume of paste (W_i) for the pozzolanic and slag cements were found to be lower than that of the ordinary Portland cement; the differences being greater for the pozzolanic cements and slight for the Portland blastfurnace cement. The differences were found to be due to differences in the degree of flocculation, the latter being influenced both by the physical and chemical properties of the fine powders replacing Portland cement.

Corresponding differences in the values of bleeding capacity were also observed. The values of minimum water-cement ratio $(W/C)_m$ for the two pozzolanic cement were 0.58 and 0.76 against a value of 0.91 for the Portland cement showing thereby a substantially lower

strength of the 'floc structure' of the pozzolanic cement pastes.

The values of W_i and $(W/C)_m$ for the pastes of one part of hydrated lime with two parts of fines (e.g., slag, fly ash and 'surkhi' or (calcined clay), however, did not show significant differences amongst themselves showing thereby that the degree of flocculation and 'floc strength' did not vary in these pastes. In other words, as far as the structure of these pastes is concerned, the chemical nature of the fines does not appear to influence the results; only the physical characteristics of the fines are important.

From the point of view of gel-space theory, the final porosity of the sediment of the fresh pastes is an important factor; a lower value being advantageous. The pozzolanic and slag cements did show lower values compared to those for the Portland cement paste prepared at an equivalent W/C ratio, but the estimated average width of pores (Powers) in the sediment of former pastes was greater.

Similarly, though the porosities of the sediment of 1:2 and 1:3 lime-fines pastes were found to range from 59.4 to 60.8 per cent against 59.4 per cent of the Portland cement at a corresponding W/C ratio, the estimated average width of pore in the former pastes was

1½ to 2 times of that in the cement paste. It is, therefore, concluded that the total value of porosity is not as important as how close are the solid particles to each other.

The sedimentation (or bleeding) rate and sedimentation volume of a fresh paste, which in turn determine the porosity and 'mean' pore size of the sediment, were found to be influenced greatly by the electrostatic charges on solid particles and the electrolyte additions such as solutions of aluminium and calcium chlorides, calcium hydroxide and sulphate, sodium hydroxide and sulphate etc. which are used in small quantities as admixtures in concrete technology.

The plots of both sedimentation volume and porosity of the slag pastes versus the increasing concentration (0.015 M to 0.50 M) of the different solutions used in their preparation showed well defined maxima and minima at certain concentrations. The changes in sedimentation volume, particularly at low concentrations, could not be explained on the basis of the chemical action between slag particles and the different electrolytes.

The results, however, could be explained in terms of changes in the degree of flocculation which was found to be explicable in terms of the

Helmholtz double layer theory. The effects of small additions of electrolytes were found to be due to their physical interaction; the electrostatic charge on the particle, valence of the counterions and similions playing important roles. The results also confirmed the assumption that the slag particles are positively charged.

The rheological behaviour of fresh pastes was also studied. The Portland cement paste showed antithixotropy (or dilatancy) at 15 minutes, a reversible behaviour at 45 minutes and thixotropy at 180 minutes. The slag cements showed the reversible behaviour both at 15 and 45 minutes and thixotropy at 180 minutes. The pozzolanic cement showed thixotropic behaviour from the very beginning.

The plastic viscosity for the Portland cement was highest while it was lowest for the pozzolanic cement, slag cements having intermediate values. The yield values of the pastes of slag and pozzolanic cements were generally lower.

The degree of flocculation in the slag pastes prepared with solutions of different electrolytes was found to be governed by a balance existing at any stage between the positive dispersing ions such as aluminium, calcium and sodium and flocculating

anions of sulphate, chloride and hydroxyl etc. The rheological behaviour of these pastes at selected contentration of the electrolytes showed that relatively a higher degree of flocculation was accompanied by a higher plastic viscosity and the predominant behaviour was thixotropic though at early periods of 15 and 45 minutes some pastes did show the reversible behaviour.

The important findings about the structure of fresh pastes deduced from the sedimentation studies were thus confirmed.

The data clearly demonstrated that even when the particle size distribution and specific surface of slags, pozzolanas and other fines were controlled, differences in the structure of the fresh pastes of the cementitious materials existed in the form of differences in 'floc strength', porosity and 'mean' pore-size etc. The latter eventually affect the gel-space ratio differently and consequently the strength and other properties of the hardened cementitious paste. Some practical applications of the findings have been discussed.

Studies on Hardened Pastes

The effects of the period of curing and water-cement ratio on the degree of hydration and strengths showed that all the clinker-based cements hydrated and developed strengths at a slower rate than

that of the Portland cement.

The strength data of the Portland blastfurnace cements (PBF and BFP), the pozzolanic cement (PZC) and the supersulphated cement (SSC) showed that the strengths of the PBF cement (clinker 65: slag 35) equalled that of the Portland cement (PC) after 28 days; the gain in strengths for the BFP (clinker 35: slag 65) and PZC (clinker 75: fly ash 25) cements from 28 to 90 days was greater than for any other cement; and that at 90 days all the cement, excepting BFP, showed strengths equal or higher than those of the Portland cement.

The hydrated solid phases formed in the pastes of the above cements from 1 to 90 days were identified with the help of differential thermal and X-ray powder analyses. The phases identified in Portlant cement pastes were tobermorite-like hydrated (gel), ettringite, monosulfoaluminate, tetracalcium aluminate hydrate, a hydrogarnet and calcium hydroxide. Small quantities of calcite and monocarboaluminate were also present as impurities.

Most of the above hydrated phases were also found to be present in the pastes of the other clinker-based cements but with some differences. For example, at 90 days when the strengths were mostly equal to those of the Portland cement paste, the differences observed

were

(a) the tobermorite phase appeared to be different in nature; either in having different CaO/SiO_2 and H_2O/SiO_2 ratios or in microstructure,

(b) ettringite was not present in PBF cement but in the BFP and PZC cements it was present in quantities greater than in the PC cement,

(c) the hydrogarnet phase in the PC cement was identified as $C_6AFS_2H_8$. In the PBF, BFP and PZC cements the hydrogarnet phase appeared to be different in nature. In the PBF cement it was present in greater quantity than in any other cement, and

(d) calcium hydroxide was present in a decreasing order in the PZC, PBF and BFP cements.

The hydrated silica and alumina bearing phases seem to mix intimately only after 28 days of paste hydration as these were indistinguishable in the thermograms of 90 days old pastes.

There was no evidence of 'silico-aluminic hardening' in the PBF and BFP cements. However, the presence of gehlinite hydrated showed evidence of this type of hardening in SSC cement.

The main hydrated phase in the SSC cement was ettringite ($3CaO.Al_2O_3.3CaSO_4.31H_2O$). The sulphate activation of the low lime and high alumina slag had shown that the strengths were highest when ettringite with SO_3/Al_2O_3 ratio of 3 was formed and it was possible only when calcined gypsum was used in a quantity (20-25 per cent) greater than that recommended (10-15 per cent)

in the literature. The other phases present were tobermorite-like hydrate, gehlinite hydrate and a small quantity of monosulfoaluminate. Tobermorite-like hydrate was present in substantial quantities at 90 days as evident from the differential thermal analysis and specific surface measurement.

The hydrated solid phases in the hardened pastes of lime-slag and lime-fly ash were tobermorite-like hydrates, tetracalcium aluminate hydrate, carbo-aluminate and sulfoaluminate hydrates, and a hydro-garnet. The X-ray data indicated the presence of 14A-tobermorite hydrate in the lime-slag mix and 10-A-tobermorite hydrate in the lime-fly ash mix. The formation of gehlinite hydrate in lime-slag mix indicates the possibility of the silico-aluminic hardening in such mixes.

The relationship between the apparent specific volume of total water (V_t) and the ratio of non-evaporable water (W_n/W_t) for the hydrated PC, PBF and SSC cements was found to be a straight line relationship and satisfied the Copeland's equation $V_t = 0.99 - 0.25\ W_n/W_t$. The apparent specific volume of the non-evaporable thus appears to be 0.74. However, no conclusion could be drawn in respect of the BFP and PZC cements because of the dispersion of the experimental points.

The specific surfaces of the cement pastes (W/C = 0.40) hydrated for 90 days were found to be 195, 183, 117, 169 and 127 sq cm per g for the PC, PBF, BFP, PZC and SSC cements respectively. The values of the 'specific surface diameter' and average pore width of the hydrated phases in the different cement pastes were estimated but these were found to be of limited use in revealing differences in the microstructure of the hydrated pastes.

Electron micrographs, on the other hand, showed important differences in the hydrated cement pastes of 90 days age. For example, hydrated PC cement showed entirely fibrous structure characteristic of the tobermorite phase. The bundled fibres were clearly visible. Some plates, probably of hexagonal symmetry and belonging to the calcium aluminate hydrate phase ($C_4A.aq.$) were also seen. The PBF cement also showed fibrous structure but the fibres were very much finer and shorter in length. Sometimes the fibres were so fine that the material appeared to be amorphous in nature. The platy crystals were present in a greater quantity in this cement. In the BFP cement the tobermorite phase consisted of fine fibres and thin sheets or flakes. The hydrated PZC cement showed fibrous structure as well as foils, characteristic of the tobermorite phase. Lath-like crystals of ettringite were also present in

significant amount in the pastes of both the BFP and PZC cements. No such structures were seen in the electron micrographs of the PC and PBF cements.

The electron microscopy of the 90 days old cement pastes showed that the calcium silicate hydrate phase formed from the hydration of clinker constituents in the slag and pozzolanic cements did not maintain its separate identity. On the other hand, it appears to undergo modifications.

The capillary or total porosity of the hardened paste did not show a precise relationship with the strength. But the strengths of all the cements, including that of the supersulphated cement, could be explained on the basis of gel-space theory. The equations correspond to that of Powers i.e., $f_c = f_c^0 x^n$ where f_c = absolute strength, f_c^0 = intrinsic strength and x = gel-space ratio and n is a reduction factor. The relationships for the different hardened pastes were

(i) $f_c = 23169\ x^{1.52}$ for the PC cement

(ii) $f_c = 23179\ x^{1.46}$ for the PBF cement

(iii) $f_c = 43601\ x^{1.83}$ for the BFP cement

(iv) $f_c = 42786\ x^{2.00}$ for the PZC cement

(v) $f_c = 21013\ x^{0.85}$ for the SSC cement

(vi) $f_c = 14890\ x^{1.29}$ for the lime-pozzolana/(slag) mixes

It is concluded that the intrinsic strength of the cement gel in the cements PBF, BFP and PZC is not lower than that of the PC cement. On the other hand, the intrinsic strengths of the BFP and PZC cements are higher. The presence of tobermorite phase in the form of very fine and short fibres and also as flakes or foils (characteristic of calcium silicate hydrate phase with low CaO/SiO_2 ratio) and that of ettringite in greater quantities appear to be responsible for higher strengths of BFP and PZC cements. The presence of hexagonal plates of C-A-H phase (i.e., $C_4A.aq.$) in the PBF cement in a greater quantity than in any other cement appears to affect the strength of this cement adversely.

The relationship $f_c = 21013\ x^{0.85}$ and the specific surface measurement show that even the secondary phases of tobermorite-like hydrate, gehlinite hydrate and probably alumina gel contribute a good deal towards the strength development of the supersulphated cement.

The reason for the lower intrinsic strength of the hydrated lime-pozzolana mixes were found to be due to comparatively a greater proportion of hydrated alumina bearing phases in comparison to that of tobermorite-like hydrates.

Hydrothermal Reactions

Development of strength as a result of hydrothermal reactions between lime and ground quartz, fly ash and slags etc. in autoclaved compacts is not clearly understood and hence was reinvestigated.

The deformation characteristics of the moist mixes of hydrated lime with fines (viz., ground quartz sand, fly ash, granulated and foamed slag) were found to be governed by the water-solid ratio and the moulding pressure. The green compacts from the different lime-fine mixes should therefore be moulded at the same value of porosity rather than under the same moulding pressure.

The hydrated solid phases formed were poorly crystallized tobermorite and xonollite in lime-ground quartz mix, 11A-tobermorite and hydrogarnet of composition C_3ASH_4 in lime-fly ash mixes, and poorly crystallized tobermorite, C_2S γ-hydrate and hydrogarnet of composition $C_3AS_2H_2$ in lime-slag mixes.

The hydrothermal reactions between lime and fines were found to be almost complete in 16 hours time at 160 lbs per sq in. as evident from the very small quantities of the unreacted lime.

The reactions have been shown to take place in the solid state and are considered to be of simple additive type i.e., mixed oxides from the component oxides. However, it was found possible to describe the hydrothermal reactions in the form of chemical equations and estimate the chemically combined water and the changes in porosities of the compacts on autoclaving. The latter were found to agree well with the experimentally determined values of non-evaporable water and porosity changes respectively.

The values of surface areas of the autoclaved products were found to be about 70 sq m per g for the hydrated lime-quartz or fly ash mixes, about 40 sq m per g for the lime-granulated slag mix and about 20 sq m per g for the lime-foamed slag mix.

The mixes of lime ground quartz and lime-granulated slag showed the highest strengths (10,000 p.s.i) and the mix of lime-foamed slag the lowest strength about (2,500 p.s.i.). The two mixes of lime fly ash possessed intermediate strengths i.e., about 4,300 p.s.i.

The strengths could not be explained on the basis of gel-space ratio. The relationship between strength and nature of hydrated phase or total porosity of the autoclaved compacts were also not found satisfactory as these were only of general nature.

The two most important findings were that the ratio of the compressive and adhesive (or splitting) strength was not the same for the compacts prepared from different mixes, and that, in some instances, the density of the autoclaved product was greater than even the density of the fines used in that particular mix. The explanation appears to be the adhesional strength of interparticulate bridges and formation of the Bernals' welds. The salient features of the mechanism of strength development are as follows :

> "Application of pressure improves the adhesion between particles by formation of primary interparticulate bridges. Strengthening of the latter and formation of Bernals' welds through solid state reactions form an initial framework within few hours of autoclaving. Further increase in strength can take place by a further conversion of the reactants into reaction products of high specific surface i.e., by increasing the cohesion. Alternatively, the strengths can be increased by increasing the number and strengths of welds i.e., working through adhesion. Both the approaches can lead to high strengths by a judicious choice of materials and methods. However, the practical limitation in either case is the aggregation which beyond a certain degree will reduce strengths through an increase in porosity".

REFERENCES

1. Powers, T.C., "Physical properties of cement paste", Proc. Fourth International Symposium on Chemistry of Cement, U.S. National Bureau of Standards, Monograph 43, vol. 2, p. 594-595 (1962)

2. Taylor, H.F.W., "The chemistry of cements", Research, vol. 14, p. 154 (April, 1964)

3. Midgley, H.G., Rosaman, D. and Fletcher, K.F., "X-ray diffraction examination of Portland cement clinker, Proc. Fourth Intl. Symposium on Chemistry of Cement, National Bureau of Standards, Monograph 43, vol. 1, p. 70 (1962)

4. Steinour, H.H., "The system $CaO-SiO_2-H_2O$ and the hydration of calcium silicates", Chem. Rev., 40, 391-460 (1947)

5. Taylor, H.F.W., "The chemistry of cement hydration", Progress in Ceramic Science, Pergamon Press (London), vol. 1, p. 89-145 (1961)

6. Powers, T.C. and Brownyard, T.L., "Studies of the physical properties of hardened Portland cement paste", Research and Development Laboratories, Portland Cement Association, Bulletin 22, Part 2, p. 488-502 (1948)

7. Reference (6), p. 846-857

8. Powers, T.C., "The physical structure and engineering properties of concrete", Research and Development Laboratories, Portland Cement Association, Bulletin 90, 28 pages (1959)

9. Powers, T.C., "Structure and physical properties of hardened Portland cement paste", J. Am. Ceram. Soc., vol. 41, no. 1 (1958)

10. Reference (1), p. 587-594

11. Reference (1), p. 602

12. Czernin, W., "Cement chemistry and physics for civil engineers", Crosby Lockwood & Sons (Ltd.) London, (1962), 39-40

13. Lea, F.M., "The chemistry of cement and concrete", Edward Arnold (Publishers) Ltd., London (1956), p. 218

14. Bogue, R.H., "The chemistry of Portland cement", Reinhold Publishing Corporation, New York (2nd edition) (1955), p. 607-686

15. Reference (1), p. 592-606

16. Kalousek, G.L., Davis, C.W. and Schmertz, W.E., "An investigation of hydrating cements and related hydrous solids by differential thermal analysis", J. Am. Concrete Inst. Proc., 45, p. 693-712 (1949)

17. Heller, L. and Taylor, H.F.W., "Hydrated calcium silicates, pt. II-Hydrothermal reactions : lime: silica ratio 1:1", J. Chem. Soc., p. 2397-2401 (1951). Also pt. III-Hydrothermal reactions of mixtures of lime : silica molar ratio 3:2, J. Chem. Soc., p. 1018-1020 (1952) and pt. IV-Hydrothermal reactions, lime : silica ratios 2:1 and 3:1, J. Chem. Soc., p. 2535-2541 (1952)

18. Nurse, R.W. and Taylor, H.F.W., "Discussion of the paper on 'the reactions and thermochemistry of cement hydration at ordinary temperature by H. Steinour", Proc. Third International Symposium on the Chemistry of Cement, Cement and Concrete Association, London, p. 311-318 (1952)

19. Taylor, H.F.W., "Studies on the hydration of Portland cement", Proc. 27th International Cong., Indust. Chem., Brussels, p. 3 (1963)

20. Barnal, J.D., "The structure of cement hydration compounds", Proc. Third International Symposium on the Chemistry of Cement, Cement and Concrete Association, London (1952), p. 216-35

21. Kalousek, G.L., "Tobermorite and related phases in the system $CaO-SiO_2-H_2O$", J. Am. Concrete Inst., Proc. 51, p. 989-1011 (1955)

22. Kalousek, G.L., "Crystal chemistry of hydrous calcium silicates : 1, substitution of aluminium in lattice of tobermorite", J. Am. Ceram. Soc., 40, p. 74-80 (1957)

23. Kalousek, G.L. and Roy, R., "Crystal chemistry of hydrous calcium silicates : II, characterization of interlayer water", J. Am. Ceram. Soc., 40, p. 236-239 (1957)

24. Kalousek, G.L. and Prebus, A.K., "Crystal chemistry of hydrous calcium silicates : III, morphology and other properties of tobermorite and related phases", J. Am. Ceram. Soc., 41, p. 124-132 (1958)

25. Grudemo, A., "The microstructure of hardened cement paste", Proc. Fourth International Symposium on the Chemistry of Cement, U.S. Bureau of Standards, Monograph 43, vol. 2, p. 616-645 (1962)

26. Grudemo, A., "Electronographic studies on the morphology of calcium silicate hydrates", Swed. Cement and Concrete Institute, Roy. Inst. Tech. Stockholm, Proc. no. 26 (1955)

27. Grudemo, A., "The silca-water system : analogies between the montmorillonoids and the calcium silicate hydrates of the tobermorite group. Some experimental data for the sorption of water in montmorillonite", Note on Research in Progress, no. 5, Swed. Cement and Concr. Research Inst. Roy. Inst. Tech. Stockholm, p. 1-43 (1956)

28. Taylor, H.F.W., "Hydrothermal reactions in the system $CaO-SiO_2-H_2O$", Proc. Intl. Symposium Reactivity of Solids, Gothenburg, 1952, p. 677-682 (1954)

29. Gard, J.A., Howison, J.W. and Taylor, H.F.W., "Synthetic compounds related to tobermorite; an electron-microscope, X-ray, and dehydration study", Mag. Concrete Research 11, p. 151-158 (1959)

30. Taylor, H.F.W., "Hydrothermal reactions in the system $CaO-SiO_2-H_2O$ and the steam curing of cement and cement-silica products", Fourth Intl. Symposium on the Chemistry of Cement, U.S. Bureau of Standards, Monograph 43, vol. 1, p. 168-187 (1962)

31. Sanders, L.D. and Smothers, W.J., "Effect of tobermorite on the mechanical strength of autoclaved Portland cement-silica mixtures", Journal of the American Concrete Instt., vol. 54, no. 2, p. 127-139 (1957)

32. Midgley, H.G., "The mineralogical examination of set Portland cement", Proc. Fourth Intl. Symp. on the Chemistry of Cement, U.S. Bureau of Standards, Monograph 43, vol. 1, p. 479-489 (1962)

33. Midgley, H.G. and Rosaman, D., ibid., p. 259-262

34. Green, K.T., "Early hydration reactions of Portland cement", Proc. Fourth Intl. Symp. on Chemistry of Cement, U.S. Bureau of Standards, Monograph 43, vol. 1, p. 359-373 (1962)

35. Megaw, H.D. and Kelsey, C.H., "Crystal structure of tobermorite", Nature, p. 177, 390-1 (1956)

36. Jones, F.E., "Hydration of calcium aluminates and ferrites", Proc. Fourth Intl. Symp. on Chemistry of Cement, U.S. Bureau of Standards, Monograph 43, vol. 1, p. 204-241 (1960)

37. Mamedor, Kh.S. and Belor, N.V., "Crystal structure of tobermorite (tobermorite phases) (in Russian), Dokaldy Akad. Nauk SSSR, p. 123, 163-165 (1958)

38. Gard, J.A., Howison, J.W. and Taylor, H.F.W., "Synthetic compounds related to tobermorite : An electron-microscopic, X-ray and dehydration study", Mag. Concr. Res. 11, p. 151-8 (1959)

39. Taylor, H.F.W. and Howison, J.W., "Relationships between calcium silicates and clay minerals", Clay Minerals Bull., 3, p. 98-111 (1956)

40. Iwai, T. and Watanabe, K., "Electron-microscopic study of portland cement hydration products-tricalcium aluminate, dicalcium ferrite, and tetracalcium aluminoferrite", Electron-Microscopy Proc. Regional Conf. Asia and Occania, 1st, Tokyo 1956, p. 288-91 (1957)

41. Czernin, W., "Electron microscopy of hardened cement pastes (in German)", Zement-kalk-Gips, 11, p. 381-3 (1958)

42. Saji, K., "Electron-microscopic study of hardened cement mortars" (in Japanese) Semento Gijutsn Neupo, 12, p. 119-23 (1958)

43. Grudemo, A., "The microstructure of hardened cement paste", Proc. Fourth Intl. Symp. on Chemistry of Cement, U.S. Bureau of Standards, Monograph 43, vol. 2, p. 632-638 (1962)

44. Funk, H., "The products of action of water on -$2CaO.SiO_2$ below 120° (in German)", Z. U. allgem, Chem. 291, p. 276-93 (1957)

45. Copeland, L.E. and Schutz, Edith G., "Discussion of the paper 'The microstructure of hardened cement paste", Proc. Fourth Intl. Symp. on Chemistry of Cement, U.S. Bureau of Standards, Monograph 43, vol.2, p. 648-655 (1962)

46. Grudemo, A., "An electronographic study of the morphology and crystallization properties of calcium silicate hydrates", Svenska Forskninginst. for Cement Och Betong Vid Kgl. Tek Hogskol Stockholm; Handlingar no. 26, (1955)

47. Tomes, L.A., Hunt, C.M. and Blaine, R.L., "Some factors affecting the surface area of hydrated Portland cement as determined by water vapour and nitrogen adsorption", J. Research National Bureau of Standars 59, p. 357-364 (1957)

48. Ludwig, N.C. and Pence, S.A., "Properties of Portland cement pastes cured at elevated temperatures and pressures", Proc. Am. Concrete Inst. 52, p. 673-687 (1956)

49. Brunauer, S., "Tobermorite gel - heart of concrete", American Scientist, V. 50, no. 1, p. 210-229 (Mar. 1962)

50. Brunauer, S., "The role of tobermorite gel in concrete", Structural Concrete, vol. 1, no. 7, p. 293-309 (1963)

51. Brunauer, S. and Greenberg, S.A., "Chemistry of Hydration of cement compounds", Proc. Fourth Intl. Symp. on the Chemistry of Cement, U.S. National Bureau of Standards, Monograph 43, vol. 1, p. 141-151 (1962)

52. Bernal, J.D., Jeffery, J.W. and Taylor, H.F.W., "Crystallographic research on hydration of Portland cement", Mag. Concrete Res., no. 11, p. 49-54 (1952)

53. Reference (25), p. 645

54. Lea, F.M., "Cement Research : Retrospect and prospect", Proc. Fourth Intl. Symp. on the Chemistry of Cement, U.S. Bureau of Standards, Monograph 43, vol. 1, p. 5-8 (1962)

55. Lea, F.M., "The chemistry of pozzolana", Proc. Symp. on the Chemistry of Cements, Stockholm, p. 460-490 (1938)

56. Malquori, G., "Portland-pozzolan cement", Proc. Fourth Intl. Symp. on the Chemistry of Cement, U.S. Bureau of Standards, Monograph 43, vol. 2, p. 988-95 (1962)

57. Keil, F., "Slag cements", Proc. Third Intl. Symp. on the Chemistry of Cement, London (1952), p. 530-568

58. Kramer, W., "Blast-furnace slag and slag cements", Proc. Fourth Intl. Symp. on the Chemistry of Cement, U.S. Bureau of Standards, Monograph 43, vol. 2, p. 970-71 (1962)

59. Kondo, Renichi, "Chemical Resistivities of various types of cements", Proc. Fourth Intl. Symp. on the Chemistry of Cement, U.S. Bureau of Standards, Monograph 43, vol. 2, p. 881-886 (1962)

60. Taylor, H.F.W., "The chemistry of cements", Research, vol. 14, p. 154 (1961)

61. Chopra, S.K., "Contribution to the discussion of the paper 'A new hypothesis of the mechanism of sulphate expansion by Chatterjee and Jeffery", Mag. Conc. Research (in press)

62. Williams, H. and Chopra, S.K., "Discussion of the paper 'Blast-furnace slags and slag cements by W. Kramer", Proc. Fourth Intl. Symp. on the Chemistry of Cement, U.S. Bureau of Standards, Monograph 43, vol. 2, p. 979-981 (1962)

63. Vivian, H.E., "Some chemical additions and admixtures in cement paste and concrete", Proc. Fourth Intl. Symp. on the Chemistry of Cement, U.S. Bureau of Standards, Monograph 43, vol. 2, p. 909-926 (1962)

64. Nagai, S., "Special masonry cement having a high slag content", Proc. Fourth Intl. Symp. on the Chemistry of Cement, U.S. Bureau of Standards, Monograph 43, vol. 2, p. 1043-55 (1962)

65. Turriziani, R. and Schippa, G., "Pozzolana-lime-calcium sulphate mortars (in Italian)", Ricerea Sci. 24, p. 1895 (1954)

66. Reference (56), p.

67. Reference (58), p. 970

68. Reference (56), p. 990

69. Locher, F.W., "Hydraulic properties and hydration of glasses of the system $CaO-Al_2O_3-SiO_2$", Proc. Fourth Intl. Symp. on the Chemistry of Cement, U.S. Bureau of Standards, Monograph 43, vol. 1, p. 275 (1962)

70. Smolczyk, H.G., "Discussion of Reference (69), p. 275

71. Copeland, L.E., Kantro, D.L. and Verbeck, George, "Chemistry of hydration of Portland cement", Proc. Fourth Intl. Symp. on the Chemistry of Cement, U.S. Bureau of Standards, Monograph 43, vol. 1, p. 433-434 (1962)

72. Eitel, W., "Electron-microscopy in cement research (in German)", Zement 31, p. 489-97 (1942)

73. Stork, J. and Bystricky, V., "Study of hardened cement paste by means of electron-microscope (in French)", Rev. des. Materiaux, no. 526-527, p. 173-179 (1959)

74. Sliepcevich, C.M., Gildart, L. and Katz, D.L., "Crystals from Portland cement hydration. An electron microscope study", Ind. Eng. Chem. 35, p. 1178-87 (1943)

75. Saji, K., "An electron microscope study on the internal structure of hardened Portland cement paste and contact layer with aggregates, especially with fly ash in cement mortar", Review of the Twelfth General Meeting, Japan Cement Engineering Association, Tokyo, p. 26-27 (May, 1958)

76. Buckle, E.R. and Taylor, H.F.W., "The hydration of tricalcium and -dicalcium silicates in pastes under normal and steam curing conditions", J. Appl. Chem. 9, p. 163-172 (1959)

77. Reference (2), p.158

78. Reference (25), p. 645 and 658

79. Srinivasan, N.R., "Discussion of the paper 'Portland pozzolan cement by Giovanui Malquori", Proc. Fourth Intl. Symp. on the Chemistry of Cement, U.S. Bureau of Standards, Monograph 43, vol. 2, p. 1002 (1962)

80. Reference (1), p. 602

81. Turriziani, R. and Schippa, G., "Differential thermal analysis of reaction products between dehydrated kaolin and lime (in Italian)", Ricerca Sci. 24, p. 366 (1954)

82. Turriziani, R. and Schippa, G., "Setting and hardening of pozzolana-lime-calcium sulphate mortars (in Italian)", Ricerca Sci. 26, p. 3387 (1956)

83. Turriziani, R. and Schippa, G., "Investigation of the quaternary solids $CaO-Al_2O_3-CaSO_4-H_2O$ by the X-ray and D.T.A. methods (in Italian)", Note 1, Ricerca Sci. 24(11), p. 2356-2363 (1954)

84. Benton, E.J., "Cement-pozzolana reactions", Highway Research Board, Bull. 239, Physical & Chemical Properties of Cement and Aggregate in Concrete. National Academy of Sciences-National Res.Council (U.S.A.), p. 56-65 (1960)

85. Turriziani, R. and Rio, A., "Remarks on some methods for testing pozzolanic cements (in Italian)", Am. Chim. 44, p. 787 (1954)

86. Turriziani, R., "Italian pozzolanas and pozzolanic cements", Silicates Inds. 23, p. 181 (1958)

87. Ludwig, U. and Schwiete, H.E., "Researches on the hydration of trass cements", Proc. Fourth Intl. Symp. on the Chemistry of Cement, U.S. Bureau of Standards, Monograph 43, vol. 2, p. 1093-98 (1962)

88. Jambor, J., " Relation between phase composition, over-all porosity and strength of hardened lime-pozzolana pastes", Mag. of Conc. Res., vol. 15, no. 45, p. 131-42 (1963)

89. Kalousek, G.L., "Studies on the cementitious phases of autoclaved concrete products made of different raw materials", J. Am. Conc. Inst. Proc., vol.50, p. 365-378 (1954)

90. Aitken, A. and Taylor, H.F.W., "Hydrothermal reactions in lime-quartz pastes", J. Applied Chemistry 10, p. 107-15 (1960)

91. Bessy, G.E., "Sand-lime bricks", National Building Studies Special Report no. 3, His Majesty's Stationery Office, London (1948)

92. Taylor, W.H. and Moorehead, D.R., "Lightweight calcium silicate hydrate : some mix and strength characteristics", Mag. of Conc. Res. vol. 8, no. 24, p. 145-50 (1956)

93. Midgley, H.G. and Chopra, S.K., "Hydrothermal reactions between lime and aggregate fines", Mag. of Concr. Res., vol. 12, no. 35, p. 73-82 (1960)

94. Bessey, G.E., "Discussion of the paper 'Properties of cement paste and concrete by T.C. Powers", Proc. Fourth Intl. Symp. on the Chemistry of Cement, U.S. Bureau of Standards, Monograph 43, vol. 2, p. 610-11 (1962)

95. Feldman, R.F. and Screda, P.J., "A datum point for estimating the adsorbed water in hydrated Portland cement", J. Appl. Chem. no. 9, vol. 13, p. 375 (1963)

96. Chopra, S.K. and Patwardhan, N.K., "Use of granulated slag in the manufacture of Portland blast-furnace cement", Indian Ceramics 2, No. 12 (1956); Investigation on the utilisation of Indian iron blastfurnace slag. Proc. symp. on Housing and Building Materials, National Buildings Organisation, New Delhi, vol. 2, p. 117-123 (1958)

97. Chopra, S.K., Rao, K.S. and Patwardhan, N.K., "Use of wet ground slag as a substitute of Portland cement in concrete", Journal National Buildings Organisation (New Delhi), p. 56-59 (June-Sept.'56)

98. Chopra, S.K. and Kishan Lall, "Sulphate activation of low lime and high alumina slag", Jr. Sci. Industr. Res. vol. 20D(6), p. 218-223 (1961)

99. Chopra, S.K. and Kishan Lall, "The manufacture of supersulphated cement from Indian slag", Indian Concrete Journal, 35(4), p. 114-116 (1961)

100. Chopra, S.K. and Kishan Lall, "Activation of slag with lime or clinker", Proc. Indian Science Congress Association, 49th Session, Part III, p. 170, (1962)

101. Rehsi, S.S. and Garg, S.K., "Evaluation of Indian fly ashes", Indian Concrete Journal vol. 37, no. 6, p. 211-217 (1963)

102. Rahman, Abdul, P.M., Rehsi, S.S. and Chopra, S.K., "Strength of brick masonry", Journal National Buildings Organisation, vol. 6, no. 4, p. 49-61 (1961)

103. Bogue, R.H., "Calculation of compounds in Portland cement", Paper no. 21, Portland Cement Association Fellowship at the National Bureau of Standards, Washington, D.C. (Oct. 1929)

104. Lea, F.M.,"The chemistry of cement and concrete", Edward Arnold (Publishers) Ltd., London, p. 93-94,
and
Midgley, H.G. and Ryder, J.F., "Microscopic methods for examining cement clinkers and slags used at the Building Research Station, Note no. D.94, Building Research Station (D.S.I.R.), Garston, Watford, U.K. (1949)

105. Indian Standard 269:1958 : Indian Standard Specification for ordinary, rapid-hardening and low heat Portland cement, Indian Standards Institution, New Delhi.

106. IS: 1489 - 1962, Indian Standard Specification for Portland-pozzolana cement

107. Khan, C.A.R. and Verman, L.C., "Cement-surkhi mortars", Indian & Eastern Engineer (June 1940)

108. IS: 1344:1959, Indian Standard Specification for surkhi for use in mortar and concrete

109. Reference (25), p. 616

110. Reference (54), p. 7

111. ACI Committee 212, "Admixtures for concrete", J. Am. Concr. Inst. vol. 60, no. 11 (Nov. 1963)

112. Symposium on 'Effect of water-reducing admixtures and set-retarding admixtures on properties of concrete', ASTM Special Technical Publication no. 266, Am. Soc. Testing Materials (1959)

113. Larson, T.D., Mangusi, J.L. and Radomshi, R.R., "Preliminary study of the effect of water-reducing retarders on the strength, air void characteristics and durability of concrete", Proc. J. Am. Conc. Inst., vol. 60, no. 12, p. 1739-53 (1960)

114. Powers, T.C., "Should Portland cement be dispersed? Research and Development Laboratories Portland Cement Association, Bull. 9, p. 117-125 (1946)

115. Rehbinder, P. and Segalova, E., "Structure formation in the hardening of building materials (governing the formation and properties of structures by surface active additions)", Proc. Second Intl. Congress of Surface Activity, vol. III, p. 492-505 (1957)

116. Mikhailov, V.V., "New developments in selfstressed concrete", Proc. World Conference on Prestressed Concrete, Lithotype Process Co., p. 25 (1957)

117. Mikhailov, V.V., "Stressing cement and the mechanism of self-stressing concrete regulation" Proc. Fourth Intl. Symp. on the Chemistry of Cement, U.S. Bureau of Standards, Monograph 43, vol. 2, p. 928-32 (1962)

118. Standard method of test for fineness of Portland cement by air permeability apparatus, ASTM Designation : (204-55) 1958, Book of ASTM Standards Part 4, American Society for Testing Materials, Philadelphia, U.S.A.

119. "Standard method of test for fineness of Portland ce cement by the turbidimeter", ASTM Designation (115-58) 1958, Book of ASTM Standards, Part 4, American Society for Testing Materials, Philadelphia 3, Pa, U.S.A.

120. Orchard, D.F., "Concrete Technology", Asia Publishing House, Bombay, vol. 2, p. 36-38 (1963)

121. Joglekar, G.D., Kumarswamy, M.P. and Bhuchar, V.M., "Particle-size distribution of hydrated lime", J. Sci. Industr. Res., vol. 12B, p. 543-45 (1953)

122. Piper, C.S., "Soil and plant analysis", The University of Adelaide, Adelaide, p. 48 (1947)

123. Brink, R.H. and Halstead, W.J., "Studies relating to testing of fly ash for use in concrete" Proc. Am. Soc. Testing Materials, Vol. 56, p. 1166-68 (1956)

124. Lea, F.M., "The chemistry of cement and concrete" Edward Arnold (Publishers) Ltd., London, p. 331 (1956)

125. Lea, F.M. and Nurse, R.W., "Permeability method of fineness measurement", Symp. on Particle-size Analysis, Trans. Inst. of Chemical Engineers, vol. 25, p. 5 (1945)

126. Chopra, S.K. and Narain, S.N., "Measurement of specific surface of fly ash", Journal of Materials Research and Standards (in press)

127. Powers, T.C., "The bleeding of portland cement paste, mortar and concrete", Research Laboratory of the Portland Cement Association, Bull. 2, (1939), p. 160

128. Steinour, H.H., "Further studies of the bleeding of Portland cement paste", Research Laboratory of the Portland Cement Association, Bull. 4, p. 88 (1945)

129. Copeland, L.E., "Specific volume of evaporable water in hardened Portland cement pastes", J. Am. Concr. Inst., vol. 52, p. 864 (1955-56)

130. Reference (1), p. 580-581

131. Reference (6), p. 497

132. Reference (128), p. 13-14

133. Reference (127), p. 25-26

134. Reference (1), p. 579

135. Steinour, H.H., "Rate of sedimentation 1. Non-flocculated suspensions of uniform spheres, II. Suspensions of uniform-size angular particles and III. Concentrated flocculated suspensions of powders", Research & Development Laboratories of Portland Cement Association, Bull. 3, (1944)

136. Mather, B., "The partial replacement of Portland cement in concrete", Am. Soc. of Testing and Materials, Special Technical Publication 205, p. 52-55 (1956)

137. Hansen, W.C., "Actions of calcium sulfate and admixtures in Portland cement pastes", Proc. Symp. on Effect of Water-reducing admixtures and set-retarding admixtures on properties of concrete, ASTM Special Technical Publication no. 266, Am. Soc. Testing & Materials, p. 3-37 (1959)

138. Reference (128), p. 54

139. Daniels, F., Williams, J.W., Bender, P., Alberty, R.A. and Cornwell, C.D., "Experimental physical chemistry", McGraw Hill Book Company, I.N.C., New York, San Francisco, Toronto, London, p. 149 (1962)

140. Eitel, W., "The physical chemistry of the silicates", The University of Chicago Press, Chicago 37, 1954, p. 378-383

141. Chopra, S.K. and Kishan Lall, (unpublished work)

142. Dellyes, R., "La rheologie des pates a ciment dans la voie humide", Rev. materiaux construct (465-466), p. 193-213; (468) p. 231-243 (1954)

143. Papadakis, M., "Etude de l ecoulement des fluids", ibid (476), p. 124-37 (1955), Rheology in the cement industry, silicates inds. 22, p. 612-615; 675-681 (1957)

144. Tattersal, G.H., "The rheology of Portland Cement pastes" Brit. J. of Applied Physics 1,6, p. 165-67 (1955)

145. Tattersall, G.H., "Structural breakdown of cement pastes at constant rate of shear", Nature, 175, p. 166 (1955)

146. Shalom Moshe and Greenberg, S.A., "The rheology of fresh portland cement pastes", Proc. Fourth Intl. Symp. on the Chemistry of Cement, U.S. Bureau of Standards, Monograph 43, vol. 2, p. 731-43 (1962)

147. Green, H., "Industrial rheology and rheological structures", John Wiley & Sons. Inc., London (1949), p. 99-107

148. "Standard Sample of Mineral Oil for Gardner Mobilometer", Henry A. Gardner Laboratory, Inc. 4723 Elin Street, Bethesda 14, MD.,

"The Mac Michael Viscometer" (Model 15-347) Fisher Scientific Company, New York

149. Reference (147), p. 36-41, and p. 126-27

150. Reference (147), p. 50-53

152. Gaskin, A.J., "Discussion of the paper on the rheology of fresh cement pastes by Ishe-Shalom and Greenberg", Proc. Fourth Intl. Symp. on the Chemistry of Cement, U.S. Bureau of Standards, Monograph 43, vol. 2, p. 744-746 (1962)

152. Forslind, E., "Water association and hydrogels", Proc. of the Second Intl. Congress on Rheology edited by V.G.W. Harison, Butterworths Scientific Publications (1954), p. 50-60

153. Reference (1), p. 580

154. Reiner, Marcus., "The rheology of concrete", Chapter 9 of Rheology: Theory & Application, vol. III, edited by F.R. Eirich (Academic Press Inc., New York, N.Y. 1959)

155. Mardles, E.W.J., "Notes on the rheology of paint", Jr. of Oil & Colour Chemists Association, vol. 25, no. 267, p. 194-210 (Sept. 1942)

156. Mysels, Karol, J., "Introduction to colloid chemistry", Interscience Publishers, Inc., New York (1959), p. 378

157. Hoon, R.C., Chopra, S.K., Vengupalaro, I.V., "Technology of artificial hydraulic lime: 1. characteristics of the argillaceous constituents", Journal Central Board of Irrigation, Special issue brought out at the Intl. Conference for High Dams, New Delhi (1951)

158. Hoon, R.C., "Development of Portland pozzolana cements for mass concrete construction", Indian Concrete Journal, vol. 26, p. 225-233 (Aug. 1952) and p. 252-258 (Sept. 1952)

159. Puri, M.L. and Khanna, R.L., "The use of calcined shale as pozzolana in mass concrete", Ind. Concrete Journal, vol. 31, (1957)

160. Chatterjee, S. and Lahiri, D., "Note on the activation of granulated blastfurnace slag", Science & Culture 22, p. 514-515 (1957)

161. Chopra, S.K., Taneja, C.A., Mohan Rai and Kishan Lall, "Development of cements for use in India", Cement & Concrete, vol. 1, no. 1, p. 1-12 (1960)

162. Jain, S.K., Maheshwari, K.M., Aggarwal, G.D., Misra, R.K. and Joshi, G.D., "Bokaro fly ash for Rihand Dam", Jour. Inst. Engrs (India), vol. 41, no. 10, part CH.1., p. 529-541 (1961)

163. Srinivasan, N.R., "Surkhi as a pozzolana", Road Research Paper 1, Central Road Research Instt., New Delhi, India (1956)

164. Puri, M.L., Bawa, N.S. and Srinivasan, N.R., "Durability of concrete with respect to sulphate attack", RILEM Symp. on Concrete & Reinforced Concrete in Hot Countries, Israel (1960)

165. Reference (3), p. 413-416

166. Reference (136), p. 52-66

167. Reference (123), p. 1170-1202

168. Nurse, R.W., "Utilization of fly ash for building material", Journal Instt. of fuel, vol. 29, no. 181, p. 85-88 (1956)

169. Vincent, Robert D., Mateos, Manuel & Davidson, Donald, T., "Variations in pozzolanic behaviour of fly ashes", Proc. Am. Soc. Testing Materials vol. 61, p. 1094-1115 (1961)

170. Chopra, S.K. and Taneja, C.A., "Utilization of the Indian blastfurnace slag", Presented at the symposium on the Utilization of metallurgical wastes held at the National Metallurgical Laboratory, Jamshedpur (March 1964)

171. Osborne, F.E., De Vries, R.C. Gee, K.H. and Kramer, H.M., "Optimum composition of blastfurnace slag as deduced from liquidus data for the quaternary system $CaO-MgO-Al_2O_3-SiO_2$", Journal of Metals, p. 33-45 (Jan. 1954)

172. Chopra, S.K., Taneja, C.A. and Mehrotra, G.S., "The mineralogy of air cooled blastfurnace slag" Indian Journal of Technology (accepted for publication)

173. Keil, F. and Gille, F., "Hydraulic properties of basic glasses with the composition of gehlinite and akermanite", Zement-Kalk-Gips 2, p. 229-232 (1949)

174. Keil, F. and Locher, F.W., "Hydraulic properties of glasses", Zement-Kalk-Gipa 11(6), p. 245-253 (1958)

175. Reference (58), p. 965-967

176. Welch, J.H., "Discussion of the paper 'Blastfurnace slags and slag cements by W. Kremer', Proc. Fourth Intl. Symp. on the Chemistry of Cement, U.S. Bureau of Standards, Monograph 43, vol. 2, p. 981 (1962)

177. Chopra, S.K. and Taneja, C.A., "State of coordination of aluminium in $CaO-Al_2O_3-SiO_2$ glasses", (unpublished work)

178. Tanaka, T., Sakai, T. and Yamane, J., "Die zusammensetzung japanischer hocho-feuschlecken fur sulfat-huttenzement", Zement-Kalk-Gips 11, p. 50-55(1958)

179. Franke, B., "Bestimmung von calciumoxyd und calciumhydroxyd neben wasserfreiein und wasserhaltigem calciumsilikat", Zeitschr. f. anorg. Chemie 147, p. 180-184 (1941)

180. Nurse, R.W., "Slag composition and its effect on the properties of supersulphate cement", Paper presented at the Convention on Production & Application of Slag Cement, Naples, 30 May - 2 June (1960)

181. Tanaka, T. and Takemoto, K., "Research on hydraulic properties of granulated blastfurnace slags", Rock Product 54, no. 7, p. 82-84 (1954)

182. Copeland, L.E. and Hayes, John C., "The determination of non-evaporable water in hardendd Portland cement pastes", Research & Development Laboratories of the Portland Cement Association Bull. 47, p. 1-9 (1953)

183. Reference (6), p. 263-64

184. Reference (6), p. 692-94

185. Powers, T.C., "Physical properties of cement paste", Proc. Fourth Intl. Symp. on the Chemistry of Cement, U.S. Bureau of Standards, Monograph 43, vol. 2, p. 585-87 (1962)

186. Brunauer, S.J., Emmett, P.H. and Teller, E, "Adsorption of gases in multimolecular layers", Jl. American Chemical Society, v. 60, p. 309 (1938)

187. Reference (6), p. 670-72, Reference (1), p. 585

188. Reference (1), p. 590-91, Reference (1), p. 586

189. Brunauer, S., Kantro, D.L. and Copeland, L.E., "The stoichiometry of the hydration of beta-dicalcium silicate and tricalcium silicate at room temperature", J. Am. Chem. Soc. 80, p. 761-67 (1958)

190. Reference (6), p. 484-88, Reference (1), p. 587, Reference (73), p. 497, Reference (13), p. 149-50

191. Malquori, G., Sersale, R. and Giordano-Orsini, P., "Discussion of the paper 'Blastfurnace slags and slag cements by W. Kramer', Proc. Fourth Intl. Symp. on the Chemistry of Cement, U.S. Bureau of Standards, Monograph 43, vol. 2, p. 976-79 (1962)

192. "Proceedings Symp. on the Chemistry of Cements" Ch. Abstracts vol. 52, p. 6746-6755 (1958)

193. Reference (13), p. 370

193A. Alexander, K.M., "Reactivity of ultrafine powders produced from siliceous rocks", Jour. Am. Concr. Inst., vol. 32, no. 5, (Nov. 1960)

194. Schiller, K.K., "Strength of highly porous brittle materials", Nature, vol. 180, 26, p. 862-63 (1957)

195. Midgley, H.G. and Chopra, S.K., "Hydrothermal reactions in lime rich part of the system CaO-SiO_2-H_2O", Mag. Concr. Res., vol. 12, no. 34, p. 19-26 (1960)

196. Roy, M. and Harker, I., "Discussion of the paper 'Hydrothermal reactions in the system CaO-SiO_2-H_2O and steam curing of cement and cement-silica products by H.F.W. Taylor", Proc. Fourth Intl. Symp. on the Chemistry of Cement,

U.S. Bureau of Standards, Monograph 43, vol. 1, p. 196-201 (1962)

197. Thorvaldson, T. and Skelton, G.R., "Steam curing of Portland cement mortars : A new crystalline substance", Can. J. Research 1, p. 148-154 (1929)

198. Kalousek, G. and Adams, M., "Hydration products formed in cement pastes at 25 to 175°C", J. Am. Concr. Inst. Proc. 48, p. 77-90 (1950)

199. Neese, H., Spangenberg, K. and Weiskirchner, W., "Contribution to the knowledge of the reaction products in steam hardened pastes of quartz flour with lime or Portland cement (in German)", Tonind. Z. 81, p. 325-332 (1957)

200. Assarson, G.O., "Hydrothermal reactions between calcium hydroxide and amorphous silica; the reactions between 180 and 220°C", J. Phys. Chem. 61, p. 473-479 (1957)

201. Rozenfeld, L.M., Ben Yaminovich, I.M. and Berezin, H.N., "Large panels of autoclaved aerated concrete without cement containing blastfurnace slag and fuel ash and ii. Kunnos, G. Ya, Lindenberg, B. Ya and Lev, N. Ya, 'Use of fuel ash concrete in Latarian S.S.R.' Beton i Zhelezobeson, 1961 (2), 68-83. (Also Library Communicated 1095 of the Building Research Station, U.K.)

202. Lecnazar, F.J., "Reactivation of prematurely hydrated Portland cements", J. Sci. & Industr. Res., vol. 21 D, no. 2, p. 33-38 (1962)

203. Assarson, G.O., "Discussion of the paper 'Hydrothermal reactions in the system $CaO-SiO_2-H_2O$ and the steam curing of cement and cement-silica products", Proc. Fourth Intl. Symp. on the Chemistry of Cement, U.S. Bureau of Standards, Monograph 43, vol. 1, p. 190-194 (1962)

204. Garner, W.E., "Chemistry of the solid state" Butterworth Scientific Publications, London, p. 303-306 (1955)

205. Thorvaldson, T., "Effect of chemical nature of aggregate on strength of steam cured Portland cement mortars", J. Am. Concr. Inst. Proc., vol. 52, p. 771 (1955)

206. Lea, F.M., "The chemistry of cement and concrete", Edward Arnold Ltd. (Publishers), London (1956), p. 227

207. Hanson, W.C., "Discussion of the paper 'Portland-pozzolan cement by Giovauni Malquori', Proc. Fourth Intl. Symp. on the Chemistry of Cement, U.S. Bureau of Standards, Monograph 43, vol. 2, p. 1000 (1962)

208. Heller, L. and Taylor, H.F.W., "Crystallographic data for the calcium silicates", Her Majesty's Stationery Office, London (1956), p. 58

209. Smith, C.O., "Identification and qualitative chemical analysis of minerals", D. Van. Nostrand Company Inc. (1953), p. 283

210. Gorden, William, A. and Gillespie, H. Aldrige, "Variables in concrete aggregates and Portland cement paste which influence strength of concrete", J. Am. Concr. Inst., v. 60, no. 8, p. 1029-52 (Aug. 1963)

211 Romesh, C.K. and Chopra, S.K., "Determination of tensile strength of concrete and mortar by the split test" Indian Concrete Journal, vol. 34, no. 9, p. 354-57 (1960)

SELECTED PUBLICATIONS

1. Gas producing agents in the production of lightweight aggregates. By S.K. Chopra, Kishan Lall and V.S. Ramachandran, Journal of Applied Chemistry, vol. 14, 1964, p. 181-185

2. Measurement of specific surface of fly ash. S.K. Chopra and S.N. Narain, Journal of Mat. Res. and Standards, ASTN (U.S.A.) (in press)

3. Contribution to the discussion of the paper 'A new hypothesis of the mechanism of sulphate expansion by Chatterjee and Jeffery, Mag. Conc. Research, London (in press)

4. The mineralogy of air-cooled blastfurnace slag, S.K. Chopra, C.A. Taneja and G.S. Mehrotra, Indian Journal of Technology (under publication)

5. Utilization of the Indian blastfurnace slag, S.K. Chopra and C.A. Taneja, Presented at the Symposium on the Utilization of Metallurgical wastes, National Metallurgical Laboratory, Jamshedpur (March 1964)

6. Discussion of the paper 'Blast-furnace slags and slag cements by W. Kramer, H. Williams, & S.K. Chopra, Proc. Fourth Intl. Symp. on the Chemistry of Cement, U.S. Bureau of Standards, Monograph 43, vol. 2, p. 979-981 (1962)

7. The preparation and chemistry of expanding cements, S.K. Chopra and Mohan Rai, Cement & Lime Manufacture vol. XXXV, no. 2, p. 17-22, 1962

8. Activation of slag with lime or clinker," S.K. Chopra and Kishan Lall, Proc. Indian Science Congress, 49th Session Cuttack, Jan., Part III 1-170 (1962)

9. Problems in manufacture and use of dolomitic lime, Mohan Rai and S.K. Chopra, Jr. N.B.O., VII (2), 16-21, 1962

10. A lightweight aggregate from Durgapur slag, S.K. Chopra and C.A. Taneja, Jr. N.B.O., VII(4), 16-20, 1962

11. Sintering fly ash for making a lightweight aggregate, S.K. Chopra, C.S. Sharma and Kishan Lall, J. Inst. of Engrs (India), 44(3), C 12, 165-174, 1963

12. A non-shrinking and low expanding cement, S.K.Chopra and Mohan Rai, JSIR, 21D(7), 239-42, 1962

13. The strength of brick masonry, P.M. Abdul Rehman, S.S. Rehsi and S.K. Chopra, Jr. N.B.O., VI(4), 49-61, 1961.

14. Sulphate activation of low lime and high alumina slag, S.K. Chopra, and Kishan Lall, JSIR, vol. 20D, no. 6, 203-206, June 1961

15. Sintered lightweight aggregate from Indian fly ashes, S.K. Chopra and Kishan Lall, Indian Concrete Journal, vol. 35, no. 5, 150-153, May 1961

16. Manufacture of supersulphated cement from Indian slag, S.K. Chopra and Kishan Lall, Indian Concrete Journal, 35(4), 114-116 (March 1961)

17. An investigation on expanding cements, Mohan Rai and S.K. Chopra, Proc. Indian Science Congress, 47th Session, Roorkee, Jan., 1961

18. Discussion on the paper, 'Manufacture and properties of Portland Blast furnace cement', S.K. Chopra, Proc. Institution of Engineers, Sept., 1960

19. Development of cements for use in India, S.K. Chopra and C.A. Taneja, Mohan Rai and Kishan Lall, Cement & Concrete, vol. 1, no. 1, 1-12 (1960)

20. Hydrothermal Reactions between lime and aggregate fines, H.G. Midgley and S.K. Chopra, Mag. Concr. Res., vol. 12, no. 35, 73-82, July 1960

21. Hydrothermal reactions in the lime, rich part of the system $CaO-SiO_2-H_2O$, H.G. Midgley and S.K. Chopra, Mg. Concr. Res., vol. 12, no. 34, 19-26, March 1960

22. Determination of Tensile strength of concrete and mortars, C.K. Ramesh and S.K. Chopra, Indian Concr. Jour., vol. 34, no. 9, 354-357, Sept. 1960

23. Brickwork in lime-pozzolana mortars, S.K. Chopra, S.S. Rehsi and B.K. Jindal. Presented at NBO Symp. on 'Defects in Masonry', National Buildings Organisation, New Delhi (April 1962)

24. Determination of tensile bond strengths, S.K. Chopra, S.P. Garg and S.S. Rehsi, Indian Builder, June, 1960

25. Development of super-sulphated cement from Indian slag, S.K. Chopra, Kishan Lall and N.K. Patwardhan, Proc. Indian Science Congress, 47th Session held at Bombay, Jan. 3-9, 1960

26. Lightweight slag aggregates for concrete, S.K. Chopra and Kishan Lall, Indian Concrete Journal, 33(8), 270-273, 1959

27. An indigenous foaming agent for low density foamed concrete, G.W. Kapse, S.K. Chopra and N.K.Patwardhan, Indian Concr. Jour., 369-371, Nov., 1958

28. Mechanical versus manual methods of compacting tensile briquettes, S.K. Chopra, Indian Ceramics, vol. 4, 111-124, 1958

29. New foaming agents, G.W. Kapse, S.K. Chopra, Research and Industry, vol. 1, no. 12, 251 (1956)

30. Use of granulated slag in the manufacture of Portland blastfurnace cement, S.K. Chopra and N.K. Patwardhan, Proc. Symp. on Housing & Building Materials, National Buildings Organisation, New Delhi, vol. 2, 117-123 (1958)

31. Use of wet ground slag as a substitute of Portland cement in concrete, S.K. Chopra, Rao, K.S. and Patwardhan, N.K., Jl. Nat. Bldgs. Organisation (New Delhi, 56-59 (June-Sept. 1956)

32. Iron blastfurnace slag as a building material, S.K. Chopra and N.K. Patwardhan, Bull. of the Central Building Res. Instt., Roorkee, vol.3, no. 2, 2-57, Dec. 1955

33. Investigation on the utilization of Indian iron blastfurnace slag, Part I as an aggregate, S.K.Chopra, CBRI Bull. vol. 3, no. 2, 58-65, Dec. 1955

34. Preliminary investigation on the utilization of Sindri Coal Ash as a Building material, S.K. Chopra JSIR, 12B, no. 3, 430-434 (1953)

35. Technology of artificial hydraulic lime 1: Characteristics of the argillaceous constituents, R.C. Hoon, S.K. Chopra, I.V. Venugopalarao, Jr. of the Central Board of Irrigation, special issue brought out at the International Conference for High Dams, New Delhi, 1951

36. Pozzolanas and pozzolanic cements, by S.K. Chopra and N.K. Patwardhan, The Indian Concrete Journal, 24, 11, 269, Nov., 1950.